Energy Management Strategies in Production Environments with Support of Solar Energy

University of Almeria

Author:

Jerónimo Ramos Teodoro

Supervisors:

Prof. Francisco Rodríguez Díaz

Prof. Manuel Berenguel Soria

Almeria

December 2020

Energy Management Strategies in Production Environments with Support of Solar Energy

Estrategias de gestión energética en entornos productivos
con apoyo de energía solar

A thesis submitted to the Department of Informatics and
the International PhD School of the University of Almeria
for the degree of Doctor of Philosophy in Informatics (RD 99/11)

Author
Jerónimo Ramos Teodoro

Supervisors
Dr. Francisco Rodríguez Díaz
Dr. Manuel Berenguel Soria

Almeria, December 2020

PUBLISHED BY THE UNIVERSITY OF ALMERIA

Photo and illustration credits: FreeImages.com/Margan Zajdowicz (book cover and Chapter 5 header), FreeImages.com/Mabel Amber (Chapter 1 header), pexels.com/Pixabay (Chapter 2 header), pexels.com/Shvets Anna (Chapter 3 header), pxels.com/Flickr (Chapter 4 header), pexels.com/Markus Spiske (Chapter 6 header), pexels.com/Fauxels (Chapter 7 header), pexels.com/Pixabay (Chapter 8 header), FreeImages.com/Colin Nixon (Bibliography header), Máriam Ramos Teodoro (ODEHubs's components icons).

Document layout credits: Mathias Legrand (The Legrand Orange Book, LaTeX template), Juan Diego Gil Vergel (adaptations of the template).

First printing, December 2020

A Ángeles,
a mis padres, Jero y Lola,
a mi hermana, Máriam,
a mi familia,
a mis compañeros y amigos.

———-

To Ángeles,
to my parents, Jero and Lola,
to my sister, Máriam,
to my family,
to my colleagues and friends.

Agradecimientos

Reza una de las citas de Christopher McCandless que «la felicidad solo es real cuando es compartida»y no podría estar más de acuerdo con él. Por ello, quiero aprovechar estas primeras páginas para expresarles mi más sincera gratitud a quienes de un modo u otro me han acompañado en este camino académico durante los últimos cinco años.

En primer lugar, quiero dar las gracias especialmente a mis directores, Paco y Manolo, por su dedicación, paciencia, confianza, y ánimo. No solo me habéis transmitido la pasión por el control automático y servido como ejemplo de académicos competentes desde el inicio de mi etapa universitaria, cuando aún era estudiante de ingeniería, sino que además me habéis brindado la oportunidad de formar parte del grupo de investigación del que sois pilares fundamentales. Valoro muchísimo vuestro apoyo a nivel científico y creativo en el desarrollo de esta tesis, pero también todos vuestros sabios consejos, que atesoro para el futuro.

Del mismo modo, agradezco todos mis compañeros del Grupo de Investigación de Automática, Robótica y Mecatrónica su permanente disposición a prestar ayuda y el ambiente que se respira en el mismo. Paco, Manolo, José Luis Guzmán, José Carlos, Antonio, Manolo Pérez, María del Mar, José Luis Torres, Domingo, José Luis Blanco, Juan Diego, Manolo Muñoz, Marta, Marina, Ángeles, Paco García, Kiko, Quique, Hui, Lidia, Pepe Carballo, Javi Bonilla, Francisco Javier, Andrzej, Javi López, Julián, Luis, es un placer teneros al lado y compartir el día a día con vosotros. Me gustaría, además, hacer mención a algunos de ellos por los recuerdos y experiencias que siempre guardaré con especial cariño: a Paco y a Manolo, porque habéis tirado del carro conmigo todo este tiempo; a José Luis Guzmán, por sus consejos y aliento para correr la media maratón, y por los zumos de cebada fermentada que hemos compartido; a María del Mar, Jorge, y Manolo Pérez, por los trabajos que hemos sacado adelante; a los jóvenes del grupo, Marta, Marina, Ángeles, Paco García, Kiko, Quique, Hui, porque nos enfrentamos a los mismos retos; a mis compadres, José Luis Torres, Domingo, Juan Diego, Manolo Muñoz, por ser referentes para mí y por asumir con naturalidad mis ausencias a la hora del desayuno; a Manolo Muñoz, por su generosa disposición para echarme una mano este último año y por nuestras andanzas en mitad de una pandemia; a Juan Diego, porque me has enseñado otro punto de vista de las cosas, porque me persuadiste para correr la media maratón, y por aventurarnos a ir Brasil de estancia (y salir a tiempo).

Tampoco puedo olvidar al Departamento de Sistemas y Automática de la Universidad Federal de Santa Catarina (Brasil), que me acogió durante tres meses como estudiante doctoral. Quisiera dar las gracias al profesor Julio Normey Rico, por aceptar hacerse cargo de nosotros, por sus observaciones e ideas para la realización de esta tesis, y por su hospitalidad para enseñarnos parte de la isla de Florianópolis. Igualmente, he de agradecer a Paulo y Gustavo toda su colaboración a este respecto y que compartieran con nosotros su tiempo de recreo, ofreciéndonos la posibilidad de sumergirnos en la cultura local. Gracias también a los becarios del departamento, especialmente a Carolina y Bruno, quienes se preocuparon de que nos integráramos en su entorno.

Por otro lado, he de reconocer la labor institucional de las entidades que han respaldado mi trabajo académico, incluyendo a la Universidad de Almería y al Departamento de Informática, con mención especial a Luis Iribarne como coordinador del programa de doctorado; a la Plataforma Solar de Almería, al Instituto Andaluz de Investigación y Formación Agraria y Pesquera, al Centro de Investigación de Energía Solar, y la Estación Experimental de la Fundación Cajamar, por su colaboración en proyectos de investigación en los que se enmarca esta tesis; y a la Agencia Estatal de Meteorología, por su prestación de servicios a estos proyectos.

Finalmente, quisiera dar las gracias a mis amigos y mi familia, por permitirme disfrutar de su compañía en el tiempo libre que le queda a uno; especialmente a Ángeles, a mis padres, Jero y Lola, y a mi hermana, Máriam, por su compresión, por su inestimable apoyo y por ser la verdadera razón de todo.

Muchas gracias a todos,
Jero

Apoyo económico:
Esta investigación no se podría haber llevado a cabo sin el apoyo económico del Ministerio Español de Economía y Competitividad, el cual ha financiado la beca de Formación para Personal Investigador (FPI) otorgada al estudiante de doctorado autor de esta tesis. Además, el trabajo también ha recibido apoyo económico parcial del proyecto ENERPRO (DPI2014-56364-C2-1-R), financiado por el Ministerio de España de Economía, Industria y Competitividad y fondos FEDER; y del proyecto CHROMAE (DPI2017-85007-R), financiado por el Ministerio de España de Ciencia, Innovación y Universidades y fondos FEDER.

Acknowledgements

One of Christopher McCandless's citations claims that "happiness is only real when shared" and I cannot but agree with it. Hence, I would like to make the most of these initial pages for expressing my sincere gratitude to whom one way or another have accompanied me in this academic pathway over the last five years.

First of all, I especially want to give thanks to my supervisors, Paco and Manolo, for their dedication, patience, confidence, and encouragement. Not only have you transmitted to me the passion for automatic control and served as examples of competent academicians from the beginning of my stage at the university, when I still was an engineering student, but you also afforded me the chance to become part of the research group of which you are part of the mainstay. I enormously value your support at a scientific and creative level for the development of this thesis, along with your wise advice, which I will treasure for the future.

In the same way, I praise all my fellows of the Automatic Control, Robotics, and Mechatronics Research Group for their permanent willingness to provide aid and for the atmosphere that is breathed in it. Paco, Manolo, José Luis Guzmán, José Carlos, Antonio, Manolo Pérez, María del Mar, José Luis Torres, Domingo, José Luis Blanco, Juan Diego, Manolo Muñoz, Marta, Marina, Ángeles, Paco García, Kiko, Quique, Hui, Lidia, Pepe Carballo, Javi Bonilla, Francisco Javier, Andrzej, Javi López, Julián, Luis, it is a pleasure to have you next to me and to share the day-to-day life with you. I would like, moreover, to mention some of them for the remembrances and experiences that I will always keep with special affection: Paco and Manolo, because you have been pulling out all the stops with me all this time; José Luis Guzmán, for his advice and inspiration to run the half marathon and for the fermented barley juice that we have shared; María del Mar, Jorge, and Manolo Pérez, for the work that we have taken forward; the youngster of the group, Marta, Marina, Ángeles, Paco García, Kiko, Quique, Hui, because we are facing the same challenges; my godfathers, José Luis Torres, Domingo, Juan Diego, Manolo Muñoz, for being my referents and for assuming with naturalness my absences at breakfast time; Manolo Muñoz, for his magnanimous willingness to lend me a helping hand this last year and for our adventures in the middle of a pandemic; Juan Diego, because you have taught me to see things from another point of view, because you persuaded me to run the half marathon, and for venturing to do the stay in Brazil together (and getting out on time).

I cannot forget either the Department of Systems and Automation of the Federal University of Santa Catarina (Brazil), which embraced me as a doctoral student for three months. I would like to thank Professor Julio Normey Rico, for accepting to be in charge of us, for his observations and ideas to accomplish this thesis, and for his hospitality to show us part of the island of Florianopolis. Equally, I have to express my gratitude to Paulo and Gustavo, for all their collaboration in this respect and for sharing with us their leisure time, offering us the opportunity to immerse ourselves into the local culture. Thank you, as well, to all the interns of the department, especially to Carolina and Bruno, who worried about keeping us integrated into their environment.

On the other hand, I have to acknowledge the institutional labour of the entities that have supported my academic work, including the University of Almeria and the Department of Informatics, with special mention to Luis Iribarne as coordinator of the PhD programme; the Solar Platform of Almeria, the Andalusian Institute for Agricultural and Fishing Research and Training, the Solar Energy Research Centre, and the Experimental Station of the Cajamar Foundation, for their collaboration in the research projects that constitute the framework of this thesis; and the Spanish National Weather Agency, for their provision of services to these projects.

Finally, I would like to give thanks to my friends and family, for letting me enjoy their company in one's remaining free time; especially to Ángeles, to my parents, Jero and Lola, and to my sister, Máriam, for their empathy, for their inestimable support and for being the real reason of everything.

Thank you very much to all,
Jero

Financial support:
This research would not have been possible without the financial support from the Spanish Ministry of Economy and Competitiveness, which has funded the fellowship for Research Staff Training (FPI) awarded to the doctoral student that authored this thesis (BES-2015-075133). In addition, this research has received partial financial support from the ENERPRO project (DPI2014-56364-C2-1-R), funded by the Spanish Ministry of Economy, Industry and Competitiveness and ERDF funds; and the CHROMAE project (DPI2017-85007-R), funded by the Spanish Ministry of Science, Innovation and Universities and ERDF funds.

Resumen

Durante los últimos años, las políticas energéticas destinadas a incrementar la eficiencia en los procesos de producción, transporte y consumo han conducido a enfoques basados en la descentralización de los mismos y la combinación de diferentes tipos de energía, con el propósito de beneficiarse del uso de los recursos e infraestructura disponibles a escala local de una forma sinérgica. En consecuencia, se espera que las energías renovables jueguen un papel clave dada su relevancia en la generación distribuida, bien para redes puramente eléctricas o bien para sistemas combinados de energía. Sin embargo, debido a su naturaleza intermitente, muchas requieren el uso de sistemas de almacenamiento, una infraestructura flexible, y estrategias de gestión que desacoplen la generación de la demanda, a fin de resultar económicamente viables.

En este sentido, el control predictivo basado en modelo ha propiciado muchos de los últimos desarrollos por su capacidad para lidiar con los objetivos operacionales (criterios económicos o medioambientales para la toma de decisiones a lo largo del tiempo) de sistemas que incluyen múltiples vectores energéticos, a la par que respeta las diferentes restricciones legales, técnicas y políticas de las instalaciones involucradas. Esta tesis presenta varias aportaciones a dicho campo del conocimiento, todas ellas alrededor de la formulación de un marco de modelado genérico de amplia aplicabilidad mediante el que representar sistemas de diversa naturaleza, complejidad, escala de tiempo y topología. Dicha formulación tiene por objetivo la complementación de modelos previos para incluir la posibilidad de definir de forma más precisa determinados procesos, como la venta de recursos de salida o la adición de cargas relacionadas con el estado de funcionamiento de ciertos dispositivos, y reducir el número de variables de decisión requeridas para modelar concentradores de energía de cierta complejidad. La posterior formalización del problema de optimización, a partir del marco de modelado desarrollado, requiere de la aplicación de control predictivo basado en modelo o estrategias de programación para la gestión de energía/recursos. Aunque la función objetivo del problema de optimización planteado en esta tesis únicamente considera aspectos económicos relativos al intercambio de recursos, no se imponen restricciones particulares sobre la misma, que bien podría seleccionarse de acuerdo con otros criterios (ambientales, energéticos...). Todo esto ha conducido al diseño de una prometedora librería de funciones con el objetivo de facilitar la implementación de estos problemas de control o reparto, considerando los principales inconvenientes de los paquetes alternativos.

La utilidad de los hitos anteriores se demuestra mediante un caso de estudio inspirado en las instalaciones correspondientes a los dos proyectos de investigación en los que el estudiante doctoral ha participado durante su formación. Para ilustrar con una aplicación real e interesante, sin pérdida de generalidad, se considera la situación legal en España entre 2015 y 2018 concerniente al autoconsumo, en la que las ventas a la red se permiten a precio de subasta y tanto la energía autoconsumida como la vertida a la red están gravadas. Esto condiciona la programación operacional, que se determina atendiendo a criterios económicos y considerando las variaciones en el precio de la electricidad a lo largo del día, de acuerdo con los datos publicados en tiempo real por el operador de mercado. Las simulaciones llevadas a cabo requerían, de antemano, estimar y validar un modelo de producción energética para los equipos fotovoltaicos, así como la combinación, limpieza y sincronización las bases de datos de las instalaciones. Los resultados obtenidos son coherentes con respecto al comportamiento intuitivamente esperado del controlador atendiendo al objetivo económico, lo cual valida el enfoque de modelado propuesto. Además, la herramienta será útil en la evaluación de prueba, en el estudio de estrategias de gestión de recursos con diferentes conjuntos de datos reales y, debido a su concepción como herramienta flexible, en entornos industriales, comerciales y domésticos. Por todas las razones anteriores, se espera que el trabajo presentado en esta tesis sea de interés al grueso de la comunidad científica.

Las reflexiones de esta tesis concluyen que el trabajo futuro debería enfocarse en añadir capacidades al marco de modelado propuesto con el fin de representar determinados procesos particulares; en desarrollar modelos precisos para los sistemas de conversión o almacenamiento y las redes de transporte; en caracterizar la incertidumbre y formular, en concordancia, esquemas de control probabilísticos; y en implementar estas características en la librería desarrollada, bien en su forma actual o considerando otros paradigmas de programación y su integración dentro de los denominados sistemas ciber-físicos.

Palabras clave: concentradores de energía, sistemas multi-energía, producción distribuida, control predictivo basado en modelo, programación lineal en enteros mixta, optimizacióin determinista, reparto económico, distritos agroindustriales, generación fotovoltaica, autoconsumo, MATLAB®, Simulink®.

Abstract

Over the last few years, energy policies aimed at increasing efficiencies in production, transportation, consumption and storage processes have led to approaches based on decentralising these processes and combining different kinds of energy to benefit from the use of available local resources and infrastructure in a synergistic way. Consequently, renewable energies are expected to play a key role given their relevance in distributed generation either for purely electrical power networks or combined energy systems. However, owing to their intermittent nature, many require the use of storage devices, a flexible infrastructure, and management strategies that decouple generation from demand in order to be economically viable.

In this regard, model predictive control has pushed forward many of the latest developments because of its capability to cope with the operational objectives (economic and/or environmental criteria for making decisions over time) of systems that include multiple energy carriers, whilst respecting the several legal, technical, and political constraints of the facilities involved. This thesis presents various contributions to that field of knowledge, all around the formulation of a widely applicable generic modelling framework for representing systems of diverse nature, complexity, timescale, and topology. The formulation is aimed at complementing previous models in order to include the possibility of defining more accurately certain processes, such as selling output resources and adding loads related to the operating state (on/off) of certain devices, and to reduce the number of decision variables for modelling complex energy hubs. The subsequent formalisation of the optimisation problem, from the developed modelling framework, requires applying model predictive control or scheduling strategies for energy/resource management. Even though the objective function of the optimisation problem posed in this thesis only considers economic aspects regarding the trade of resources, no restrictions are placed on the particular objective function, which could be selected according to other criteria (environment, energetic resources...). All that has led to devise a promising software library aimed at easing the implementation of this control or dispatch problems, considering the main drawbacks of the alternative packages.

The utility of the above milestones is demonstrated by means of a case study inspired in the facilities corresponding to the two research projects in which the doctoral student has been participating during his tuition. To provide a real and captivating application for the developed approach, without loss of generality, the legal situation in Spain concerning self-consumption between 2015 and 2018 has been considered, in which sales to the grid are allowed at the pool price and both the self-consumed energy and that injected to the grid are taxed. This conditions the operational scheduling, which is determined attending to economic criteria and considering the variations in the electricity price throughout the day according to the real-time data published by the market operator. The performed simulations required, in advance, to estimate and validate an energy production model for the photovoltaic equipment and the combination, cleansing, and synchronisation of the databases of the facilities. The results obtained are coherent with respect to the intuitively expected behaviour of the controller regarding the economic objective, which validates the proposed modelling approach. In addition, the tool will be useful in assessing multiple "what-if" scenarios and studying resource management strategies with different sets of real data and, because of its conception as a flexible tool, in industrial, commercial, or home environments. For all the above reasons, it is hoped that the work presented in this thesis will be of interest to the wider scientific community.

The final reflections of this thesis conclude that future work should focus on adding capabilities to the proposed modelling framework in order to represent certain particular processes, developing precise models for conversion/storage devices and transportation networks, characterising uncertainty and formulating probabilistic control schemes accordingly, and implementing these features in the developed library, either in its current form or considering other programming paradigms and its integration within the so-called cyber-physical systems.

Keywords: energy hubs, multi-energy systems, distributed production, model predictive control, mixed-integer linear programming, deterministic optimisation, economic dispatch, agro-industrial districts, photovoltaic generation, self-consumption, MATLAB®, Simulink®.

Contents

List of Figures

List of Tables

List of Abbreviations

AC	Alternating current. XXXI, XXXII, 59, 123, 133
AEMET	Spanish State Meteorological Agency, from Spanish *Agencia Estatal de Meteorología*. 60, 112
AFEM	Assessing Future Electricity Markets. 34
AIMMS	Advanced Interactive Multidimensional Modeling System. 20, 21, 25
AMPL	A Mathematical Programming Language. 20, 24, 25, 33, 121
ANN	Artificial neural network. 130
ARM	Automatic Control, Robotics and Mechatronics. 6, 112
ARMA	Auto-regressive moving average. 130
BARON	Branch-And-Reduce Optimization Navigator. 20, 121
BHI	Beam horizontal irradiance. XXXI, 60
CC	Chance constraints. 20, 22, 24, 29
CCGA	Column-and-constraint generation algorithm. 23, 24
CHROMAE	Control and Optimal Management of Heterogeneous Resources in Agroindustrial Production Districts Integrating Renewable Energies. 5, 7, 8, 12, 13, 20, 37, 39, 43, 47, 59, 73, 85
CIEMAT	Research Centre for Energy, Environment and Technology, from Spanish *Centro de Investigaciones Energéticas, Medioambientales y Tecnológicas*. 39
CIESOL	Solar Energy Research Centre, from Spanish *Centro de Investigación de Energía Solar*. 39, 40, 55, 60, 64, 67, 69, 70, 87, 91, 92, 96, 103, 112
CIGRE	International Council on Large Electric Systems, from French *Conseil International des Grands Réseaux Électriques*. 24
CoPro	Improved Energy and Resource Efficiency by Better Coordination of Production in the Process Industries. 35
CORDIS	Community Research and Development Information Service. 34

CPS Cyber-physical system. 28
CVaR Conditional value at risk. 20, 24, 25
DC Direct current. XXXI, XXXII, 59, 69, 123, 124
DER-CAM Distributed Energy Resources Customer Adoption Model. 20
DHI Diffuse horizontal irradiance. XXXI, 60, 100, 112
DIMMER District Information Modeling and Management for Energy Reduction. 34
DMG Distributed multi-generation. 3, 4
DNI Direct normal irradiance. XXXI, 60, 100, 112
DP Dynamic programming. 19, 24, 29
DPS Distributed production system. 15, 22
DST Daylight saving time. XXX, 61, 89, 97
DYMASOS Dynamic Management of Physically Coupled Systems of Systems. 35
EH Energy hub. 3, 4, 7–9, 15, 16, 20–22, 25–28, 33, 34, 36, 47–49, 51–55, 57, 71–77, 80, 81, 83–85, 87, 91, 92, 95, 96, 105, 109–112
EHCM Energy Hub Component Modelling. 21
ENERPRO Control and Energy Management Strategies in Production Environments with Support of Renewable Energy. 5, 7, 8, 12, 13, 37, 39, 59, 85
ESC Energy Science Center. 34
ETH Swiss Federal Institute of Technology, from German *Eidgenössische Technische Hochschule*. 34
EU European Union. 1, 2
FHS Final Hourly Schedule. 90, 99, 112
FPI Research staff training, from Spanish *formación de personal investigador*. 6
FVDS Final Viable Daily Schedule. 90, 99
GA Genetic algorithm. 19, 25, 26, 28
GAMS General Algebraic Modeling System. 20–26, 29, 33
GHI Global horizontal irradiance. XXXI, 60, 100, 112
GRG Generalized reduced-gradient. 27
HOMER Hybrid Optimization Model for Electric Renewable. 20, 23, 28, 33
HVAC Heating, ventilation air conditioning. 24
ICTs Information and communication technologies. 3, 4
IEA International Energy Agency. 41
IEEE Institute of Electrical and Electronics Engineers. 23, 24, 26, 27, 29, 30
IFAPA Andalusian Institute for Agricultural and Fishing Research and Training, from Spanish *Instituto Andaluz de Investigación y Formación Agraria y Pesquera*. 39
IMES Integration of Sustainable Multi-Energy-Hub Systems at Neighbourhood Scale. 34
IMP Institut Mihajlo Pupin. 26
INEOS Inspec Ethylene Oxide Specialities. 29
JCR Journal Citation Reports. 9, 10
JRC Joint Research Centre. 34
LHV Lower heating value. 97

LP	Linear programming. 19, 25–27
LPV	Linear parameter varying. 129
LQP	Linear quadratic programming. 19, 29
LUSYM	Leuven University System Modeling. 21
MATLAB	Matrix Laboratory. XXXI, 7, 8, 20–29, 33, 47, 71, 73, 85, 103, 113, 121
MBDS	Matching Basis Daily Schedule. 90
MCS	Monte Carlo simulations. 20, 22, 25, 26
MDP	Markov decision processes. 20, 24
ME	Mean error. XXXI, 67, 68
MES	Multi-energy system. 3, 4, 8, 9, 15, 16, 20–22, 26–28, 33–36, 57, 71, 109, 110
MG	Microgrid. 3, 5, 15, 16, 22, 23, 25, 26, 28, 30, 35, 110–112
MILP	Mixed-integer linear programming. 19, 22–29, 57, 85, 111
MINLP	Mixed-integer nonlinear programming. 19, 22, 24, 26–29, 57
MIQCQP	Mixed-integer quadratically constrained quadratic programming. 19, 23, 24
MIQP	Mixed-integer quadratic programming. 19, 23, 26, 27
MOST	MATPOWER Optimal Scheduling Tool. 21
MPC	Model predictive control. 4, 5, 7, 9, 21–24, 26, 27, 29, 35, 53, 83, 98, 109, 110, 112, 129
MRS	Multi-resource system. 110
MS	Microsoft. 29
NLP	Nonlinear programming. 19, 24, 26
NOCT	Normal operating cell temperature. XXXI–XXXIII, 62, 64
NRMSE	Normalised root-mean-square error. XXXI, 67–69
NSGA	Non-dominated Sorting Genetic Algorithm. 25
OBDS	Operating Basis Daily Schedule. 90
ODEHubs	Optimal Dispatch for Energy Hubs. 8, 52, 57, 71–84, 92, 94, 95, 98, 108, 109, 111–113
OMIE	Iberian Energy Market Operator - Spanish Pole from Spanish *Operador del Mercado Ibérico de Energía - Polo Español, S.A.*. 88, 89, 99, 101, 112
PEGASE	Pan European Grid Advanced Simulation and State Estimation. 29
PEM	Point estimate method. 20, 24, 26
PlaMES	Integrated Planning of Multi-Energy Systems. 35
Plan4Res	Community Research and Development Information Service. 35
PNMPC	Practical nonlinear model predictive control. 28, 29
PSA	Solar Platform of Almeria, from Spanish *Plataforma Solar de Almería*. 39, 41, 42, 70, 87
PSO	Particle swarm optimisation. 19, 22, 23, 26, 28
PV	Photovoltaic. 3, 7, 13, 36, 39, 40, 44, 55, 59, 60, 62, 64, 69, 70, 83, 84, 87, 88, 91, 92, 96, 112
PVDS	Provisional Viable Daily Schedule. 90
QP	Quadratic programming. 19, 22–24
REE	Electrical Network of Spain from Spanish *Red Eléctrica de España*. 89

RES Renewable energy sources. 2–5, 22, 29, 70, 106, 110
RO Robust optimisation. 19, 24, 26, 27
RTO Real-time optimisation. 5
RWTH Rhenish-Westphalian Institute of Technology, from German *Rheinisch-Westfälische Technische Hochschule*. 35
SBB Simple Branch and Bound. 26
SNOPT Sparse Nonlinear Optimizer. 24
SOCP Second-order cone programming. 19, 27, 29
SP Stochastic programming. 19
SUN4GREEN Maximising Sunlight Resources for Cost, Energy and Yield Efficient Greenhouses. 12
TDNN Time delay neural network. 130
TEP197 TEP stands for Production Technologies, from Spanish *Tecnologías de la Producción*, which indicates the area to which the research group belongs. 197 is its identification number within the Andalusian Plan of Research, Development, and Innovation. 6
TRNSYS Transient System Simulation. 22, 61
TU Technical University, from German *Technische Universität*. 35
UAL University of Almeria. 6
UK United Kingdom. 25, 27, 34
UoM University of Manchester. 27
US United States. 22, 24, 26
UTC Coordinated Universal Time or Universal Time Coordinated. 89
VPP Virtual power plant. 3, 4, 15, 16, 22–26, 28, 110

Nomenclature

Chapters 4, 6 and 7

Latin symbols	Units	Description
$\boldsymbol{C}$	Multiple units	$N_o \times N_p$ coupling matrix
C	Multiple units	Element of $\boldsymbol{C}$
$\boldsymbol{C_{ch}}$	-	$N_o \times N_o$ diagonal matrix of charge efficiencies
C_{ch}	-	Element of $\boldsymbol{C_{ch}}$
$\boldsymbol{C_{di}}$	Multiple units	$N_{di} \times N_p$ device coupling matrix (referred to their inputs)
C_{di}	Multiple units	Element of $\boldsymbol{C_{di}}$
$\boldsymbol{C_{dis}}$	-	$N_o \times N_o$ diagonal matrix of discharge efficiencies
C_{dis}	-	Element of $\boldsymbol{C_{dis}}$
$\boldsymbol{C_{do}}$	Multiple units	$N_{do} \times N_p$ device coupling matrix (referred to their outputs)
C_{do}	Multiple units	Element of $\boldsymbol{C_{do}}$
$\boldsymbol{C_i}$	-	$N_i \times N_p$ input coupling matrix
C_i	-	Element of $\boldsymbol{C_i}$
$\boldsymbol{C_s}$	-	$N_o \times N_o$ diagonal matrix of resource degradation
C_s	-	Element of $\boldsymbol{C_s}$
$\boldsymbol{c}$	Multiple units	$1 \times N_i$ vector containing the price of each input of the energy hub
c	Multiple units	Element of $\boldsymbol{c}$
$\boldsymbol{D_i}$	Multiple units	$N_{di} \times 1$ vector of devices' flows (referred to their inputs)

D_i	Multiple units	Element of $\boldsymbol{D_i}$
$\boldsymbol{D_o}$	Multiple units	$N_{do} \times 1$ vector of devices' flows (referred to their outputs)
D_o	Multiple units	Element of $\boldsymbol{D_o}$
H	-	Length (in samples) of the control horizon
$\mathcal{H}$	-	Set of N_h networked energy hubs
h, h'	-	Energy hub in $\mathcal{H}$
$\boldsymbol{I}$	Multiple units	$N_i \times 1$ vector of input flows
I	Multiple units	Element of $\boldsymbol{I}$
k	-	Discrete time instant
N_d	-	Number of conversion devices of the energy hub
N_{di}	-	Number of input flows of all the conversion devices that form the energy hub
N_{do}	-	Number of output flows of all the conversion devices that form the energy hub
$\boldsymbol{N}_{h,h'}$	-	$N_o(h) \times 1$ vector of exported flows from h to h'
$\boldsymbol{N}_{h',h}$	-	$N_i(h) \times 1$ vector of imported flows from h' to h
N_h	-	Number of energy hubs
N_i	-	Number of input flows of the energy hub
N_o	-	Number of output flows of the energy hub
N_p	-	Number of paths between inputs and outputs of the energy hub
T	min	Sample time
t	min	Continuous time instant
$\boldsymbol{M}$	Multiple units	$N_o \times 1$ vector of market sales flows
M	Multiple units	Element of $\boldsymbol{M}$
$\boldsymbol{O}$	Multiple units	$N_o \times 1$ vector of output flows
O	Multiple units	Element of $\boldsymbol{O}$
$\boldsymbol{P}$	Multiple units	$N_p \times 1$ vector of flows between inputs and outputs or "path vector"
P	Multiple units	Element of $\boldsymbol{P}$
p_E	€$/kWh$	Local supply company tariff prices
p_{ES}	€$/MWh$	Electricity prices from daily and intraday markets
p_{PV}	€$/kWh$	Variable charges over the 3.0A access fee for the self-consumed energy
$\boldsymbol{Q_{ch}}$	Multiple units	$N_o \times 1$ vector of charge flows
Q_{ch}	Multiple units	Element of $\boldsymbol{Q_{ch}}$
$\boldsymbol{Q_{dis}}$	Multiple units	$N_o \times 1$ vector of discharge flows
Q_{dis}	Multiple units	Element of $\boldsymbol{Q_{dis}}$

$\boldsymbol{S}$	Multiple units	$N_o \times 1$ vector of stored resources
S	Multiple units	Element of $\boldsymbol{S}$
$\boldsymbol{s}$	Multiple units	$1 \times N_o$ vector containing the price of sold resources
s	Multiple units	Element of $\boldsymbol{s}$

Greek symbols	Units	Description
$\boldsymbol{\delta}$	-	Binary matrix
δ	-	Binary variable
$\boldsymbol{\delta_{ch}}$	-	$N_o \times N_o$ binary diagonal matrix of charge flow activation
δ_{ch}	-	Element of $\boldsymbol{\delta_{ch}}$
$\boldsymbol{\delta_{D_i}}$	-	$N_{di} \times N_{di}$ binary diagonal matrix of devices' flow activation (referred to their inputs)
δ_{D_i}	-	Element of $\boldsymbol{\delta_{D_i}}$
$\boldsymbol{\delta_{D_o}}$	-	$N_{do} \times N_{do}$ binary diagonal matrix of devices' flow activation (referred to their outputs)
δ_{D_o}	-	Element of $\boldsymbol{\delta_{D_o}}$
$\boldsymbol{\delta_{dis}}$	-	$N_o \times N_o$ binary diagonal matrix of discharge flow activation
δ_{dis}	-	Element of $\boldsymbol{\delta_{dis}}$
$\boldsymbol{\delta_I}$	-	$N_i \times N_i$ binary diagonal matrix of input flow activation
δ_I	-	Element of $\boldsymbol{\delta_I}$
$\boldsymbol{\delta_O}$	-	$N_o \times N_o$ binary diagonal matrix of output activation
δ_O	-	Element of $\boldsymbol{\delta_O}$
$\boldsymbol{\delta_M}$	-	$N_o \times N_o$ binary diagonal matrix of market sales flow activation
δ_M	-	Element of $\boldsymbol{\delta_M}$
η	-	Efficiency
κ	-	Constant of proportionality that relates the production of a device to its demand

Other symbols	Units	Description
$\mathbf{1}$	-	Identity matrix

Sub-scripts	Units	Description
ch	-	Charge
d,D	-	Device
di	-	Device input
do	-	Device output
dis	-	Discharge
h,h'	-	energy hub in $\mathcal{H}$
i,I	-	Input
m,M	-	Market
o,O	-	Output
p,P	-	Path
s,S	-	Storage
$1...n$	-	Position/number of a element in a vector or matrix $(row, column)$

Super-scripts	Units	Description
max	-	Upper limit of a vector
min	-	Lower limit of a vector
$(1...n...m)$	-	Different elements of a set

Chapter 5

Latin symbols	Units	Description
A_c	m^2	Total area of the array c
A_m	m^2	Area of the module
a	V	Modified ideality factor of the diode
B	-	Relative day for the Equation of Time
C_{pv}	-	Gross efficiency of the field that will be an element the coupling matrices presented in Chapter 4
$C_{T,Eg}$	$°C^{-1}$	Fitting coefficient (0,0002677 $°C^{-1}$ for silicon)
$D_{i,pv}^{max}$	kW	Upper limit of the flow (solar radiation) entering the device (field) which will be an element of the $\boldsymbol{D_i^{max}}$ vector (see Chapter 4)
DoY	-	Day of the year (from 1 to 365 or 366)
DST	h	Offset due to daylight saving time
E_g	eV	Material bandgap energy

$E_{g,st}$	eV	Material bandgap energy at standard conditions (1.12 eV for silicon)
EoT	s	Result of evaluating the so-called Equation of Time
$\mathcal{F}$	-	Set of arrays that form the photovoltaic field
f_{eV}	J/eV	Conversion factor from electron-volts to joules (1.602 · 10^{-19} J/eV)
G	kW/m^2	Global horizontal irradiance (GHI), sum of G_b and G_d
G_b	kW/m^2	Beam horizontal irradiance (BHI)
G_{bn}	kW/m^2	Direct normal irradiance (DNI)
G_d	kW/m^2	Diffuse horizontal irradiance (DHI)
G_{NOCT}	W/m^2	Irradiance at NOCT conditions (800 W/m^2)
G_{st}	W/m^2	Irradiance at standard conditions (1000 W/m^2)
G_T	kW/m^2	Incident solar irradiance on a tilted surface
h_s	h	Solar time
h_o	h	Official time
I	A	Current generated by the module
I_L	A	Light current
I_{mpp}	A	Current generated by the module at maximum power point
I_o	A	Diode reverse saturation current
I_{sc}	A	Short-circuit current
k	-	Discrete time instant
k_B	J/K	Boltzmann constant (1.381 · 10^{-23} J/K)
ME	Multiple units	Mean error
N_c	-	Number of arrays that form the photovoltaic field
N_{pa}	-	Number of modules connected in parallel
$NRMSE$	%	Normalised root-mean-square error
N_s	-	Number of cells of the module
N_{se}	-	Number of modules connected in series
n_d	-	Ideality factor of the diode (as provided by the *PV Array* MATLAB®'s block)
n_{days}	-	Total number of days of the year (365 or 366, depending on if it is a leap year or not)
$P_{c,ac}$	kW	AC power supplied to the grid by the array c
$P_{c,ac}(j)$	kW	AC power produced by the array c at instant j
$\hat{P}_{c,ac}(j)$	kW	Estimate of the AC power produced by the array c at instant j
$P_{c,dc}$	kW	DC input power to the inverter of the array c

$P_{inv,ac}$	kW	AC output power from the inverter of the array c
$P_{inv,ac,r}$	kW	Nominal AC output power from the inverter of the array c
$P_{inv,dc,r}$	kW	Nominal DC input power to the inverter of the array c
q	C	Electronic charge ($1.602 \cdot 10^{-19}$ C)
R^2	-	Coefficient of determination
R_b	-	Ratio of beam radiation on a tilted plane to that on the plane of measurement (usually horizontal)
R_s	Ω	Series resistance
R_{sh}	Ω	Shunt resistance
S_T	W/m^2	Effective irradiance absorbed by the module
$S_{T,st}$	W/m^2	Effective irradiance absorbed by the module at standard conditions
T	min	Sample time
t	min	Continuous time instant
T_a	$°C$	Ambient temperature
$T_{a,NOCT}$	$°C$	Ambient temperature at NOCT conditions (20 $°C$)
T_m	$°C$	Temperature of the module
$T_{m,NOCT}$	$°C$	Temperature of the module at NOCT conditions
$T_{m,st}$	$°C$	Temperature of the module at standard conditions (25 $°C$)
V	V	Voltage of the module
$V_{c,dc}$	V	DC input voltage to the inverter of the array c
V_{mpp}	V	Voltage of the module at maximum power point
V_{oc}	V	Off-load voltage

Greek symbols	**Units**	**Description**
β	$°$	Slope angle of the modules
γ	$°$	Surface azimuth angle or deviation between the orientation of the field and the south (east negative and west positive)
δ	$°$	Declination of the sun, which measures the displacement of the sun due to translation of the earth
$\eta_{c,ac}$	-	Transmission efficiency from the inverter to the point of supply of the array c

$\eta_{c,inv}$	-	Efficiency of the inverter connected to the array c
$\eta_{c,mpp}$	-	Maximum power point efficiency of the of the array c
θ	$\circ$	Angle of incidence
θ_z	$\circ$	Zenith angle (angle of incidence on a horizontal surface, when $\beta = 0°$)
$\mu_{V,oc}$	$\%/°C$	Temperature coefficient for V_{oc}
$\mu_{I,sc}$	$\%/°C$	Temperature coefficient for I_{sc}
ρ_g	-	Ground reflectance (assumed to be of 0.1)
ϕ	$\circ$	Latitude where the field is located (south negative and north positive)
ψ	$\circ$	Longitude where the field is located (from 0 to 360 degrees west)
ψ_{ref}	$\circ$	Longitude of the standard meridian for the local time zone (from 0 to 360 degrees west)
ω	$\circ$	Hour angle, which measures the displacement of the sun due to rotation of the earth

Subscripts	**Units**	**Description**
ac	-	Alternating current
c	-	Array of the photovoltaic field
dc	-	Direct current
inv	-	Inverter
m	-	Module
mpp	-	Maximum power point
$NOCT$	-	Normal operating cell temperature (NOCT) ($G_{NOCT} = 800\ W/m^2$, $T_{a,NOCT} = 20\ °C$, and wind speed of 1 m/s)
oc	-	Open circuit
sc	-	Short-circuit
st	-	Standard conditions ($G_{st} = 1000\ W/m^2,\ T_{c,st} = 25\ °C$)
r	-	Nominal value

Energy Management Strategies in Production Environments with Support of Solar Energy

1. Introduction

Chapter Summary

In this introductory chapter, Section 1.1 offers a brief description of the current concerns in the environmental panorama and their impact on energy policies, which bolster the need for more research and constitute incentives for this thesis. Sections 1.2 and 1.3 present its general layout, including the research objectives and context, and Sections 1.4–1.6 contain the personal and scientific achievements derived from the same one. Finally, Section 1.7 sketches out the rest of the chapters.

1.1 Background and Motivation

Nowadays science is more concerned than ever with giving solutions to some of humanity's most complex challenges, such as climate change. In spite of the scepticism that still remains about it, there exists scientific evidence, and a broad consensus, on anthropogenic climate change and its repercussions for both the environment and our societies [1]. The drivers of climate change alter the energetic balance in the earth, can have a natural or anthropogenic origin and are quantified in terms of "radiative forcings", which lead to a near-surface warming when larger than zero (mainly as a result of greenhouse gases) [2]. Although the worldwide impact is difficult to measure because it affects directly and indirectly both natural and human systems, some of the most immediate metrics, related to weather conditions, can provide a snapshot of the state at a particular place when historical data are taken into account. In this regard, Figure 1.1 ranks the nationwide situation in Europe from zero (less affected) to a hundred (more affected), a score which has been calculated according to four indicators (data collected from 2014, 2015, and 2017): surface temperatures, sea temperatures, sea levels, and precipitation [3]. It is not surprising that, given this situation and its foreseeable impact, many states and organisations have started to support a shift of paradigm towards sustainable development policies. In particular, the European Union (EU) adopted a road map with the overarching aim of making Europe climate neutral in 2050, which has engaged politicians in putting concrete initiatives forth.

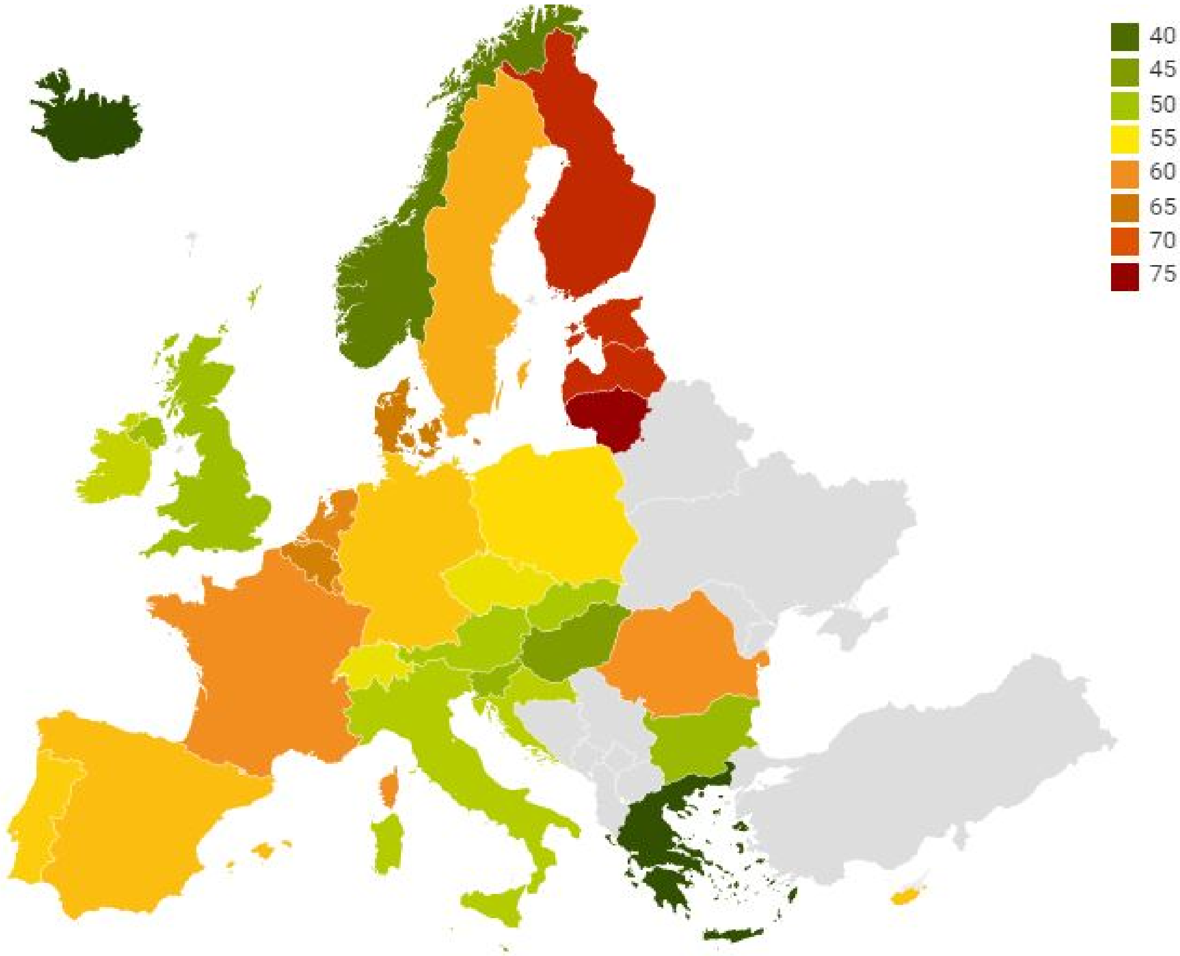

Figure 1.1. Climate change effects on European countries considering surface temperatures, sea temperatures, sea levels, and precipitation. Source: [3]

Among its interim targets there were three key goals in the European Union (EU) for 2020: reducing greenhouse gas emissions by at least 20% (from 1990 levels), increasing the share of renewable energy to 20% and achieving a 20% improvement in energy efficiency (savings of primary energy consumption) [4]. Whereas the latter two are close to be achieved but yet to be assessed in the reports of the European Commission, the European Union (EU) reached a 23% reduction in greenhouse gas emissions in 2018 and there are updated numbers for 2030: 40% (with incoming proposals to raise to 55%), 32% and 32.5% in the same goals [5]. In fact, all of them contribute to the fight against climate change either directly, by attacking the main agent causing global warming (greenhouse gases), or indirectly, by reducing the dependence on fossil fuels, which tend to be the main source of primary energy [6], thanks to the energy efficiency and to the employment of alternatives such as renewable energy sources (RES). The European Green Deal is one of the latest documents, released by European Commission, that provides an action plan to make the EU's economy sustainable, encompassing the above-mentioned objectives and introducing new legislation on innovation, circular economy, biodiversity, farming and building renovation [7].

According to the report "Sector Coupling in Europe: Powering Decarbonization" published by BloombergNEF in partnership with Eaton and Statkraft, the pathway to a green low-carbon future passes through the electrification of the sectors of the economy with higher consumption of fossil fuels: transport, industry and buildings.

This could take place directly, plugging these sectors into the grid via the proliferation of electric devices such as vehicles or heating systems; or indirectly, by using electricity to produce bio-fuels or hydrogen (from electrolysis) that provide heat to cover the demand of those sectors [8], as substitutes for fossil fuels. The same report points out that this situation “will require more flexible resources such as battery storage and gas peaker plants”, undoubtedly owing to the use RES. Some of them, such as photovoltaic (PV) and wind generation, increase the likelihood of mismatch between generation and make the operation of the grid more complex [9] and, given their intermittent nature, they require storage systems and suitable management strategies that decouple generation from demand in order to be economically viable [10].

Over the last few years, these energy policies aimed at increasing the efficiency and flexibility in production, transportation, consumption and storage processes have led scientists to formulate approaches based on the decentralisation of these processes and the combination of different kinds of energy to benefit from the use of available local resources and infrastructure in a synergistic way [11]. Some recent proposals have been focused on reducing the number of conversions from primary sources to points of consumption [12], exploiting renewable energy sources (RES) [13] and sustainable low carbon alternatives [14], or providing flexibility and stability to supply systems [15]. In this regard, recent concepts such as distributed multi-generation (DMG) [11] and multi-energy system (MES) [16] have come to set a general framework to characterise systems that employ various energy carriers, including the usual terminology, pending issues, and common structures. Mancarella distinguished within the so-called multi-energy systems (MESs), other contemporary concepts like microgrids (MGs), virtual power plants (VPPs) and energy hubs (EHs) as being general aggregation concepts aimed at integrating distributed energy resources into power system operation and planning, potentially resulting in new business models, as oppose to conventional large-scale power plants [16].

A formal definition of the energy hub (EH) concept was given for the first time by Geidl et al. [17] in 2006: a unit where multiple energy carriers can be converted, conditioned, and stored. According to Mancarella, it was developed “to model, from a technical perspective, generic MESs” [16]. This is often done by means of a simplified model based on the input-output interactions inside the system (balance equations), as exemplified in resource dispatch problem in 2007 by Geidl and Andersson [18]. Since then, many authors have applied this concept to different problems, such as resource management, introducing robust optimisation algorithms [19], methodologies to enhance the representation of operational constraints [20] or to facilitate the automatic modelling of arbitrary EH configurations [21], and demand-side management strategies [22]. In addition, the EH modelling framework has been implemented in microgrid (MG) management problems [23], including its integration into vehicle to grid systems [24]. The concept is also used in problems related to economic dispatch [25], or optimal device configuration in systems with storage elements [26]. A recent review on common resources and converters in EH’s models shows that most works focus on electricity and thermal heating technologies, paying less attention to other material resources (such as solid fuels, water, carbon dioxide or hydrogen) [27]. However, since both EHs and MESs can contain energy or material flows, the term “resource” will be preferred versus “energy” from now on.

One existing obstacle for the development of distributed multi-generation (DMG) is that the legal frameworks are still under development and each resource supply and distribution network usually operates under its own rules. Electricity power systems have one of the most extensive juridical frameworks, despite the still-present administrative and legal barriers [28], which has set the fundamental basis for smart grid development and self-consumption [29]; this has been thanks to recent advancements in information and communication technologies (ICTs), as well as those in automation and electronics.

Indeed, the term “smart" in smart grid [30] alludes to the use of information and communication technologies (ICTs), as well as process control and automation in decision making, to optimally operate distributed electricity grids. Although some of these techniques are not exclusively applied in the electricity sector—the petrochemical industry has been using model predictive control (MPC) since the end of the last century [31]—its large-scale use among different producers is still nascent, since “energy sectors have been traditionally decoupled from both operational and planning viewpoints" [16]. This view and current energy policies are however changing thanks to the appearance of MESs and EHs, whose advantages with respect to the traditional view of energy carriers have been set forth by Long as listed below [32]. Although they specifically refer to MES, they are germane to any distributed system with multiple energy carriers (EHs or hybrid virtual power plants (VPPs), for instance).

- *With MESs in general, the smart grid concept can be extended from the power system into the multi-energy domain to achieve an increase in the number of degrees of freedom with which to match energy supply with demand, improving overall system flexibility.*
- *Greater utilisation of primary energy sources is possible through the improved efficiencies enabled by distributed multi-generation technologies e.g. combined heat and power.*
- *The capacity credit of intermittent renewable energy resources can be improved. For example, electrical energy produced by wind that would otherwise be curtailed during periods of low electricity demand can be diverted to heat buffered sections of the system via power to heat technologies (e.g. heat pumps).*
- *Converting hard/expensive to store electrical energy into vectors where storage is easier/cheaper (e.g. with power to gas technology) can further improve system flexibility and reduce capital and operational expenditure for system operators.*
- *A potential exists for greater resource-market interaction for energy end-users who can modify their energy use to take advantage of energy pricing fluctuations (i.e. through time-of-use, real-time, dynamic tariffs etc.). For example, switching an electrically sourced heat demand (e.g. heat pump) to that supplied by gas (e.g. combined heat and power) during periods where electricity is expensive.*
- *Opportunities exist for MESs to provide ancillary services to the electrical networks through the provision of flexible demand/production that is capable of switching its primary energy source should system conditions require it (e.g. for peak demand management, secondary frequency response etc.).* [32, p. 26]

A quick look at some of the above-cited works, related to distributed generation, shows that many of the decision-making processes in this field rely on solving optimisation problems, either for design or management purposes, since this allows a practitioner to determine the choicest option (i.e. the most suitable set of variables) for a given problem; which is usually done according to certain criterion (as discussed in 2.1.2) and in the presence of operational, technical, economical, and legal constraints. In this regard, a proper control scheme can resolve issues related to the dispatch of resources/energy, providing generation schedules, accommodating more RES and making adequate use of the existing infrastructure (e.g. transmission/distribution networks or storage systems). Model predictive control (MPC), which encompasses a family of control techniques (cooperative, hierarchical, economic MPC...), presents itself as a promising methodology to fulfil the necessities of DMG since it considers how the system will change over time (receding horizon principle) as well as constraints in the problem formulation [33].

To the best of the author’s knowledge, many of these control approaches come from the field of chemical engineering which has traditionally used a hierarchy of levels or layers to distinguish different tasks performed in industry [34]. These are defined attending to the frequency at which decisions are taken (i.e. how often the control actions are calculated), the kind and quantity of involved equipment, and the level of abstraction.

Many contributions employ hierarchical control strategies in which MPC can act in either the regulatory or the supervisory layers [35] as well, and, in this regard, there is a dichotomy between Economic MPC and real-time optimisation (RTO) with MPC [36]. Long discusses both approaches in his thesis [32] and how the existence of uncertainty affecting the system behaviour is sometimes handled by using certainty equivalent MPC [37]. From his ideas, one can conclude that, when it comes to certain energy management applications, it is acceptable to assume (a) that the lower level regulatory controllers have a dynamic fast enough with respect to the sampling interval of the upper layers and they do not need to be considered for optimisation purposes (the corresponding steady-states are instead considered), (b) that due to the presence of them stability is not a primary concern, and (c) that for demonstration purposes a general uncertain optimisation problem can be converted into a deterministic one. This is the basis of many of the articles found in the literature about energy dispatch which deals with the energetic management of a campus [38] or the energy dispatch of a MG [39], to name a few, and also the basis of this thesis, where the control problem corresponds to the computations performed in upper layers.

1.2 Aim and Objectives

The memorandum of the research plan constitutes the formal commitment between the supervisors and the doctoral student in which the motivation, objectives, and methodologies are verbalised. From the same one and from a broad review of updated references, some of which are also presented in Chapter 2, the previous section encompasses a series of ideas that justify the interest of this thesis. The methodologies drafted in the said memorandum correspond to the content of Chapters 3-7 and the objectives, barely differing from the ones originally stated, are enumerated below in order to be associated with the contributions of the developed research work in Section 1.4.

- O1. Development of physical models for generators, consumers, and storage elements from a modular philosophy and with different levels of abstractions that allows simulating the short, medium and long-term dynamics of the system and is used for optimisation. The spotlight will be put on energy-hub-type modelling paradigms.
- O2. Characterisation of the production, demands, and disturbances.
- O3. Experimental validation of the developed models in steady-state and dynamic conditions.
- O4. Application of the models to the development of strategies for optimisation and coordination of production processes from an economic point of view. Control alternatives for energetically interconnected systems will be assessed, such as model predictive control (MPC).
- O5. Application of the above achievements to the facilities of the Control and Energy Management Strategies in Production Environments with Support of Renewable Energy (ENERPRO) and Control and Optimal Management of Heterogeneous Resources in Agroindustrial Production Districts Integrating Renewable Energies (CHROMAE)'s reference production systems (see Section 1.3 and Chapter 3).

In a broad sense, all these concrete objective are aimed at enhancing the energetic management in districts' environments, with special attention to the agro-industrial sector and RES, which are incentives for research in the Almerian ecosystem (e.g. ENERPRO and CHROMAE projects) and in many other agricultural regions around the globe.

1.3 Research Context

This thesis is the fruit of five years' research, from January 2016 to December 2020, with the Automatic Control, Robotics, and Mechatronics Research Group (ARM-TEP197) and the Area of System Engineering and Automatic Control at the Department of Informatics, all belonging to the University of Almeria (UAL). It was thank to the fellowship for Research Staff Training (FPI), awarded by the Spanish Ministry of Economy and Competitiveness (BES-2015-075133), that its author was able to perform his research and teaching duties and afford the three-month stay at Brazil. Such fellowship is associated with the ENERPRO project (see its test-bed plant in Figure 1.2), whose main objectives are enumerated below, as defined in its website [40].

E1. *Development of methodologies for obtaining models of processes that contain renewable energy sources to produce/consume process heat, electricity, water and CO_2. Development of estimators and predictors of generation and demand stages.*

E2. *Development of hierarchical, hybrid and, in general, MPC control and management strategies to optimise production from the economic, security and energy and water use points of view in heterogeneous systems, using a coordinated and comprehensive approach.*

E3. *Implementation and validation of the strategies in the production environment selected as test-bed plant. This will facilitate the development of the different tasks of the project over realistic conditions. Possible extensions to more complex environments like campus or industrial clusters will be demonstrated.*

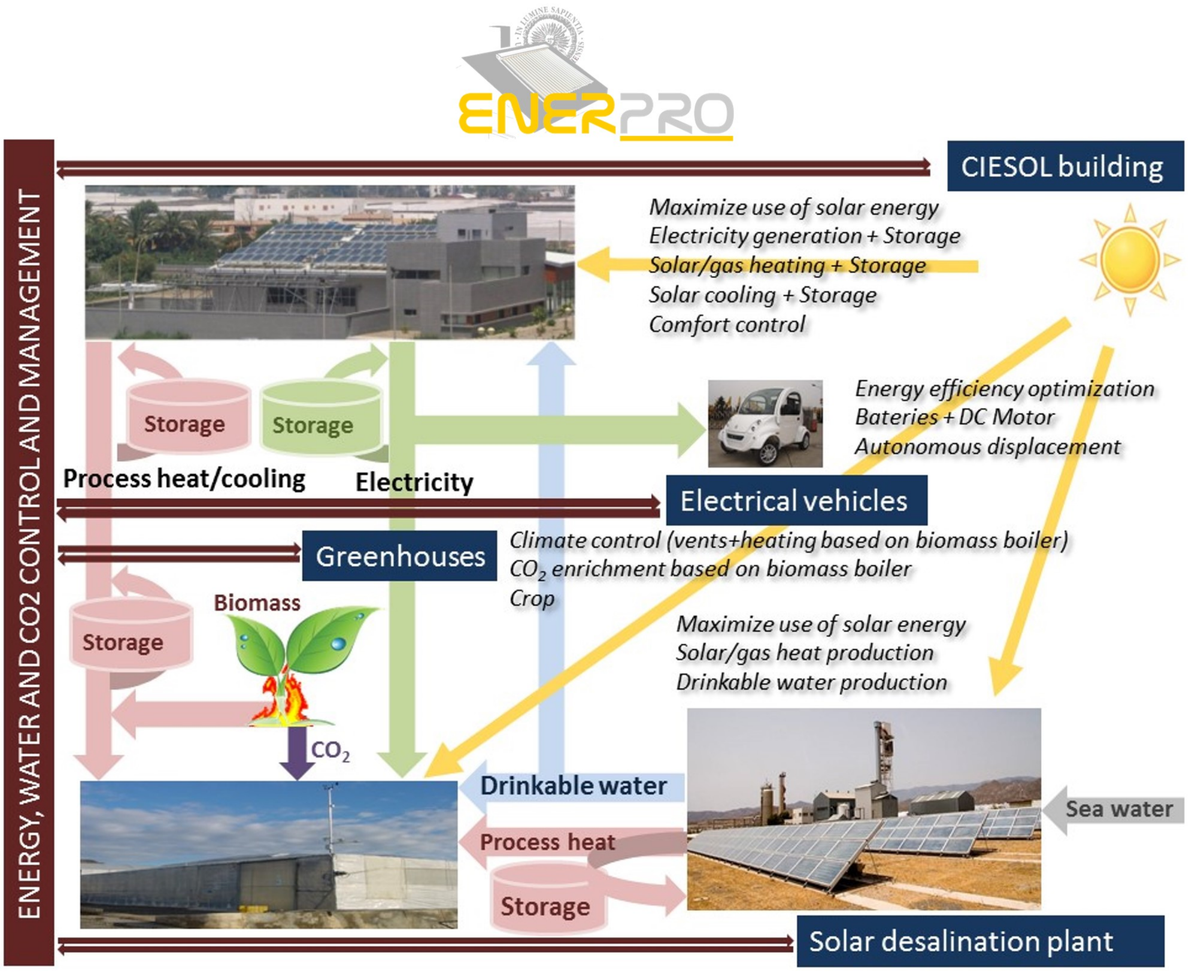

Figure 1.2. ENERPRO's research approach and functional diagram of the test-bed plant

By the time he joined the project, in 2016, there were some processes of the ENERPRO's test-bed plant (Figure 1.2) already characterised, so the initial efforts were put into integrating their models from a global perspective. As the idea was to align a realistic tuition programme with the project's objectives, the so-called "energy hubs" (EHs) were chosen as a paradigm of systems with similar necessities as ENERPRO's test-bed plant. The literature around that concept showed that it had been proposed to represent plants with different kind of resources (E1), that the resulting models were being employed in optimisation problems to schedule the production of energy, often by means of MPC (E2), and that the basic formulation, even if oversimplified at times, allows considering networks of EHs in a straightforward way (E3). The core contribution that helped to fulfil E1 and E2 arrived in 2018 [41], based on the rest of articles published by that time. After a one-year extension, the project ended in December 2018 but, in the same year, the PhD student was assigned to the CHROMAE project, devised for the furtherance of the same line of research (see the objectives below), but more focused on the agricultural sector and on larger systems, as the number of elements and interactions increased in comparison with ENERPRO's (see Figure 1.3) [42].

C1. Characterisation and modelling of the resource flows and inter-relations between the plants conforming the district, considering their consumption, production and storage under the approach of distributed multi-generation and multi-energy systems. The main aim is to develop a simulation environment involving the consumption and production of heterogeneous resources in agri-food districts (easy to extrapolate to other activities) which allows us to analyse concrete use cases, test new management approaches and take decision aimed at maximising their use.

C2. Development of new control strategies for the descriptive variables of plants comprising the district, so that their objectives may be accomplished optimising, at the same time, the use of the resources by means of model predictive control techniques.

C3. Development of high-level control and optimal integrated management strategies for those resources required to operate the plants inside an agro-industrial district using control techniques such as centralised and distributed model predictive control, optimal control and rule-based control, among other. All these techniques consider both economic and environmental criteria and their efficient use.

From 2018 to 2020, the formulation of the problem that considered ENERPRO's test-bed plant was accommodated for CHROMAE's district, in order to meet C1, C2 and C3 objectives. However, this was taken a step further by considering to perform analyses in networked EHs, which was formally posed in 2019 [43] (E3, C3), and by developing a tool in MATLAB® and Simulink® [44] that allows analysing concrete cases in a flexible and simple way (C1). On the other hand, the review initiated in 2016 became consolidated as an article that has been recently submitted and is under review [45].

Although ENERPRO and CHROMAE have been the main driving forces for the work accomplished during this thesis and the publications presented in Section 1.5, they have led his author to participate in two other parallel, but complementary, lines of research: one related to PV production (SUN4GREEN's research contract), where the models presented in Chapter 5 and their computer code were adapted to predict the energy yield by a set of experimental panels with reflectors located on the roof of a greenhouse; and the other to resource management in greenhouses (CARBON4GREEN research project), which involves part of the knowledge on modelling, control and optimisation gained during the postgraduate stage.

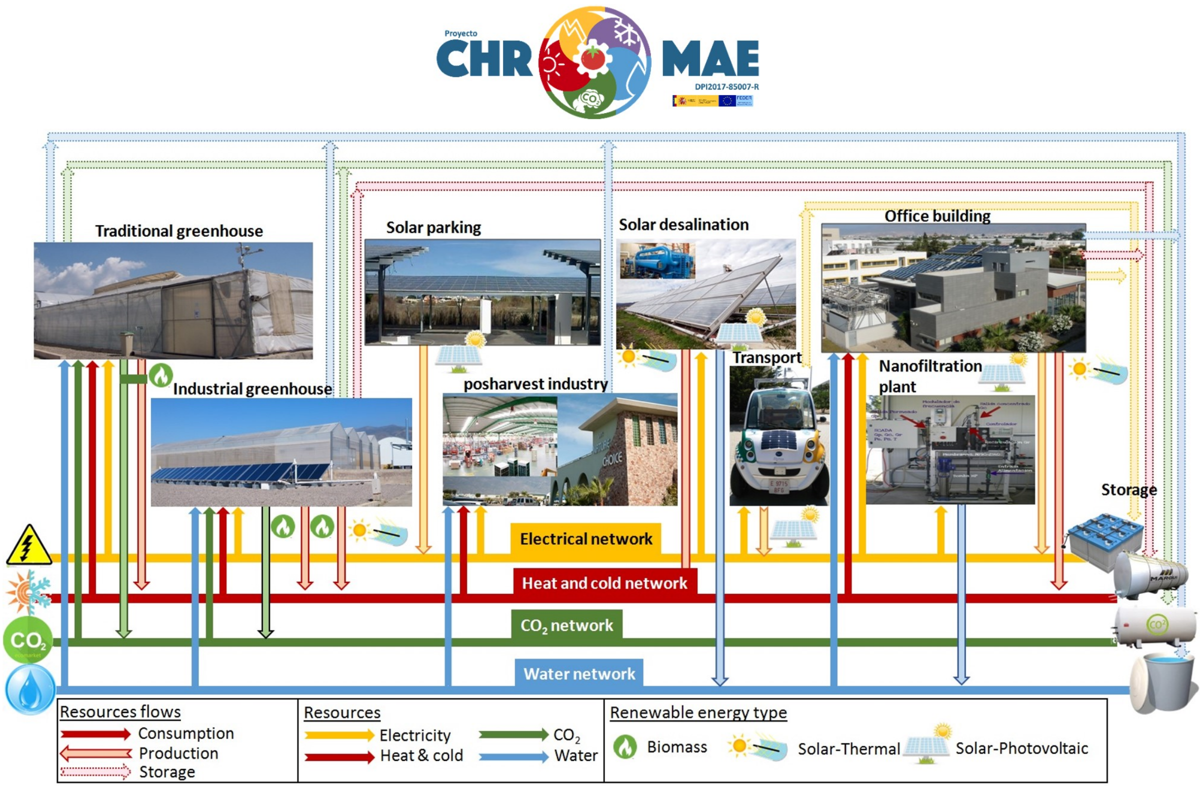

Figure 1.3. Flow of heterogeneous resources among the different elements of the CHROMAE's agro-industrial district

1.4 Main Contributions

Given the potential impact that the next developments could have in the energetic panorama, outlined in Section 1.1, the research plan arranged in accordance with them (Section 1.2), and the objectives of ENERPRO and CHROMAE projects (Section 1.3), the main contributions of this thesis, with respect to them, are constituted by three major breakthroughs in the field of EHs and MESs that merit attention for being the core development outcomes of this thesis.

- Formulation of a widely applicable generic modelling framework for representing EHs or MESs of diverse nature, complexity, time-scale and arbitrary topology; i.e. arrangements may contain any amount of energy carriers (inputs), loads (outputs), conversion devices (alternate operation or co-generation) and splits/combinations of resource flows. This was aimed at complementing previous models in order to include the possibility of representing more accurately certain processes, such as selling output resources and adding loads related to the operating state (on/off) of certain devices, and to reduce the number of decision variables for modelling complex EHs, which entails reducing the computation effort. Objectives related: O1, E1, E3, C1.
- A software library called Optimal Dispatch for Energy Hubs (ODEHubs), which stands for Optimal Dispatch for Energy Hubs. It is based on the proposed framework and has been devised to ease the implementation of control or dispatch problems considering the main drawbacks of possible alternative packages (see Subsection 2.1.4). It is composed by a set of MATLAB® and Simulink® files and freely available on Github (https://github.com/ual-arm/odehubs). The package can generate the constraints in MATLAB® code and obtain the optimal dispatch schedule for the deterministic mixed-integer linear problem that represents the defined system. Objectives related: O1, O3, O4, O5, E1, E2, C1, C3.

- Formalisation of the optimisation problem required to apply MPC-based or scheduling strategies for energy/resource management in EHs or MESs. Even though the objective function posed in Chapter 4 only considers economic aspects regarding the trade of resources, no restrictions are placed on the particular objective function, which could be selected according to other criteria (e.g. environmental issues or multi-objective optimisation). Objectives related: O4, E2, C3.

In addition, another three achievements are part of the practical knowledge contained in this thesis, which is more closely related to the cases of application of both projects.

- Testing the proposed approach's validity on several case studies. For the sake of conciseness, in this document only the most complex, but illustrative, modelling example is presented in Chapter 7, which includes multiple material and energetic resources, and unusual inputs (such as seawater and biomass), outputs (CO_2 enrichment for a greenhouse), and converters (a solar-powered desalination plant and an absorption chiller). To make the analysis more realistic, it was considered the legal framework for systems with self-consumption, and therefore operational scheduling is determined considering variations in the electricity price throughout the day. Objectives related: O3, O5, E3.
- Validation of a model for photovoltaic production based on the solar irradiance on sloped surfaces and the equivalent circuit for photovoltaic cells. It was characterised according to the parameters of the facilities involved in this thesis and its inputs are historical or forecast radiation data. Objectives related: O2, O3, E1.
- Combination, cleansing, and synchronisation of the databases of the facilities in order to identify consumption profiles for simulation purposes. Objectives related: O2, E1, C1.

Note that C2 was not attached to any of the above contributions because it is related to lower lever control, and out of the scope of this thesis. On the other hand, the use of robust control strategies and uncertainty analyses were partially tackled during the stay in Brazil, in relationship with O2 and O4 and with the development of predictors and estimators. In particular, the work centred on obtaining preliminary forecast models and adapting the formulation of the problem to include chance constraints according to the presence of uncertainty in solar radiation forecasts, which will be further discussed in Section 8.3.

1.5 Publications

The research work of this thesis is supported by the publications listed below, where the name of the PhD candidate and author of this thesis has been highlighted in bold font. At the date of submission of this document, the contributions consist of two papers published, and another one under review, in journals indexed in the Journal Citation Reports (JCR) database, four international conferences, and five national conferences, which will be cited in the closing summary of contributions of each chapter to point out their relevance. He also took part in three other local conferences, on the occasion of the Annual Meeting of the PhD Programme in Informatics of the University of Almeria, in which the progress of research work is periodically shared among the members of the Department of Informatics and the academic community.

1.5.1 Scientific Journals

J. Ramos-Teodoro, F. Rodríguez, M. Berenguel, and J. L. Torres, "Heterogeneous resource management in energy hubs with self-consumption: Contributions and application example," *Applied Energy*, vol. 229, pp. 537–550, 2018. Impact factor in 2018 (Journal Citation Reports (JCR)): 8.426. Journal Rank in Category in 2018 (JCR): 8/103 (Q1) in Energy & Fuels; 5/138 (Q1) in Engineering, Chemical. Reference: [41]

J. Ramos-Teodoro, A. Giménez-Miralles, F. Rodríguez, and M. Berenguel, "A flexible interactive tool for modelling and optimal dispatch of resources in agri-energy hubs," *Sustainability*, vol. 12, no. 21, pp. 8820–8844, 2020. Impact factor in 2019 (JCR): 2.576. Journal Rank in Category in 2019 (JCR): 26/41 (Q3) in Green & Sustainable Science & Technology; 120/265 (Q2) in Environmental Sciences. Reference: [44]

J. Ramos-Teodoro, F. Rodríguez, and M. Berenguel, "Cutting-edge approaches in control, management and design of distributed production systems: Microgrids, virtual power plants, energy hubs, and multi-energy systems," *IEEE Access*, **(submitted to the journal and under review)**. Impact factor in 2019 (JCR): 3.745. Journal Rank in Category in 2019 (JCR): 35/156 (Q1) in Computer Science, Information Systems; 61/266 (Q1) in Engineering, Electrical & Electronic; 26/90 (Q2) in Telecommunications. Reference: [45]

1.5.2 International Conferences

J. Ramos-Teodoro, F. Rodríguez, and M. Berenguel, "Modelling based on the energy hub paradigm of a greenhouse agricultural exploitation with support of renewable energies," in *Proceedings of the I Iberian Symposium on Horticultural Engineering*, Lugo, Spain, 2018. Reference: [46]

J. Ramos-Teodoro, F. Rodríguez, M. Castilla, and M. Berenguel, "Modelling production, consumption and storage of heterogeneous resources of an agro-industrial district with renewable energies," in *Proceedings of the X Iberian Congress on Agro-Engineering*, Huesca, Spain, 2019, (in Spanish). Reference: [43]

A. Giménez-Miralles, **J. Ramos-Teodoro**, F. Rodríguez, and M. Berenguel, "Case study of the ODEHubs tool for energetic and material resources management of a Mediterranean traditional greenhouse," in *Proceedings of the II Iberian Symposium on Horticultural Engineering*, Ponte de Lima, Portugal, 2020, (in Spanish). Reference: [47]

J. Ramos-Teodoro, M. Castilla, J. D. Álvarez, F. Rodríguez, and M. Berenguel, "Economic dispatch of a bioclimatic office building considering thermal energy, electricity and water demands," in *Proceedings of the 18th International Conference on Renewable Energies and Power Quality*, Granada, Spain, 2020. Reference: [48]

1.5.3 National Conferences

J. Ramos-Teodoro, J. D. Álvarez, F. Rodríguez, and M. Berenguel, "Economic management of energy hubs with heterogeneous resources through MINLP," in *Proceedings of the IV CEA Symposium on Modelling, Simulation and Optimisation*, Valladolid, Spain, 2018, (in Spanish). Reference: [49]

J. Ramos-Teodoro, F. Rodríguez, and M. Berenguel, "Photovoltaic facilities modelling for an energy hub management with heterogeneous resources," in *Proceedings of the XVI CEA Symposium on Control Engineering*, Almeria, Spain, 2018, (in Spanish). Reference: [50]

J. Ramos-Teodoro, F. Rodríguez, and M. Berenguel, "Comparative study of energy management in an agro-industrial plant with self-consumption," in *Proceedings of the I Congress for Young Researchers on Agri-Food Science*, Almeria, Spain, 2018, (in Spanish). Reference: [51]

F. Rodríguez, **J. Ramos-Teodoro**, M. Berenguel, and P. Lorenzo, "Economic management of the carbon enrichment in a tomato greenhouse with different sources of CO_2," in *Proceedings of the "Adding Value to CO_2" Congress (3rd edition)*, Madrid, Spain, 2019, (in Spanish). Reference: [52]

J. Ramos-Teodoro, A. Giménez-Miralles, F. Rodríguez, and M. Berenguel, "Simulation of scenarios of economic dispatch in multi-energy systems," in *Proceedings of the XVIII CEA Symposium on Control Engineering*, Murcia, Spain, 2020, (in Spanish). Reference: [53]

1.5.4 Local Conferences

J. Ramos-Teodoro, "Energy management strategies in production environments with support of solar energy," in *Proceedings of the I Annual Meeting of the PhD Programme in Informatics of the University of Almeria*, Almeria, Spain, 2018, (in Spanish). Reference: [54]

J. Ramos-Teodoro, "Heterogeneous resource management in energy hubs with self-consumption," in *Proceedings of the II Annual Meeting of the PhD Programme in Informatics of the University of Almeria*, Almeria, Spain, 2019, (in Spanish). Reference: [55]

J. Ramos-Teodoro, "Contributions to control and management of distributed production systems: State-of-the-art and development of a library for simulations," in *Proceedings of the III Annual Meeting of the PhD Programme in Informatics of the University of Almeria*, Almeria, Spain, 2020, (in Spanish). Reference: [56]

1.6 Other Research, Teaching and Educational Activities

Regarding the rest of milestones that evidence the acquisition of competencies needed for the world of research, there are two which have been key: one is the three-months stay (01/07/2018-30/09/2018) at the Department of Systems and Automation of the Federal University of Santa Catarina (Florianopolis, Brazil), within the Research Group on Renewable Energies led by Professor Julio Elías Normey Rico, which satisfies one of the requirements to receive the Acknowledgement of International PhD; the other corresponds to the three research projects and the research contract in which the doctoral student has collaborated (see the next subsection), as they provided a solid background in planning research. Another contribution that does not fit as publication per se but settled the course of this thesis at its early stage is the thesis that was presented by the candidate to obtain the Master's Degree in Industrial Engineering.

J. Ramos-Teodoro, "Energy management of a heterogeneous production system under the energy hub paradigm," Master's thesis, Department of Systems Engineering and Automation, University Carlos III of Madrid, Madrid, Spain, 2017, (in Spanish). Reference: [57]

As part of his tuition, the author of this thesis has also accepted several invitations to review works related to either the topics treated in this thesis or the area of knowledge of the PhD programme. In particular, such articles were submitted to congresses as the "22nd IEEE International Conference on Emerging Technologies and Factory Automation (ETFA)" and the "21st IFAC World Congress" and the following journals: Applied Energy, Journal of Green Engineering, International Journal of Robotics Research, Journal of Cleaner Production, and *Revista Iberoamericana de Automática e Informática Industrial*.

Attending to educational and teaching involvement, the PhD candidate has been engaged in five editions of the European Researchers' Night (from 2016 to 2020), one of the actions funded by the Marie Skłodowska-Curie programme; three of the European Robotics Week (from 2017 to 2019); five of the First Lego League (from 2016 to 2020); and several other activities under educational programmes of the University of Almeria. Meanwhile, in academia, he has participated in a Group of Innovation and Good Teaching Practices whose outcome consists in two scientific contributions, as summarised in Subsection 1.6.2, and he has been giving classes in the subjects listed below and acted as co-supervisor in two Bachelor's theses [58, 59].

- Computer Control, 221 hours, BEng Industrial Electronics Engineering.
- Industrial Automation, 59 hours, BEng Industrial Electronics Engineering.
- Itinerary of Automation, 30 hours, MEng Industrial Engineering.
- IoT Applications, 29 hours, MEng Technologies and Applications in Informatic Engineering.

1.6.1 Collaboration in Research Projects and Contracts

UAL18-TEP-A055-B, Optimisation of an Integral Heating and Carbon Enrichment System in Greenhouses (CARBON4GREEN). Council of Economy, Knowledge, Business and University of the Regional Government of Andalusia. Research project under the 2014-2020 Operational FEDER Programme of Andalusia. Chief/Principal Investigator: Jorge Antonio Sánchez Molina (University of Almeria). 01/10/2019–30/09/2021. 72 000 €.

DPI2017-85007-R, Control and Optimal Management of Heterogeneous Resources in Agroindustrial Production Districts Integrating Renewable Energies (CHROMAE). Spanish Ministry of Economy, Industry and Competitiveness. Research project under the National Programme for Research Aimed at the Challenges of Society. Chief/Principal Investigator: Francisco Rodríguez Díaz (University of Almeria). 01/01/2018–30/06/2021. 164 308,32 €. Reference: [42]

Counselling for the Development of Models for Designing Photovoltaic Greenhouses from External Conditions under the Framework of the Maximising Sunlight Resources for Cost, Energy and Yield Efficient Greenhouses (SUN4GREEN) European Project (Grant Agreement Nº. 756006). Research contract under the SUN4GREEN European Project. Sponsor: Rufepa Tecnoagro, S.L. Chief/Principal Investigator: Jorge Antonio Sánchez Molina (University of Almeria). 01/11/2018–31/10/2019. 96 709,25 €.

DPI2014-56364-C2-1-R, Control and Energy Management Strategies in Production Environments with Support of Renewable Energy (ENERPRO). Spanish Ministry of Economy and Competitiveness. Research project under the National Programme for Research Aimed at the Challenges of Society. Chief/Principal Investigator: Manuel Berenguel Soria (University of Almeria). 01/01/2015–31/12/2018. 176 297 €. Reference: [40]

1.6.2 Projects and Publications Related to Teaching and Education

19_20_1_27C, Development of a Low-Cost Hardware-in-the-Loop Prototype for Teaching Automation in Engineering Degrees. Call for Creating Groups of Innovation and Good Teaching Practices in the University of Almeria. Biennium 2019 and 2020. Chief/Principal Investigator: María del Mar Castilla Nieto (University of Almeria). 01/01/2015–31/12/2018. 1200 €.

M. Castilla, F. Rodríguez, J. D. Álvarez, J. G. Donaire, and **J. Ramos-Teodoro**, "Design of a prototype based on the hardware-in-the-loop paradigm for practical classes of automation in engineering degrees," in *2019 Teaching Innovation Meeting*, Almeria, Spain, 2019. Reference: [60]

M. Castilla, F. Rodríguez, J. D. Álvarez, J. G. Donaire, and **J. Ramos-Teodoro**, "A hardware-in-the-loop prototype to design benchmarks for automation and control education," in *Proceedings of the 21st IFAC World Congress*, Berlin, Germany, 2020. Reference: [61]

1.7 Outline of the Thesis

The remainder of this thesis is organised as follows: Chapter 2 provides a review on the subjects of interest for this thesis to readers, classifying a set of articles according to their methodologies and subject of study; in Chapter 3, the facilities of the ENERPRO and CHROMAE projects are introduced, with special attention to the parameters employed or assumed in the subsequent chapters; Chapter 4 presents the core elements of the proposed modelling framework, including the conversion and storage models and the formulation of the optimisation problem; Chapter 5 is devoted to demonstrate the validation of the PV production models in two of the facilities; the main characteristics of the software library developed during this thesis are described in Chapter 6; Chapter 7 contains the case study which illustrates how both the modelling framework and the library can be used to obtain the dispatch of resources of an agro-industrial cluster; and Chapter 8 draws the main conclusions of this work and some promising lines of research for the future.

2. Literature Review

Chapter Summary

In this chapter a review on the subjects of interest for this thesis is provided to readers. Sections 2.1–2.3 are devoted to analysing in detail a wide collection of articles which help to identify current scientific gaps and set the main technical and terminological background for the remaining chapters. On the other hand, Section 2.4 contains information about groups of research and ongoing projects related to this thesis, mainly at European level, and Section 2.5 adds supplementary information on some of the models usually employed for the estimation of the availability and consumption of resources, particularly solar radiation, energy, water and CO_2.

2.1 Production Systems and Energy Management

The term “production system" is often defined from the business viewpoint as “a collection of people, equipment, and procedures organised to perform the manufacturing operations of a company (or other organisation)" [62]. It is then a generic concept that encompasses from the physical facilities and their own layout to the material and human resources that support production operations. Although most of the terminology mentioned in this thesis originated within the energy context [63], not necessarily linked to business, one can talk about production systems if a laxer definition is considered thereof.

Certainly, manufacturing operations consists in transforming input material or energy resources into different output resources increasing its utility or quantifiable value in economic, physical, or other terms. As this transformation does not need to be accomplished by a company, the production activity can be contextualised in a diverse range of elements (country, neighbourhood, dwelling, building ...), in a way similar to what Mancarella proposed regarding MESs [16]. Then, a production system will hereafter refer to “any device or entity where material or energy resources are transformed". Based on analysis to date, publications filling gaps in the field of the energy management have introduced a variety of different concepts (e.g. MGs, VPPs, EHs, or MESs) to refer to distributed production system (DPS).

These articles share factors such as objectives, techniques, methodologies, tools... but most surveys treat these concepts separately, and therefore there is a lack of updated reviews including several of those approaches together. In this section, information from specific publications and from reviews on production systems is collected to present an updated comparison focused but not limited to the above-mentioned concepts. In particular, it is aimed at providing a global overview in terms of employed terminology, context, purpose, mathematical models, optimisation strategies, and tools (software and programming); as well as a series of articles classified from that perspective, whose analysis helps to identify their strengths and weaknesses.

There is extensive literature based on the previous definition of production system but the search has been mainly focused on the articles that mention in their title or keywords some of the terms of greater relevance, due to their growing tendency from 2000 to mid-2020, applicable to production systems. Figure 2.1 illustrates this in two graphs which show similar information, but use different scales to correctly appreciate the differences between the number of articles on MGs, in Figure 2.1a, and the others terms, in Figure 2.1b: MESs, EHs and VPPs. By scrutinising some of the bibliographic references given in the articles found in this way, some additional keywords, recapped at the end of Section 2.2, were extracted and then employed instead of the four original terms to encompass a wider variety of publications.

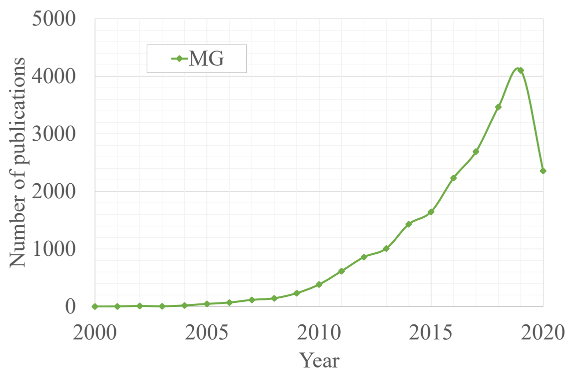

(a)

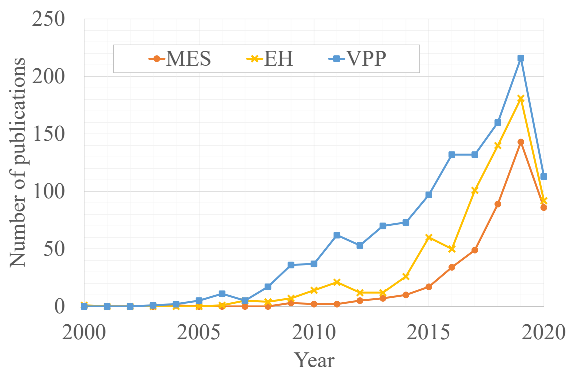

(b)

Figure 2.1. Published documents from 2000 to mid-2020 that include in their title or keywords the terms microgrid (MG), multi-energy system (MES), energy hub (EH), or virtual power plant (VPP). Source: Scopus database [64]

In order to elaborate on the reasons for selecting the features that, once analysed, would allow differentiating the articles' contributions, an introductory diagram that distinguishes them is presented in Figure 2.2. It also summarises the content of this section and includes the elements that will compose the headers of the tables, as well a non-exhaustive list of its attributes. All this information is complemented below, and the drawbacks of this classification will be further discussed in Chapter 8.

2.1.1 Context

Context may comprise a number of aspects large enough (i.e. technical, geographical, social, cultural, economic, legal...) to difficult a short description of the situation and status of a production system. Following a holistic approach, some authors refer to the "perspectives" (namely spatial, multi-fuel, multi-services, and network) of the multi-energy systems [16]. Other reviews include storage and conversion devices, and the kind of resources either as the main element of the analysis [27] or within an extensive survey [65].

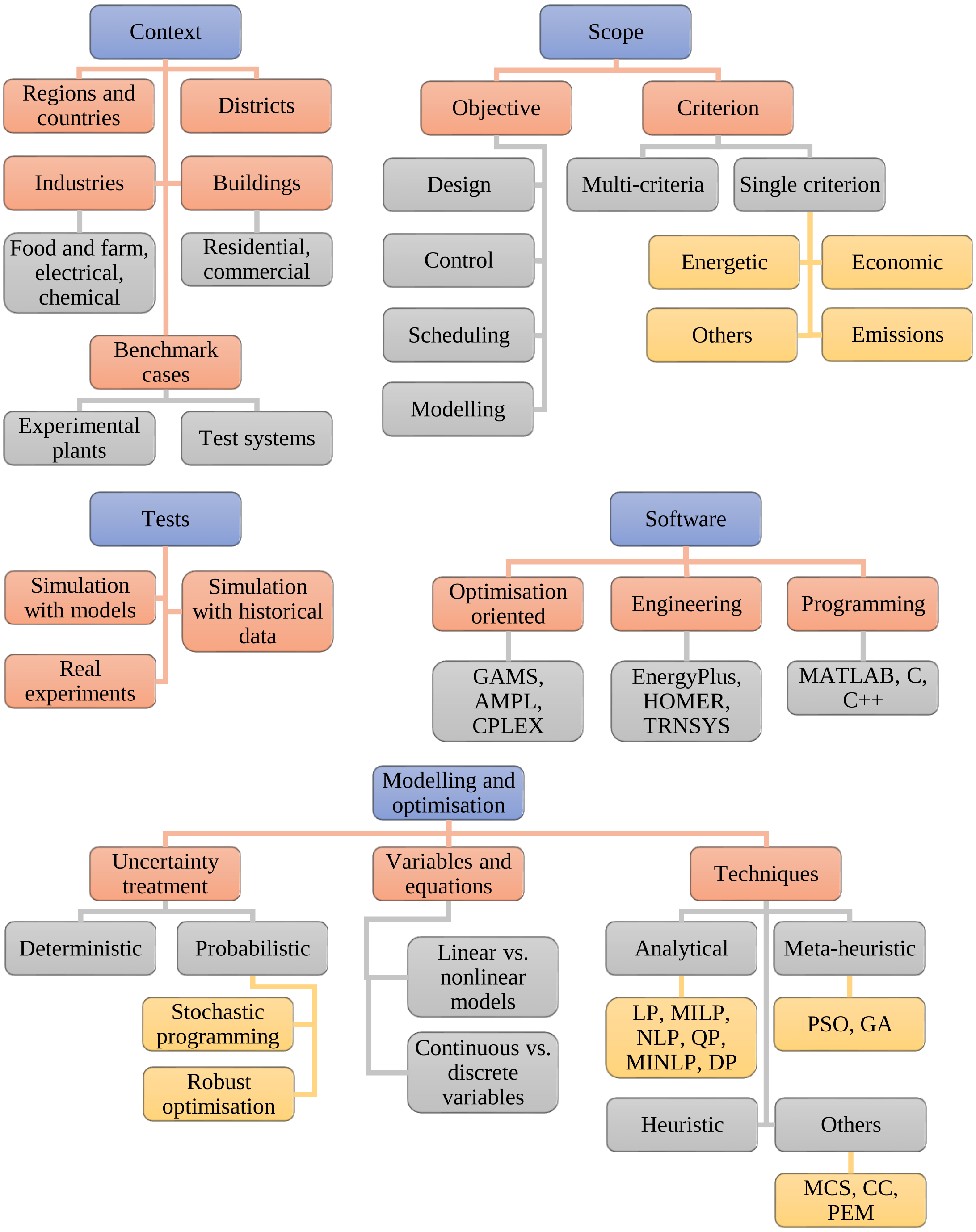

Figure 2.2. Classification diagram on DPS-related papers, according to the characterisation presented in Section 2.2. Acronyms in this figure are defined in the text and the list of abbreviations.

For the sake of uniformity and simplicity the activity sector, the location and/or the scale will be considered enough factors to help to contextualise each work. Attending to the first one, facilities can be industrial, commercial, residential, farming-related, to name a few examples, or even a group of several types. With regard to location, even if understood in geographical terms as a specific city or country, it may also give an idea of the social and economic panorama. Finally, the scale of the system embraces a diverse range of elements such as single devices, plants, districts, cities, regions, or countries. Although those three factors may not be explicitly mentioned in the context column of the following table—some articles deal, for example, with predefined test system without a defined location—the description given will provide a broad outlook of them, including (if possible) the location where the study was performed.

2.1.2 Scope

The following element of analysis, part of the scope, is the objective, distinguishing at least four possibilities which are sometimes closely related: design, scheduling, control, and modelling. The problem with which each work deals usually belongs to one of those categories whose relationships and conception will be explained in more detail as follows.

- Design. Determining the size and layout of the elements that compose a production system is a recurrent engineering problem usually addressed by using different levels of abstraction depending on the application. In practical terms, it includes both the devices (reactors, generators, boilers, turbines, ...) and the transmission systems. Expansion planning is one of the terms recently coined within the field of energy systems [66]. In respect of its relation to the other objectives, some of the analyses carried out, include the simulation of scenarios in which the operation of the system is scheduled, during a certain time interval, to obtain possible designs on which to choose the best alternative [67]. Needless to say that models are usually required for this purpose.
- Scheduling and control. Both concepts answer the question of how a production system should be operated over time, including, for example, the equipment operating point, maintenance tasks, or alarms management. In control engineering the control actions affecting the system may depend on the scheduling process carried out at a hierarchically higher level, to which many authors allude with the term real-time optimisation. This term is indistinctly used in either production management [68] or resources allocation during maintenance tasks [69]. On other occasions, a similar structure is referred to as "supervisory layer" [70]. Although the idiosyncrasies of scheduling and control could be more deeply discussed, the criterion taken here in order to differentiate both possibilities, when the authors do not explicit the objective, is whether their work deals with a closed-loop approach (control) or an open-loop one (scheduling).
- Modelling. Although models are also employed even in works whose objective is one of the above, in other situations the proposal is substantial enough to only present a detailed (and validated or justified) description of the system's behaviour. This usually concerns either conceptual models (such as control or communications architectures), which focus on illustrating the structure and interactions usually in a schematic way [71], or high-fidelity models, involving, for example, differential-algebraic equations and computational methods. In the second case, the resulting models are especially useful to perform simulations that help to understand the system's dynamics and to make decisions based on them (as exemplified in [67]).

In addition to the objective, another important fact to take into account is the criterion according to which the work is carried out or, simply put, the considerations that are made to choose between alternative designs, control actions, or plans. Although the economic criterion usually prevails over others, there are works that apply environmental criteria (such as carbon dioxide emissions generated by an activity [72]), the use of primary [73] or renewable [71] energy sources, or a mix of criteria [26]. These criteria may result from complex relationships as happens, for example, with economic analyses that distinguish between operation and maintenance costs and investment cost [74], but, for the sake of conciseness, only a brief description will be provided for each of the reviewed articles.

2.1.3 Modelling and Optimisation

Many authors employ mathematical models and present optimisation problems in their research, and therefore the ongoing formulations deserve special attention. Once the variables that allow characterising the system' operating conditions are chosen, both the objective function, which is usually defined from the scope (objective and criterion) of the study and the constraints that represent the system' behaviour, determine the kind of problem to solve. The Neos Server website [75–77] provides valuable information to non-experts about the taxonomy of optimisation, where four major facets are discussed: continuous versus discrete, constrained versus unconstrained, single-objective versus multi-objective, and deterministic versus stochastic. From those, only the first and the last ones deserve special attention because all the reviewed models contain constraints in order to suitably represent the reality and the objective function is determined by the criterion (as so defined above), which will be analysed for each work. In addition, linearity is another factor that researchers consider as it is directly related to the solving techniques, mainly distinguishing between linear problems and nonlinear problems. Also, readers should bear in mind from now on that problems are considered nonlinear if the models contain at least one nonlinear expression or equation, and non-continuous if they include at least one integer (discrete) variable.

On the one hand, according to Neos Server website [75–77], "some models only make sense if the variables take on values from a discrete set, often a subset of integers", which include, for instance, binary variables for reproducing on/off states in some devices. When problems include at least one integer variable, they become discrete optimisation problems that tend to be harder to solve than continuous optimisation problems. On the other, as models constitute a simplification of the reality, according to the treatment of the variables subject to uncertainty, they are mainly divided into deterministic or probabilistic problems. The classification considered here can be complemented by the one found in the reference [78], which covers the most common sources of uncertainty as well, whose analysis is beyond the scope of this thesis.

- Deterministic optimisation. There exist problems that never contain random variables, that is to say, an exact knowledge of the production system is assumed, and the value of the cost function exclusively depends on the value of the decision variables. Three main approaches can be employed for solving these problems: analytical techniques such as linear programming (LP), linear quadratic programming (LQP), quadratic programming (QP), second-order cone programming (SOCP) nonlinear programming (NLP), mixed-integer linear programming (MILP), mixed-integer quadratic programming (MIQP), mixed-integer quadratically constrained quadratic programming (MIQCQP), mixed-integer nonlinear programming (MINLP), or dynamic programming (DP); heuristic techniques, based on practical rules for each specific problem; and metaheuristics that use generalist rules in order to arrive at a solution as close to optimal, for example, genetic algorithms (GAs) or particle swarm optimisation (PSO). Note that as metaheuristics generate random points while trying to converge to a usually sub-optimal solution, the use of these algorithms is sometimes referred to as "stochastic optimisation" [79], but a different definition is considered in this thesis, as given below.
- Probabilistic or stochastic optimisation. Other kinds of problems contain random variables that can be expressed through a probability density function: in other words, a random component or uncertainty on the knowledge of the production system is assumed and the value of the cost function varies regardless of the value of the decision variables. Two main branches of problems are distinguished, stochastic programming (SP), if the uncertainty is characterised through probability density functions, and robust optimisation (RO), when the only information considered are the bounds within which certain parameter is contained. This implies a greater complexity and is the main reason why many techniques from deterministic

optimisation are adapted for the stochastic problem (some authors add a “P" at the beginning of the above-mentioned acronyms [80]). Other widespread techniques useful to deal with uncertainty are Markov decision processes (MDP) modelling, Monte Carlo simulations (MCS), conditional value at risk (CVaR) analysis, which can be done, at the same time, through Monte Carlo simulations (MCS) [81], point estimate method (PEM) [80] and reformulating the problem into chance constraints (CC) [70].

2.1.4 Tests and Software

One of the two last aspects to consider is the type of test performed attending to both the environment where the experiments are performed (simulators or real devices) and the origin of the data employed in the case of simulations, which usually come from standard datasets or models (provided by other entities, researchers...), hypothetical statements (e.g. some climatic variables are considered constant), or from historical measurements within the facilities.

Furthermore, these analyses are addressed by using multifarious tools that include programming environments and engineering software. In the first case, tools such as CPLEX [82], GAMS [83] or AMPL [84], use their own programming languages aimed at defining the optimisation problem in a straightforward way; whereas other such as MATLAB® [85], consist in an interpreted language widely used in technical computing for different purposes. In both cases and depending on the type of problem treated, different optimisation algorithms can be employed (e.g. Gurobi [86] or BARON [87]), either because they are incorporated within each tool or by integrating external resolution algorithms from other developers. Also, MATLAB® is often combined with YALMIP [88] or TOMLAB [89] because the way optimisation problems are defined with these toolboxes is similar to other optimisation-oriented tools’ such as GAMS or AMPL. Regarding engineering or specific software, they either tend to integrate all of the above in a more or less opaque manner to users in tools for modelling, operating or planning MESs [16] such as DER-CAM [90], eTransport [91], HOMER [92], or EnergyPlus [93], to name a few.

Another package that merits attention when it comes to object-oriented programming is Modelica, which counts for example with a library for the control of building energy systems [94]. Note that the following section may include programs that have not been enumerated in this one because they are mentioned in just one of the reviewed papers. In order to have a more complete vision, readers are referred to a couple of reviews on district-scale [95] and urban [96] energy systems, where the spotlight is mainly on consolidated and specific engineering software for design and analysis; and another two focused on broader contexts [97, 98] which comprise less mature applications relying on general-purpose programming environments or languages, such as the above-mentioned CPLEX [82], GAMS [83], and AMPL [84], but also AIMMS [99], MATLAB® [85], R [100] and Python [101].

To the author’s knowledge, MATLAB® is extensively employed in this field of research, both as a standalone version and combined with other optimisation-assisted modelling tools. It happens to be one of the more common programming languages as well, together with Python and GAMS [97], but despite its potential, to date, very few specific tools for dealing with the most common problems in EHs have been developed and made freely available. As introduced in Section 1.3, one the objectives of the CHROMAE project was to build a simulation environment which has eventually materialised in form of the tool described in Chapter 6. It was developed in MATLAB® after assessing the current alternatives that make use of this language, which are outlined below.

1. Ehub Modeling Tool [102]. It consists of a set of MATLAB® scripts for creating input case study data, which are sent and then executed in the optimisation package AIMMS. It also incorporates R code for visualising the results of the simulations. A subsequent version was released in Python, including a graph-based modelling tool. Software available at `https://github.com/hues-platform/ehub-modeling-tool`.
2. EHCM Toolbox [103]. An object-oriented programming tool that was conceived to deal with the control necessities of a building and entirely in MATLAB®. Consequently, it might lack flexibility in certain aspects, which is counterbalanced by a sophisticated model for batteries and the possibility to integrate detailed building dynamics from another toolbox. Software available at `https://control.ee.ethz.ch/software/BRCM-Toolbox1.html`.
3. MATPOWER Optimal Scheduling Tool (MOST) [104]. It is an extension of the MATPOWER package, a free and open-source set of MATLAB® files for solving steady-state electric power scheduling problems. MOST can be used to solve from simple deterministic unconstrained problems to stochastic, security-constrained, combined unit-commitment and, multi-period optimal power flow problems. The current implementation is limited to DC power flow modelling of the network, so it is a bit limited when it comes to MESs and EHs. Software available at `https://github.com/MATPOWER/most`.
4. IMAKUS [105]. This is the name given to a deterministic model of the German power system aimed at making investment decisions on storage and conventional generation assets. Although it was implemented in MATLAB® code using a generic formulation, its authors do not clarify its possible use on other regions or with other resources than electricity. No support website.
5. LUSYM [106]. A tool quite similar to MOST in the sense that it is focused on the electricity sector and allows introducing nearly the same constraints in the problem. The main difference resides in the use of GAMS together with MATLAB®, which are interfaced so that GAMS is used for solving the optimisation problem and MATLAB® for processing the input and output data. No support website.
6. EUPowerDispatch [107]. Another tool for the optimal dispatch of the power system, but particularised at European level, and it uses GAMS and MATLAB® in the same way that LUSYM does. More information available at `https://ses.jrc.ec.europa.eu/eupowerdispatch-model`.
7. Software Library for MESs (no official name yet) [32]. Probably, the most flexible and complete of the alternatives, based on object-oriented programming, and derived from the generalised modelling framework for MESs proposed by Long [32]. It is intended to be used for MPC applications rather than scheduling problems. The same version was built both in Python and MATLAB®, although none of them is freely available. No support website.

All these tools have helped in one way or another to establish the basis from which developers can keep providing new algorithms and procedures to the field of energy and resource management. Nonetheless, there is still room for improvement in certain aspects that the researchers might demand: less experienced users might struggle with coding and there exists no graph-based modelling tool for MATLAB® environment that allows one to formulate and solve resource dispatch problems, four out of the seven packages are focused on purely electric systems (3, 4, 5, 6), only three are freely available online and properly documented (1, 2, 3), and some of them require third-party software that is subject to a license (1, 5, 6). These drawbacks are overcome in the software resulting from this thesis, as detailed in Chapter 6.

2.2 Classification and Analysis

In order to arrange the information of interest for this thesis, the seventy publications that have been analysed to extract the features stated in the previous section are compiled in Tables 2.1–2.5. Note that the main keyword employed during search appears in the caption of each table (MGs, VPPs, EHs, and MESs), although some of the articles may be related to more than one term. In particular, there are sixty articles related to them (fifteen each) and ten articles sorted into the "other terms" denomination.

2.2.1 Smart Grid and Microgrids

Among the terms applicable to DPS, the microgrid concept [108] arose in order to integrate the distributed generation of energy and the planning and operation of the electric grid [109]. MGs can be defined as low and medium voltage distribution grids where different energy resources need to be managed in coordinated or isolated mode. They constitute one of the main elements of the future smart grid [30], whose decentralisation and coordinated management would enhance the traditional operational approach. Readers are referred to the following reviews on this topic for more information: the first one is related to control and management strategies [110], the second also tackles modelling and planning together with such strategies [111] and a third one which analyses markets, architectures and technologies within transactive energy systems [112].

Although they emerged within the electrical energy field, their use has been extended to systems that combine different types of energy such as cogeneration [113] or trigeneration [90] and therefore they have become relevant MESs. There are also examples of MGs that employ material resources such as biomass [70], drinking water [114] or hydrogen [115, 116]. The scope of application is quite broad as well: commercial buildings [90], residential urban [117] and rural areas [118], agri-food industries [71], a mixture of these ones [119]. Other fields of special interest include the management of MGs during grid-connected and islanded modes [120, 121], and the integration of electric vehicles through MPC [122], rule-based control [123] or scheduling strategies that consider uncertainty [124]. Table 2.1 compiles fifteen articles, cataloguing their characteristics.

Table 2.1. Classification of the reviewed literature on microgrids (MGs)

Ref.	Context	Scope	Test	Modelling and optimisation	Software
[70]	Sugar cane industry (Brazil)	Control (MPC) Energetic criterion	Simulation with historical demand and weather	Probabilistic, CC, QP	MATLAB® YALMIP CPLEX
[71]	Agro-industry (Piedmont, Italy)	Scheduling Energetic and RES usage multi-criteria	Real experiments	Deterministic, MILP + conceptual model	Own software
[90]	Commercial buildings (San Francisco, US)	Design (yearly scheduling) Economic criterion	Simulation with hotel model and historical price	Deterministic, MILP	DER-CAM (GAMS + CPLEX)
[113]	Community MG (Lesotho)	Design (yearly scheduling) Economic criterion	Simulation with demand model	Deterministic, nonlinear, PSO	μ-Grid [125]
[114]	Remote areas (Aegean Sea, Greece)	Design (yearly scheduling) Economic criterion	Simulation with models	Probabilistic, MINLP, PSO, MCS	GenOpt TRNOPT TRNSYS

Table 2.1. (Continued). Classification of the reviewed literature on microgrids (MGs)

Ref.	Context	Scope	Test	Modelling and optimisation	Software
[115]	Experimental MG (Seville, Spain)	Control (MPC) Energetic criterion	Real experiments	Deterministic vs. probabilistic scenarios	MATLAB® GAMS
[116]	System based on a experimental MG (Seville, Spain)	Control (MPC) Economic and energetic multi-criteria	Simulation with historical demand and weather	Deterministic, QP, MIQP	Not mentioned
[117]	Residential buildings (unlocated)	Control (MPC) vs. scheduling Economic criterion	Simulation with historical demand and weather	Deterministic, MILP	MATLAB® YALMIP CPLEX
[118]	Village and commercial building (India)	Design (yearly scheduling) Economic criterion	Simulation with historical demand and weather	Deterministic	HOMER
[119]	Threee different agents (unlocated)	Daily scheduling Economic and reliability multi-criteria	Simulation with models	Deterministic vs. probabilistic, PSO	Not mentioned
[120]	Five different agents (unlocated)	Daily scheduling Economic criterion	Simulation with models	Deterministic	MATLAB®
[121]	Six distributed generation units (unlocated)	Control Energetic criterion	Simulation with models	Probabilistic, linear, robust control	MATLAB® YALMIP
[122]	MG with external agents (unlocated)	Control (MPC) Economic criterion	Simulation with historical weather	Deterministic, MIQCQP, stepwise linearised	TOMLAB MATLAB® CPLEX
[123]	Experimental MG (Almeria, Spain)	Control Energetic criterion	Simulation with historical demand and weather	Deterministic, linear, heuristic rules	MATLAB®
[124]	IEEE 33-bus test system (unlocated)	Scheduling Economic criterion	Simulation with models	Probabilistic, MINLP, PEM	Not mentioned

2.2.2 Virtual Power Plants

Similarly, virtual power plants [126] originated because of the need of managing electrical systems constituted by a delimited cluster of producers and consumers interacting together that emulate the behaviour of a single generation plant (hence the “virtual" adjective is added, since it is not a plant by itself). It is possible to find reviews on their integration into the electrical system [127] and the treatment of uncertainties in modelling [128].

So far, just a few studies have included resources in VPPs other than purely electric generation, cogeneration or trigeneration [16]. Even so, some recent works include thermal [80, 129] or natural gas [130] supply networks or contribute with formulating short-term [131, 132] and medium-term strategies to schedule the distribution of energy [133] or maintenance tasks [134], and proposing management architectures [135]. Others merit attention for considering a novel adaptative robust optimisation problem for electricity markets solved through a column-and-constraint generation algorithm (CCGA) [136], using bi-level planning approaches [137–139], establishing a system-theoretic foundation to realise the vision of distribution-level VPPs [140], and mitigating cyber-attack effects through a robust dispatch [141]. Table 2.2 compiles fifteen articles, cataloguing their characteristics.

Table 2.2. Classification of the reviewed literature on virtual power plants (VPPs)

Ref.	Context	Scope	Test	Modelling and optimisation	Software
[80]	VPP with four zones + thermal energy (Canada)	Daily scheduling Economic criterion	Simulation with historical demand and weather	Probabilistic, MILP, PEM	GAMS CPLEX
[129]	IEEE 13-bus test system (unlocated)	Daily scheduling Economic and risk multi-criteria	Simulation with historical demand, weather and prices	Probabilistic vs deterministic, MILP, CVaR	Gurobi
[130]	VPP with nine nodes + gas (China)	Daily scheduling Economic and risk multi-criteria	Simulation with historical demand and weather	Probabilistic, RO, CC, MILP, CVaR	GAMS CPLEX
[131]	VPP with batteries (Iberian electricity market)	Daily and intraday scheduling Economic criterion	Simulation with historical demand, production and prices	Probabilistic, MILP	AMPL CPLEX
[132]	VPP operating within the electricity market (Spain)	Daily and intraday scheduling Economic criterion	Simulation with historical prices and production	Probabilistic, DP, MDP, CVaR	MATLAB® QUASAR Own software
[133]	VPP (Šibenik County, Croatia)	Weekly scheduling Economic criterion	Simulation with historical prices and models	Deterministic, MILP, uncertain scenarios	GAMS CPLEX
[134]	IEEE 6-bus and 18-bus test systems (unlocated)	Maintenance scheduling Economic criterion	Simulation with models	Deterministic, MINLP, uncertain scenarios, CVaR	GAMS
[135]	VPP (unlocated)	Scheduling Economic and comfort multi-criteria	Conceptual model (no tests)	Deterministic, MILP	CPLEX or Gurobi suggested
[136]	VPP (Spain)	Daily scheduling Economic criterion	Simulation with historical prices and models	Probabilistic, adaptative RO, CCGA	GAMS CPLEX
[137]	Commercial or residential VPPs with 2100 HVACs (unlocated)	Daily scheduling Economic criterion	Simulation with models	Deterministic, bi-level MIQCQP (MILP + NLP)	TOMLAB MATLAB® CPLEX SNOPT
[138]	IEEE 9-bus test system (unlocated)	Daily and intraday scheduling Economic criterion	Simulation with models	Deterministic, QP	Not mentioned
[139]	CIGRE medium voltage European benchmark distribution network (Germany)	Daily and intraday scheduling Economic criterion	Simulation with historical production and demand	Probabilistic (daily) and deterministic (intraday)	MATLAB® Gurobi MAT-POWER
[140]	IEEE 37-bus test system and residen-tial/comercial VPPs (Anatolia, California, US)	Control (MPC) Energetic criterion	Simulation with historical weather and demand	Deterministic, QP	Not mentioned
[141]	IEEE 123-bus test system (unlocated)	Control (MPC) Economic criterion	Simulation with models	Deterministic vs. probabilistic	MATLAB®

Table 2.2. (Continued). Classification of the reviewed literature on virtual power plants (VPPs)

Ref.	Context	Scope	Test	Modelling and optimisation	Software
[142]	VPP with electric vehicles (unlocated)	Daily scheduling Economic and risk multi-criteria	Simulation with historical prices, production and vehicles	Deterministic and probabilistic, LP, MCS, CVaR	Not mentioned

2.2.3 Energy Hubs

The energy hub concept [17] was probably the first approach capable of dealing with different energy vectors, that is, energy flows and material resources. Their authors [18] define it as "the interface between producers, consumers and transport infrastructure, which from the point of view of a system provides the relationship between the inputs, outputs, conversion and storage of different energy vectors". Recently, an extensive survey [65] and a comprehensive review [143] have been published on this topic. Other articles have been published with the aim of analysing a bit more specific aspects on EHs, such as the type of conversion elements and resources [27], or optimal scheduling in presence of uncertainty [78].

As this approach was not initially circumscribed to electric systems, it has been used in a wide variety of contexts, such as the energy analysis [144] and design [67] of buildings, designing [145] or resizing [72] the district level supply systems or energy management in greenhouses [73], residential districts [146], countries [147] or interconnected EHs [148]. With regard to the main advances, there are different formulations that seek to improve the ability to represent real systems, for example, using stepwise functions to deal with nonlinear models [20], including demand response programs [149] considering the effect of valves opening in turbine efficiency curves [25], or reducing the number of required variables to define the problem [41]. Some authors have even proposed hybrid approaches between MGs and EHs [150] and there are also examples of robust optimisation [19] and heuristic strategies [151]. Table 2.3 compiles fifteen articles, cataloguing their characteristics.

Table 2.3. Classification of the reviewed literature on energy hubs (EHs)

Ref.	Context	Scope	Test	Modelling and optimisation	Software
[67]	Buildings (London, UK)	Design (yearly scheduling) Economic and CO_2 emissions multi-criteria	Simulation with models and historical weather	Deterministic, bi-level GA + MILP	EnergyPlus AIMMS MATLAB® CPLEX NSGA-II
[72]	Districts, village with twenty-nine buildings (Zernez, Switzerland)	Design (yearly scheduling) CO_2 emissions criterion	Simulation with models and historical weather	Deterministic, LP	EnergyPlus MATLAB® CPLEX
[73]	Greenhouses (Ontario, Canada)	Daily scheduling Criteria comparison	Simulation with historical demands, price and weather	Deterministic, MILP + uncert. analysis (MCS)	AMPL CPLEX
[144]	Dwellings (unlocated)	Daily scheduling Criteria comparison	Simulation with models	Deterministic, MILP	GAMS CPLEX

Table 2.3. (Continued). Classification of the reviewed literature on energy hubs (EHs)

Ref.	Context	Scope	Test	Modelling and optimisation	Software
[145]	Administrative center, district (Beijing, China)	Design (Seasonal daily scheduling) Economic criterion	Simulation with historical weather and prices	Deterministic, MILP	CPLEX Gurobi YALMIP
[146]	Fifty residential buildings (US)	Daily scheduling Economic criterion	Simulation with historical weather and demands	Deterministic, NLP, consensus optimisation	Not mentioned
[147]	Country (China)	Design (yearly scheduling) Economic criterion	Simulation with historical demands	Deterministic, linear, heuristic rules	EnergyPLAN
[148]	IEEE 33-bus test system with four EHs (unlocated)	Daily scheduling Economic criterion	Simulation with models	Deterministic, MILP	GAMS CPLEX
[20]	Office building (Zurich, Switzerland)	Weekly scheduling CO_2 emissions criterion	Simulation with models and historical weather	Deterministic, LP vs. MILP	EnergyPlus MATLAB® CPLEX
[149]	Three theoretical EHs (one in Waterloo, Canada)	Daily scheduling Economic criterion	Simulation with historical demands and prices	Deterministic vs probabilistic, PEM, MCS, MINLP	GAMS SBB/CONOPT
[25]	Multiple theoretical EHs (unlocated)	Scheduling Criteria comparison	Simulation with models	Deterministic, nonlinear, MINLP, PSO, GA and others	MATLAB®
[41]	Experimental industrial cluster (Almeria, Spain)	Control (MPC) Economic criterion	Simulation with historical demands, price and weather	Deterministic, MILP	MATLAB®
[150]	Sugar cane industry (Brazil)	Control (MPC) Energetic criterion	Simulation with historical weather	Deterministic, bi-level MIQP	MATLAB® YALMIP CPLEX
[19]	Theoretical EH (Waterloo, Canada)	Daily scheduling Economic criterion	Simulation with models	Probabilistic, RO	CPLEX
[151]	Set of buildings (IMP Campus, Belgrade, Serbia)	Daily scheduling Economic criterion	Simulation with historical demands, price and weather	Deterministic, LP	MATLAB® CPLEX

2.2.4 Multi-Energy Systems

The denomination multi-energy system aroused, from a generic perspective, in order to encompass all the methodologies related to energy carriers' management, including the above-mentioned approaches: MGs, VPPs and EHs. Mancarella offers an extensive discussion about the characteristics of MES [16] and other authors [96] agree that it is the “extension of the smart grid, beyond electric power", that is, including other resources of the energy sector. It has been anticipated that this concept could be applied at different scales and integrate small systems into larger systems, which means modelling from homes to regions or countries, including intermediate geographical levels such as buildings, industries, districts or cities. Based on Mancarella's concept, reviews on MESs modelling [152], necessary infrastructure [153] and useful tools [96] have recently been carried out. Among the issues addressed in publications where MESs are expressly mentioned, there are some remarkable contributions regarding their modelling: a flexible framework that allows including bidirectional flows [38], Sankey diagrams have been proposed as well as suitable alternative [154], and, in more specific contexts, some works have dealt with the techno-economic analysis of a biofuel-based MES [155] or the British system in future scenarios [156, 157]. Moreover, there has been some research on the design of MESs in buildings [158] and districts [159], as well as other systems including storage devices [26], active distribution networks [160] and coordinated expansion planning [161]. With respect to the operation strategies, robust optimisation has been employed to obtain the optimal flows in smart districts [162, 163], and also deterministic models in district heating networks [164], regional energy systems [165], and commercial buildings [166]. Table 2.4 compiles fifteen articles, cataloguing their characteristics.

Table 2.4. Classification of the reviewed literature on multi-energy systems (MESs)

Ref.	Context	Scope	Test	Modelling and optimisation	Software
[26]	Residential district (Zurich, Switzerland)	Design (yearly scheduling) Economic and CO_2 emissions multi-criteria	Simulation with historical demands, price and weather	Deterministic, MILP	CPLEX
[38]	Set of three buildings (UoM Campus, UK)	Control (MPC) Economic criterion	Simulation with historical demands	Deterministic, MIQP	CPLEX
[154]	District (UoM Campus, UK)	Modelling and analysis	Simulation with historical prices and demands	Deterministic (no optimisation)	MATLAB® + Excel
[155]	Polygeneration system (unlocated)	Modelling, energetic and economic analysis	Simulation with models	Deterministic (no optimisation)	Aspen Plus
[156] [157]	Country (Great Britain)	Modelling and design Economic criterion	Simulation with models and historical data	Deterministic, nonlinear	EnergyPlus MATLAB®
[158]	Buildings (Turin, Italy)	Design (seasonal values) Criteria comparison	Simulation with models	Deterministic, LP	EnergyPlus GRG2 algorithm
[159]	Administrative center, district (Beijing, China)	Design (seasonal daily scheduling) Economic criterion	Simulation with historical weather and prices	Deterministic, MILP	CPLEX YALMIP MATLAB®
[160]	IEEE 33-bus and 23-node gas systems + eights EHs (unlocated)	Design (yearly scheduling) Economic criterion	Simulation with historical production and demand	Probabilistic, MINLP, SOCP	CPLEX
[161]	14-bus MES (unlocated)	Design (yearly values) Economic criterion	Simulation with models	Deterministic, MILP, Benders decomposition	Not mentioned
[162]	District with twenty-six buildings (Manchester, UK)	Daily scheduling Economic criterion	Simulation with historical demands	Probabilistic, MILP + RO (two stages)	MATLAB® Own software
[163]	Fifty residential buildings, district (England, UK)	Daily scheduling Economic criterion	Simulation with historical weather and prices	Probabilistic, MILP	Not mentioned

Table 2.4. (Continued). Classification of the reviewed literature on multi-energy systems (MESs)

Ref.	Context	Scope	Test	Modelling and optimisation	Software
[164]	District heating network (Changchun, China)	Daily scheduling Economic criterion	Simulation with models	Deterministic, MILP	MATLAB® YALMIP CPLEX
[165]	Multiple district networks (unlocated)	Daily scheduling Economic and environmental multi-criteria	Simulation with models	Deterministic, MINLP, solvers comparison	CPLEX
[166]	Commercial building (Wuhan, China)	Control (MPC) Economic criterion	Simulation with historical weather and demands	Deterministic, MILP and MINLP, GA, PSO	Gurobi

2.2.5 Other Terms

In addition to the four main approaches discussed here, other terms appear—sometimes accompanying the previous ones—in publications whose research topic and scope are related to the kind of problems analysed so far.

An example of this are the so-called cyber-physical systems (CPSs), a new concept that integrates many ideas of control and automation engineering, computing techniques, and information and communication technologies. Most of the scientific contributions are focused on proposing conceptual models, control and communications architectures, or cybersecurity and computational techniques (blockchain, big data ...), but there are others on production systems, such as the electricity grid [167], which are by definition CPS when interacting with computer control components and communication networks. In particular, there are examples of controlling the thermal supply in residential networks [168] or integrating energy management in industry [169].

Furthermore, the terms energy dispatch [170], economic dispatch [25, 171], optimal dispatch [172], and resource allocation [173] are employed for applications similar to those of MESs and EHs, and there are even articles in which none of the above terms is expressly mentioned including energy management in houses [74], distribution networks [174], and controlling coupled plants via practical nonlinear model predictive control (PNMPC) [175]. The eTransport model is another example which, according to their authors [91], has been developed "around case studies submitted by the industrial sponsors", long before MGs, VPPs, EHs, MESs started to grow in popularity. Only one of those is presented in Table 2.5, which compiles ten articles, cataloguing their characteristics.

Table 2.5. Classification of the reviewed literature including other terms related to DPS

Ref.	Context	Scope	Test	Modelling and optimisation	Software
[74]	Off-grid house (Hesarak, Tehran, Iran)	Design (yearly scheduling) Economic and reliability multi-criteria	Simulation with historical demand	Deterministic	HOMER MATLAB®

Table 2.5. (Continued). Classification of the reviewed literature including other terms related to DPS

Ref.	Context	Scope	Test	Modelling and optimisation	Software
[91]	Residential areas (Norway)	Scheduling (exp. planning) Economic criterion (emissions penalty)	Simulation with historical prices	Deterministic, MILP, DP	eTransport (C++ + COIN + MS Access + MS Visio)
[168]	Residential areas (unlocated)	Control and scheduling Economic criterion	Simulation with models	Deterministic, heuristic rules, MILP	Not mentioned
[169]	Battery manufacturing plant (unlocated)	Control (MPC) Economic criterion	Simulation with historical demand and prices	Deterministic, MINLP	Not mentioned
[170]	Regions, IEEE and PEGASE test systems (Europe)	Control or scheduling Economic criterion	Simulation with models	Deterministic, SOCP, Benders decomposition	GAMS MOSEK MATLAB®
[171]	IEEE 6-bus and 118-bus test systems (unlocated)	Daily scheduling Economic criterion	Simulation with models	Probabilistic, MINLP, CC	CPLEX
[172]	District heating network (unlocated)	Daily scheduling Economic criterion	Simulation with models	Probabilistic, CC, MILP, Benders decomposition	CPLEX YALMIP
[173]	Different production plants (INEOS, Köln, Germany)	Control or scheduling Economic criterion	Simulation with models	Deterministic, LQP, Lagrange multipliers	Not mentioned
[174]	Hybrid power plant including IEEE 39-bus system (unlocated)	Daily scheduling Economic, RES usage and security multi-criteria	Simulation with historical demands	Deterministic, heuristic rules, MILP, Benders decomposition	Not mentioned
[175]	Greenhouses and desalination (Almeria, Spain)	Control (MPC) Energetic criterion	Simulation with historical demand and weather	Deterministic, PNMPC	MATLAB®

2.3 Holistic View of Production Systems

In order to elaborate on the results that summarise the characteristics of the reviewed papers, a bar chart for each of the columns in the previous table is included below (Figures 2.3–2.8). For visualisation reasons, the scope column has been split into two charts, according to the objectives (Figure 2.5) and the criterion (Figure 2.6), as considered in Section 2.1. Note that, except in Figure 2.7 and 2.8, each chart encompasses seventy publications in total, which are matched with just one of the label on the vertical axis as explained below. In Figure 2.7 and 2.8 publications can be counted more than once since they either combine or compare different models and resolution techniques or use more than one computer program. The subsequent paragraphs describe these charts and include, between brackets, the total number of articles within each category.

According to Figure 2.3, most work is developed within the context of districts and urban areas (20), followed by benchmark cases (13) which include, among others, experimental MGs and IEEE test systems. The publications that comprise theoretical systems and those whose framework is not clearly delimited have been included into the “Others” category (15), which is the second in importance. The production systems of industries (7), buildings (8) and region and countries (7) are treated in a fewer, but significant, number of articles.

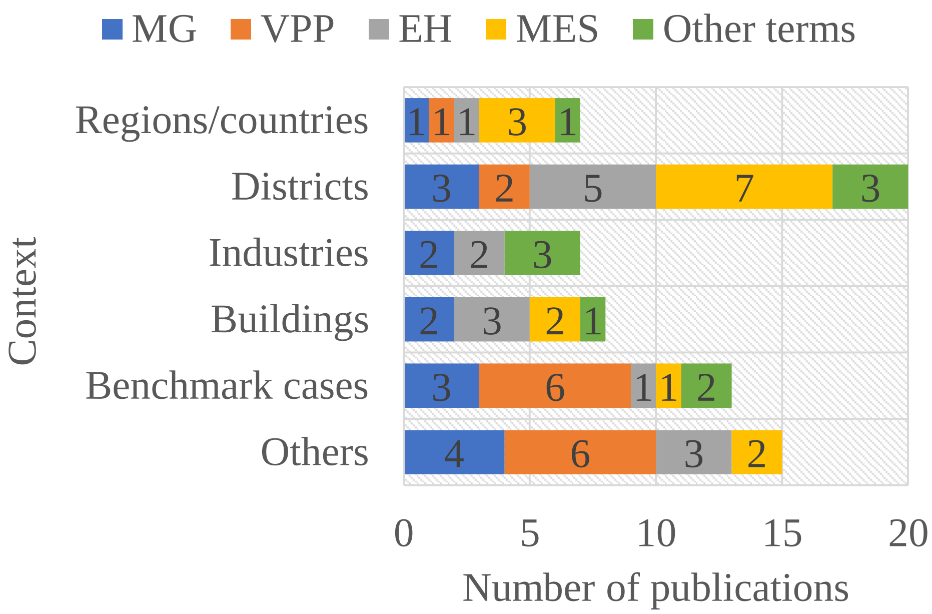

Figure 2.3. Classification summary of the most usual contexts in the reviewed papers

As mentioned in Section 2.1, the objectives considered here are so interrelated that they may appear together. For this reason, Figure 2.4 is arranged in a hierarchical form in which if a work shares more than one objective, only the upper label on the vertical axis is considered. To illustrate this point, consider for example references [78] and [170] in Table 2.5: they have been classified as “Design” and “Scheduling” respectively. In essence, scheduling comprises a meaningful number of publications (38) if compared with the remaining objectives, namely design (15), control (14) and modelling, which is the basis for most control and designing techniques, but it appears independently only in certain analysis and simulation studies (3).

This is partially due to the fact that many applications are related to the electricity markets, whose operation consist of hourly bids for selling/purchasing energy that are scheduled in advance. Another singular fact is that proportionally more control strategies seem to be applied on MGs, probably because they include more tractable elements in comparison with other approaches on large scale systems, the low-level controllers of which are neglected.

With regard to the criteria applied in each work, Figure 2.5 shows an overwhelming majority of the economic one (43) in single criterion cases, over the others (energetic, with 7 publications, and emissions, with 2), due again to the fact that money is the main incentive in electricity markets. It is still considered even in many multi-criteria (12) and criteria comparison (6) studies, which are categories that encompass heterogeneous criteria as further detailed in Tables 2.1–2.5. Considering as single criterion CO_2 or other gases emissions and energetic issues is usually related to design and control strategies.

Considering the kind of tests presented in Tables 2.1–2.5, Figure 2.6 is arranged into four categories. Most authors employ measurements from real system or databases related to them

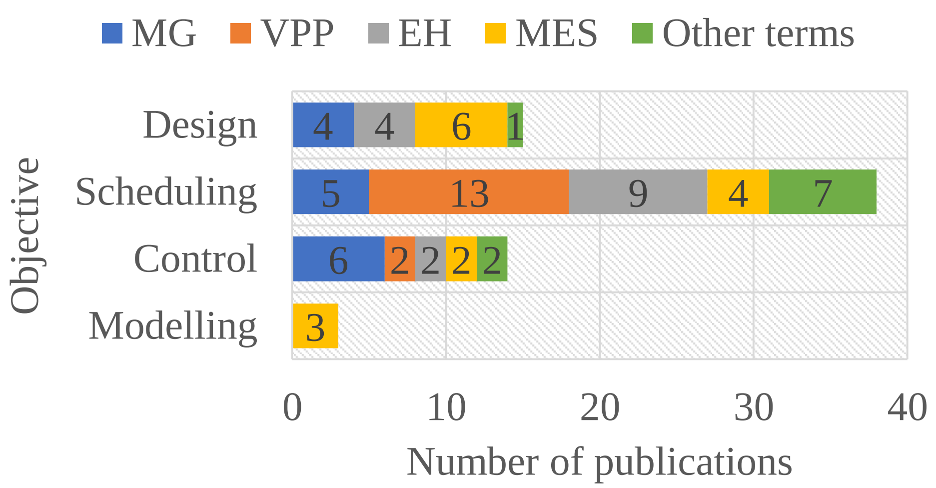

Figure 2.4. Classification summary of the most usual objectives in the reviewed papers

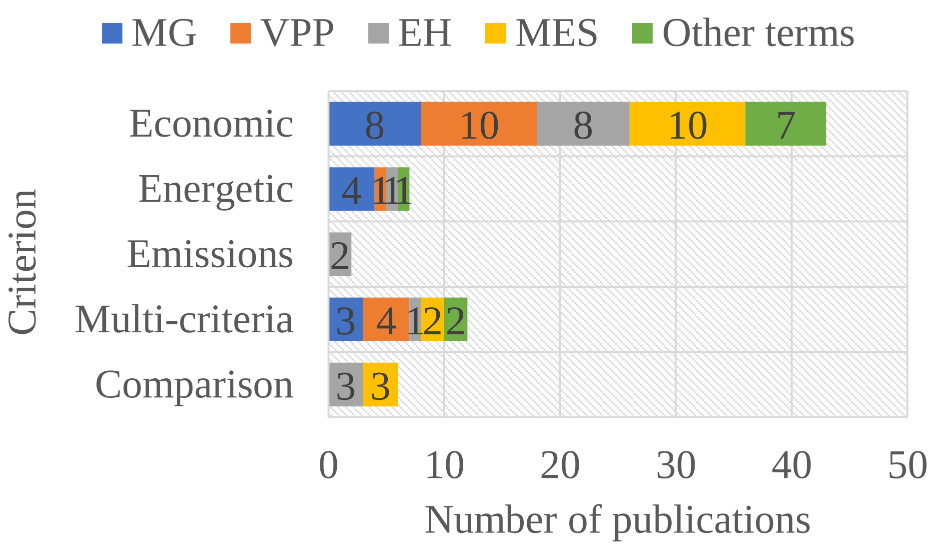

Figure 2.5. Classification summary of the most usual criteria in the reviewed papers

as inputs for the model they use in simulation environments (44). Regardless of the number of sources, “Simulation with data" means that at least part of the inputs come from historical records (price, production, demand, weather conditions...). In other cases, data are obtained through models (seasonal or mean values, predictive models...) or their origin is not explicitly mentioned (23). Finally, in a small number of cases related to scheduling or control techniques, real experiments are carried out over the systems (2) or they do not perform any test (1).

Owing to the heterogeneity in the terms included in the “Modelling and optimisation" column, readers are referred to Figure 2.2 in order to understand the terms that appear in Figure 2.7. Note that the six first constitute three binomial categories according to Figure 2.2 of which uncertainty treatment was discussed in Section 2.1 and the two remaining, as well as the kind of technique, can be easily characterised from the acronyms in Tables 2.1–2.5. At this point, the authors would like to remark that these aspects could not be fully analysed because of the scarcity of information in some papers, which hinder this task. They have been disregarded in the linearity, continuity and techniques categories in Figure 2.7.

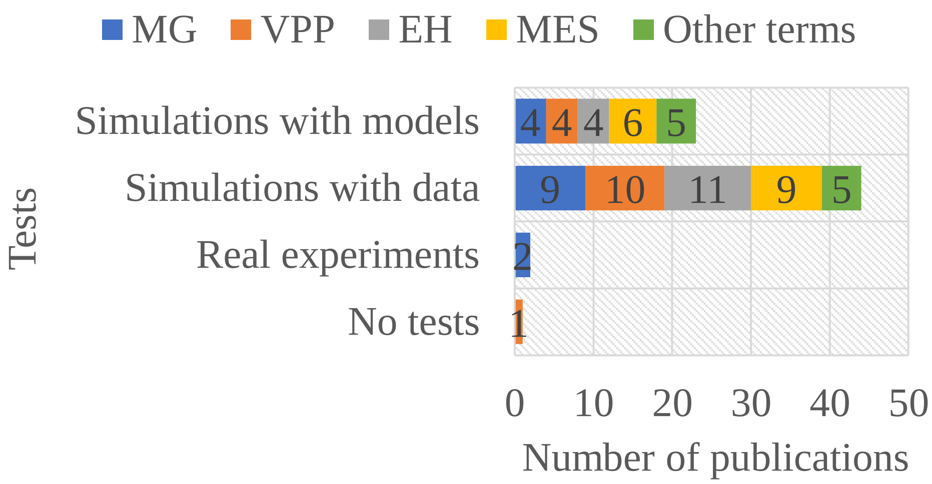

Figure 2.6. Classification summary of the most usual tests in the reviewed papers

Most publications use deterministic (56), linear (34) models with integer variables (43), solving the problem through analytical methods (56). Continuous formulations are not abundant (12) since the capacity to model certain devices is limited, and neither do heuristic (3) and meta-heuristic (10) approaches because of their sometimes-higher computational burden or their possible convergence to sub-optimal results. In contrast, probabilistic (17) and nonlinear (23) models, which tend to represent real systems with major fidelity, appear with frequency.

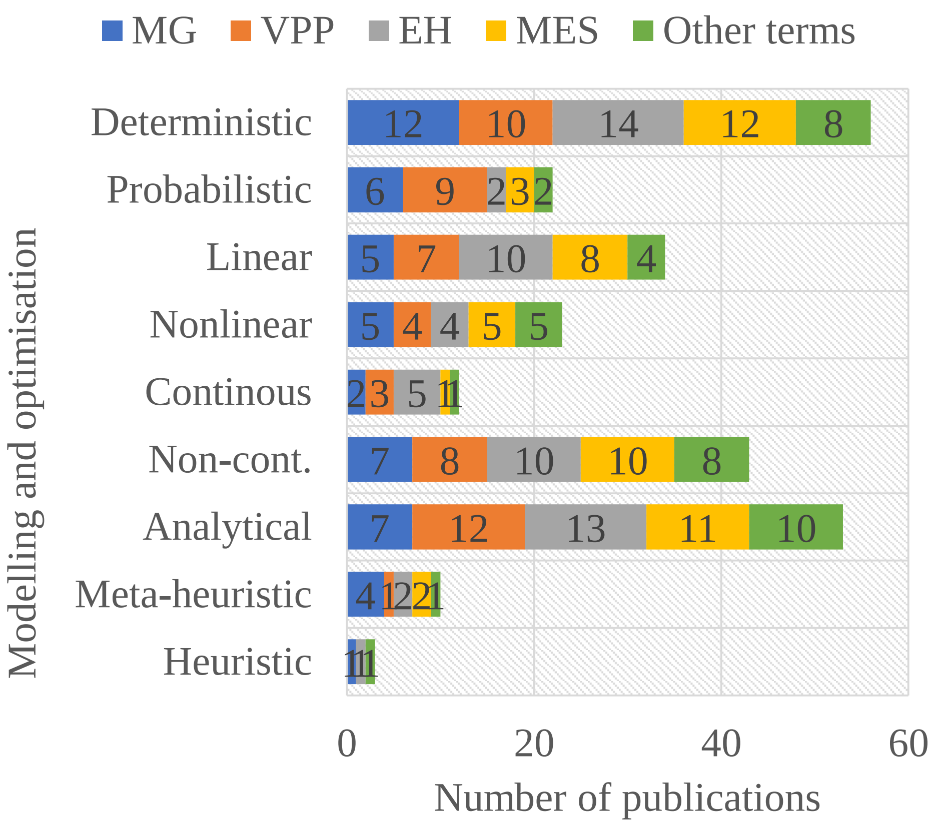

Figure 2.7. Classification summary of the uncertainty treatment, continuity (use of integer variables), linearity and techniques in the reviewed papers

Lastly, the names of the tools and programs that are used in more than one work are compiled in Figure 2.8, whereas those which do not are considered all together under the “Others" label (14). CPLEX is the principal choice for many authors (29), followed by GAMS (11) and AMPL (2) as optimisation packages that include both a modelling layer and basic solvers that can be used in combination with other software. Apart from these, Gurobi appears as another important optimiser (5), although it relies on other tools for programming the model. MATLAB® is the second noteworthy program (25), extensively employed in engineering and with its own programming language, for which other developers provide optimisation-assisted modelling tools such as YALMIP (7) and TOMLAB (2). HOMER (2) and Energy Plus (5) are the only relevant engineering software mentioned in the reviewed articles, although there is however also a substantial number of them that do not allude to any software (13).

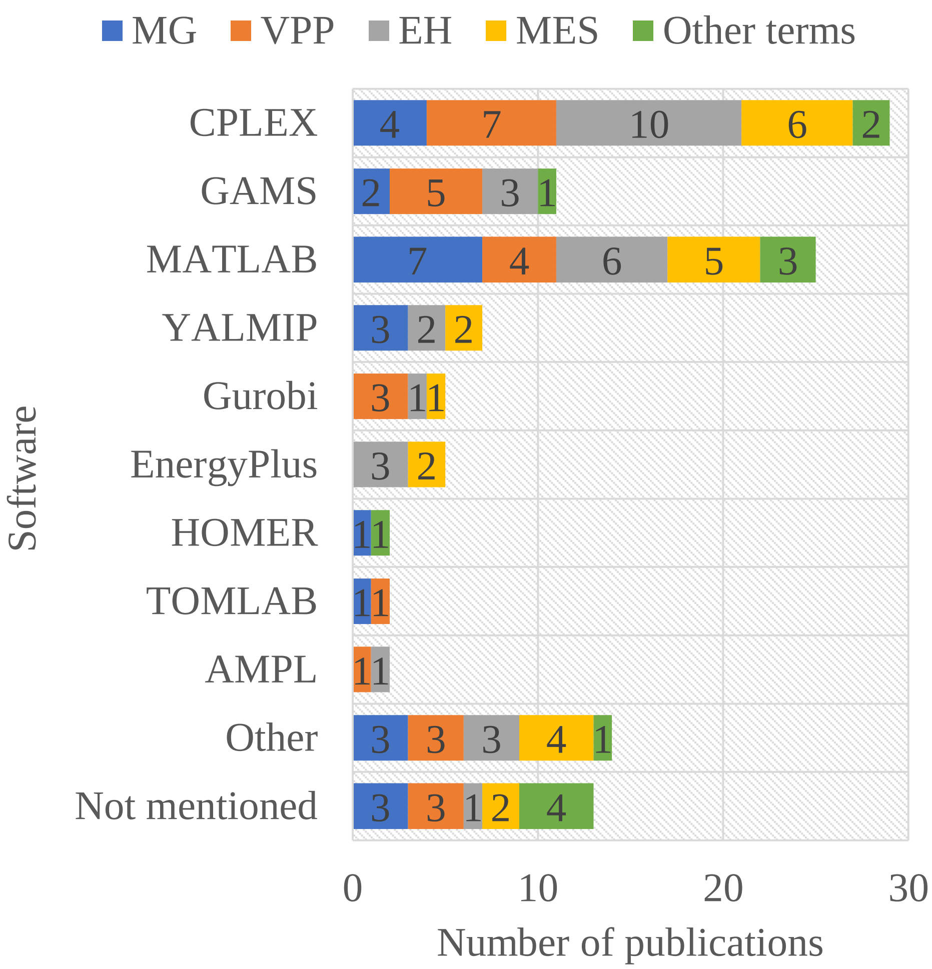

Figure 2.8. Classification summary of the most usual software in the reviewed papers

2.4 Related Research Groups and Projects

There are many groups and projects at national and international level which merit attention because of their scientific contributions to the field of distributed production systems, especially when it comes to EHs and MESs. However, for practical issues, it is not the purpose of this section to make an exhaustive list of them, but only to cite the most relevant ones either because some of their members gave birth to papers that have become a milestone, with plenty of cites from other publications, or just because they have come into sight during the bibliographic review and the research work of this thesis.

At European level, the Energy Science Center (ESC) integrates numerous research groups from the Swiss Federal Institute of Technology, from German *Eidgenössische Technische Hochschule* (ETH) Zurich (Switzerland), among which the Electrical Systems Laboratory stands out for past contributions related to EHs, led by Göran Andersson (Professor Emeritus since 2016) and Martin Geidl [17, 18, 176], who proposed and have disseminated such term since 2006. Some recent projects, as IMES and AFEM [177], have dealt with the decentralised production of electrical energy integrating renewable sources, emphasising the evaluation of MESs and their markets with perspectives for the future. They have been further in two new projects where platforms for modelling (Figure 2.9) and control of energy systems are being developed. Similarly, the Urban Energy Systems Laboratory [178], which belongs to the research centre Empa, has been involved with Energy Science Center (ESC) and dedicates its time to researching integrated MESs, with several works published over the last few years [20, 67, 72, 95, 179]. Both the ETH Zurich and Empa participate in the proposal of the Swiss Competence Center for Energy Research on Future Energy Efficient Buildings & Districts [180], which is closely related to the above-mentioned projects.

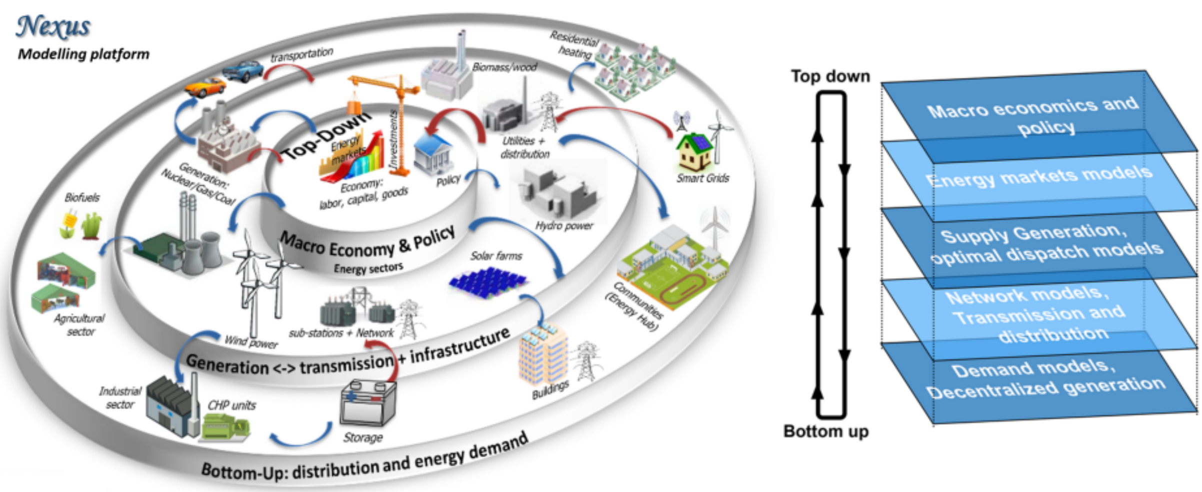

Figure 2.9. Vision of the Integrated Energy Systems Modelling Platform from the ESC. Source: ESC Research Projects [177]

Another representative research group in Europe, from the University of Manchester (United Kingdom (UK)), is the Electrical Energy and Power Systems Group [181] where a significant number of the works cited in this thesis have been performed during this decade [16, 32, 38, 154, 156, 157, 162, 163, 182, 183], and whose efforts are focused on the design and operation of power-system plants, and future smart transmission and distribution networks. Actually, the term MES was coined by Professor Pierluigi Mancarella [16], former member of the group, and the group took part in the already finished DIMMER project [184].

Additional research projects under the “Horizon 2020” and previous programmes can be found on the Community Research and Development Information Service (CORDIS) website [185], including a global map elaborated by the Joint Research Centre (JRC) [186] “with the most comprehensive inventory of smart grid projects in Europe”, where the aforementioned DIMMER and IMES appear. There are, however, some that cannot be found through this tool because they do not specifically tackle smart grid-related issues, but they still are intended to provide solutions for MESs.

For example, the SmarThor project, undertaken by the association of Belgian partners EnergyVille, deals with the development of a platform with which controlling an experimental MES [187]. Also, the TU Dortmund and the RWTH Aachen, from Germany, have been immersed in far-reaching projects as DYMASOS [188], CoPro [189], Plan4Res [190] and PlaMES [191], among whose objectives are the development of tools and methods for optimal planning and management of industrial complexes and energy systems. In this regard, the MESCOS simulator that was devised in the RWTH Aachen, allows the analysis of MES including district-scale gas, electricity, and heat supply, for which could constitute a basis for those projects.

At Spanish level, the Industrial Automatics and Robotics Group of the University of Seville works in optimal energy management in MGs through MPC [24, 115, 116, 122, 192–195] and participated in the DYMASOS project; the Control and Supervision of Processes Group of the University of Valladolid on modelling, simulation, control, and optimisation in industrial processes [68, 69] and participated in the CoPro project; and the Advanced Control Systems Group of the Polytechnic University of Catalonia on applying MPC techniques and game theory for water management [196, 197], to name a few. Beyond Europe, it could be highlighted the Power and Energy Systems Group from the University of Waterloo (Canada), whose lines of research consist of distribution systems planning and management [73, 198]; and the Research Group on Renewable Energies from the Federal University of Santa Catarina (Brazil), whose application areas include the automation and control of renewable energy systems [23, 24, 70, 150] and was the host institution during the three-months stay of the PhD candidate.

2.5 Other Subjects of Interest: Resource Prediction Models

Given the amount of different technologies involved in distributed production systems, this section is aimed at just providing a short overview, which does not need to be exhaustive for the purpose of this thesis, of some of the ones that are more relevant, which are employed in the plant analysed in Chapter 7. In particular, the model presented in Chapter 4 would require forecasting the availability of supplies (i.e. inputs) such as solar radiation and the loads or demanded resources, namely electricity, water, thermal power, etc. when employed in MPC schemes to operate the plant. Although the approach considered in this thesis is limited to a deterministic scenario where the forecast data are replaced by historical records, a basic review was conducted in order to introduce the readers to some of the methods and models usually employed in the literature to obtain those predictions.

To start with, among the different criteria by which models can be classified, the distinction between first principles and data-driven modelling is widely used because of its correlation with the knowledge of the system to be modelled, which is probably related to the main question that researchers and engineers need to answer about the model: How much time and effort should be put into achieving a suitable level of detail for a particular application? Czop et al. discussed the main characteristics of both modelling approaches and their hybridisation into a new category (grey-box models) [199].

Mathematical models based on first principles (also called transparent-box models) are formulated from physical, chemical, and biological fundamentals in form of differential, difference or partial derivative equations. Some authors identify in them three categories of parameters: geometrical, physical, and phenomenological. As Czop et al. define:

> *Geometrical and physical parameters are deduced from construction or operational documentation. The phenomenological parameters are the adjustable ones, which are estimated or adjusted based on their roughly known values* [199, p. 179].

Their main drawbacks are that they require a deep a priori understanding of the underlying phenomena occurring in each process to derive those equations and the difficulty to determine the phenomenological parameters. They are however quite useful, especially for simulation, because they allow providing a detailed insight of the system to other non-experts and figuring out its behaviour regardless of the operation conditions (i.e. from fewer experimental datasets).

On the contrary, data-driven models (also called black-box models) establish mathematical relationships without considering the inherent nature of the system, by using statistical, fitting and machine learning techniques on sets of experimental data. As Gil remarks:

> *In this case, their validity and performance strongly depend on a good selection of the dependent and independent variables, an adequate design of the experiments to be performed in the real facility, and an appropriate selection of the structure of the model* [200, p. 12].

But, as long as the number of datasets is enough to cover the whole range of operation of the system and any variation on the external conditions, this kind of models are much more rapid to develop and deploy.

2.5.1 Solar Radiation

The two main forms to yield energy from the sun have been the topic of numerous publications: solar thermal and PV systems. Both share the bases of how solar radiation reaches the surface of the earth and interacts with its atmosphere, although the subsequent production process is modelled according to the physics behind each technology.

Many of the prediction tools with a certain degree of accuracy require to know the amount of radiation on tilted surfaces, for which different models have been proposed, as shown in Duffie and Beckman's book [201]. The simplest version considers isotropic atmosphere and distinguishes at least between direct radiation, which does not interact with the atmosphere, and therefore its direction depends solely on the terrestrial location (latitude and longitude) of the said surface; and diffuse radiation, whose direction differs from direct radiation's due to the phenomena of reflection, absorption, refraction, etc. To calculate both components, it must be taken into account the meteorological conditions together with other geometric factors such as the earth's orbit, or the movement and the inclination of its axis of rotation.

The same book includes more information about solar production technologies and several basic concepts on PV solar energy [201], although other sources offer more detail on the latter ones as well as their application in practical situations [202]. In these cases, production is usually estimated based on the parameters offered by the manufacturers and on the equivalent circuit for PV cells, as did de Soto et al. to estimate performance [203].

Other approaches consist in using data-driven or statistics model, rather than physical, such as time-series analysis [204] and neural networks [205], sometimes within hybrid approaches that include autoregressive moving average models [206, 207]. Furthermore, when tackling this problem, it is necessary to be clear about the frequency and prediction horizon, since they determine the choice of the type of model. For example, Perez et al. used a numerical climate model, as a result of a process of different prediction stages, for a horizon of up to six days and another model, based on the analysis of satellite images instead, for the short-term prediction of up to six hours.

2.5.2 Energy, Water and CO_2 Consumption in Agro-Industrial Districts

In practical applications, operating MESs and EHs requires forecasting their energetic and material needs from real-time information, which is pertinent to the nature, complexity, and scale thereof. This subsection outlines some of the methods employed to predict them in buildings and greenhouses, the consumers of the ENERPRO and CHROMAE projects with a higher degree of uncertainty due to stochastic phenomena: these are the weather and the human behaviour.

A compilation of the methods for predicting consumption in buildings distinguished up to five types, which are actually in line with the criterion mentioned at the beginning of Section 2.5: engineering methods, which are based on first principles; statistical methods, artificial neural networks, support vector machines, which correspond to data-driven models; and grey models (hybridisation of the two main approaches) [209]. Engineering methods intend to determine the energy dynamics of the entire building or its rooms from thermal equations and there is usually a distinction between detailed and simplified methods. Whilst the former ones use complex functions to precisely calculate energy consumption (including information on outdoor weather conditions, the building's construction material, its use and comfort needs), the latter try to reduce the number of model variables by simplifying, for example, the climatic conditions when the internal thermal loads are dominant, which makes them principally useful when there is a lack of information about some of the model's inputs. They are expressly appropriate when it comes to determining the thermal loads because of their direct relation to the meteorological conditions, but they may result inaccurate to catch certain power consumption patterns related to human events. Statistical methods, and analogously the rest of methods, try to correlate energy consumption or indicators with certain influence variables, such as weather conditions, for which it is necessary to have historical data and they include, among other techniques, Fourier series, multiple linear regression, or auto-regression.

The demand for water in urban environments has been an object of study from temporal and spatial perspectives since the last century [210]. House-Peters and Chang presented an in-depth review of the publications on this topic, together with a summary of the methods and the explanatory variables commonly used, namely ambient temperature, precipitation, wind speed, evapotranspiration, water price, rate structure, population growth and income, in the case of temporal analyses; and age, household size, education, floor area, number of bedrooms, size of outdoor space, outdoor pool or garden, proportion of single-family households, housing typology, normalised difference of vegetation index, urban heat island, and conservation policy, in the case of spatial analyses. The complexity of the models scrutinised in their review ranges from individual domestic to regional consumption, and the time scale from hourly to quarterly or seasonal consumption. Furthermore, most of them are based on data-driven analysis, mainly regressions, whereas the ones based on first principles seem to have been relegated to an inferior place by the scientific community [210]. Regarding the former ones, Herrera et al. performed a comparison of models (artificial neural networks, projection pursuit regression, multivariate adaptive regression splines, support vector regression, random forests, and a weighted pattern-based model) to forecast the hourly urban water demand of a city spotted in the south-east of Spain, identifying support vector regression models as the most accurate, closely followed by the multivariate adaptive regression splines, projection pursuit regression and random forest models [211].

Regarding greenhouses, there is extensive literature on how to evaluate their energetic and material needs but, for the purpose of this section, most of the information has been extracted from a book co-authored by the supervisors of this thesis [212]. As Rodríguez et al. enlightened, the main demands correspond to thermal energy (cooling and heating), water and CO_2, which are directly related to the inside climate and therefore, indirectly, to the crop growth; that is, depending on the type of yield, the main variables that need to be kept within certain ranges are temperature, humidity, and CO_2 concentration in the air. Rodríguez et al. explain in detail the mass and energy balances occurring inside the greenhouse from which those variables can be computed over time (first principle models), for example: the thermodynamic behaviour of the greenhouse is determined from the incoming radiation and the heat transfer processes between the air, the cover, and the soil; the humidity and the water needs are usually calculated from the evapotranspiration, which can be forecast by coupling the climatic model with the crop's; and the CO_2 concentration from the photosynthetic activity of the plantation. Apart from the dynamic equations governing these phenomena, Rodríguez et al. indicate that there are alternative models: on the one hand, what they call pseudo-physical climate models, similar to the simplified engineering methods for buildings; and, on the other, data-driven models that include linear models obtained from the step or impulse response of the system, linear fuzzy models, nonlinear Volterra models, and nonlinear artificial neural networks. In any case, the same forecast variables (temperature, humidity, and CO_2 concentration) allow quantifying the energetic and material needs.

There other resources that are treated as inputs to the greenhouse, such as fertilisers or herbicides, which will not be taken into account in this thesis (although they fit in the proposed modelling framework) because their integration into distributed supply networks, in economic and legal terms, is not probably viable nowadays. However, in greenhouses with a certain degree of development or automation, especially when they make use of equipment like dehumidifiers, artificial lighting, forced ventilation, or electric-powered heating systems, neglecting the electric consumption might not be reasonable. As this tends to depend on the usage of the actuators employed to control the variables mentioned in the above paragraph, they can be as well quantified from the crop's model and needs, which is the approach taken by Rodríguez et al. to obtain the cost incurred by the actuators [212].

2.6 Contributions and Related Publications

The content of Sections 2.1–2.3, which gave rise to the article that has been submitted to IEEE Access [45], analyses the most remarkable common elements (employed terminology, context, research purpose, mathematical models, optimisation strategies, and tools) that can be found in publications related to this. They have been first defined and characterised, and then used to classify seventy of the works available in the current literature in tabular form and to elaborate graphs accounting for all the assessed aspect, which allows to present a holistic view on distributed production systems to the reader. On the other hand, Section 2.4 gives visibility to some of the already consolidated groups in this field, and Section 2.5 provides a short overview of the forecast models developed by other authors for some of the production technologies involved in the following chapters.

3. Description of Experimental Facilities

Chapter Summary

In Chapter 1, the ENERPRO and CHROMAE projects and their relation with this thesis were briefly described. In this chapter, the facilities that compose the demonstration and reference plants in each project are described with special attention to the parameters employed or assumed in the subsequent chapters. The size of these plants (see Figures 1.3 and 1.2), the kind of resources interchanged, and the presence of elements such as the greenhouse and the desalination plant allow their designation as agro-industrial cluster or district. Although some of these facilities are physically apart, they will be considered a single ensemble which can be modelled under the proposed framework. Sections 3.1, 3.4 and 3.5 introduce the building of the Solar Energy Research Centre (CIESOL), a PV parking and an electric vehicle located at the University of Almeria campus, respectively; Section 3.2 two of the desalination plants and nanofiltration plant at the facilities of the Solar Platform of Almeria (PSA); and Section 3.3 two greenhouses, one located at the Experimental Station of the Cajamar Foundation and the other at the Andalusian Institute for Agricultural and Fishing Research and Training (IFAPA). Most of the information regarding these facilities was collected and can be found in the master's thesis presented in 2017 [57].

3.1 CIESOL building

The Solar Energy Research Centre (CIESOL) was founded in 2005 thanks to an agreement between the University of Almeria and the Centre for Energy, Environment and Technology (CIEMAT) of the Ministry of Economy and Competitiveness [213]. The centre is located at the University of Almeria campus (36.83ºN, 2.41ºW), in a building which receives the same name as the centre: CIESOL building (Figure 3.1). This has a total surface area of 1071,92 m^2, laid out on two floors, and was built following bioclimatic criteria, incorporating several energy-saving passive and active strategies. A vast network of sensors allows recording and monitoring information in order to determine, or at least estimate with a high degree of confidence, CIESOL's energy consumption, outdoor and indoor climate conditions, and occupancy, among others.

Figure 3.1. Backside picture of the CIESOL building where the photovoltaic field and the field of solar collectors are visible in the rooftop

Although the main facilities and their features are summarised below, readers are referred to Castilla et al.'s book which contains a detailed description of CIESOL [214]. The PV field counts with forty-two Atersa A-222P modules, facing south (azimuthal angle of 21º east), with a surface area of 1,63 m^2 and a slope angle of 22º, and distributed in three arrays of fourteen collectors each connected in series (seven on the left and seven on the right at the highest part of the roof, as shown in Figure 3.1). Each array feeds a CICLO-3000 inverter where the electrical parameters related to production are measured and sent to a database, mainly direct current and voltage and alternate current and voltage at each inverter.

The solar-assisted air-conditioning and heating system, whose schematic is available at CIESOL's website [213], consist of eighty Solaris CP1 flat solar collectors, facing south (azimuthal angle of 21º east), with surface area of 2,02 m^2 and a slope angle of 30º, and distributed in ten arrays of eight collectors each (five arrays left and five right in Figure 3.1, behind the PV field); a YAZAKI WFC SC20 absorption machine (LiBr-H_2O) with a cooling a capacity of 70 kW and a performance between 0,7 and 0,9 (depending on the operation conditions); a SULZER EWK 100 cooling tower with a capacity of 170 kW; two storage tanks for hot water with a capacity of 5000 L each; an auxiliary heater with a capacity of 100 kW; two CIPRIANI Scambiatori heat exchangers with a capacity of 100 kW each; another two storage tanks for cold water with capacities of 2000 L and 3000 L; an underground cooling system; and the set of fan-coils distributed inside the building. There is also a support Ciatesa Hidropack WE 360 with cooling and heating capacities of 76,4 kW and 82,6 kW, respectively, and electric consumption of 26 kW (coefficient of performance of 2.73 and energy efficiency ratio of 3.23).

The meteorological station located in the rooftop measures outdoor temperature, relative humidity, solar radiation (including the component used in Chapter 5), or wind speed, among other variables. There are also some redundant sensors placed in the ventilated façades of CIESOL (facing South-East) in order to improve the accuracy of those measurements. +

Regarding the remaining sensors, indoor air temperature, relative humidity, and CO_2 concentration can be gauged in certain points inside the building and six of the fan-coil units (located in two offices, three laboratories and the meeting room) incorporate flowmeters and thermocouples to estimate the amount of thermal power supplied to the room.

3.2 Solar Platform of Almeria

The Solar Platform of Almeria is the largest centre destined for the research, development and testing of concentrating solar technology [215], located at the municipality of Tabernas, Almeria (37.09ºN, 2.35ºW). It dates from 1981, when founded by the International Energy Agency (IEA), but it was not until 1987 that became part of CIEMAT, which today integrates and organises the activities carried by each of the PSA's divisions: the Solar Concentration System Units, the Thermal Storage and Solar Fuels Unit, the Solar Desalination Unit, and the Solar Water Treatment Unit. Among their facilities (Figure 3.2), there are three involved in the development of this thesis that belong to the latter two units: the multi-effect distillation (AQUASOL system), membrane distillation, and nanofiltration plants.

Figure 3.2. Aerial view of the Solar Platform of Almeria where the facilities involved in this thesis can be spotted at the right bottom part of the picture

3.2.1 AQUASOL system

The AQUASOL system consists of a fourteen-stage multi-effect distillation unit (Figure 3.3a) designed, manufactured and installed by ENTROPIE in 1987, with forward feed configuration, a nominal feed flow of 8 m^3/h, a distillate production of 3 m^3/h, and a thermal consumption of 200 kW [216]; a double-effect absorption heat pump (LiBr-H_2O) from the same company, which is connected to the last stage of the distillation unit so that the low pressure steam is recovered in order to reduce the amount of energy consumed by the system [217]; an ATTSU RL200 fire-tube steam boiler that ensures the operation conditions in absence of solar radiation; and a water thermal storage system and a field of solar collectors which have been renovated during ENERPRO project. Initially, the system was composed of two tanks with a capacity of 12 m^3 each and 252 CPC Ao Sol 1.12x solar collectors, with a total area of around 500 m^2, but in 2015 the field was replaced by another one of sixty Wagner LBM 10HTF collectors, with a total area of around 606 m^2 and the same slope angle (35º), and the tanks by another pair with a total capacity of 40 m^3.

3.2.2 Membrane Distillation Pilot Plant

This plant (Figure 3.3b) was conceived for evaluating solar thermal desalination applications and testing different commercial and prototypical membrane distillation modules, and readers are referred to [218] work to extend the information given in this subsection [218]. The modules can be fed from two solar fields of flat-plate collectors: one consisting of ten Solaris CP1 Nova collectors with a total surface of 20 m^2, and another of four Wagner LBM 10HTF collectors with a total surface of 40 m^2. Both are connected as well to an intermediate water storage tank of 1500 L which can act as a heat buffer for thermal regulation or be bypassed, when appropriate. The installation is fully automated and monitored (inlet and outlet temperatures plus flows) allowing the heat flow to be regulated up to a temperature of about 90 ºC. A separate water circuit can be used for cooling purposes or for the steady-state operation of the plant, where the distillate and brine flows are collected and mixed together to be fed again into the desalination modules.

3.2.3 Nanofiltration Pilot Plant

As in the previous case, PSA's nanofiltration plant (Figure 3.3c) is used as a test bed for water treatment experiments at pilot scale. It consists of three membranes which can work in parallel or series, that is, the main stream of wastewater can be divided, in order to be filtered in each membrane, or entirely pass from one to the next. In either case, this results in a permeate stream (with low content of micropollutants that are able to break through the membranes) and a concentrate stream (rich in them), part of which is fed back to the tank containing the wastewater (recirculation stream). The system is configured to control the flow and electrical conductivity of each stream (permeate, concentrate and recirculated), as well as the transmembrane pressure, thanks to the pressure, temperature, and flow meters and to the valves installed at certain points in the circuit. As the operation range of the plant depends on the amount of pollutants in the water, indirectly determined by the electrical conductivity of the stream, readers are referred to the most recent publication on this plant for further information, where the static behaviour was tested using a feed stream (H_2O + NaCl) with a conductivity of 2300 µS/cm [219].

(a) (b) (c)

Figure 3.3. Experimental plants at the Solar Platform of Almeria involved in this thesis: multi-effect distillation unit (a), membrane distillation (b), and nanofiltration (c) pilot plants

3.3 Industrial and Traditional Agricultural Production

As the scope of CHROMAE needed to involve the usual elements in the Almerian agricultural ecosystem, from farmers to food industries, two types of greenhouses were selected for the project (Figure 3.4): a Mediterranean traditional greenhouse of the Experimental Station of the Cajamar Foundation (36.79º N, 2.72º W), colloquially known as *Las Palmerillas* [220], and an industrial greenhouse of the Andalusian Institute for Agricultural and Fishing Research and Training placed at one of their research centres in the municipality of *La Mojonera* (36.78º N, 2.71º W).

3.3.1 *Las Palmerillas*'s Greenhouse

This parral-type greenhouse [221] has a total surface area of 877 m^2 (37.8 m × 23.2 m), a polyethylene cover, automated ventilation with lateral windows in the northern and southern walls, flap roof windows in each span, and fine-mesh anti-trip nets. The greenhouse orientation is east–west, the crop rows are aligned north–south, and the cropping conditions are very similar to the ones in commercial greenhouses, continuously monitoring several climatic parameters within the greenhouse. Outside, a weather station measures air temperature, relative humidity, solar radiation, liquid precipitations, and wind speed. In addition, the greenhouse has a heating system consisting of a GP 95 propane heater and a Missouri 150000 multi-fuel boiler, which is part as well of the CO_2 storage and enrichment system [222].

3.3.2 IFAPA's Greenhouse

It is a gable multi-span greenhouse of 1000 m^2 of surface area with an exchangeable plastic-mesh cover, and east–west orientation. As in the other greenhouse, several climatic parameters (including temperature, humidity and CO_2 concentration) are constantly monitored inside the greenhouse and it has a hybrid heating system integrated by a biomass boiler of 225 kW, a thermal production system (with a main storage tank of 7 m^3 and an inertial tank of 2 m^3), a CO_2 storage and enrichment system, and a weather station which measures the same variables as *Las Palmerillas*'s station.

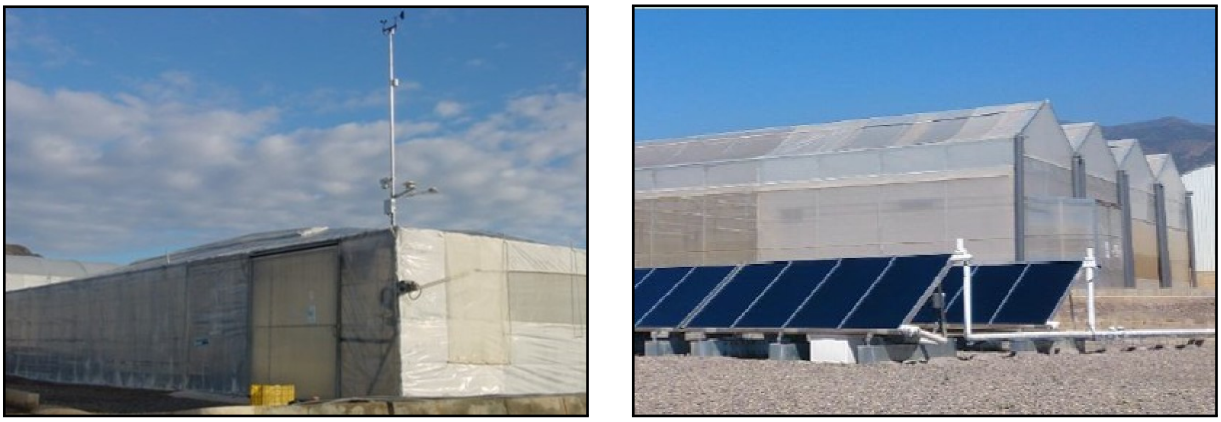

(a) (b)

Figure 3.4. Experimental greenhouses involved in this thesis: *Las Palmerillas*'s Greenhouse (a) and IFAPA's Greenhouse (b)

3.4 Photovoltaic Parking

The PV parking of the University of Almeria (36.83ºN, 2.40ºW), shown in Figure 3.5a, consists of ten arrays of 483 Conergy PA 240P modules (twenty-one in series and twenty-three in parallel) connected to a Fronius Agilo 100 inverter (4830 modules and ten inverters in total) for production purposes, as well as another three arrays, for experimental testing, connected to their respective Fronius IG Plus 55v3 inverters, and distributed as follows: twenty-four Conergy PA 240P modules (twelve in series and two in parallel) in the first group, twenty-four Conergy Power Plus 240M modules (twelve in series and two in parallel) in the second and seventy-two First Solar FS-380 modules (eight in series and nine in parallel) in the third. All the modules have a slope angle of 7º and are facing south (azimuthal angle of 21º east).

3.5 UAL-eCARM Electric Vehicle

The so-called UAL-eCARM (Figure 3.5b) is an electric vehicle manufactured by Changzhou Greenland Vehicle Co. Ltd. (LITA GLe2-2S model) which has been tweaked over the last years in order to make it an autonomous vehicle. According to the manufacturer's specifications, the prototype weights 460 kg without the batteries (760 kg with them) and has an autonomy of 90 km and a maximum speed of around 45 km/h.

The extra hardware components consist of voltage and current meters to measure energy consumption and monitor the state of the batteries, different sensors for navigation and mapping (GPS and inertial measurement units, several encoders for steering control and odometry, a pair of cameras and a laser which are part of the artificial vision system), and two motors which compose the new drive-by-wire system (one at the steering column and the other one connected to brakes' hydraulic system) [223]. The car still maintains its original 48-volts motor of 4,3 kW, which is controlled through a potentiometer, so that none of the pedals is functional any more. Two embedded computers serve as an interface for all these peripherals, under the OpenMORA architecture. Owing to its deterioration, the original batteries were recently replaced by a new pack of eight batteries model 6V-GEL, fabricated by Trojan Battery Company [123].

(a) (b)

Figure 3.5. Photovoltaic parking (a) and electric vehicle (b) at the University of Almeria

4. Distributed Production and Dispatch

Chapter Summary

This chapter contains a broad description of the models programmed in MATLAB® for the tool presented in Chapter 6 and the case study of Chapter 7. Section 4.1 details the insights of the modelling proposal of this thesis to represent EH and Section 4.2 formalises the management strategy aimed at achieving the lowest operation cost of the EH. In Section 4.3 the formulation of the former sections is extended to be applied for performing equivalent analyses in networked EHs. Section 4.4 offers helpful information on how to define the parameters of the model proposed in the previous sections and Section 4.5 compiles the conceptual models of the distinguishable EHs in the CHROMAE project.

4.1 Modelling of Energy Hubs

In broad terms, the models of most EHs represent energy and mass balances between a set of input resources that can be transformed into another set of output resources. These resources are represented mathematically through variables which constitute the respective input and output vector elements. The basic relationship proposed by Geidl and Andersson [18] is based on a coupling matrix $\boldsymbol{C}$ that represents the conversion process between multiple energy carriers in steady-state ($\boldsymbol{L} - \boldsymbol{C}\boldsymbol{P} = 0$), where $\boldsymbol{P}$ are the input powers or sources and $\boldsymbol{L}$ the output powers or loads. The coefficients of this matrix are given by the product of the efficiencies of all the conversion units or devices that intervene in the conversion and the so-called dispatch factors that need to be introduced whenever one energy carrier splits up to several flows inside the EH. Additional constraints may consider power limits, the presence of storage systems, and necessary energy balances among these dispatch factors.

This has led to formulations that have progressively introduced elements to represent conversion and storage processes more accurately but share a similar basis. Actually, there is usually a distinction between the conversion and storage models [19] and the systems represented are supposed to contain their devices close enough to assume that resource losses only occur in conversion and storage processes. In order to formulate a linear model, the use of dispatch factors [18] must be avoided; thus Parisio et al. suggested introducing as many variables as there are conversion devices, rearranging the input vector and the coupling matrix in a new equation which relates them to the output vector [19]. A similar approach was adopted by Evins et al. which combined an input–output equation with the one proposed by Parisio et al. [20].

In contrast to other proposals in the literature, such as Parisio et al.'s, the model developed in this thesis defines a "path vector" whose elements are decision variables for each possible path between inputs and outputs [41]. This allows avoiding the nonlinear relationships of Geidl and Andersson's model when two dispatch factors are multiplied in the coupling matrix [18], and to formulate the conversion model of complex EHs more simply, with fewer decision variables. The input and internal flows are obtained from the elements of the path vector and suitably defined coupling matrices. Some outputs or loads can be considered dependent on the fact that certain device is turned on or off, which was taken into account in the model by arranging Geidl and Andersson's equation $\boldsymbol{L} - \boldsymbol{C}\boldsymbol{P} = 0$. All the equations that encompass these and other circumstances are presented below, although, for the sake of simplicity, most of them will appear here in matrix notation. In addition, the term "power" will be superseded by "flow" or just omitted, since not only energy carriers are considered, but also material resources. Furthermore, the novel elements introduced have been highlighted in blue in Fig. 4.1

Considering the most common elements in previous approaches (represented in black in Fig. 4.1), the conversion and storage model of a general EH needs a minimum set of variables representing the structure of the system to be defined. Therefore, let N_i represent the number of input flows, N_o the number of output flows, N_p the number of paths between these inputs and outputs, and N_d the number of conversion devices with a total amount of N_{di} input flows and N_{do} output flows. Also, the equations are represented in discrete time, with a uniform sample time $T = t(k+1) - t(k)$, where k constitutes any discrete-time instant.

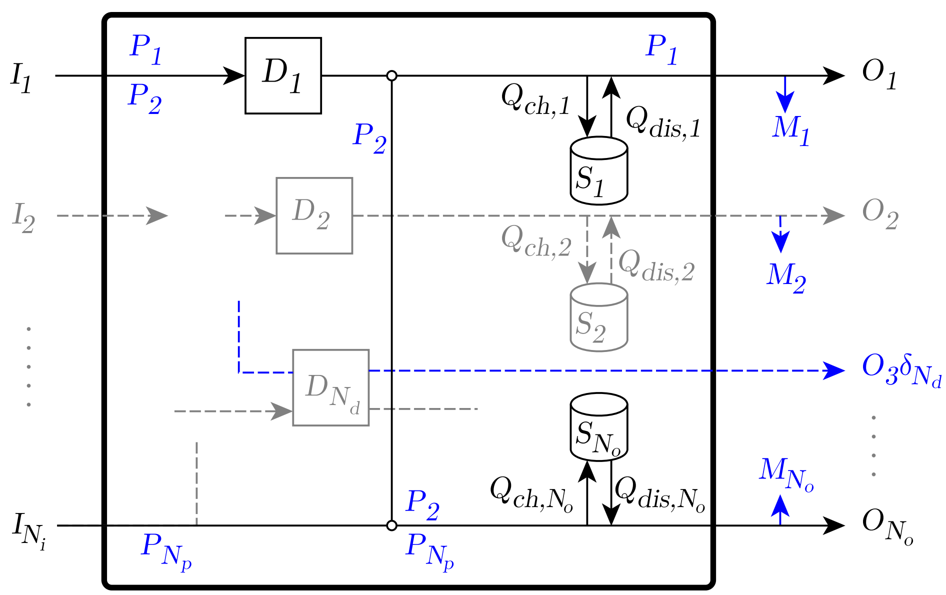

Figure 4.1. Schematic diagram of a general EH with storage at the output ports. The novel elements introduced in this thesis are highlighted in blue: binary variables attached to certain outputs, paths between the inputs and outputs, and output resource sales.

4.1.1 Conversion Model

The conversion processes need to satisfy balance conditions at each time step, as stated in Equation (4.1),

$$\boldsymbol{\delta_O}(k)\boldsymbol{O}(k) + \boldsymbol{M}(k) = \boldsymbol{C}(k)\boldsymbol{P}(k) - \boldsymbol{Q_{ch}}(k) + \boldsymbol{Q_{dis}}(k), \tag{4.1}$$

where $\boldsymbol{P}$ is the $N_p \times 1$ vector of flows between inputs and outputs or "path vector", $\boldsymbol{M}$ is the $N_o \times 1$ vector of market sales flows, $\boldsymbol{O}$ is the $N_o \times 1$ vector of output flows, $\boldsymbol{Q_{ch}}$ is the $N_o \times 1$ vector of charge flows, $\boldsymbol{Q_{dis}}$ is the $N_o \times 1$ vector of discharge flows, $\boldsymbol{C}$ is the $N_o \times N_p$ coupling matrix, and $\boldsymbol{\delta_O}$ is the $N_o \times N_o$ binary diagonal matrix of output activation.

Additionally, the relationship between the internal $\boldsymbol{P}$ vector flows and both the input flows to the EH itself must be established, as defined in Equation (4.2), and the input–output flows in each device, as given in Equations (4.3) and (4.4),

$$\boldsymbol{I}(k) = \boldsymbol{C_i}\boldsymbol{P}(k), \tag{4.2}$$

$$\boldsymbol{D_i}(k) = \boldsymbol{C_{di}}(k)\boldsymbol{P}(k), \tag{4.3}$$

$$\boldsymbol{D_o}(k) = \boldsymbol{C_{do}}(k)\boldsymbol{P}(k), \tag{4.4}$$

where $\boldsymbol{I}$ is the $N_i \times 1$ vector of input flows, $\boldsymbol{D_i}$ is the $N_{di} \times 1$ vector of devices' flows (referred to their inputs), $\boldsymbol{D_o}$ is the $N_{do} \times 1$ vector of devices' flows (referred to their outputs), $\boldsymbol{C_i}$ is the $N_i \times N_p$ input coupling matrix, $\boldsymbol{C_{di}}$ is the $N_{di} \times N_p$ device coupling matrix (referred to their inputs), and $\boldsymbol{C_{do}}$ is the $N_{do} \times N_p$ device coupling matrix (referred to their outputs). Note that in Reference [41] only one equation was defined, instead of two, to limit the flows through the devices of the EH.

Except vector $\boldsymbol{O}$, which a priori does not contain decision variables (see Subsection 4.1.4 for the opposite case), and vector $\boldsymbol{P}$, which is indirectly limited by the production capacity of the conversion devices from the following equations, the remaining vectors need to be constrained in order to ensure that the conversion devices do not exceed their defined capacities. That is the raison d'être of Equations (4.5)–(4.8),

$$\boldsymbol{M^{min}}(k)\boldsymbol{\delta_M}(k) \leq \boldsymbol{M}(k) \leq \boldsymbol{M^{max}}(k)\boldsymbol{\delta_M}(k), \tag{4.5}$$

$$\boldsymbol{I^{min}}(k)\boldsymbol{\delta_I}(k) \leq \boldsymbol{I}(k) \leq \boldsymbol{I^{max}}(k)\boldsymbol{\delta_I}(k), \tag{4.6}$$

$$\boldsymbol{D_i^{min}}(k)\boldsymbol{\delta_{D_i}}(k) \leq \boldsymbol{D_i}(k) \leq \boldsymbol{D_i^{max}}(k)\boldsymbol{\delta_{D_i}}(k), \tag{4.7}$$

$$\boldsymbol{D_o^{min}}(k)\boldsymbol{\delta_{D_o}}(k) \leq \boldsymbol{D_o}(k) \leq \boldsymbol{D_o^{max}}(k)\boldsymbol{\delta_{D_o}}(k), \tag{4.8}$$

where the superscripts "max" and "min" refer to the upper or lower limit of each vector (for instance, $\boldsymbol{I^{max}}$ determines the maximum amount of resources that can enter the EH), and the rest of δ symbols define diagonal binary variables that indicate if the flow is allowed or not. In particular, $\boldsymbol{\delta_M}$ is the $N_o \times N_o$ binary diagonal matrix of market sales flow activation, $\boldsymbol{\delta_I}$ is the $N_i \times N_i$ binary diagonal matrix of input flow activation, $\boldsymbol{\delta_{D_i}}$ is the $N_{di} \times N_{di}$ binary diagonal matrix of devices' flow activation (referred to their inputs), $\boldsymbol{\delta_{D_o}}$ is the $N_{do} \times N_{do}$ binary diagonal matrix of devices' flow activation (referred to their outputs).

4.1.2 Storage Model

In order to properly meet resource demand, most previous models in the literature introduce storage devices, as represented in Fig. 4.1. The storage dynamic is assumed to be linear and, without loss of generality [176], devices are considered to be located only at the output flows. The storage processes need to satisfy balance conditions between consecutive time steps, so that the state of the system varies according to the amount of resources charged or discharged, as stated in Equation (4.9),

$$\boldsymbol{S}(k+1) = \boldsymbol{C_s}(k)\boldsymbol{S}(k) + \boldsymbol{C_{ch}}(k)\boldsymbol{Q_{ch}}(k) - \boldsymbol{C_{dis}}(k)\boldsymbol{Q_{dis}}(k), \tag{4.9}$$

where $\boldsymbol{Q_{ch}}$ is the $N_o \times 1$ vector of charge flows, $\boldsymbol{Q_{dis}}$ is the $N_o \times 1$ vector of discharge flows, $\boldsymbol{S}$ is the $N_o \times 1$ vector of stored resources, $\boldsymbol{C_{ch}}$ is the $N_o \times N_o$ diagonal matrix of charge efficiencies, $\boldsymbol{C_{dis}}$ is the $N_o \times N_o$ diagonal matrix of discharge efficiencies, and $\boldsymbol{C_s}$ is the $N_o \times N_o$ diagonal matrix of resource degradation.

Note that, as in conversion devices, the above variables need to be constrained in order to ensure that the storage devices do not exceed their capacities, through Equations (4.10)–(4.12),

$$\boldsymbol{Q_{ch}^{min}}(k)\boldsymbol{\delta_{ch}}(k) \leq \boldsymbol{Q_{ch}}(k) \leq \boldsymbol{Q_{ch}^{max}}(k)\boldsymbol{\delta_{ch}}(k), \tag{4.10}$$

$$\boldsymbol{Q_{dis}^{min}}(k)\boldsymbol{\delta_{dis}}(k) \leq \boldsymbol{Q_{dis}}(k) \leq \boldsymbol{Q_{dis}^{max}}(k)\boldsymbol{\delta_{dis}}(k), \tag{4.11}$$

$$\boldsymbol{S^{min}}(k) \leq \boldsymbol{S}(k) \leq \boldsymbol{S^{max}}(k), \tag{4.12}$$

where the superscripts "max" and "min" refer to the upper or lower limit of each vector (for instance, $\boldsymbol{S^{max}}$ determines the maximum amount that each storage system may store), and the rest of the δ symbols define diagonal binary variables that indicate if the flow is allowed or not. In particular, $\boldsymbol{\delta_{ch}}$ is the $N_o \times N_o$ binary diagonal matrix of charge flow activation, $\boldsymbol{\delta_{dis}}$ is the $N_o \times N_o$ binary diagonal matrix of discharge flow activation.

4.1.3 Simultaneous Constrained Processes

Additional constraints are required in order to take into account certain processes that cannot occur at the same time. Three situations can be distinguished: preventing the charge and discharge of the same storage systems, by means of Equation (4.13),

$$\boldsymbol{\delta_{ch}}(k) + \boldsymbol{\delta_{dis}}(k) \leq \boldsymbol{1}, \tag{4.13}$$

where $\boldsymbol{1}$ is the identity matrix (note that $\boldsymbol{I}$ already denotes a variable of the model); avoiding the use of the same infrastructure for acquiring and selling resources (a typical situation in power and water supply), as expressed in Equation (4.14),

$$\delta_{I,i}(k) + \delta_{M,o}(k) \leq 1, \tag{4.14}$$

where i and o respectively denote the elements of $\boldsymbol{\delta_M}$ and $\boldsymbol{\delta_I}$ with common infrastructure; and impeding that some devices operate simultaneously, as stated in Equation (4.15),

$$\delta_{D,d^{(1)}}(k) + \cdots + \delta_{D,d^{(n)}}(k) \leq 1, \tag{4.15}$$

where $d^{(1)}...d^{(n)}$ refer to the elements of $\boldsymbol{\delta_{D_i}}$ or $\boldsymbol{\delta_{D_o}}$ corresponding to non-simultaneous converters. Owing to the definition of $\boldsymbol{P}$, the variables corresponding to the outputs of a device that produces different resources at the same time (e.g. a combined heat and power system or a boiler with carbon capture) must equal the input amount of that device. Equation (4.16) satisfies that balance,

$$P_{p^{(1)}}(k) + ... + P_{p^{(n)}}(k) = P_{p^{(n+1)}}(k) + ... + P_{p^{(m)}}(k), \tag{4.16}$$

where $p^{(1)}...p^{(n)}...p^{(m)}$ correspond to simultaneous converter outputs.

These situations will be exemplified in Chapter 7, although the following explanations are provided for a better understanding:

- In Equation (4.14), when an input resource (e.g. electricity) is supplied from a public utility network through a certain medium, the supply facility (e.g. electrical wiring) cannot be employed at the same time for selling resources since this means establishing a flow in the opposite direction.
- In Equation (4.15), if for any reason two devices cannot operate together (e.g. a device virtually split into two different ones, such as a reversible heat pump), the flows through each can be limited by making their corresponding binary variable equal to zero.
- In Equation (4.16), some devices can supply different output resources from their input (e.g. a combined heat and power system), so although each produced resource constitutes a different path in $\boldsymbol{P}$, their upstream flow is the same (the fuel input) and so are the sums of elements in $\boldsymbol{P}$ corresponding to each output of the device.

4.1.4 Device-Dependent Fixed and Variable Loads

Note that the arrangement above proposed to consider loads coming from the use of a particular device consisted in adding any necessary element to vector $\boldsymbol{O}$ and using $\boldsymbol{\delta_O}$ in Equation (4.1). However, this solution is only suitable in the case of fixed demands, since the model does not contemplate the possibility of adding variable demands, proportionally to the flow of the device. One straightforward way to iron out this situation consists in redefining the elements of $\boldsymbol{O}$ so that the demand equals the proportional flow of the device or, in what turns out to be equivalent, redefining matrices $\boldsymbol{C}$ and $\boldsymbol{\delta_O}$. In the following paragraphs, both situations are exemplified by using a hypothetical EH in order to elucidate how the previous formulation needs to be adapted, which is relevant for programming.

Let Figure 4.2 represent a simplified example of an EH where an electric pump is in charge of keeping the water pressure of an irrigation facility. In order to ease the understanding of this example, free water discharge and no electricity storage or market sales flows are considered. The path vector only has two elements, that is, the number of possible paths in the EH: $I_1 \rightarrow D_1 \rightarrow O_1$ (P_1) and $I_2 \rightarrow O_2$ (P_2), so in this concrete case $\boldsymbol{C_i}$ becomes the identity matrix and $\boldsymbol{P} = \boldsymbol{I}$. Thus, the balance equations of the conversion processes and their limits, i.e. Equations (4.1)–(4.4), (4.7), and (4.8), adopt the form of Equations (4.17)–(4.22),

$$\begin{bmatrix} 1 & 0 \\ 0 & \delta_{D,1}(k) \end{bmatrix} \begin{bmatrix} O_1(k) \\ O_2(k) \end{bmatrix} = \begin{bmatrix} C_{1,1}(k) & 0 \\ 0 & C_{2,2}(k) \end{bmatrix} \begin{bmatrix} P_1(k) \\ P_2(k) \end{bmatrix} - \begin{bmatrix} Q_{ch,1}(k) \\ 0 \end{bmatrix} + \begin{bmatrix} Q_{dis,1}(k) \\ 0 \end{bmatrix}, \tag{4.17}$$

$$\begin{bmatrix} I_1(k) \\ I_2(k) \end{bmatrix} = \begin{bmatrix} 1 & 0 \\ 0 & 1 \end{bmatrix} \begin{bmatrix} P_1(k) \\ P_2(k) \end{bmatrix}, \tag{4.18}$$

$$D_{i,1}(k) = \begin{bmatrix} 1 & 0 \end{bmatrix} \begin{bmatrix} P_1(k) \\ P_2(k) \end{bmatrix}, \tag{4.19}$$

$$D_{o,1}(k) = \begin{bmatrix} C_{1,1}(k) & 0 \end{bmatrix} \begin{bmatrix} P_1(k) \\ P_2(k) \end{bmatrix}, \tag{4.20}$$

$$D_{i,1}^{min}(k)\delta_{D,1}(k) \le D_{i,1}(k) \le D_{i,1}^{max}(k)\delta_{D,1}(k), \tag{4.21}$$

$$D_{o,1}^{min}(k)\delta_{D,1}(k) \le D_{o,1}(k) \le D_{o,1}^{max}(k)\delta_{D,1}(k), \tag{4.22}$$

where the non-zero elements of the coupling matrices $\boldsymbol{C}$ and $\boldsymbol{C_{do}}$ would be equal to one because no transformation of resources exits in the EH, and $\boldsymbol{\delta_O}$ contains the binary variable related to the activation of the pump ($\delta_{D,1}$).

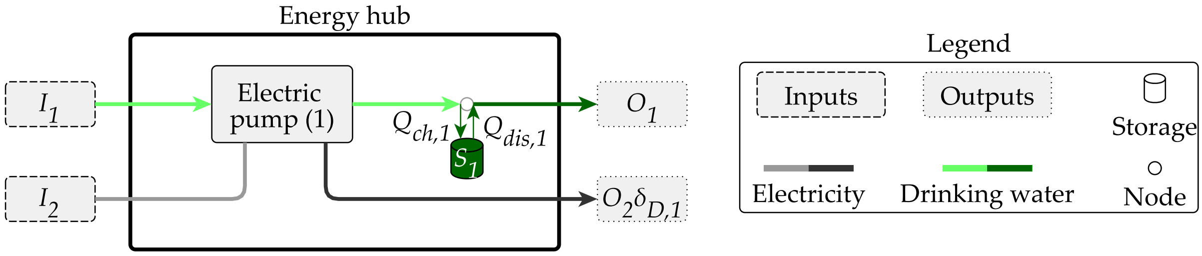

Figure 4.2. Hypothetical EH where the electric pump (D_1) works at any time there exists a flow between the public supply network (I_1) and the water demand (O_1) or the storage tank ($Q_{ch,1}$). I_2 represents the electricity from the power grid that covers the pump's demand (O_2).

Now, if the electric pump is assumed to have a constant consumption, O_2 would be equal to that value instead of constituting a decision variable in the optimisation problem, which is the case contemplated in Subsection 4.1.1. However, if a consumption proportional to the pumped water flow is considered instead, with a constant of proportionality κ, Equation (4.17) needs to be reformulated as follows. First, it must be defined whether the consumption is proportional to the inlet or the outlet flow, which would lead to two different expressions $O_2 = \kappa D_{i,1} = \kappa P_1$ or $O_2 = \kappa D_{o,1} = \kappa C_{1,1} D_{i,1} = \kappa C_{1,1} P_1$, respectively. Only the second expression will be used from now on as it will allow generalisations to the first one. In any case, as both P_1 and $\delta_{D,1}$ are decision variables, their product would turn the optimisation problem into a nonlinear one when substituting O_2 into Equation (4.17). To avoid this, $\delta_{D,1}$ can be removed from $\boldsymbol{\delta_O}$ (making that element equal to one) since P_1 is already constrained by the on/off state of the pump, through Equations (4.21) and (4.22), which leads to transforming Equation (4.17) into Equation (4.23),

$$\begin{bmatrix} 1 & 0 \\ 0 & 1 \end{bmatrix} \begin{bmatrix} O_1(k) \\ \kappa C_{1,1}(k) P_1(k) \end{bmatrix} = \begin{bmatrix} C_{1,1}(k) & 0 \\ 0 & C_{2,2}(k) \end{bmatrix} \begin{bmatrix} P_1(k) \\ P_2(k) \end{bmatrix} - \begin{bmatrix} Q_{ch,1}(k) \\ 0 \end{bmatrix} + \begin{bmatrix} Q_{dis,1}(k) \\ 0 \end{bmatrix}, \tag{4.23}$$

or equivalently, arranging matrix $\boldsymbol{C}$, into Equation (4.24),

$$\begin{bmatrix} 1 & 0 \\ 0 & 1 \end{bmatrix} \begin{bmatrix} O_1(k) \\ 0 \end{bmatrix} = \begin{bmatrix} C_{1,1}(k) & 0 \\ -\kappa C_{1,1}(k) & C_{2,2}(k) \end{bmatrix} \begin{bmatrix} P_1(k) \\ P_2(k) \end{bmatrix} - \begin{bmatrix} Q_{ch,1}(k) \\ 0 \end{bmatrix} + \begin{bmatrix} Q_{dis,1}(k) \\ 0 \end{bmatrix}. \tag{4.24}$$

Just to recap all of the above and as a rule of thumb, in case of device-dependent variable demand, the following modifications must be performed in the model presented previously: removing from $\boldsymbol{\delta_O}$, by making equal to one, all the elements of its diagonal related to those demands; setting to zero the analogous rows in $\boldsymbol{O}$; and including in the columns of $\boldsymbol{C}$ related to that device the suitable conversion/transformation coefficients multiplied by the negative constant of proportionality between the demand and the flow through the device. Part of the ODEHubs's code was generated to perform these modifications in the model.

4.2 Resource Dispatch within Energy Hubs

The above equations and the ones of similar models are usually employed as constraints in optimisation problems. Their solution allows determining the best set of flows at each sample time according to certain criteria (which were discussed in Subsection 2.1.2), that is, the amount of resources that need to get in or out of the storage systems, to be obtained from the sources of supply or to be sold in the markets; or, in terms of the decision variables in Equations (4.1)–(4.16), the values for charge, discharge, and market sales flows, the binary variables and the "path vector". In this thesis, the management strategy aimed at achieving the lowest operation cost is applied by solving the optimisation problem stated in equation (4.25),

$$\begin{aligned} \min \quad & \sum_{k=0}^{H-1} (\boldsymbol{c}(k)\boldsymbol{I}(k) - \boldsymbol{s}(k)\boldsymbol{M}(k)) \\ \text{s.t.} \quad & \text{Equations (4.1)–(4.16)}, \end{aligned} \tag{4.25}$$

where $\boldsymbol{c}(k)$ is the $1 \times N_i$ vector containing the price of each input, $\boldsymbol{s}(k)$ is the $1 \times N_o$ vector containing the price of sold resources (in terms of energy, mass, or volume), and H is the length (in samples) of the control horizon. Note that, depending on the units of the sample time T and the vectors, additional terms might need to be introduced in Equations (4.9) and (4.25) to convert between time units (see for example [41]).

In real applications, note that solving this optimisation problem just as it is and using the decision variables, which can constitute set-points for lower-level control loops, during the whole horizon H matches the definition of scheduling given in Subsection (2.1.2). This would require forecasting the demand of each resource an even some parameters of the model, which may be subjected to uncertainty. As introduced in Section 1.1, one solution would consist in solving this optimisation problem iteratively in order to dynamically update the decision variables and so the values of the set-points. Such approach is known as in the literature as model predictive control or receding horizon control, where the operation schedule is calculated by repeatedly solving the above-mentioned problem and only taking into account the decision variable values at the current discrete-time instant.

4.3 Interconnected Energy Hubs

The above model can be extended in order to perform equivalent analyses in networked EHs which share different resources. Let $\mathcal{H}$ represent the set of N_h networked EHs, h one of those EHs and h' any different one. Note also that N_i and N_o can take different values in each EH depending on their number of input and output flows, so they will be expressed as function of h in the following paragraphs. Since Equations (4.1) and (4.2) need to be satisfied in each EH, they can be arranged into Equations (4.26) and (4.27) to consider the existence of such network and multiple EHs,

$$\begin{aligned} \boldsymbol{\delta_O}(k,h)\boldsymbol{O}(k,h) + \boldsymbol{M}(k,h) + \sum \boldsymbol{N}_{h,h'}(k,h) = \\ = \boldsymbol{C}(k,h)\boldsymbol{P}(k,h) - \boldsymbol{Q_{ch}}(k,h) + \boldsymbol{Q_{dis}}(k,h), \quad \forall h, h' \in \mathcal{H} : h' \neq h, \end{aligned} \tag{4.26}$$

$$\boldsymbol{I}(k,h) + \sum \boldsymbol{N}_{h',h}(k,h) = \boldsymbol{C_i}(h)\boldsymbol{P}(k,h), \quad \forall h, h' \in \mathcal{H} : h' \neq h, \tag{4.27}$$

where $\boldsymbol{N}_{h,h'}$ is the $N_o(h) \times 1$ vector of exported flows from h to h', and $\boldsymbol{N}_{h',h}$ is the $N_i(h) \times 1$ vector of imported flows from h' to h. Equations (4.3)–(4.16) would be as well particularised for each $h \in \mathcal{H}$ by simply changing the argument k for k, h in each term of these equations.

Moreover, as occurred with the production and storage limits in Subsections 4.1.1 and 4.1.2, the amount of resources exchanged between EHs need to be constrained according to the capacities of the network. Equations (4.28) and (4.29) set the maximum and minimum amount of imports and exports, respectively, whereas Equation (4.30) avoids bidirectional flows from happening,

$$\boldsymbol{N}^{min}_{h',h}(k,h)\boldsymbol{\delta_{h',h}}(k,h) \leq \boldsymbol{N}_{h',h}(k,h) \leq \boldsymbol{N}^{max}_{h',h}(k,h)(k)\boldsymbol{\delta_{h',h}}(k,h), \qquad \forall h,h' \in \mathcal{H} : h' \neq h, \tag{4.28}$$

$$\boldsymbol{N}^{min}_{h,h'}(k,h)\boldsymbol{\delta_{h,h'}}(k,h) \leq \boldsymbol{N}_{h,h'}(k,h) \leq \boldsymbol{N}^{max}_{h,h'}(k,h)(k)\boldsymbol{\delta_{h,h'}}(k,h), \qquad \forall h,h' \in \mathcal{H} : h' \neq h, \tag{4.29}$$

$$\boldsymbol{\delta_{h',h}}(k,h) + \boldsymbol{\delta_{h,h'}}(k,h) \leq \mathbf{1}, \quad \forall h,h' \in \mathcal{H} : h' \neq h, \tag{4.30}$$

where the superscripts “max” and “min” refer to the upper or lower limit of each vector, $\delta_{h',h}$ is the $N_i(h) \times N_i(h)$ binary diagonal matrix of imported flow activation from h' to h, and $\delta_{h,h'}$ is the $N_o(h) \times N_o(h)$ binary diagonal matrix of exported flow activation from h to h'. Equation (4.30) allows the transmission losses to be taken into account, whenever they need to, as is the case for most energy exchanges,

$$\boldsymbol{N}_{h',h}(k,h) = \boldsymbol{C}_N(k,h,h')\boldsymbol{N}_{h',h}(k,h'), \quad \forall h,h' \in \mathcal{H} : h' \neq h, \tag{4.31}$$

where $\boldsymbol{C}_N(k,h,h')$ is the $N_i(h) \times N_o(h')$ diagonal matrix of transmission efficiencies from h' to h, and $\boldsymbol{N}_{h',h}$ is the $N_o(h') \times 1$ vector of exported flows from h' to h.

Finally, the cost function would require to be modified in consonance to the desired strategy to manage the set of EHs. The simplest case consists in considering a centralised approach in which the objective is to minimise the total cost, without additional terms related to the use of the network nor considering particular interests of each EH, which leads transforming Equation (4.25) into Equation (4.32),

$$\begin{aligned} \min \quad & \sum_{h \in \mathcal{H}} \sum_{k=0}^{H-1} (\boldsymbol{c}(k,h)\boldsymbol{I}(k,h) - \boldsymbol{s}(k,h)\boldsymbol{M}(k,h)) \\ \text{s.t.} \quad & \text{Equations (4.3)–(4.16) particularised for each } h, \\ & \text{Equations (4.26)–(4.31).} \end{aligned} \tag{4.32}$$

4.4 Conversion and Capacity Models

The element of the vectors that bound the flows within the energy hub (denoted with the superscripts “max” and “min”) and of the coupling matrices that contain values of efficiencies (denoted with the letter “C”) are defined in coherence with the physical component that they represent. Most common values in the above matrices and vectors are defined by setting the lower bound to zero and the upper bound to infinite for unconstrained flows, and setting the efficiencies to zero (instead of minus infinite, which would lead to having undesirable reverse flows) when there is no possible flow among devices/EHs or to one in lossless conversion/transportation processes. Many other the processes occurring in the EH are actually characterised as having complex dynamics which cannot be entirely reflected in the above equations without these being reformulated, affecting how the former parameters are defined.

Such issues have been already tackled, for example, by Evins et al. who proposed methods to prevent devices from starting up too frequently and to turn the nonlinear dynamic of load-dependent efficiencies into step-wise curves. In order to keep things simple, the approach of this thesis lies in using constants, usually from manufacturers' specifications and considering that they cover the main range of operation of each device; or time-variant coefficients, which should be deductible from the models that dictate the behaviour of each process. The latter one is the reason why the parameters of the model presented in Equations (4.1)–(4.16), and so the ones in Section 4.3, depend on k. This is relevant to both the PV facilities and the fields of solar collectors, whose production along the day, needs to be calculated with the models presented in the next chapter.

4.5 Conceptual Models of CHROMAE's Energy Hubs

Although the use of the proposed modelling framework is further exemplified in Chapter 7, this section sketches out the main elements of the facilities presented in Chapter 3 as help for configuring them in the developed software library, a task to be accomplished by the staff involved in the CHROMAE project. Apart from defining the parameters of each equipment as clarified in the previous section, either by using constant or time-variant coefficients, it is important to determine, as a first step, the variables representing the structure of the system to be defined (see Section 4.1): input flows, output flows, market sales flows, and conversion/storage devices. Be aware of the fact that the following descriptions are only based on the basic elements of each EH, as depicted in Figure 4.3, and therefore these structures might well increase in complexity if a more precise model of the processes is required (for example, in the following cases the electric consumption associated with some of the impulsion systems, such as air conditioning units', has been disregarded or included as part of a general load). In addition, note that some conversion devices are related to as many identifiers (without mathematical style, since they are not variables by themselves) as their number of outputs because they are split into two virtual devices (with a single output) for modelling purposes.

- Traditional greenhouse (h1). Inputs: (I_1), propane (I_2) and biomass (I_3) from local suppliers, and water from the public network (I_4). Outputs: electricity to operate the actuators (O_1), thermal power (O_2) and CO_2 (O_3) for the inside climate, electricity for the CO_2's impulsion pump (O_4), irrigation water demand (O_5), electricity for the irrigation pump (O_6), electricity to discharge the water well (O_7). Market sales: surplus CO_2 released into the atmosphere (M_3). Devices: GP 95 propane heater (D_1), Missouri 150000 multi-fuel boiler (D_2 and D_3), and irrigation pump (D_4).
- Industrial greenhouse (h2). Inputs: electricity from the grid (I_1), solar radiation (I_2), biomass from local suppliers (I_3), and water from the public network (I_4). Outputs: electricity to operate the actuators (O_1), thermal power (O_2) and CO_2 (O_3) for the inside climate, electricity for the CO_2's impulsion pump (O_4), irrigation water demand (O_5), electricity for the irrigation pump (O_6), electricity to discharge the water well (O_7). Market sales: surplus CO_2 released into the atmosphere (M_3). Devices: solar collectors (D_1), Missouri 150000 multi-fuel boiler (D_2 and D_3), and irrigation pump (D_4).
- CIESOL building (h3). Inputs: electricity from the grid (I_1), solar radiation (I_2 and I_3), propane from local suppliers (I_4), and water from the public network (I_5). Outputs: electricity for the building's equipment (O_1), cooling (O_2) and heating (O_3) thermal power for the inside climate, sanitary water demand (O_4). Devices: Atersa PV modules (D_1), Solaris solar collectors (D_2, YAZAKI absorption machine D_3), Ciatesa reversible heat pump (D_4 and D_5), and auxiliary heater (D_6).

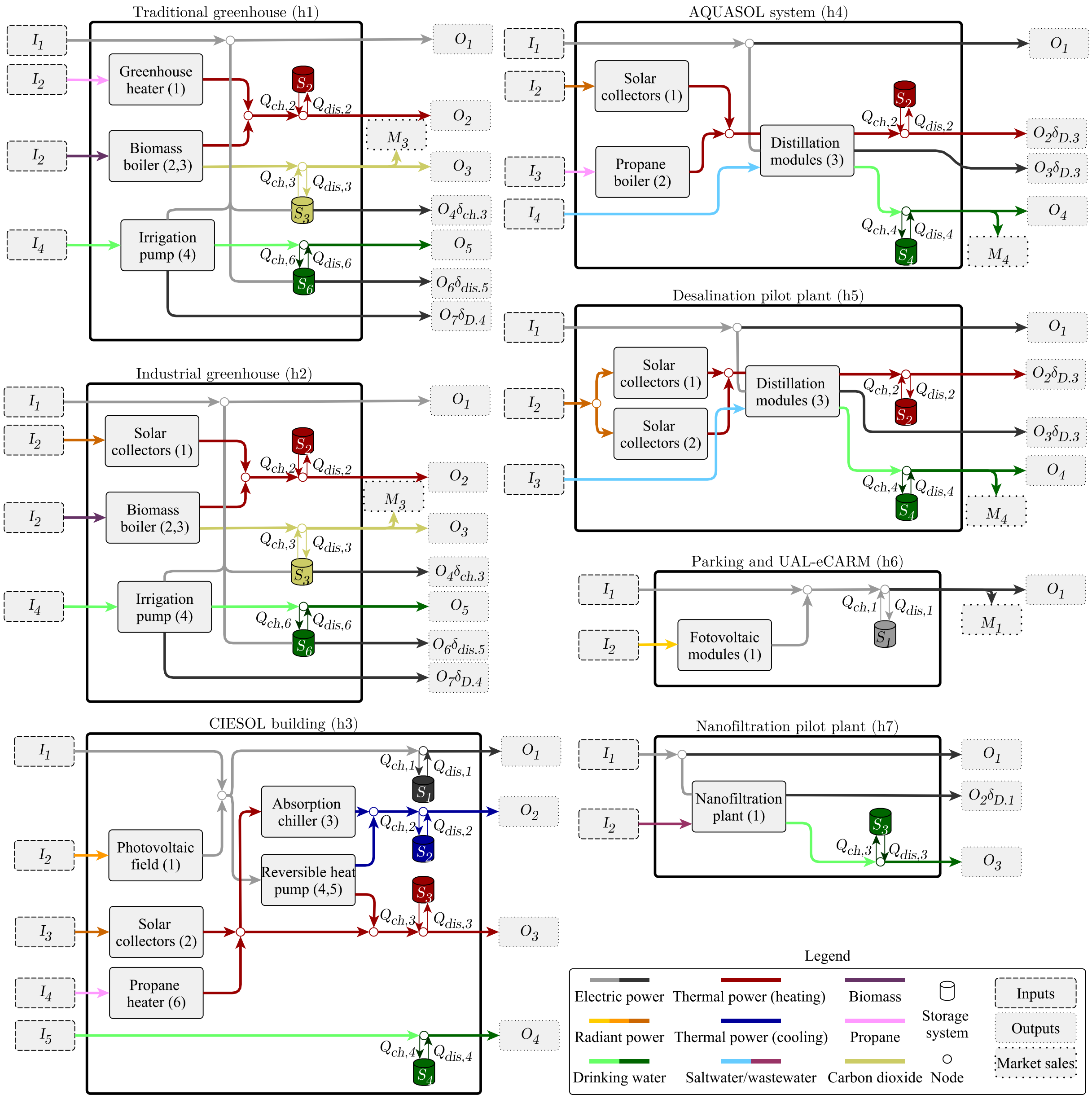

Figure 4.3. Structures of the EHs distinguished in the CHROMAE project

- AQUASOL system (h4). Inputs: electricity from the grid (I_1), solar radiation (I_2), propane from local suppliers (I_3), and artificial seawater for experimentation (I_4). Outputs: electricity to operate the actuators (O_1), thermal power (O_2) and electricity (O_3) for the distillation modules, distilled water demand (O_4). Market sales: distilled water sold through the public network (M_4). Devices: Wagner solar collectors (D_1), ATTSU fire-tube steam boiler (D_2), and distillation modules (D_3).
- Desalination pilot plant (h5). Inputs: electricity from the grid (I_1), solar radiation (I_2) and artificial seawater for experimentation (I_3). Outputs: electricity to operate the actuators (O_1), thermal power (O_2) and electricity (O_3) for the distillation modules, distilled water demand (O_4). Market sales: distilled water sold through the public network (M_4). Devices: Solaris solar collectors (D_1), Wagner solar collectors (D_2), and distillation modules (D_3).
- Parking and UAL-eCARM (h6). Inputs: electricity from the grid (I_1) and solar radiation (I_2). Outputs: electricity demand (O_1). Market sales: electricity sold through the grid (M_1). Devices: fotovoltaic modules (D_1).

- Nanofiltration pilot plant (h7). Inputs: electricity from the grid (I_1) and artificial wastewater for experimentation (I_2). Outputs: electricity to operate the actuators (O_1), electricity for the nanofiltration modules (O_2), purified water demand (O_3). Market sales: purified water sold through the public network (M_3). Devices: nanofiltration modules (D_1).

4.6 Contributions and Related Publications

This chapter encompasses two of the main contributions of this thesis, as introduced in Section 1.4, which are the ones related to the formulation of a generic modelling framework and the formalisation of the control problem. Note that the above-presented framework is applicable to EHs or MESs of diverse nature, complexity, time-scale and arbitrary topology, and no restrictions have been placed on the particular objective function, which could be selected according to other criteria different from the economic one. Except for the content of Subsection 4.1.4, the rest of Sections 4.1 and 4.2 constitutes part of the paper published in Applied Energy [41] and gave rise to some of the analyses presented in conferences [46, 48, 49, 51, 52]. In particular, one of them, with a formerly adopted approach based on MINLP [49], led to the current formulation of the problem employing MILP, and the other are applications of the proposed modelling framework to different case studies. Subsection 4.1.4 was developed and introduced in ODEHubs later, but it is equally part of the paper published in Sustainability [44], in which the software library is described as well. Both Sections 4.3 and Sections 4.5 were presented as part of a case study in the X Iberian Congress on Agro-Engineering [43] and, although it has not been are not incorporated in ODEHubs, it is expected that the fundamentals of networked EHs analysed in Section 4.3 help to include this capability in a future release. The content of Section 4.4 has not been presented as is in any of the publications, but still has quite a lot of illustrative value for the following chapters.

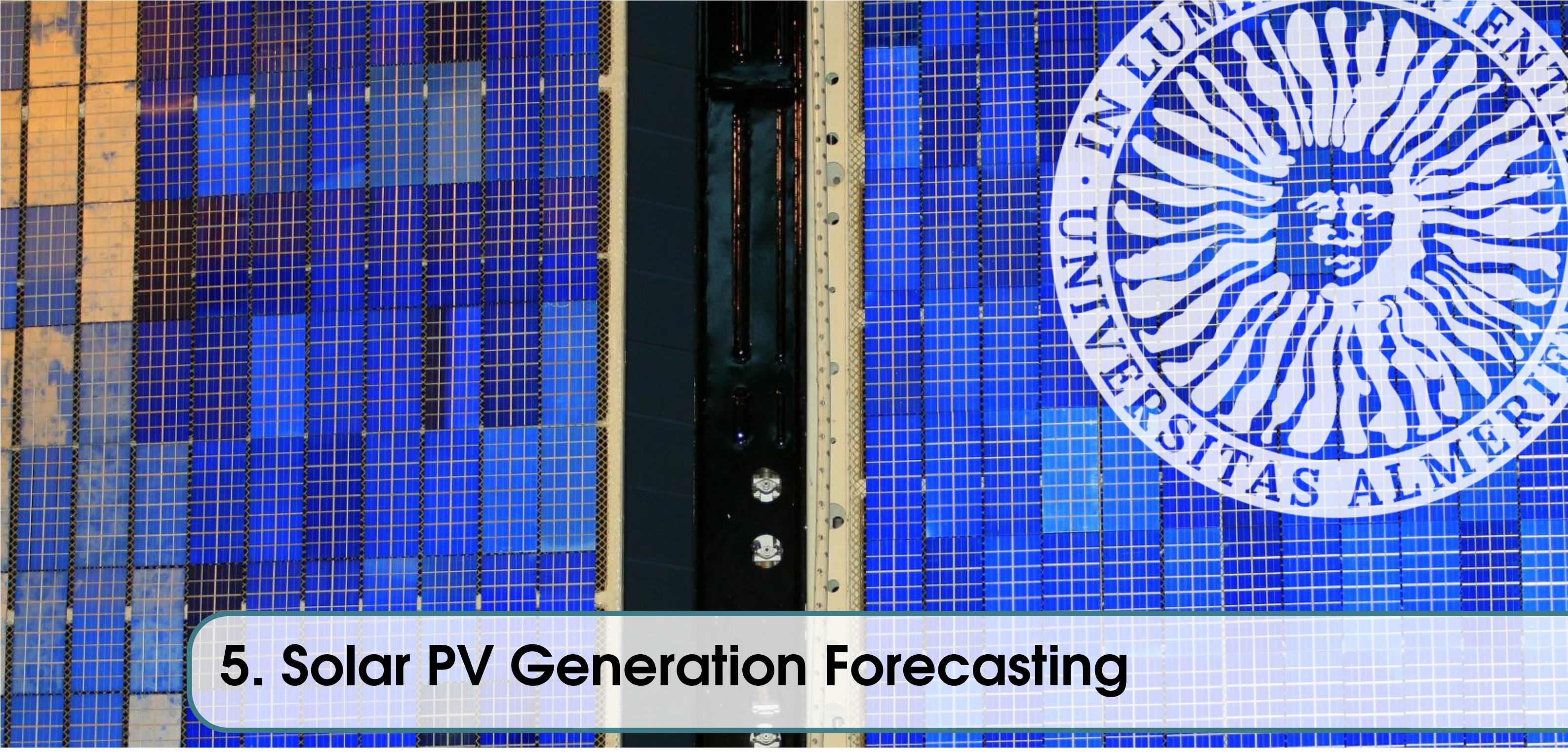

5. Solar PV Generation Forecasting

Chapter Summary

Photovoltaic (PV) production is especially relevant for the ENERPRO and CHROMAE projects and, also in order to provide an example of dealing with time-variant coefficients (bear in mind Section 4.4), in this chapter the models employed to calculate its estimate are presented. Section 5.1 specifies how PV fields can be integrated within the proposed modelling framework. Sections 5.2 and 5.3 introduce the main first principles models that have been well established in the literature for solar radiation on sloped surfaces and for photovoltaic (PV) cells, respectively. Section 5.4 details the arrangements made to consider the inversion and transmission losses in the photovoltaic (PV) facilities, including curve fitting for some of the parameters. Finally, in Section 5.5 real data is employed to test the validity of the parameters characterised in the previous sections.

5.1 Time-Variant Coefficients for PV Facilities

Considering a uniform sample time $T = t(k+1) - t(k)$, where k constitutes any discrete time instant, as in Chapter 4, the relationship between the incident radiation on an array of PV modules, the amount of direct current (DC) power produced by them, and the one supplied to the alternating current (AC) grid can be obtained by arranging Equation (23.7.1) from Duffie and Beckman's book into Equation (5.1),

$$P_{c,ac}(k) = G_T(k) A_c \eta_{c,mpp}(k) \eta_{c,inv}(k) \eta_{c,ac}, \tag{5.1}$$

where $P_{c,ac}$ is the amount of AC power supplied to the grid by the array, G_T is the incident solar irradiance on the (tilted) surface of the array c (see Section 5.2 for calculations), A_c is the total area of the array c (see Section 5.3 for technical information), $\eta_{c,mpp}$ is the maximum power point efficiency of the of the array c (see Section 5.3 for calculations), $\eta_{c,inv}$ is the efficiency of the inverter connected to the array c (see Section 5.4 for calculations), and $\eta_{c,ac}$ is the transmission efficiency from the inverter to the point of supply of the array c (see Section 5.4 for calculations).

The following sections describe the way these parameters are computed in the programmed code, and once their value is known, the transformation to the variables and constraints employed in Chapter 4 would be as stated in Equations (5.2) and (5.3) for a device D^{pv} representing the entire PV field with a set $\mathcal{F}$ of N_c arrays,

$$D_{i,pv}^{max}(k) = G_T(k) \sum_{c \in \mathcal{F}} A_c, \tag{5.2}$$

$$C_{pv}(k) = \sum_{c \in \mathcal{F}} \frac{\eta_{c,mpp}(k)\eta_{c,inv}(k)\eta_{c,ac}}{N_c}, \tag{5.3}$$

where $D_{i,pv}^{max}$ is the upper limit of the flow (solar radiation) entering the device (field) which will be an element of the $\boldsymbol{D_i^{max}}$ vector (see Chapter 4), and C_{pv} is the gross efficiency of the field which will be an element of the coupling matrices presented in Chapter 4.

5.2 Solar Irradiance on Sloped Surfaces

Although both the anisotropic and the isotropic sky model have been implemented, the validation and the case study presented in this thesis were carried out only using the second one, which is described below based on the explanations found in Duffie and Beckman's book [201]. Firstly, the total solar irradiance on a tilted surface is given by Equation (5.4),

$$G_T(k) = G_b(k)R_b(k) + G_d(k)\frac{1+\cos\beta}{2} + G(k)\rho_g\frac{1-\cos\beta}{2}, \tag{5.4}$$

where G_b is the beam horizontal irradiance (BHI), G_d is the diffuse horizontal irradiance (DHI), G is the global horizontal irradiance (GHI), that is, the sum of $G_b(k)$ and $G_d(k)$, R_b is the ratio of beam radiation on a tilted plane to that on the plane of measurement (usually horizontal), ρ_g is the ground reflectance (assumed to be of 0.1), and β is the slope angle of the modules.

To forecast the production, it is necessary to know the three terms of the irradiance on the horizontal plane, which in practice can be provided by organisms such as the Spanish National Weather Agency AEMET. For the validation presented in this section, the historical data recorded by the CIESOL's weather station were used instead. In either case, the beam irradiance tends to be indirectly determined from the direct normal irradiance (DNI) on the horizontal plane (or direct beam irradiance), which is the magnitude actually measured by the pyrheliometers. Their relationship is given by Equation (5.5),

$$G_b(k) = G_{bn}(k)\cos\theta_z, \tag{5.5}$$

where G_{bn} is the direct normal irradiance (DNI), and θ_z is the zenith angle.

Except $\rho_g(k)$ and the irradiances, the rest of variables appearing in Equation (5.4) are geometrical parameters to take into account the position of the sun in the sky, which are related by means of Equations (5.6), (5.7), and (5.8),

$$R_b(k) = \frac{\cos\theta(k)}{\cos\theta_z(k)}, \tag{5.6}$$

$$\begin{aligned}\cos\theta(k) = {} & \sin\delta(k)\sin\phi\cos\beta - \sin\delta(k)\cos\phi\sin\beta\cos\gamma + \cos\delta(k)\cos\phi\cos\beta\cos\omega(k) \\ & + \cos\delta(k)\sin\phi\sin\beta\cos\gamma\cos\omega(k) + \cos\delta(k)\sin\beta\sin\gamma\sin\omega(k),\end{aligned} \tag{5.7}$$

$$\cos\theta_z(k) = \sin\delta(k)\sin\phi + \cos\delta(k)\cos\phi\cos\omega(k), \tag{5.8}$$

where θ is the angle of incidence, γ is the surface azimuth angle or deviation between the orientation of the field and the south (east negative and west positive), ϕ is the latitude where the field is located (south negative and north positive), δ is the declination of the sun, which measures the displacement of the sun due to translation of the earth, and ω is the hour angle, which measures the displacement of the sun due to rotation of the earth. Note that Equation (5.8) correspond to Equation (5.7) particularised for $\beta = 0°$, i.e. a horizontal surface.

Most of the above parameters depend on the design of the field and are constants since these fields are supposed to be static (without solar tracking), but for the rest Equations (5.9)–(5.13) provide the way to calculate them from ordinary variables such as time and day,

$$\delta(k) = 23.45 \sin\left(360 \frac{284 + DoY(k)}{n_{days}(k)}\right), \tag{5.9}$$

$$\omega(k) = 360 \frac{h_s(k) - 12}{24}, \tag{5.10}$$

$$h_s(k) = h_o(k) + \frac{24}{360}(\psi_{ref} - \psi) + \frac{1}{3600} EoT(k) - DST(k), \tag{5.11}$$

$$\begin{aligned} EoT(k) = 13.752(0.075 + 1.868 \cos B(k) - 32.077 \sin B(k) \\ - 14.615 \cos 2B(k) - 40.89 \sin 2B(k)), \end{aligned} \tag{5.12}$$

$$B(k) = (1 - DoY(k))360/n_{days}(k), \tag{5.13}$$

where DoY is the day of the year (from 1 to 365 or 366), n_{days} is the total number of days of the year (365 or 366, depending on if it is a leap year or not), h_s is the solar time (expressed in hours), h_o is the official time (expressed in hours), ψ is the longitude where the field is located (from 0 to 360 degrees west), ψ_{ref} is the longitude of the standard meridian for the local time zone (from 0 to 360 degrees west), EoT is the result of evaluating the so-called Equation of Time (expressed in seconds), DST is the offset due to daylight saving time (expressed in hours), and B is the relative day for the Equation of Time.

In above and the following equations, when sunrise (or sunset) occurs at time k or nearly that time the cosine of θ_z will tend zero and therefore R_b will take very large values that tend to infinite [201]. Since they are employed to obtain the integrated production between two time steps (usually one-hour intervals), the procedure to avoid that problem consist in calculating the above variables for the midpoint of each interval, which in such cases must range from the sunrise to the end of the time step (or from the start of the time step to the sun set), similar as TRNSYS software does [224]. On the other hand, the parameters of the fields employed in the validation are recapped in Table 5.1 from Chapter 3.

Table 5.1. Location and geometry of the PV fields

Parameter	**Parking**	**CIESOL**
Latitude (ϕ)	36.83º	36.83º
Longitude (ψ)	-2.40º	-2.41º
Slope (β)	7º	22º
Orientation (γ)	-21º	-21º

5.3 Equivalent Circuit for Photovoltaic Cells

The model of the equivalent circuit for PV cells "can be used for an individual cell, a module consisting of several cells, or an array consisting of several modules" [201], and it is easy to apply because the parameters required can be deduced from the ones given by the manufacturers at standard conditions ($G_{st} = 1000\ W/m^2$, $T_{m,st} = 25\ °C$). Considering the four types of PV modules described in Chapter 3, Atersa A-222P (M1), Conergy PA 240P (M2), Conergy Power Plus 240M (M3), First Solar FS-380 (M4), the characteristics from their datasheet required to fit the model are presented in Table 5.2.

Table 5.2. Technical characteristics of the PV modules at standard conditions

Parameter	**M1**	**M2**	**M3**	**M4**
Area of the module (A_m)	1.628 m^2	1.652 m^2	1.652 m^2	0.720 m^2
Number of cells (N_s)	60	60	60	154
Off-load voltage (V_{oc})	37.20 V	37.00 V	38.00 V	60.80 V
Short-circuit current (I_{sc})	7.96 A	8.54 A	8.45 A	1.88 A
Voltage at max. power point (V_{mpp})	29.84 V	30.20 V	30.89 V	48.5 V
Current at max. power point (I_{mpp})	7.44 A	7.95 A	7.90 A	1.65 A
Temperature coeff. for V_{oc} ($\mu_{V,oc}$)	-0.35 %/ºC	-0.32 %/ºC	-0.34 %/ºC	-0.27 %/ºC
Temperature coeff. for I_{sc} ($\mu_{I,sc}$)	0.05 %/ºC	0.04 %/ºC	0.06 %/ºC	0.04 %/ºC
NOCT* ($T_{m,NOCT}$)	47 ºC	45 ºC	48 ºC	45 ºC

*Normal operating cell temperature (NOCT) at $G_{NOCT} = 800\ W/m^2$ irradiance, $T_{a,NOCT} = 20\ °C$ ambient temperature, and wind speed of 1 m/s. This is the only parameter not measured at standard conditions.

On the other hand, the model of the equivalent circuit is given by the five parameters shown in Equation (5.14), from which the $I - V$ curve can be obtained,

$$I(k) = I_L(k) - I_o(k)\left[e^{\left(\frac{V(k)+I(k)R_s(k)}{a(k)}\right)} - 1\right] - \frac{V(k) + I(k)R_s(k)}{R_{sh}(k)}, \qquad (5.14)$$

where I_L is the light current, I_o is the diode reverse saturation current, R_s is the series resistance, R_{sh} is the shunt resistance, a is the modified ideality factor of the diode, I is the current generated by the module and V is the voltage of the module. However, Equation (5.14) is not valid for any situation, but its parameters need to be updated according to the operating conditions and the technical characteristics of the PV modules. Duffie and Beckman describe the procedure to do so, although this is not reproduced here because Simulink® and its *PV Array* block were used instead to transform Table 5.2 into Table 5.3, which contains the five parameters at reference conditions (in this case, the standard conditions at which the manufacturer made the measurements of Table 5.2). Note that a_{st} is not obtained directly but by means of Equation (5.15), according to the definition of that parameter that the authors give [201],

$$a_{st} = k_B n_d T_{m,st} N_s / q, \qquad (5.15)$$

where k_B is the Boltzmann constant ($1.381 \cdot 10^{-23}$ J/K), n_d is the ideality factor of the diode (as provided by *PV Array*), $T_{m,st}$ is the temperature of the module at standard conditions (25 ºC), N_s is the number of cells of the module (see Table 5.2), and q is the electronic charge ($1.602 \cdot 10^{-19}$ C).

Table 5.3. Parameters of the equivalent circuit at standard conditions for the PV modules

Parameter	**M1**	**M2**	**M3**	**M4**
Light current ($I_{L,st}$)	7.97 A	8.56 A	8.46 A	1.93 A
Diode reverse saturation current ($I_{o,st}$)	0.186 nA	0.0639 nA	0.140 nA	1.64 pA
Series resistance ($R_{s,st}$)	0.39 Ω	0.31 Ω	0.32 Ω	3.31 Ω
Shunt resistance ($R_{sh,st}$)	280 Ω	162 Ω	237 Ω	263 Ω
Modified ideality factor of the diode (a_{st})	1.52 V	1.45 V	1.53 V	2.20 V

From Table 5.3, the five parameters of Equation (5.14) can be updated at each time step, considering the relationships given by Equations (5.16)–(5.21),

$$\frac{a(k)}{a_{st}} = \frac{T_m(k) + 273}{T_{m,st} + 273}, \tag{5.16}$$

$$I_L(k) = \frac{S_T(k)}{S_{T,st}}[I_{L,st} + \mu_{I,sc}(T_m(k) - T_{m,st})], \tag{5.17}$$

$$\frac{I_o(k)}{I_{o,st}} = \left(\frac{T_m(k) + 273}{T_{m,st} + 273}\right)^3 e^{\left(f_{eV}\frac{E_{g,st}}{k_B(T_{m,st}+273)} - f_{eV}\frac{E_g(k)}{k_B(T_c(k)+273)}\right)}, \tag{5.18}$$

$$\frac{E_g(k)}{E_{g,st}} = 1 - C_{T,Eg}(T_m(k) - T_{m,st}), \tag{5.19}$$

$$\frac{R_{sh}(k)}{R_{sh,st}} = \frac{S_{T,st}}{S_T(k)}, \tag{5.20}$$

$$R_s(k) = R_{s,st}, \tag{5.21}$$

where T_m is the temperature of the module, $T_{m,st}$ is the temperature of the module at standard conditions, E_g is the material bandgap energy, $E_{g,st}$ is the material bandgap energy at standard conditions (1.12 eV for silicon), f_{eV} is the conversion factor from electron-volts to joules ($1.602 \cdot 10^{-19}$ J/eV), $C_{T,Eg}$ is a fitting coefficient (0,0002677 $^{\circ}C^{-1}$ for silicon) [201], S_T is the effective irradiance absorbed by the module, and $S_{T,st}$ is the effective irradiance absorbed by the module at standard conditions. Note in these equations that temperatures must be introduced in Kelvin in Equations (5.16) and (5.18) and that, according to Table 5.2, $\mu_{I,sc}$ must to be multiplied by I_{sc} and divided by 100 in order to be transformed from percentage to absolute value (which some manufacturers provide too).

Regarding the last two parameters that would require to be determined in order to apply the above equations, the effective absorbed solar ratio ($S_T(k)/S_{T,st}$) is estimated by applying the Fresnel's equations and the Snell's law, as well as re-arranging Equation (5.4) to consider the effect of the air mass, the incidence angle and the spectroscopic behaviour of the materials. Readers are referred to Chapter 5 in Duffie and Beckman's book or to the conference paper related to this thesis for further information, but most of the parameters involved have been presented in Section 5.2 and the new ones required are related to the cover of the modules, which is made of glass. A glazing thickness of 3.2 mm, a glazing extinction coefficient of 4 m^{-1}, and an air-glass refractive index of 1.526 were considered in all cases.

On the other hand, the module temperature is calculated from Equation (5.22),

$$T_m(k) = T_a(k) + (T_{m,NOCT} - T_{a,NOCT})\frac{G_T(k)}{G_{NOCT}}\left(1 - \frac{\eta_{c,mpp}(k)}{0.9}\right), \tag{5.22}$$

where T_a is the ambient temperature, and the rest of parameters have been defined previously (see Table 5.2 for NOCT conditions). As the efficiency appears in this equation (all the modules forming an array are considered to have the same efficiency), the temperature of the module is obtained by iteratively computing the equations presented in this section from an initial guess of $\eta_{c,mpp} = 0.12$ and with a termination criterion based on the change of the efficiency, which must be less than 0.001 in two consecutive steps to force convergence ("since the module efficiency is not a strong function of temperature, the process will converge rapidly" [201]). Each new value is obtained assuming that the maximum power point is being tracked in the facilities and neglecting the effect of the wind on the module temperature in Equation (5.22). As demonstrated by Duffie and Beckman [201], differentiating Equation (5.14) with respect to V and setting the result equal to zero leads to Equation (5.23),

$$\frac{I_{mpp}(k)}{V_{mpp}(k)} = \frac{\frac{I_o(k)}{a(k)} e^{\left(\frac{V_{mpp}(k)+I_{mpp}(k)R_s(k)}{a(k)}\right)} + \frac{1}{R_{sh}(k)}}{1 + \frac{R_s(k)}{R_{sh}(k)} + \frac{I_o(k)R_s(k)}{a(k)} e^{\left(\frac{V_{mpp}(k)+I_{mpp}(k)R_s(k)}{a(k)}\right)}}, \tag{5.23}$$

where I_{mpp} is the current generated by the module at maximum power point, and V_{mpp} is the voltage of the module at maximum power point; and, on the other hand, Equation (5.14) needs to be satisfied at the same point, which results in Equation (5.24),

$$I_{mpp}(k) = I_L(k) - I_o(k) \left[e^{\left(\frac{V_{mpp}(k)+I_{mpp}(k)R_s(k)}{a(k)}\right)} - 1 \right] - \frac{V_{mpp}(k) + I_{mpp}(k)R_s(k)}{R_{sh}(k)}. \tag{5.24}$$

The simultaneous solution of both equations allows determining the maximum power point current and voltage, and therefore the efficiency of the array, as concluded in Equation (5.25),

$$\eta_{c,mpp}(k) = \frac{V_{mpp}(k)I_{mpp}(k)}{G_T(k)A_m(k)1000}. \tag{5.25}$$

5.4 Inversion and Transmission Losses

Owing to the heterogeneity of the available data and the differences found in the two facilities under study, the methods to calculate the inversion and transmission losses in this section rather provide a rough estimate of them, which for the purpose of the developed models will be enough.

On the one hand, CIESOL's data-set consist of minutely data from October 2013 to April 2017 of the inverters' electrical measurements (direct and alternating current, voltage and power) so that no transmission losses are considered because they are located very close to the PV field ($\eta_{c,ac} = 1$ for all the CIESOL's arrays). The inconvenience is that the manufacturer of those CICLO-3000 inverters does not offer information on their efficiency, and therefore they need to be determined from the above-mentioned measurements. Figure 5.1 shows the exponential curves fitted to the data of the three inverters, where some isolated samples and the ones corresponding to efficiencies greater than one have been eliminated, especially in the inverters 1 and 3. Despite being identical devices and arrays, the curves' parameters differ each other and although the correlation coefficients (R^2) are close to one, it would be advisable a more in-depth analysis, probably including additional variables such as the DC voltage (multiple regression), to improve these results. The main inconvenience would be that this equipment cannot be studied under laboratory conditions because it is part of the building's power supply system. Considering the actual results, the efficiency of each inverter is computed in Equation (5.3) after obtaining the amount of power produced by the array to which they are connected ($P_{c,dc}$) and substituting that value in the corresponding exponential curve (see Figure 5.1).

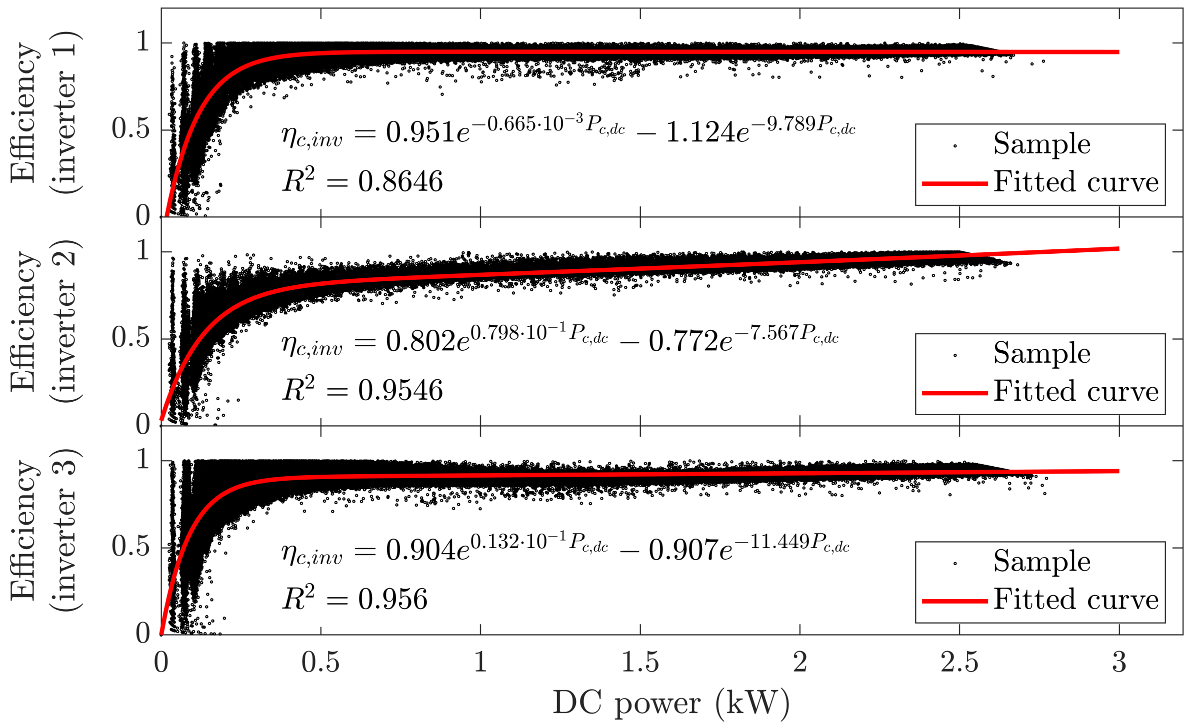

Figure 5.1. Curve fitting for the inverters of CIESOL's PV field

On the other hand, the data-set of the parking only contains the gross daily power produced from January 2013 to March 2014, measured by the general electric meter, and the monthly production of this one and the inverters, hence there is no way to certainly know any of the electrical variables related to the inverters nor the fields, required to better fit the model. Instead, the efficiency curves of the manufacturer are considered for each kind of inverter (Fronius Agilo 100 and Fronius IG+ 55v3, see Section 3.4), summarised in Table 5.4, and the transmission losses are approximated by means of a simple linear regression between the two monthly measurements, which leads to an efficiency of $\eta_{c,ac} = 0.978$ for all the parking's arrays (see Figure 5.2).

Table 5.4. Efficiencies of the parking's inverters as a function of the DC input voltage (minimum, nominal and maximum) and the AC output power, according to the manufacturer's datasheet

AC output power as percentage of the nominal value ($P_{inv,ac}$)	**Efficiencies in percentage** ($\eta_{c,inv}$) **Fronius Agilo 100 460 V / 640 V / 820 V**	**Fronius IG+ 55v3 230 V / 370 V / 500 V**
5% of $P_{inv,ac,r}$	90.5 / 88.3 / 84.8	90.5 / 91.6 / 89.9
10% of $P_{inv,ac,r}$	94.6 / 93.2 / 91.5	91.5 / 92.2 / 90.8
20% of $P_{inv,ac,r}$	96.6 / 95.7 / 94.7	93.4 / 93.6 / 93.3
25% of $P_{inv,ac,r}$	96.9 / 96.2 / 95.4	94.1 / 94.2 / 93.3
30% of $P_{inv,ac,r}$	97.0 / 96.5 / 95.7	94.4 / 94.5 / 93.8
50% of $P_{inv,ac,r}$	97.2 / 96.8 / 96.3	94.7 / 95.4 / 94.7
75% of $P_{inv,ac,r}$	96.9 / 96.6 / 96.1	95.2 / 95.7 / 95.0
100% of $P_{inv,ac,r}$	96.5 / 96.2 / 95.7	95.3 / 95.9 / 95.2

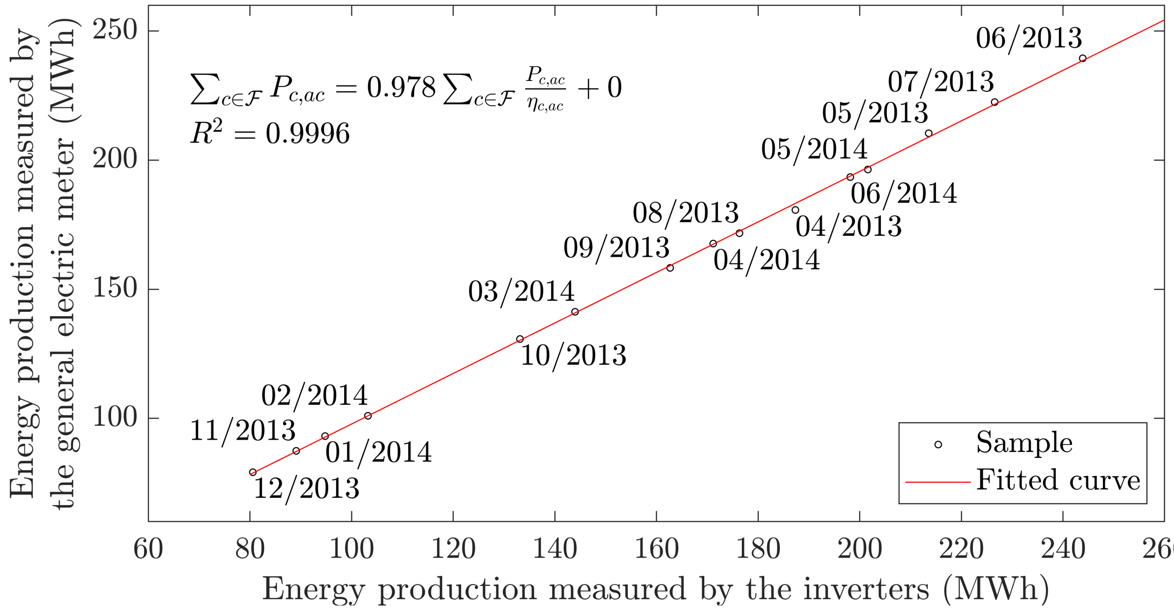

Figure 5.2. Curve fitting for the transmission losses of the parking's PV field

Since the arrays consist of modules of the same type, and neglecting any transmission loss occurring between the modules and the inverter's input, in each case the DC input voltage ($V_{c,dc}$) and power ($P_{c,dc}$) to the inverter can be obtained considering the fundamentals of Section 5.3, as expressed in Equations (5.26) and (5.27),

$$V_{c,dc}(k) = V_{mpp}(k)N_{se}, \tag{5.26}$$

$$P_{c,dc}(k) = V_{mpp}(k)I_{mpp}(k)N_{se}N_{pa}/1000, \tag{5.27}$$

where N_{se} is the number of modules connected in series, and N_{pa} is the number of modules connected in parallel. Note that curves in Figure 5.1 directly provide the value of the inverter's efficiency at each k, but, for the parking, several operations need to be carried out on the values of Table 5.4, as explained below.

- First, column 1 is expressed in terms of absolute values (instead of percentages of $P_{inv,ac,r}$) for each type of inverter, considering the AC nominal output powers given in Table 5.5.
- Second, for each voltage, and given the efficiencies of Table 5.4, it is possible to calculate the equivalent DC input power that would replace the values of column 1 by applying $P_{c,dc} = P_{inv,ac}/\eta_{c,inv}$.
- Third, from a double linear interpolation of the values yield by Equations (5.26) and (5.27), the actual efficiency of the inverter is obtained at each k.

Table 5.5. DC nominal input power and AC nominal output power of the parking's inverters, according to the manufacturer's datasheet

Nominal power values	**Fronius Agilo 100**	**Fronius IG+ 55v3**
DC input power ($P_{inv,dc,r}$)	104.4 kW	5.25 kW
AC output power ($P_{inv,ac,r}$)	100 kW	5 kW

5.5 Model Validation

In order to validate the above-presented model, different approaches were considered for CIESOL and the parking. In the first case, the daily mean error (ME), normalised root-mean-square error (NRMSE) and the coefficient of determination R^2 were calculated for the estimation of the generated power at a one-minute resolution, and normalised by the difference of the maximum and minimum values of the data, as stated in Equations (5.28), (5.29), and (5.30),

$$ME = \sum_{j=1}^{1440} \sum_{c \in \mathcal{F}} \frac{P_{c,ac}(j) - \hat{P}_{c,ac}(j)}{1440}, \tag{5.28}$$

$$NRMSE = \frac{\sqrt{\sum_{j=1}^{1440} \sum_{c \in \mathcal{F}} \frac{(P_{c,ac}(j) - \hat{P}_{c,ac}(j))^2}{1440}}}{\max(P_{c,ac}(j)) - \min(P_{c,ac}(j))}, \tag{5.29}$$

$$R^2 = 1 - \frac{\sum_{j=1}^{1440} \sum_{c \in \mathcal{F}} (P_{c,ac}(j) - \hat{P}_{c,ac}(j))^2}{(P_{c,ac}(j) - \sum_{j=1}^{1440} \sum_{c \in \mathcal{F}} P_{c,ac}(j)/1440)^2}, \tag{5.30}$$

where $P_{c,ac}(j)$ is the AC power produced by the array c at min j, and $\hat{P}_{c,ac}(j)$ is the estimate of the AC power produced by the array c at min j. Figure 5.3 shows a bar diagram containing the distribution of these indices over the period of time analysed, where the gaps between data correspond to missing or inconsistent samples (mainly unfeasible power values or incomplete records due to electrical outages, maintenance operations, or sensor failures). They are especially noticeable in the NRMSE because its value is always greater than 1,51, as summarised in Table 5.6, and therefore those gaps are easily identified by the absence of bars.

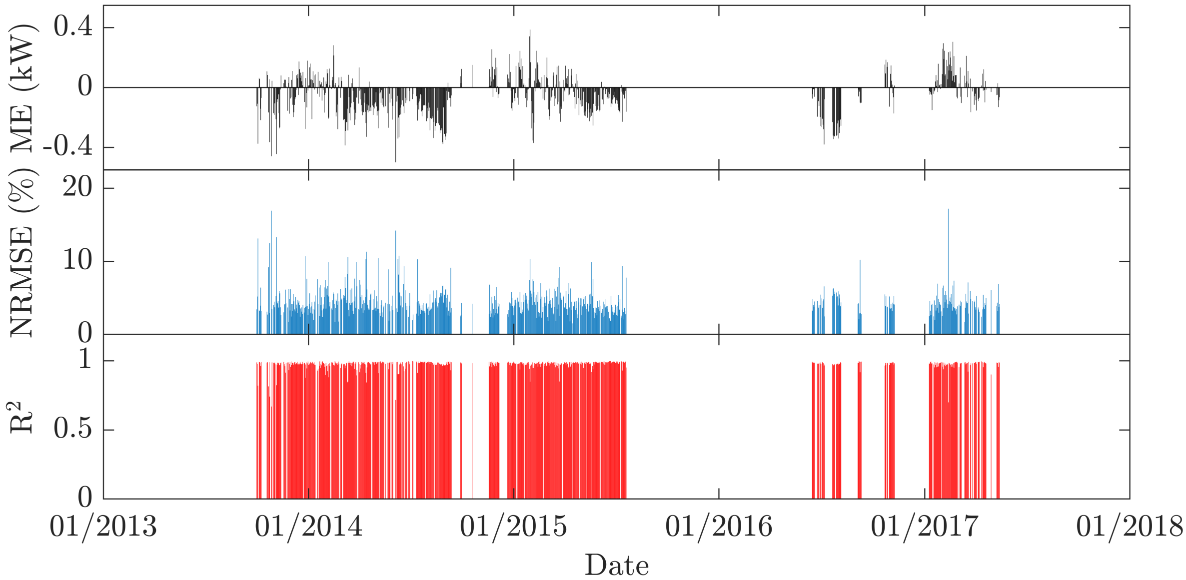

Figure 5.3. Distribution of the ME, NRMSE, and R^2 from the data available for CIESOL

In order to give a further idea of the fitting, Figure 5.4 presents both the worst and the best performing predictions in terms of absolute NRMSE (Figure 5.4a) and considering the same index but, as an additional condition to examine the performance with clear sky, only among the days in which the mean power generated is greater than 4 kW (Figure 5.4b); and, in Figure 5.5, the ordinary and cumulative probability distribution histograms (i.e. the frequencies of observations divided by the total number of samples) are also shown for the one-minute data.

Table 5.6. Reference values of the ME and the NRMSE for the fitted model (CIESOL)

Model fitting indicators	**Maximum**	**Minimum**	**Mean**	**Median**
ME	0.387 kW	-0.499 kW	-0.057 kW	-0.056 kW
NRMSE	17.19%	1.51%	4.51%	4.14%
R^2	0.9974	0.0072	0.9667	0.9824

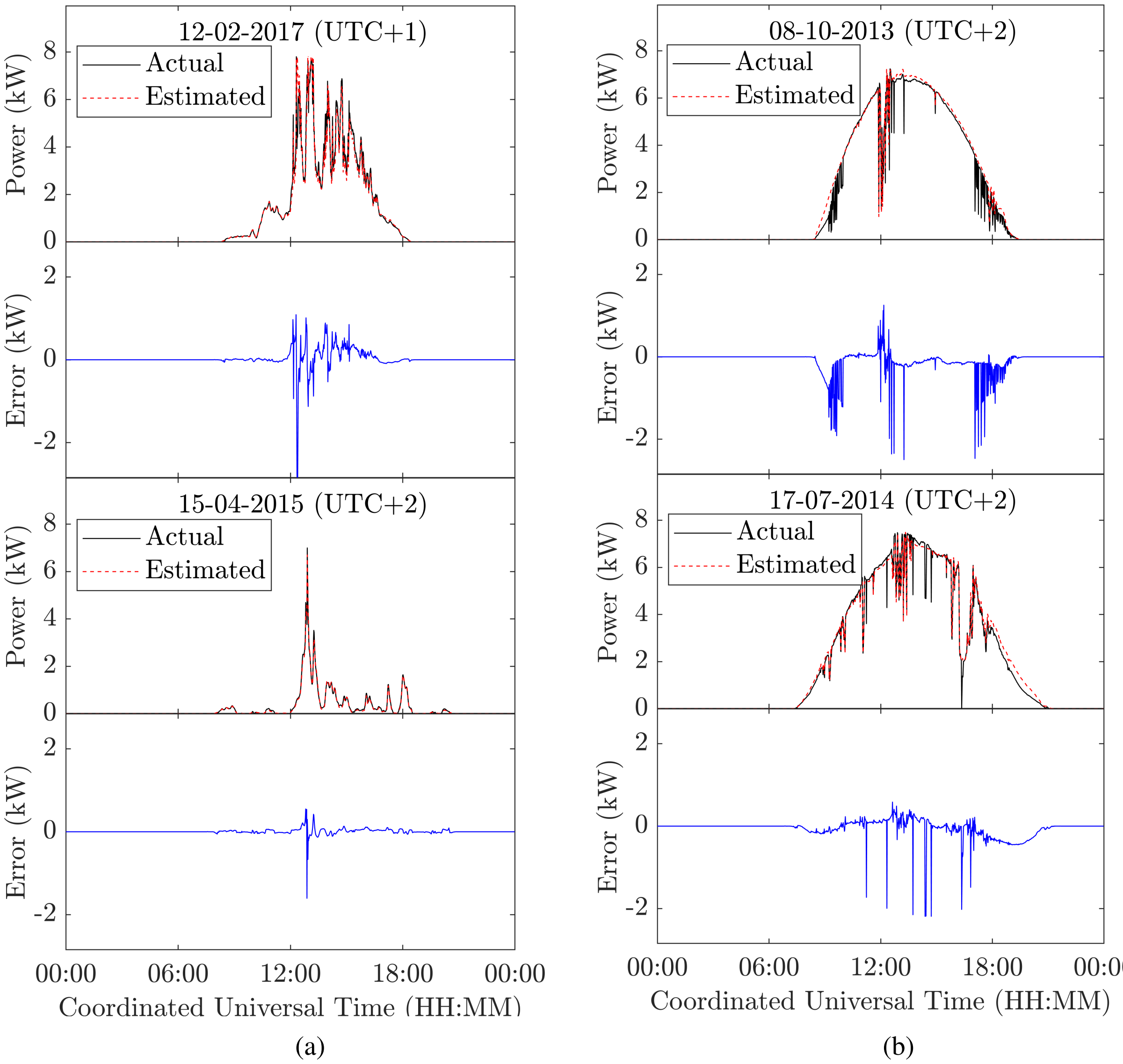

Figure 5.4. Worst (top) and best (bottom) validation for CIESOL's PV field in different days. The days were selected according to the absolute value of the NRMSE (a) and considering the same index but, as an additional condition to examine the performance with clear sky, only among the days in which the mean power generated is greater than 4 kW (b).

Note that the mean value of the ME is negative in the above results, which implies that the model tends to slightly overestimate the production. This confronts with the fundamentals of the isotropic sky, the usually conservative choice because the amount of radiation on sloped surfaces is underestimated.

Unfortunately, the facilities are not prepared to measure such magnitude directly, which would open the door to calibrate the equations presented in Section 5.2 separately and then they could be used as "ground truth" to do the same with the subsequent equations (the model presented in Section 5.3 could be as well validated with the DC magnitudes measured by the inverters). This suggests possibilities for improving the model which is still enough accurate for control purposes, especially if compared with similar values of the coefficient of determination found in the literature just for the model of the modules (equivalent to the Section 5.3 of this thesis): Zhou et al. validated their model with values ranging from 0.96 to 0.98 (single-diode model and data corresponding to four typical days) [225] and Ma et al. reached values of up to 0.998, which the authors recognise to be "much higher than those seen in the literature", by using a two-diode model and three example days [226]. The probability distribution histograms in Figure 5.5, constructed from 450948 samples and 672 intervals, also support these claims and shows an approximate symmetry of the error's distribution with respect to the mean value.

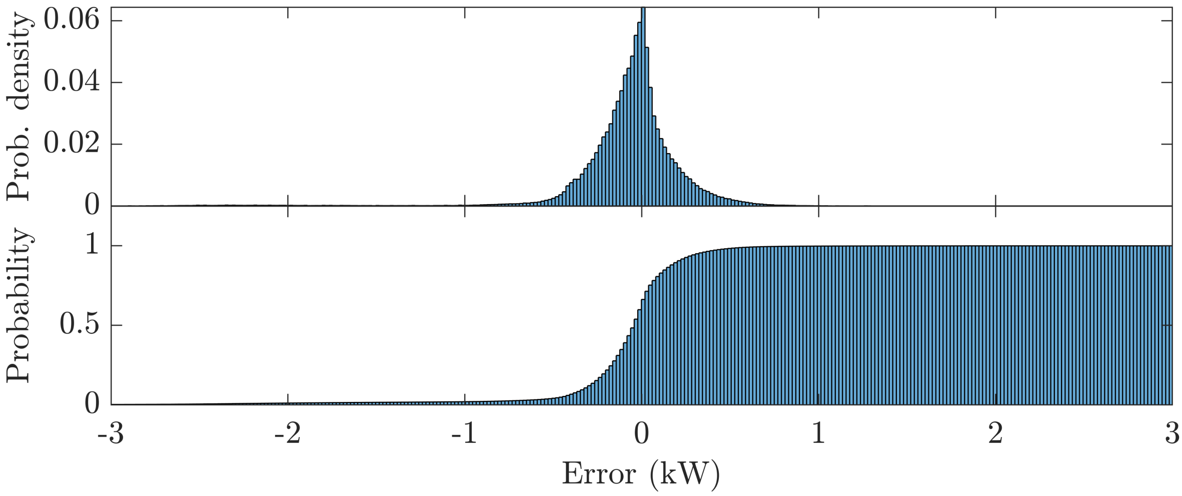

Figure 5.5. Ordinary and cumulative probability distribution histograms of the one-minute error for CIESOL's PV field

On the other hand, the results for the parking are encapsulated in Figure 5.6, which presents both the validation and the values of the indices defined above, which have been calculated for the whole period of data by changing the units and the amount of samples in Equations (5.28), (5.29), and (5.30), that is, using MWh instead of kW and replacing 1440 (the number of minutes in a day) by 292 (the number of days with consistent data). In comparison to CIESOL, the results are not hopeless because the model still provides a good estimate of the energy yield (see the 0.9524 coefficient of determination and the 5.6% NRMSE), although the mean error is again negative but significantly higher. The probability distribution histograms in Figure 5.7, constructed from 292 samples and 17 intervals, also reflect this deviation from the ideal zero mean value and shows again an approximate symmetry of the error's distribution with respect to this one. Counting with more concrete electric parameters and over a longer period would help to enhance the accuracy of these models, which is a pending issue for future research.

5.6 Contributions and Related Publications

The above sections present one of the contributions, as introduced in Section 1.4, corresponding to the practical knowledge of this thesis, which consists in the validation of the PV model for the research facilities. This is related with the projects' objectives and, in particular with the characterisation of the production in the above-presented plants (O2), hence the spotlight was put on this technology because the solar resource is their main RES but also one of the major sources of uncertainty. Moreover, at the time the doctoral student started to work on this, there were already calibrated models of the fields of solar collectors located in CIESOL [227] and the PSA [228], but none for the PV fields. The ones shown in this chapter will be employed in Chapter 7 to set the time-variant coefficients, i.e. the maximum amount of solar energy that can be transformed into electricity and the process's efficiency at a given time. The content of this chapter is the fruit of a publication in the XVI CEA Symposium on Control Engineering [50].

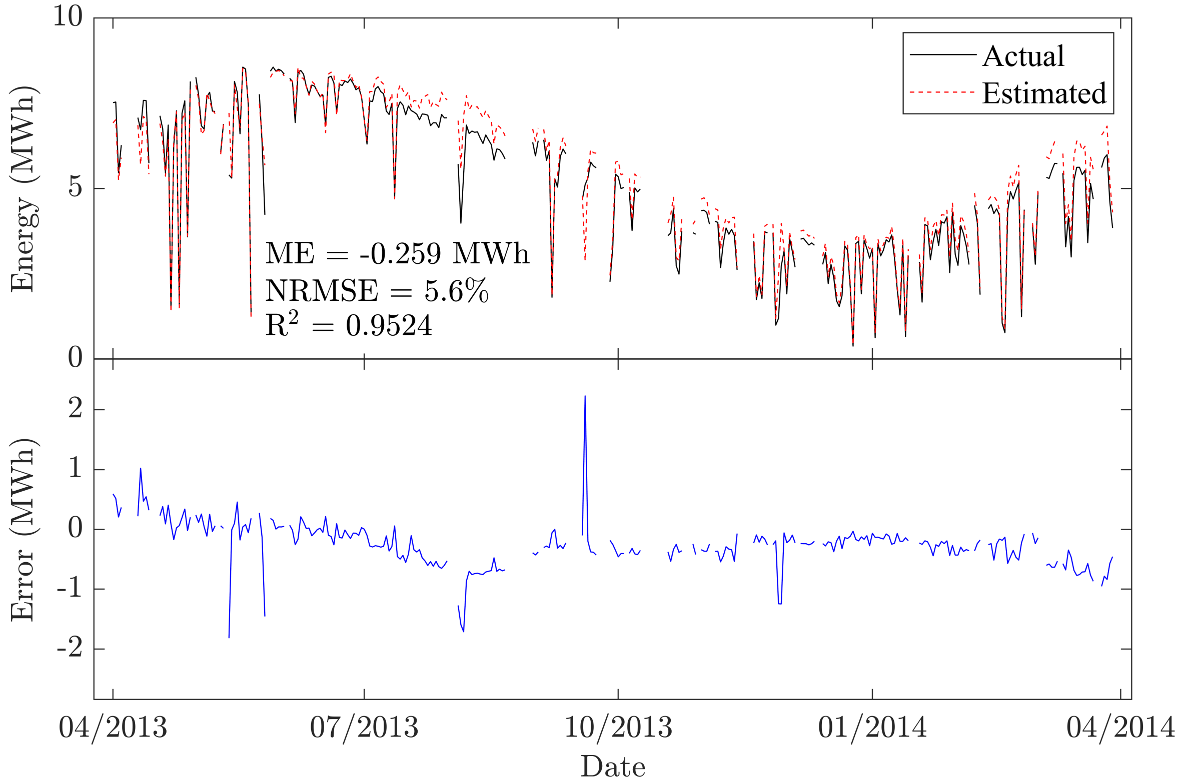

Figure 5.6. Validation for the parking's PV field over the period of data

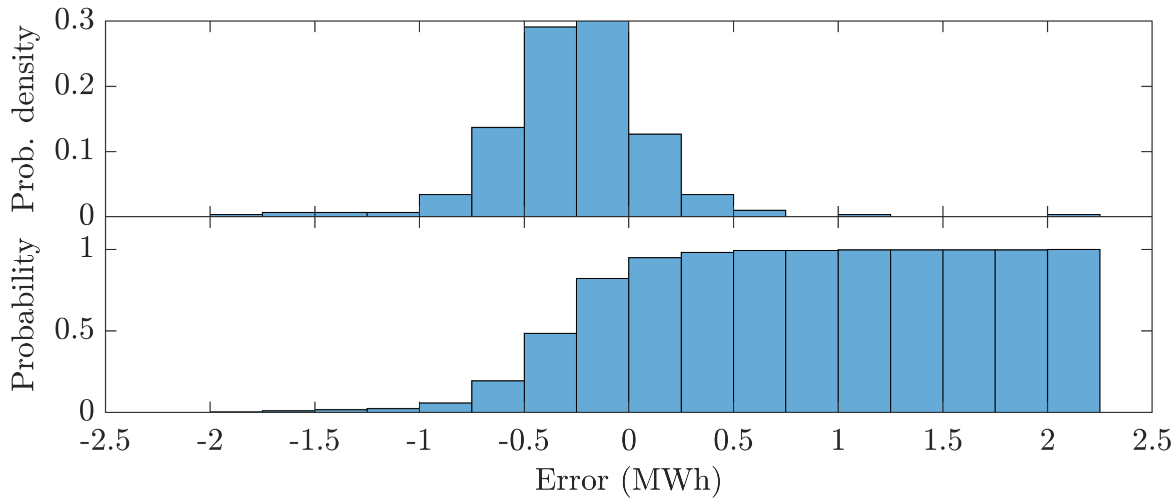

Figure 5.7. Ordinary and cumulative probability distribution histograms of the daily error for the parking's PV field

6. Software Implementation

Chapter Summary

As introduced in Chapter 4, the dispatch of energy and resources in EHs involves the definition and resolution of optimisation problems, which can be more easily done thanks to the toolbox presented in this chapter. Section 6.1 outlines its main characteristics, architecture, functions, and files. Section 6.2 describes the utility of the blocks implemented in a Simulink® library, which can be used to define the model of an EH within the proposed modelling framework, and their configurable parameters; Section 6.3 enlightens the main configuration parameters of ODEHubs that need to be defined for any simulation (regardless of the method employed to set the model); and Section 6.4 provides an introductory example of how to configure the model of a simple EH in Simulink®.

6.1 ODEHubs Toolbox

Given the alternatives presented in Subsection 2.1.4, the tool developed in this thesis, called ODEHubs, presents significant improvements with respect to those. First, multiple carriers can be considered in the dispatch problem thanks to the general model for EHs and MESs that has been incorporated and, what is more important, the system can be defined via Simulink® blocks, by analogy with its input–output graph representation, or with MATLAB® code. Second, it allows the users to choose between two optimisation modes and different solvers: on the one hand, MPC-based (receding horizon strategy) or scheduling (fixed horizon); on the other, the internal MATLAB® function *intlinprog*, so no third-party software installation is required, or any compatible external solver through YALMIP [88] (for instance CPLEX [82]). Finally, the set of MATLAB® and Simulink® files that compose this tool is freely available on Github (https://github.com/ual-arm/odehubs), together with the 'ready-to-use' data-set of the case study presented in Chapter 7. ODEHubs consists of a set of functions and files that allow obtaining the optimal dispatch or scheduling of any system that can be modelled according to the equations presented in Chapter 4.

Users can manually define the characteristics of an EH (number of elements, flow relationship, etc.) and configure certain parameters depending on their needs. In order to serve as a short guide for anyone interested in the tool, the main functions and settings are described in the following lines, considering the general flowchart of the software presented in Figure 6.1), although specific documentation will be made available on the website of the tool.

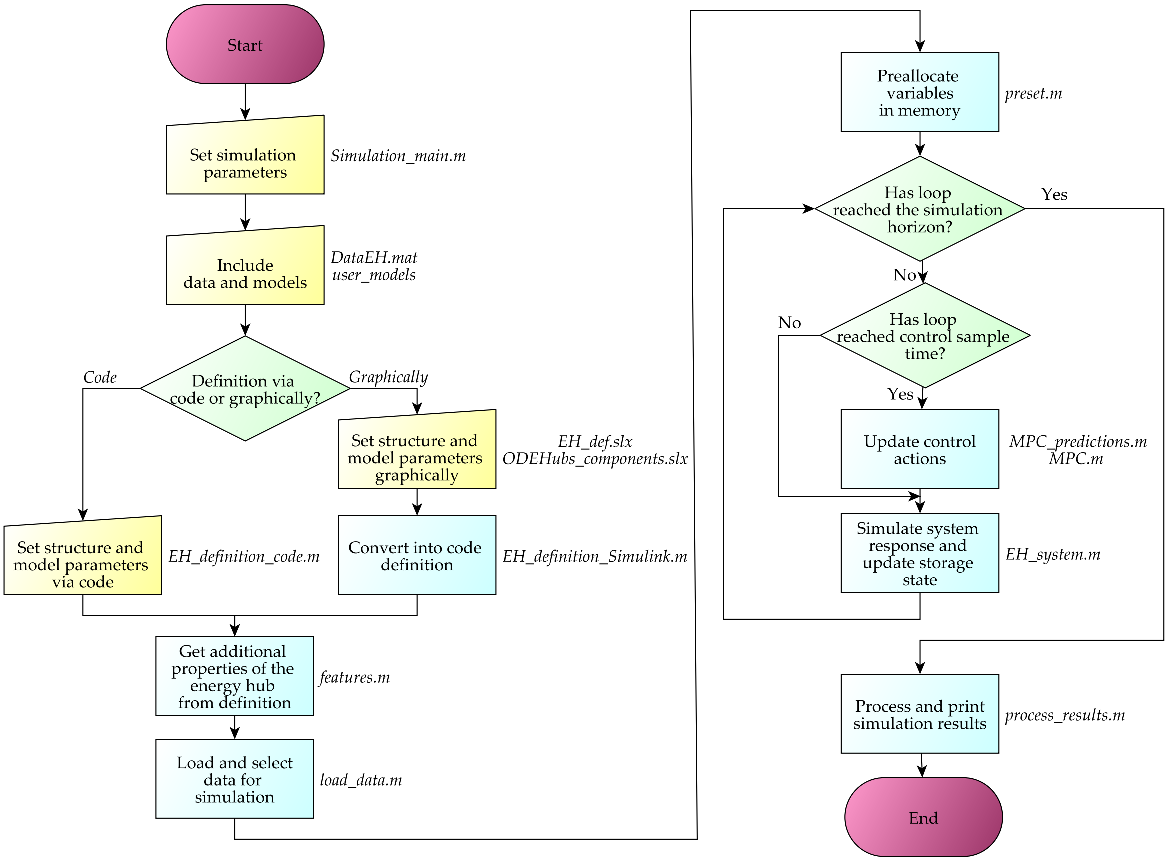

Figure 6.1. Flowchart of the Optimal Dispatch for Energy Hubs (ODEHubs) library that shows the processes involved in defining and simulating an EH and the main files or folders related to them (in italics)

The first step required to use ODEHubs, and from which the model is generated and adapted to be introduced in the optimisation solver, consists in defining the problem which involves manipulating three or four files, depending on whether the problem is defined graphically or by programming (see their names next to yellow trapezia in Figure 6.1). Except for *Simulation_main.m*, which is placed in the root directory, the rest of them can be found in the *definition* folder. Note also that although the manual procedures, which are described below, have been included sequentially in Figure 6.1, they are actually interchangeable.

- *Simulation_main.m* is the base of the flowchart and is where most functions are called. At the beginning of the file a set of parameters, whose use is clarified below, are declared and users might need to modify these lines prior to simulation. A *struct* variable called *EH* is created during its execution and used to store variables and communicate them to other functions.
- The folder *user_models* contains any function that users might need to define time-variable parameters in Equations (4.1)–(4.16) and in Equation (4.25). They need to be arranged following the syntax *parameter = function (data,date,samples,tm)*, so that *parameter* is a vector of values obtained from *data* (which is an automatically filtered version of *dataEH*) starting at the time declared in *date*, in each *tm* period of time during the horizon *samples*.

- *DataEH.mat* is a file, in the binary data container format that the MATLAB® program uses, with a single *timetable* variable called *dataEH* stored in it. This type of variable allows the grouping of column-oriented data in a table where each row represents a date and time. Thus, the columns consist of all the time-dependent variables required to simulate the system, such as the demanded outputs or weather conditions. Users are responsible for including the data that they need in this format, with the freedom to choose the name of each column/variable. Columns may be empty if no data are required to be loaded, but the *timetable* needs to be generated according to the simulation start time and horizon (see Section 6.3).
- *EH_definition_code.m* is the function employed to set the properties of the EHs, and it includes the parameters related to Equations (4.1)–(4.16) and to Equation (4.25), via MATLAB® code. The file provided by the authors of this work for the case study presented in Chapter 7 can be used as a template for other systems just by adapting its content.
- *ODEHubs_components.slx* is the Simulink® library, which, with the support of the content of the *user_models* folder, incorporates the predefined models of several storage and conversion devices developed during the CHROMAE project [42] (Figure 6.2). Its blocks, which are described in the next section, are employed to build Simulink® models that represent any EH either by copying and pasting from the library or by dragging from the library browser if *ODEHubs_components.slx* is added. As in any other library, the file is locked when first opened, but users, and even the developers in future releases of ODEHubs, might add new blocks if necessary.
- *EH_def.slx* is the default name given to the Simulink® model employed to define the EH graphically, although any other syntactically valid name can be used if specified in *Simulation_main.m*, which easily allows changing between different EHs in each simulation. A brief example of how to build the model within it is provided in Section 6.4.

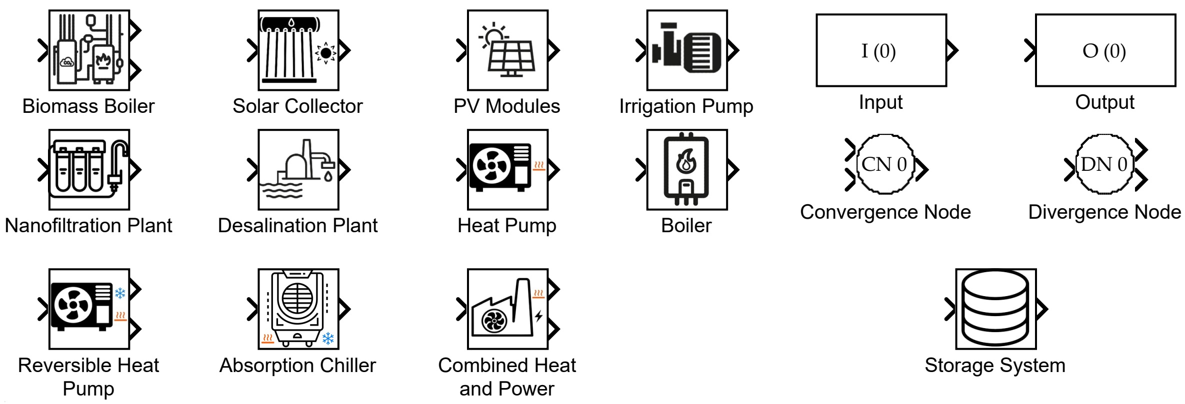

Figure 6.2. ODEHubs's library components defined in Simulink®, which can be used to define customised systems either by including their elements in Simulink®'s browser or by copying them from the library file. The name that appears under each block can be changed when the block is included in a Simulink® model, as well as the labels within *Input* and *Output* blocks.

The remainder functions are not intended to interact with the users directly, but they are part of the automatic process of calculating the dynamic of the EH and storing and displaying the final results. They are distributed in different folders according to their purpose, but all of them appear in *Simulation_main.m* and are responsible for calling other specific functions. *EH_definition_Simulink.m*, *features.m*, and *preset.m* arrange the input data from the users to be processed by other functions; *load_data.m* loads the content of *DataEH.mat* and filters it by time according to values specified by the users; *MPC_predictions.m*, and *MPC.m* provide an updated dispatch of the EH's resources at each sample time specified for the control actions;

EH_system.m simulates the response of the EH at each sample time specified for the system's dynamic; and *process_results.m* aggregates the flows during the simulation horizon and displays the scheduled dispatch. At this point, note that including *MPC_predictions.m* and *EH_system.m* is a mere formal aspect because they currently make use of the same models and variables; thus, the control layer's dynamic will always match the one of the systems (except if different sample times are chosen for them). However, they will be useful in future releases of ODEHubs, which are expected to incorporate capabilities to simulate non-deterministic scenarios as well as different control strategies that deal with uncertainty.

6.2 ODEHubs's Block Library

The model presented in Section 4.1 can be configured both graphically and via code and, in either case, the parameters that need to be introduced in ODEHubs are related to the elements of the above matrices, that is, the technical features of the devices that compose the EH. These can be defined (in the *Model* tab) in either of the following ways: as a numeric data type in the case of static coefficients, as a *string* containing the name of a variable of the *dataEH timetable* corresponding to the value of such parameter at each sample time, as a *string* containing the name of a function in the folder *user_models*, which provides the value of this parameter at each sample time, or as a *cell array* composed of one or several of the latter ones.

ODEHubs's block library will be used in this section to elaborate on that, since it might be more intuitive than programming code. Figure 6.2 shows the types of blocks that need to be used in the definition diagram, which were designed based on the elements found in the model presented in Section 4.1.4 and the appearance of the descriptive diagrams in many works related to EHs (see Figure 4.2, for example). They can be classified as follows.

- N_i *Input* blocks (Figure 6.3a, Table 6.1) characterise the available resources of the EH. Their main parameters are the cost of acquiring the resource, part of vector $\boldsymbol{c}$, and the maximum and minimum values of the input flow, which compose vectors $\boldsymbol{I^{max}}$ and $\boldsymbol{I^{min}}$.
- N_o *Output* blocks (Figure 6.3b, Table 6.2) characterise the loads or demands of the EH. Their main parameter is the value of this flow, part of vector O or, alternatively, the constant of proportionality mentioned in Section 4.1.4, if it is a variable device-dependent load. The mask of these blocks allows defining such dependence as well as enabling the sale of resources through that output, in which case additional parameters are made visible and editable: the price of selling the resource, part of vector $\boldsymbol{s}$, and the maximum and minimum values of the market flow, which compose vectors $\boldsymbol{M^{max}}$ and $\boldsymbol{M^{min}}$.
- N_o or less *Storage System* blocks (Figure 6.5a, Table 6.5) need to be used to characterise the storage devices of the EH. The output of each of these blocks must be connected any *Output* block where energy, mass, or volume is stored. Their parameters, which are arranged in tabs, allow defining the charge and discharge flows and the capacity of each storage system, so they are elements of the vectors $\boldsymbol{Q_{ch}^{min}}$, $\boldsymbol{Q_{ch}^{max}}$, $\boldsymbol{Q_{dis}^{min}}$, $\boldsymbol{Q_{dis}^{max}}$, $\boldsymbol{S^{min}}$, and $\boldsymbol{S^{max}}$; as well as the efficiency of each storage process, taking part of the matrices $\boldsymbol{C_{ch}}$, $\boldsymbol{C_{dis}}$, and $\boldsymbol{C_s}$. Additionally, the initial state of the storage system must be defined $\boldsymbol{S}(0)$ in the *Storage* tab.
- *Convergence Node* and *Divergence Node* blocks (Figure 6.4, Tables 6.3–6.4) do not currently have any utility but, because of the way Simulink® treats the signals between blocks, they will be needed in future releases to allow merging and splitting flows numerically in simulations via Simulink®. The diagrams must incorporate these blocks whenever several flows converge into a single flow (the sum of the original flows equals the resulting flow) or whenever a flow diverges into different sub-flows (the sum of the sub-flows equals the original flow). Their only configurable parameter is the number of converging or diverging flows.

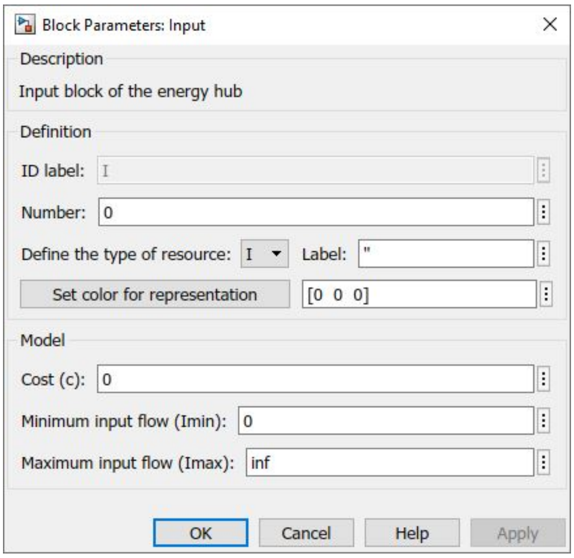

(a)

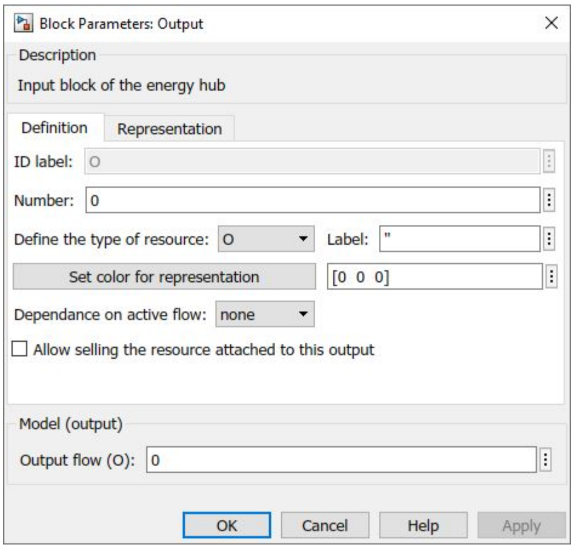

(b)

Figure 6.3. Parameters of the *Input* (a) and *Output* (b) blocks

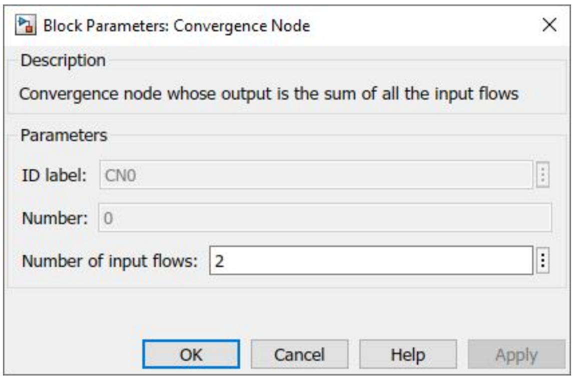

(a)

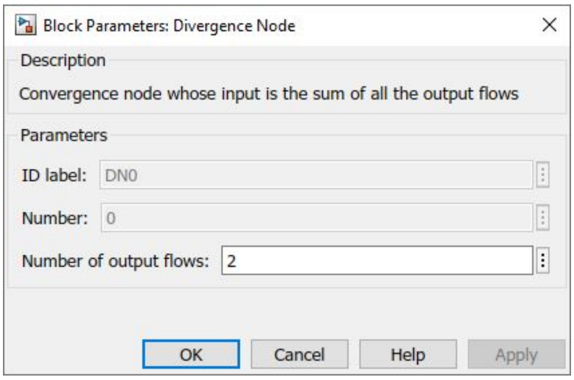

(b)

Figure 6.4. Parameters of the *Convergence Node* (a) and *Divergence Node* (b) blocks

- N_d *Device* blocks (Figure 6.5b, Table 6.6) corresponding to devices need to be included in the Simulink® model employed to define the EH graphically. As depicted in Figure 6.2, ODEHubs's library consists of some predefined blocks with the same parameters: limits for the input(s) and output(s) of each device, related to vectors $\boldsymbol{D}_{di}^{min}$, $\boldsymbol{D}_{di}^{max}$, $\boldsymbol{D}_{do}^{min}$, and $\boldsymbol{D}_{do}^{max}$; and, the conversion factor(s) between them, which are required to build matrices $\boldsymbol{C}$, $\boldsymbol{C}_{di}$, and $\boldsymbol{C}_{do}$. At present, three different types of blocks can be distinguished: type 0, for those with a single input and a single output (*Solar Collector*, *PV Modules*, *Irrigation Pump*, *Nanofiltration Plant*, *Desalination Plant*, *Heat Pump*, *Boiler*, and *Absorption Chiller*); type 1, for those with a single input and a two simultaneous outputs (*Biomass Boiler* and *Combined Heat and Power*); and type 2, for those with a single input and a two non-simultaneous outputs (*Reversible Heat Pump*). The main difference is that the types 1 and 2 are virtually divided into two devices (one for each output) and therefore, their model-related parameters need to be defined as a *cell array* composed of as many numeric data and/or *strings* as the number of outputs of the device. Despite this distinction and the variety of icons employed for each kind of device (only for representation purposes), all these blocks have the same configuration parameters (see Figure 6.5b, Table 6.6).

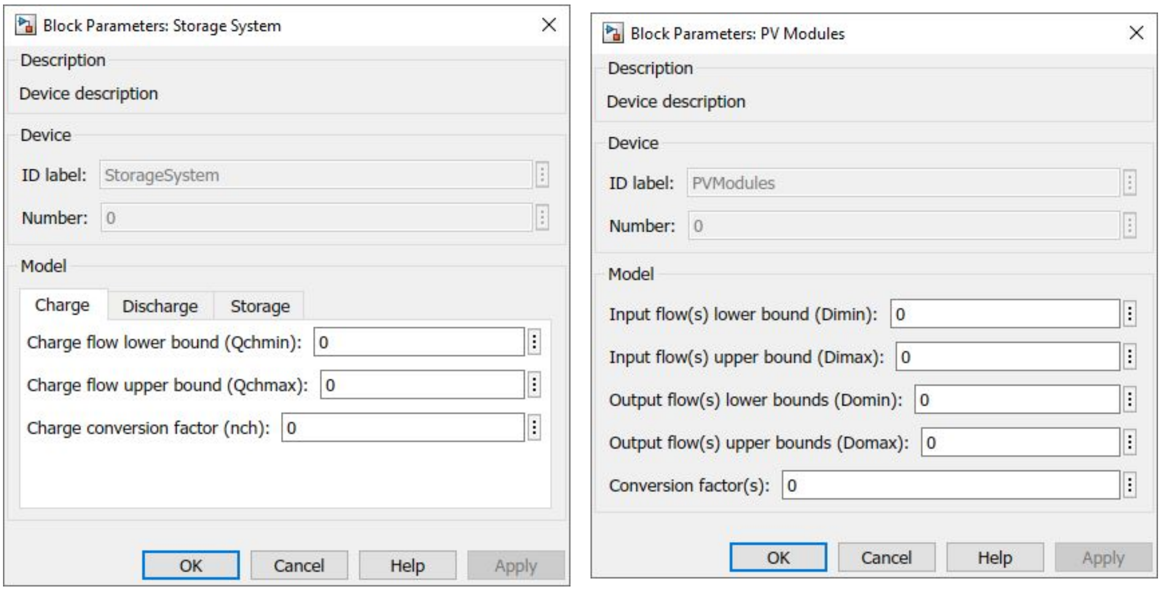

Figure 6.5. Parameters of the *Storage System* (a) and *Device* (b) blocks

Table 6.1. Properties of the *Input* block

Icon	Block's *name* and description
I (0)	*Input*. It allows to define and configure the parameters corresponding to an input resource of the EH.
Parameter [Tab]	**Description**
ID label [Definition]	Optional identifier of the input only for representation purposes. By default "I", which stands for "Input". It can be indirectly redefined by the users from the two following parameters.
Type of resource [Definition]	Optional identifier. It is intended to define the type of resources with a single letter from a drop-down menu that contains the Latin alphabet. By default "I", which stands for "Input".
Label [Definition]	Optional identifier. It is intended to identify the input within a set of inputs with the same type of resource. By default an empty *string*.
Number [Definition]	Unique identifier of the input that can be defined by the users for representation or data management purposes. It is used by ODEHubs's internal functions and, by default, ODEHubs redefines any of these duplicate identifiers in EH's Simulink® model. It determines the position of the element corresponding to that input in the $\boldsymbol{I}$ vector. By default zero.

Table 6.1. (Continued). Properties of the *Input* block

Parameter [Tab]	**Description**
Set colour for representation [Definition]	Clicking this button opens a pop-up window to select from a palette the colour used to represent the input. Alternatively, the RGB colour can be directly defined as a three-component vector in the box on the right side of this button. By default black.
Cost (c) [Model]	Definition of the element of $\boldsymbol{c}$ corresponding to the input. By default zero.
Minimum input flow (Imin) [Model]	Definition of the element of $\boldsymbol{I}^{min}$ corresponding to the input. By default zero.
Maximum input flow (Imax) [Model]	Definition of the element of $\boldsymbol{I}^{max}$ corresponding to the input. By default infinite.

Table 6.2. Properties of the *Output* block

Icon	**Block's *name* and description**
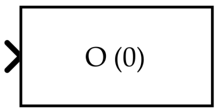	*Output*. It allows to define and configure the parameters corresponding to an output resource of the EH.

Parameter [Tab]	**Description**
ID label [Definition]	Optional identifier of the output only for representation purposes. By default "O", which stands for "Output". It can be indirectly redefined by the users from the two following parameters.
Type of resource [Definition]	Optional identifier. It is intended to define the type of resources with a single letter from a drop-down menu that contains the Latin alphabet. By default "O", which stands for "Output".
Label [Definition]	Optional identifier. It is intended to identify the output within a set of outputs with the same type of resource. By default an empty *string*.
Number [Definition]	Unique identifier of the output that can be defined by the users for representation or data management purposes. It is used by ODEHubs's internal functions and, by default, ODEHubs redefines any of these duplicate identifiers in EH's Simulink® model. It determines the position of the element corresponding to that output in the $\boldsymbol{O}$ vector. By default zero.

Table 6.2. (Continued). Properties of the *Output* block

Parameter [Tab]	Description
Set colour for representation [Definition]	Clicking this button opens a pop-up window to select from a palette the colour used to represent the output. Alternatively, the RGB colour can be directly defined as a three-component vector in the box on the right side of this button. By default black.
Dependence on active flow [Definition]	It is intended to define the element of the $\boldsymbol{\delta_O}$ matrix corresponding to the output. The drop-down menu allows the users to choose among the following options: "none" (by default), which makes the element of $\boldsymbol{\delta_O}$ equal to one, and therefore no dependence is established; and "charge", "discharge", or "device", which enable additional drop-down menus to select the label (and also the device's output in the case of "device") of the block corresponding to the device-dependent load. With the latter three options, the element of $\boldsymbol{\delta_O}$ is made equal to $\delta_{ch,o}$, $\delta_{dis,o}$ or $\delta_{D,d}$, respectively (bear in mind that o and d refer to generic outputs and devices, as defined in Chapter 4); and a checkbox ("Proportional demand") is shown to specify if it is a fixed or variable load (see Subsection 4.1.4).
Allow selling the resource attached to this output [Definition]	Checkbox to enable the "Model (market sales)" tab, where the price of selling the resource, part of vector $\boldsymbol{s}$, and the maximum and minimum values of the market flow, which compose vectors $\boldsymbol{M^{max}}$ and $\boldsymbol{M^{min}}$, are defined. By default unchecked.
Output flow (O) [Model (output)]	Definition of the element of $\boldsymbol{O}$ corresponding to the output. Default option if the "Proportional demand" checkbox is unchecked. By default zero.
Constant of proportionality (k) [Model (output)]	Definition of the κ corresponding to the output, only visible if the "Proportional demand" checkbox is checked. By default zero.
Price (s) [Model (market sales)]	Definition of the element of $\boldsymbol{s}$ corresponding to the output. Only visible if the corresponding checkbox is checked. By default zero.
Minimum sales flow (Mmin) [Model (market sales)]	Definition of the element of $\boldsymbol{M^{min}}$ corresponding to the output. Only visible if the corresponding checkbox is checked. By default zero.
Maximum sales flow (Mmax) [Model (market sales)]	Definition of the element of $\boldsymbol{M^{max}}$ corresponding to the output. Only visible if the corresponding checkbox is checked. By default infinite.
Flow label [Representation]	Title of the left vertical axis in the figures generated by ODEHubs. The *cell array* format allows splitting the text into different rows. By default an empty *string*.

Table 6.2. (Continued). Properties of the *Output* block

Parameter [Tab]	**Description**
Storage label [Representation]	Title of the right vertical axis in the figures generated by ODEHubs. The *cell array* format allows splitting the text into different rows. By default an empty *string*.
Axis factor [Representation\Right/Left axis]	Re-scaling factor for the default axis' limits generated by ODEHubs. Not applicable if it is set equal to zero, in which case the limits defined by the users through the following parameters are considered. By default one.
Lower limit [Representation\Right/Left axis]	Lower limit for the vertical axis, as defined by the users and only applicable if the axis factor is set equal to zero. By default zero.
Upper limit [Representation\Right/Left axis]	Upper limit for the vertical axis, as defined by the users and only applicable if the axis factor is set equal to zero. By default zero.

Table 6.3. Properties of the *Convergence Node* block

Icon	**Block's *name* and description**
	*Convergence Node*. It allows to merge flows converging at one junction.

Parameter [Tab]	**Description**
ID label [Parameters]	Full identifier of the block used by ODEHubs's internal functions. It is composed by "CN", which stands for "Convergence Node", and the number of the block.
Number [Parameters]	Unique identifier assigned by ODEHubs according to the amount of *Convergence Node* blocks in the Simulink® model. By default zero.
Number of input flows [Parameters]	Number of flows converging at the junction, as defined by the user. It determines the internal structure of the block and the appearance of the icon, which will have as many input ports as the number of flows. By default two.

Table 6.4. Properties of the *Divergence Node* block

Icon	**Block's *name* and description**
	*Divergence Node*. It allows to split flows diverging at one junction.
Parameter [Tab]	**Description**
ID label [Parameters]	Full identifier of the block used by ODEHubs's internal functions. It is composed by "DN", which stands for "Divergence Node", and the number of the block.
Number [Parameters]	Unique identifier assigned by ODEHubs according to the amount of *Divergence Node* blocks in the Simulink® model. By default zero.
Number of output flows [Parameters]	Number of flows diverging at the junction, as defined by the user. It determines the internal structure of the block and the appearance of the icon, which will have as many output ports as the number of flows. By default two.

Table 6.5. Properties of the *Storage System* block

Icon	**Block's *name* and description**
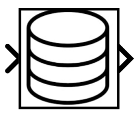	*Storage System*. It allows to define and configure the parameters corresponding to a storage system, attached to certain output, of the EH.
Parameter [Tab]	**Description**
ID label [Device]	Full identifier of the block used by ODEHubs's internal functions and automatically inherited from the *Output* block to which the *Storage System* block is connected.
Number [Device]	Unique identifier of the *Output* block to which the *Storage System* block is connected. By default zero.
Charge flow lower bound (Qchmin) [Model\Charge]	Definition of the element of Q_{ch}^{min} corresponding to the storage system. By default zero.
Charge flow upper bound (Qchmax) [Model\Charge]	Definition of the element of Q_{ch}^{max} corresponding to the storage system. By default zero.
Charge conversion factor (nch) [Model\Charge]	Definition of the element of C_{ch} corresponding to the storage system. By default zero.

Table 6.5. (Continued). Properties of the *Storage System* block

Parameter [Tab]	**Description**
Discharge flow lower bound (Qdismin) [Model\Discharge]	Definition of the element of Q_{dis}^{min} corresponding to the storage system. By default zero.
Discharge flow upper bound (Qdismax) [Model\Discharge]	Definition of the element of Q_{dis}^{max} corresponding to the storage system. By default zero.
Discharge conversion factor (ndis) [Model\Discharge]	Definition of the element of C_{dis} corresponding to the storage system. By default zero.
Capacity lower bound (Smin) [Model\Storage]	Definition of the element of S^{min} corresponding to the storage system. By default zero.
Capacity upper bound (Smax) [Model\Storage]	Definition of the element of S^{max} corresponding to the storage system. By default zero.
Degradation conversion factor (ns) [Model\Storage]	Definition of the element of C_s corresponding to the storage system. By default zero.
Storage initial state (S0) [Model\Storage]	Definition of the element of S corresponding to the storage system at $k = 0$. By default zero.

Table 6.6. Properties of the *Device* blocks

Icon	**Block's *name* and description**
Multiple icons (see Figure 6.2)	Multiple names (*Solar Collector*, *PV Modules*, *Irrigation Pump*, *Nanofiltration Plant*, *Desalination Plant*, *Heat Pump*, *Boiler*, *Absorption Chiller*, *Biomass Boiler*, *Combined Heat and Power*, and *Reversible Heat Pump*). It allows to define and configure the parameters corresponding to a device of the EH.
Parameter [Tab]	**Description**
ID label [Device]	Identifier of the block for representation purposes, which is automatically inherited from the name of the block and also used by ODEHubs's internal functions. Hence, it can be changed by the users only and directly in the Simulink® model, which forces its uniqueness.

Table 6.6. (Continued). Properties of the *Device* blocks

Parameter [Tab]	Description
Number [Device]	Unique identifier of the device given by ODEHubs, which is used by its internal functions. By default zero.
Input flow(s) lower bound (Dimin) [Model]	Definition of the element(s) of $\boldsymbol{D}_i^{min}$ corresponding to the device. For devices with multiple outputs, this parameter needs to be introduced as a *cell array*. By default zero.
Input flow(s) upper bound (Dimax) [Model]	Definition of the element(s) of $\boldsymbol{D}_i^{max}$ corresponding to the device. For devices with multiple outputs, this parameter needs to be introduced as a *cell array*. By default zero.
Output flow(s) lower bound (Domin) [Model]	Definition of the element(s) of $\boldsymbol{D}_o^{min}$ corresponding to the device. For devices with multiple outputs, this parameter needs to be introduced as a *cell array*. By default zero.
Output flow(s) upper bound (Domax) [Model]	Definition of the element(s) of $\boldsymbol{D}_o^{max}$ corresponding to the device. For devices with multiple outputs, this parameter needs to be introduced as a *cell array*. By default zero.
Conversion factor(s) [Model]	Definition of the efficiency (or efficiencies) corresponding to each output of the device that will form the matrices $\boldsymbol{C}_{di}$, $\boldsymbol{C}_{do}$, and $\boldsymbol{C}$. For devices with multiple outputs, this parameter needs to be introduced as a *cell array*. By default zero.

6.3 Main Configuration Parameters

Apart from setting the model's parameters, ODEHubs's users might want to customise the output of the program in order to suit their needs, which can be done in the *Simulation_main.m* file. Among the configuration parameters, one can select if third-party solvers are invoked, define the solver's options, select the start date for simulation (*dataEH* needs to be accordingly defined) and which results are presented (system response or control actions), and if they are exported as images or not. However, in the author's opinion, the parameters with which new users could more easily struggle are those related to sample time and horizon, which are described below based on the interpretation of Figure 6.6: the dashed arrows indicate when the control action is updated and the dark grey squares which control actions computed.

- *EH.simparam.nm* defines the simulation horizon and thus, depending on *EH.simparam.tm*, how many times the loop is executed to obtain the evolution of the system according to its dynamic, that is, updating the state of the storage systems through *EH_system.m* (which is still in its beta phase).
- *EH.simparam.tm* defines the time between two consecutive steps of the system's simulation.
- *EH.simparam.tm_MPC* defines the time between two consecutive updates of the control action, which is calculated by *MPC.m* and kept constant at each iteration if the variable *EH.simparam.tm_MPC* is greater than *EH.simparam.tm*. On the other hand, together with *EH.simparam.H_MPC*, it determines the number of samples of the model employed for optimisation. It cannot be lower than the sample time of the system *EH.simparam.tm*.

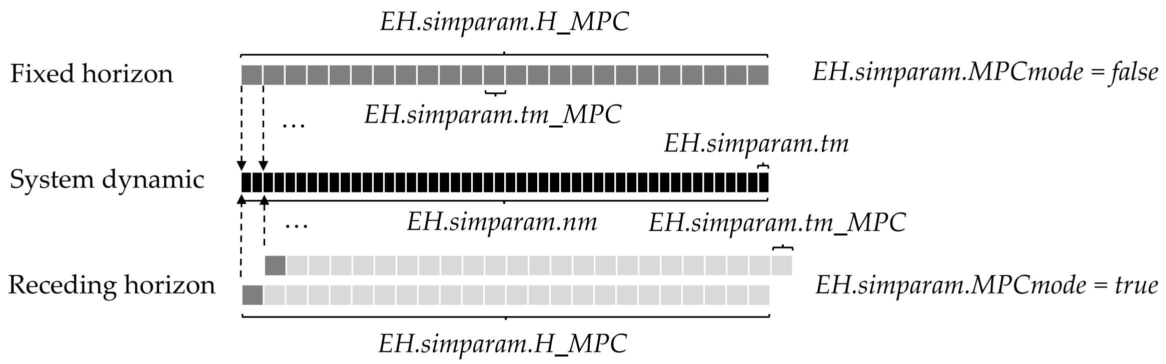

Figure 6.6. Interpretation of the configuration parameters related to sample time and horizon for the system and the control layer depending on the selected mode.

- *EH.simparam.H_MPC* defines the control horizon, which can be lower than *EH.simparam.nm* if only the first control action is computed (receding horizon strategy) but needs to be equal to this one for scheduling mode (fixed horizon strategy). In the first case (MPC mode active), ODEHubs allows users to apply the variable horizon strategy exemplified in [41].
- *EH.simparam.MPCmode* determines whether the fixed horizon strategy or the receding horizon strategy is applied. Note that *dataEH* must contain data for *EH.simparam.nm* in the first case and for *EH.simparam.nm* plus *EH.simparam.H_MPC* in the second one.

6.4 Example of Definition via Simulink®

Let the EH presented in Figures 6.7 and 6.8 serve as an example to explain how to use ODEHubs, which consist of the PV parking and the UAL-eCARM (the simplest EH of the CHROMAE project, as introduced in Section 4.5).

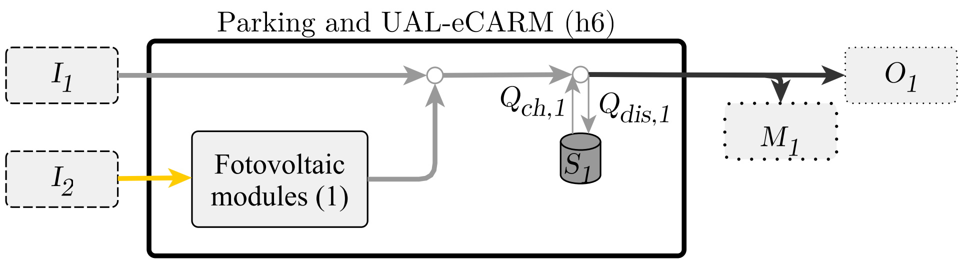

Figure 6.7. Conceptual model of the EH example defined with ODEHubs's blocks

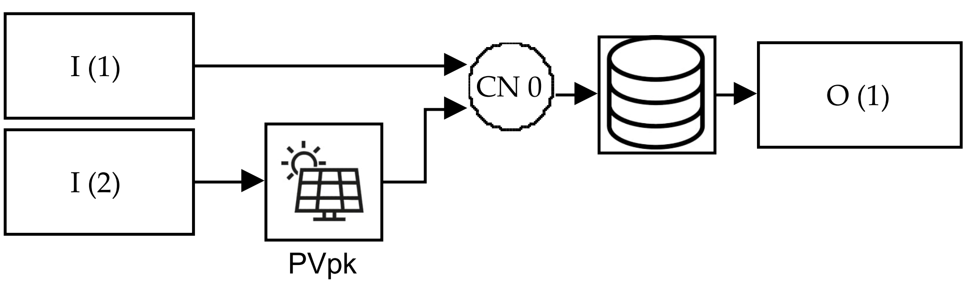

Figure 6.8. Simulink® model of the EH example defined with ODEHubs's blocks

In Figure 6.7, all the elements but M_1, which is encapsulated in an *Output* block, are related to a reciprocal block of ODEHubs's library (see Figure 6.2). Note that, in the previous chapters and in Figure 6.7, the origin or destination nodes of the different arrows representing the flows within the EH have been depicted by circles. Except for the *Storage System* blocks, which also encapsulate these nodes, in the rest of the cases those circles are converted into either a *Convergence Node* block or a *Divergence Node* block. S_1, the charge and discharge flows ($Q_{ch,1}$ and $Q_{dis,1}$) and the said node are represented by a *Storage System* block. I_1, I_2, and O_1 (together with M_1) are substituted by their respective *Input* and *Output* blocks, and the PV field is replaced by it own block (*PV Modules*). These changes result in the Simulink® model of Figure 6.8. In Figure 6.8, the numbers in round brackets appear once each block has been configured, as shown in the below figures, but even if these numbers are not defined by the users and have been left equal to zero (default value) ODEHubs will give them a new value to identify each block, as it will do for, the *PV Modules*, *Storage System* block and *Conversion Node* blocks (i.e. the "CN 0" will turn into "CN 1" the first time *EH_definition_Simulinik.m* is executed).

With respect to the particular configuration of each block, Figures 6.9–6.11 contain the parameters used in this example for clarification purposes. The main changes are summarised below and bear in mind that the users must accordingly define each parameter to ensure the dimensional coherence in the operations that ODEHubs will perform.

- Figure 6.9 shows that the cost of solar radiation (I_2) is nil, whereas electricity (I_1) is assumed to have a cost of 0.15 units. They would be represented in yellow and grey colours, respectively, and, in both cases, no constraints have been imposed on the input flows (default values of zero and infinite for I^{min} and I^{max}).
- Figure 6.10a presents some of the parameters of the storage system (the rest of them are defined in the other tabs) related to the charge flow, which limited to a maximum of 3 units and has an efficiency of 0.7.

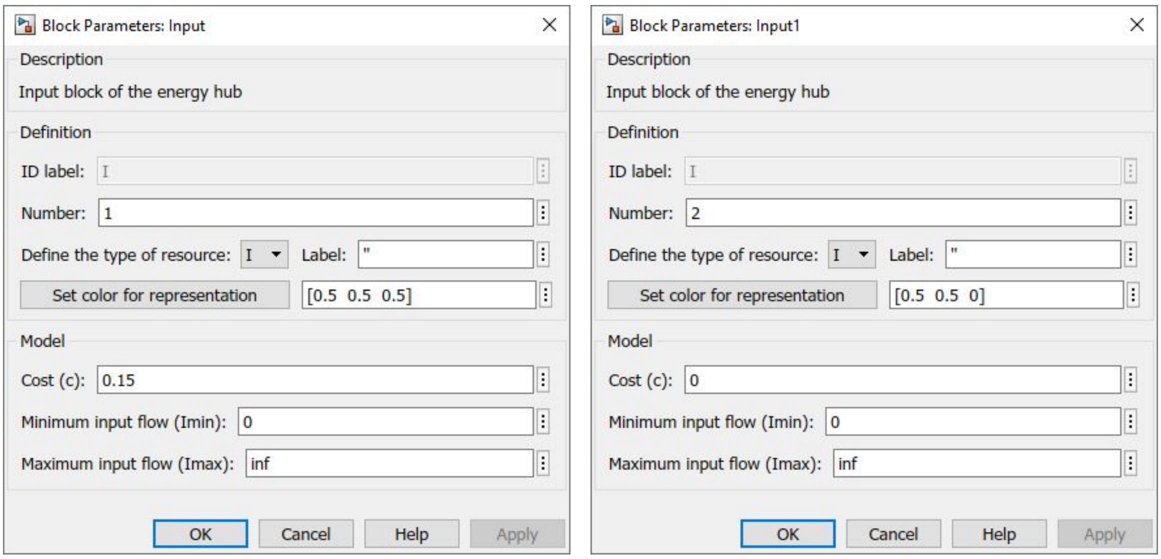

(a) (b)

Figure 6.9. Parameters of the *Input* blocks in the Simulink® model of the EH example

- Figure 6.10b serves to exemplify how parameters different than constant coefficient are defined. Although the output power of the field is not directly capped, the function *Dimax_pvpk_func* is in charge of providing the maximum amount of power from the sun at each time instant, calling other dependent functions where the models explained in Chapter 5 have been implemented;

npvpk_func has the same purpose but for the gross efficiency of the field. In these cases, the users are responsible for providing appropriate functions and note that the use of inverted commas is mandatory to define a *string*. Furthermore, any parameter or set of parameters (separated by commas, in the second case) can be introduced as a *cell array* by putting them between curly brackets (e.g. *npvpk_func*).

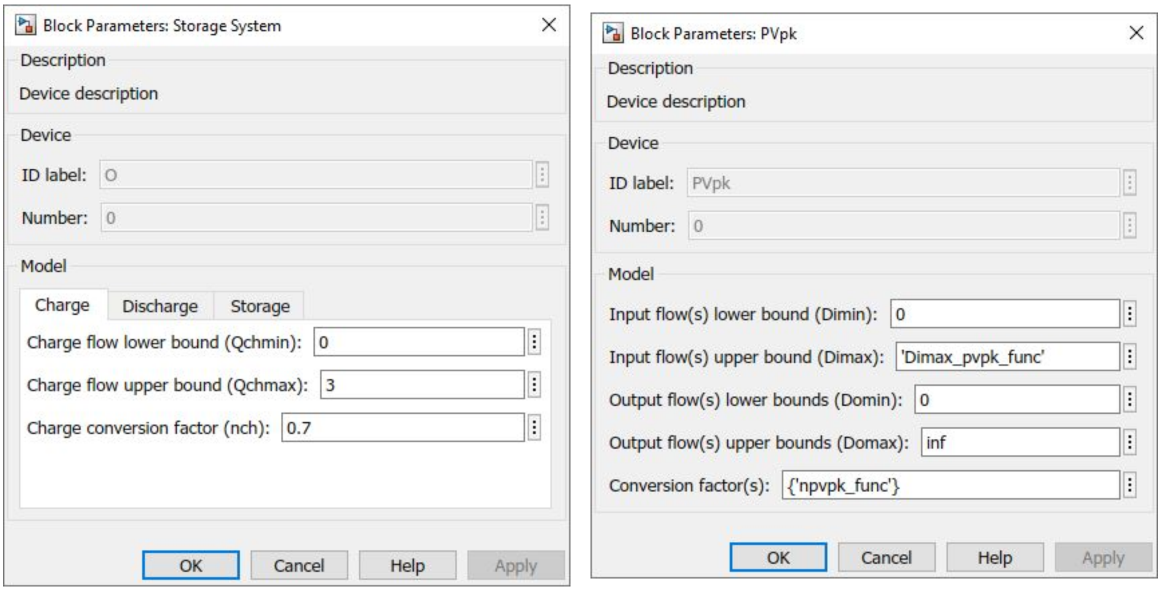

(a) (b)

Figure 6.10. Parameters of the *Storage System* (a) and *PV Modules* (b) blocks in the Simulink® model of the EH example

- Figure 6.11 illustrates how to configure the sale of resources in an output block. In contrast to Figure 6.3b, there is an additional tab visible because the checkbox is checked. The price of the sold electricity is assumed to be of 0.1 units and no constraints have been imposed on the sale flow (default values of zero and infinite for M^{min} and M^{max}). In this case, the demand of electricity would be represented in black, and "Campus_demand" represents a variable, included in the database (*DataEH.mat*), that contains its values at each time instant.

6.5 Contributions and Related Publications

This chapter presents one of the core contributions of this thesis, as introduced in Section 1.4, that is, the software library, the main enhancements of the which with respect to other alternatives have been highlighted in Section 6.1. In brief, it is composed by a set of MATLAB® and Simulink® files, which has been developed to ease the definition and resolution of EH-related optimisation problems and is freely available on Github (https://github.com/ual-arm/odehubs). The package can generate the constraints of the problem defined in Chapter 4 in MATLAB® code and obtain the optimal dispatch schedule for the deterministic MILP problem that represents the system. This will be elucidated in Chapter 7, demonstrating its use and clarifying how the problem is particularised for a given EH, via a case study based on the facilities of the ENERPRO and CHROMAE projects. The preliminary versions of this tool were presented in two conferences [47, 53], and the content of this chapter, together with Subsection 4.1.4, are included in the paper published in Sustainability [44].

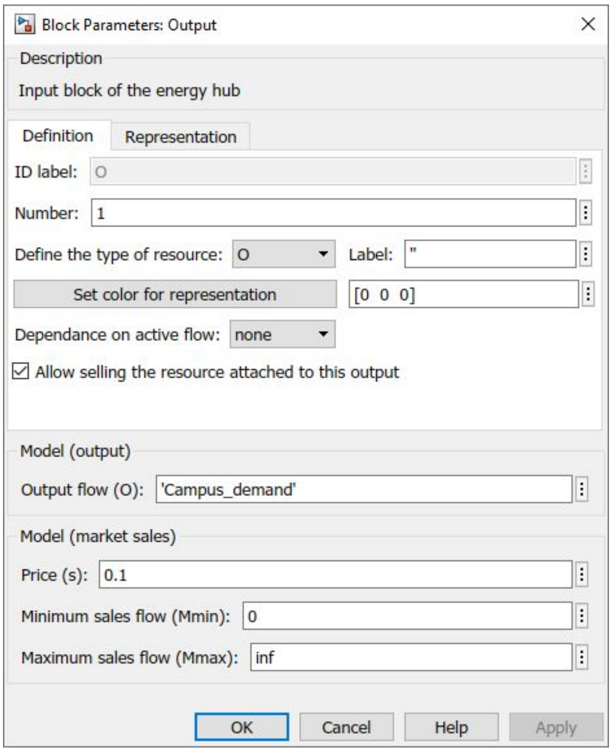

Figure 6.11. Parameters of the *Output* block in the Simulink® model of the EH example

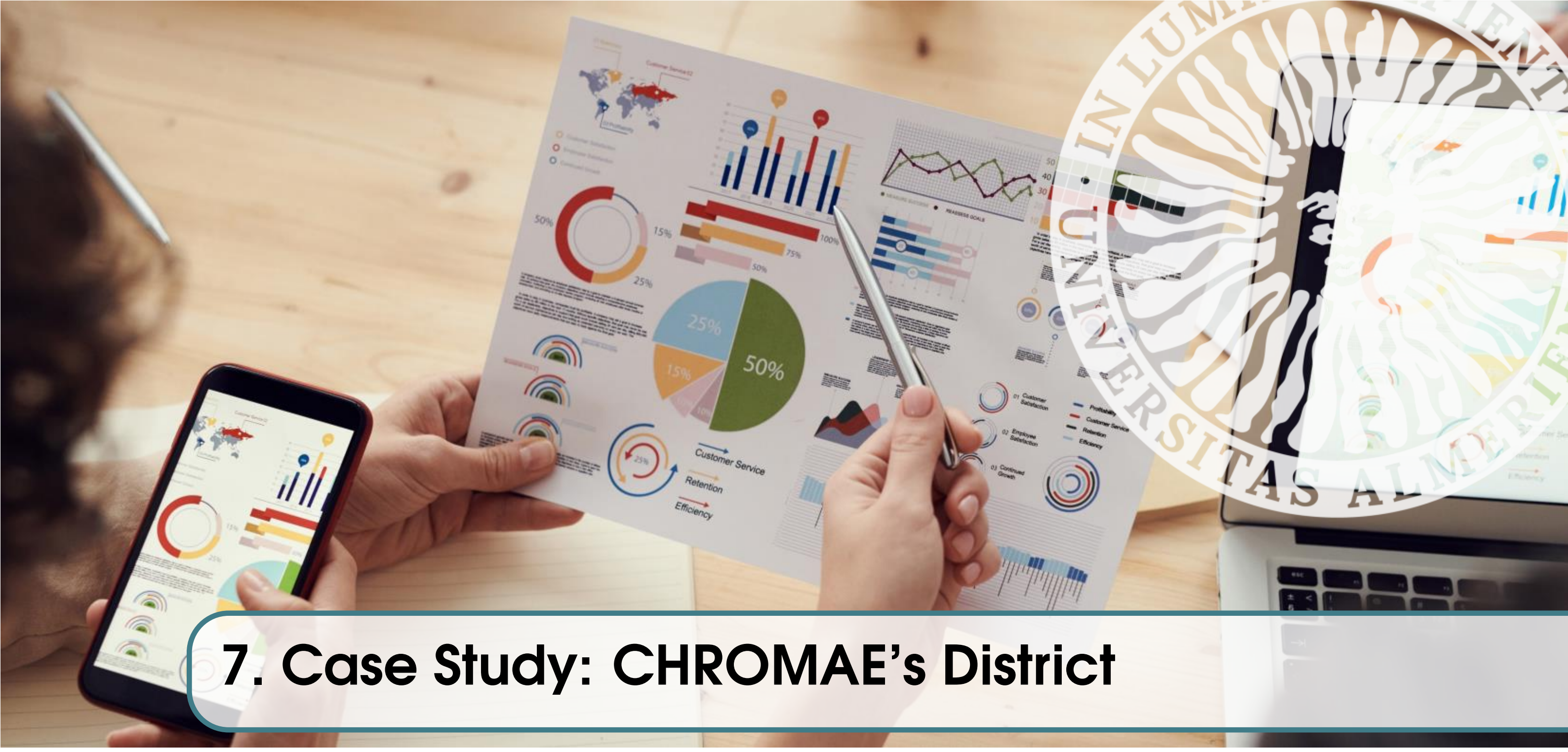

7. Case Study: CHROMAE's District

Chapter Summary

This chapter presents a case study to exemplify the utility of the modelling framework proposed in Chapter 4 by means of a complex EH inspired in the potential synergy of the facilities presented in Chapter 3. To provide a real and captivating application for the developed approach, without loss of generality, the legal situation in Spain concerning self-consumption between 2015 and 2018 is considered, in which sales to the grid are allowed at the pool price and both the self-consumed energy and that sales to the grid are taxed. This conditions the operational scheduling, which is determined considering the economic criteria of Section 4.2 and therefore the variations in the electricity price throughout the day according to the real-time data published by the market operator.

Section 7.1 introduces the needs and relationships within the considered agro-industrial district. Section 7.2 outlines the operation of the electricity market, whose prices condition the scheduling, and give a view of the types of self-consumers legally recognised (during 2015-2018 and at present). Section 7.3 shows how to particularise the model presented in Chapter 4 for the case study. Finally, the last two sections (Section 7.4 and Section 7.5) contain a description of the scenarios considered in the simulations and a critical discussion of the results obtained in simulations.

7.1 Test-Bed Plant Description

The agro-industrial district, employed to exemplify and clarify the content of the previous chapters, includes most of the facilities presented in Chapter 3: the CIESOL building, the PV parking and the UAL-eCARM electric vehicle located at the University of Almeria campus, the AQUASOL system of the PSA research centre and the parral-type greenhouse of Cajamar's Experimental Station. Although these facilities are physically apart, they are considered a single ensemble which can be modelled under the EH framework since their devices can convert, interchange and store resources, as shown in Figure 7.1.

CIESOL and the parking area can produce electricity through their PV systems, for themselves and for the rest of the cluster; heat is generated from the solar collector facilities; combustion equipment (with a CO_2 capture system for the greenhouse), or the HVAC system in CIESOL (which can also provide cooling for the building) and the desalination plant can produce drinking water, required both by the greenhouse and CIESOL. The public electricity and water utility network can serve as a backup or allow the sale of surplus resources.

The full description of them can be found in Chapter 3 but, for the purpose of this case study, only the most relevant devices are taken into account, whose technical characteristics allow establishing the operational limits and conversion factors described in Section 4.1. Since each facility has its own database, all data needed to be cleaned, synchronised, and analysed to determine the demand or load profiles of each resource type as well as to model the converter devices. Furthermore, the hourly electricity price data for daily and intraday markets were acquired from OMIE's website [229]. This was done for the 2013-2017 period to have a wide enough set of data available from which to select specific days for simulations.

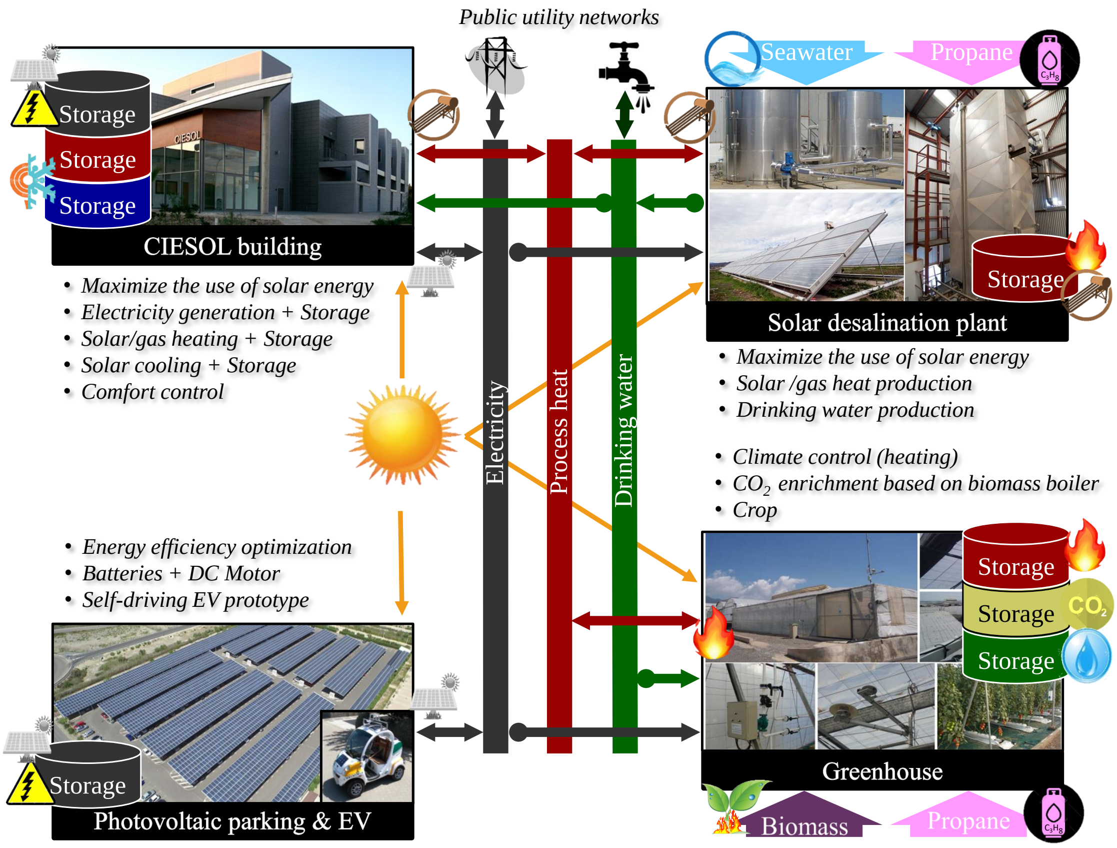

Figure 7.1. Functional diagram of the case study, where each facility can demand, supply and store different resources

7.2 Spanish Self-Consumption Regulations and Electricity Market

The Royal Decree 900/2015 [230] regulated Spanish electricity supply and generation for self-consumption since it came into force until replaced by the Royal Decree-Law 15/2018 [231] and the Royal Decree 244/2019 [232]. All of them apply to any renewable generation facility connected in some way to the public grid, but not to isolated ones, and they distinguish several kinds of self-consumption, as summarised below according to each regulation.

Royal Decree 900/2015:

- Self-consumers type 1, whose facilities are placed within a grid on their property and which are registered solely for self-consumption (not production). The capacity is limited to 100 kW and the owner of the facilities must also be the holder of the power purchase agreement. Energy is only generated for self-consumption and, although surplus energy can be exported through the public grid, it is not economically remunerated or penalised.
- Self-consumers type 2, whose facilities are registered as production facilities (in addition to self-consumption facilities). The owner and the holder of the power purchase agreement do not have to be the same legal entity. Surplus energy can be indirectly sold through retailers (who are in charge of purchasing the energy excess which they will benefit from by selling it to other consumers) at the pool price, discounting a generation fee of 0.5 €/MWh [233] and a 7% tax (IVPEE) [234] on the production. In addition, self-consumed energy is taxed according to the variable charges fees published by the government.

Royal Decree 244/2019:

- Self-consumers without surplus, which are registered solely for self-consumption (not production) and they own facilities with control of the feed-in (i.e. zero injection).
- Self-consumers with a surplus, whose facilities are registered as production facilities (in addition to self-consumption facilities) and they can inject energy on the public distribution network. Other two categories are distinguished within this one.
  - Self-consumers with surplus and economic compensation, whose facilities need to satisfy certain legal and technical criteria (e.g. the capacity is limited to 100 kW). The surplus energy exported through the public grid is not economically remunerated but compensated depending on the signed contract. For those in the free market the price is agreed with the retailer, whereas for those in the regulated one it is set according to the pool market (as in the following case but capped, so that there is no profit, and with a different fee).
  - Self-consumers with surplus and without economic compensation, which either do not fit in the above category or willingly decide to adhere to this one. Surplus energy can be sold at the pool price, discounting a generation fee of 0.5 €/MWh [233].

From the above, it becomes clear that the current legislation benefits self-consumption facilities while keeping a similar framework in which, essentially, the former self-consumers type 2 are not taxed any more for the energy self-consumed and self-consumers type 1 can now perceive a remuneration for their surplus energy. Although the modelling approach proposed would be adaptable of any of these situations, self-consumption type 2 (Royal Decree 900/2015) will be hereinafter considered for being the more complex case.

With regard to the Spanish electrical power system, this is operated by two independent entities: the market operator, *OMI - Polo Español* (OMIE) [235], which performs the economic management of the daily and intraday markets; and the system operator, *Red Eléctrica de España* (REE) [236], which is in charge of technical issues such as determining the feasibility of the dispatch provided by OMIE (thus affecting the final scheduling and price). Both companies are involved in the market transactions, but they do not participate directly in electricity trading.

As in the rest of the European Union, the daily market is a marginal pricing market: hourly prices and trading volumes are set at the point where the supply and demand curves meet. Considering Coordinated Universal Time (UTC) according to daylight saving time (DST, which implies using UTC+1 in winter and UTC+2 in summer), purchase and sale bids for the next day must be presented by agents to the market operator before 12:00 h for them to be included in a matching procedure (carried out by the Euphemia algorithm [237]).

Once this process is finished, the results are sent to the system operator to check the technical viability. The Matching Basis Daily Schedule (MBDS) is published before 13:00 h and updated several times a day, attending to technical and administrative constraints: the Operating Basis Daily Schedule (OBDS) before 14:00 h, the Provisional Viable Daily Schedule (PVDS) before 16:00 h, and the Final Viable Daily Schedule (FVDS) before 17:00 h.

On the other hand, the purpose of the intraday market is to adjust the Final Viable Daily Schedule by again presenting the sale and purchase bids. Only agents who have previously participated in the daily market session can submit bids, and they can only do it for the same hourly periods in which they have participated. This is structured into six sessions, as presented in Table 7.1 and Figure 7.2 for 2018 (this has changed since then [238]), which end with the publication of the Final Hourly Schedule (FHS); thus, prices are updated twice before the day begins and four times (taking into account the three first hours of the first session) before the day ends.

Table 7.1. Intraday market schedule in 2018 (UTC+1/UTC+2). Source: [235]

Session number	**1**	**2**	**3**	**4**	**5**	**6**
Session opening	17:00	21:00	01:00	04:00	08:00	12:00
Session closing	18:45	21:45	01:45	04:45	08:45	12:45
Matching results	19:30	22:30	02:30	05:30	09:30	13:30
Breakdowns	19:50	22:50	02:50	05:50	09:50	13:50
FHS publication	20:45	23:45	03:45	06:45	10:45	14:45
Schedule horizon	27 h	24 h	20 h	17 h	13 h	9 h
Hourly periods	22-24	1-24	5-24	8-24	12-24	16-24

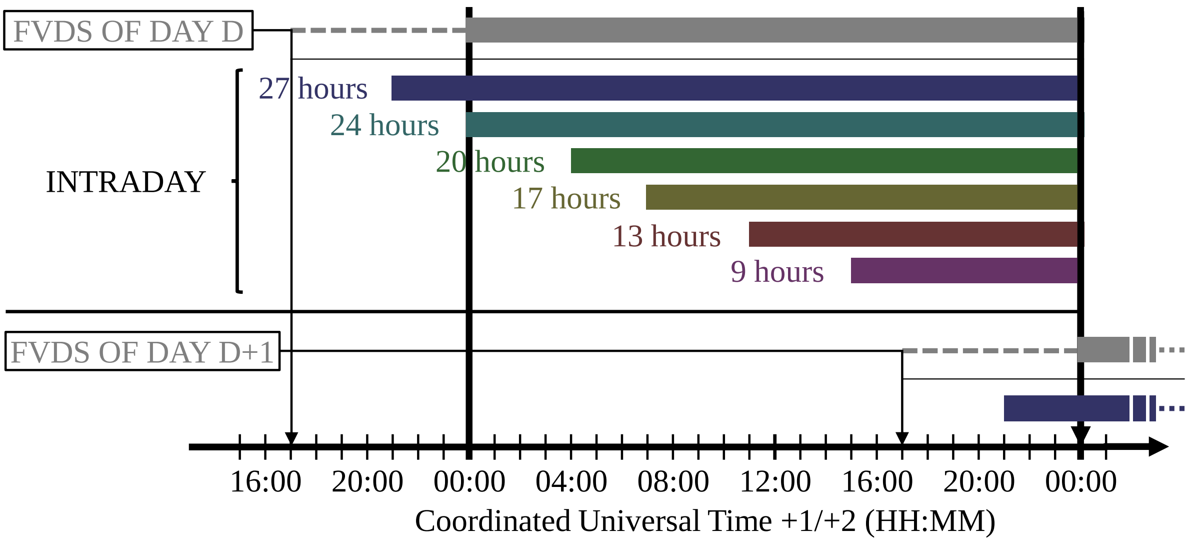

Figure 7.2. Daily market and intraday market distribution in 2018. Time axis label refers to both summer (UTC+2) and winter periods (UTC+1). Source: [235]

7.3 Modelling under the Proposed Approach

This subsection constitutes a real application example of the extended EH model proposed in Chapter 4. In the cluster described above, and depicted in Figure 7.1, resources can be identified as inputs or outputs depending on their origin and destination. In broad terms, inputs are comprised of raw materials and outputs of a load or demand from any of the facilities. These, together with the conversion and storage devices for each facility, form the EH illustrated in Figure 7.3. The following paragraphs provide details of the elements in Equations (4.1)–(4.16) particularised for this example.

7.3.1 Decision Variables and Constraints

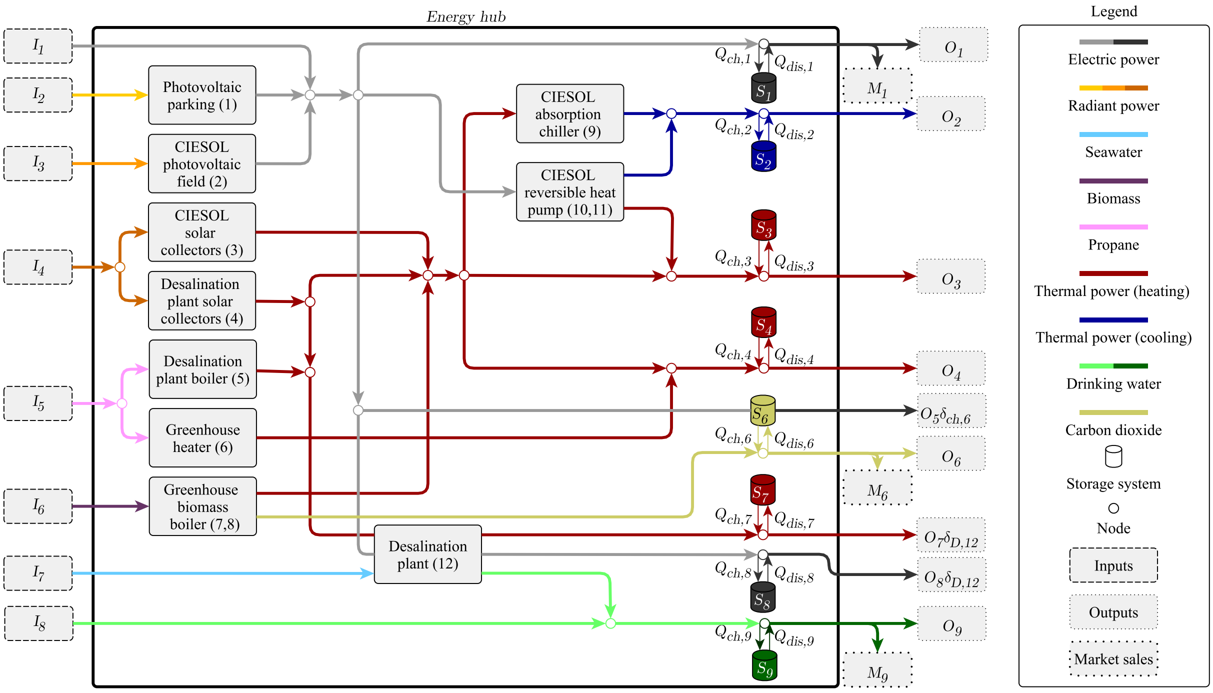

Figure 7.3. Schematic diagram of the real EH example. The individual equipment for each facility constitutes the conversion devices, whereas the public utility networks can interchange resources through I_1, I_8, M_1, and M_8. Some resources are represented by different colours, depending on the variables associated to them, in order to clarify the results in Section 7.5.

Figure 7.3 represents the example case, which consists of an EH with eight inputs and nine outputs, three of which coincide with resources available for sale (a description of each is offered in Table 7.2). Moreover, considering single-input and single-output converters so as to be able to set suitable constraints, and therefore to have two independent converters for both the greenhouse biomass boiler and the CIESOL reversible heat pump, a total amount of twelve converters (numbered within round brackets in Figure 7.3) can be identified. Different resource flows are distinguished by colours, as indicated in the legend, and nodes are employed to discern converging or diverging flows from any other crossing line caused by picturisation. As in the general model, input, output, charge, discharge, market sales, and storage vectors are defined based on top to bottom input and output resources. Radiant power has been split into three different inputs because each has a different economic cost (remember, PV generation for self-consumption type 2 is taxed).

Table 7.2. Input, output, and market variables description

Figure 7.3	Figure 7.4	Description	Units
I_1	Ei	Electricity from the public utility network	kW
I_2	Rpvpk	Radiant power received from parking PV modules	kW
I_3	Rpvcs	Radiant power received from CIESOL PV modules	kW
I_4	Rsc	Radiant power received from solar collectors	kW
I_5	Pi	Propane for fossil fuel combustion systems	kg/h
I_6	Bi	Wood pellets for the biomass boiler	kg/h
I_7	Si	Seawater for the desalination plant	m^3/h
I_8	Wi	Drinking water from the public utility network	m^3/h
O_1	Eo	Electricity for CIESOL and the greenhouse	kW
O_2	Co	Thermal power (cooling) for CIESOL	kW
O_3	Hcs	Thermal power (heating) for CIESOL	kW
O_4	Hgh	Thermal power (heating) for the greenhouse	kW
O_5	Esgh	Electricity for the greenhouse's CO_2 pump	kW
O_6	Go	Carbon dioxide for the greenhouse	kg/h
O_7	Hdp	Thermal power (heating) for the desalination plant	kW
O_8	Edp	Electricity for the desalination plant	kW
O_9	Wo	Water for CIESOL and the greenhouse	m^3/h
M_1	-	Electricity sold through the public utility network	kW
M_6	-	Carbon dioxide released from storage	kg/h
M_9	-	Water sold through the public utility network	m^3/h

According to Figure 7.3, only electricity, CO_2 and water sales are allowed, and there is no storage system for the electricity required by the CO_2 compression pump. Thus, for the sake of simplicity, the variables M_2, M_3, M_4, M_5, M_7, M_8, S_5, $Q_{ch,5}$, and $Q_{dis,5}$ are not represented.

However, they still constitute elements of the market sales, storage, charge, and discharge vectors, so the upper and lower limits of these variables have to be zero. Note that M_6 refers to CO_2 released (not sold) as this constitutes an arrangement for avoiding unfeasible solutions when the storage is full.

Similar representations of EHs are found in the literature, but this was devised in accordance with Simulink®'s block-oriented philosophy. Bearing in mind Figure 7.3, the implementation in ODEHubs is nearly immediate, as shown in Figure 7.4. Note that, the labels within some blocks are customisable for representation purposes, although by default, ODEHubs names each input and output to present the results according to the number in round brackets, matching the notation in Figure 7.3. ODEHubs also renames the *Storage System* blocks according to the label of the *Output* block to which they are connected.

In Figure 7.4, the labels within *Input* and *Output* blocks and the name of each device have been chosen to identify the kind of resources and device, but they are related to Figure 7.3 as specified in the second column of Table 7.2. With respect to the devices, their label correspond to the numeration in Figure 7.3 as indicated in round brackets: PVpk (D_1), PVcs (D_2), SCcs (D_3), SCdp (D_4), PBdp (D_5), PBgh (D_6), BBgh (D_7 and D_8), AC (D_9), HP (D_{10} and D_{11}), DP (D_{12}). In addition, M_1, M_6, and M_9 are intentionally missing because they are internally included in their respective *Output* blocks, which have been configured to allow the sale of the resources attached to that output (see Figure 6.3b).

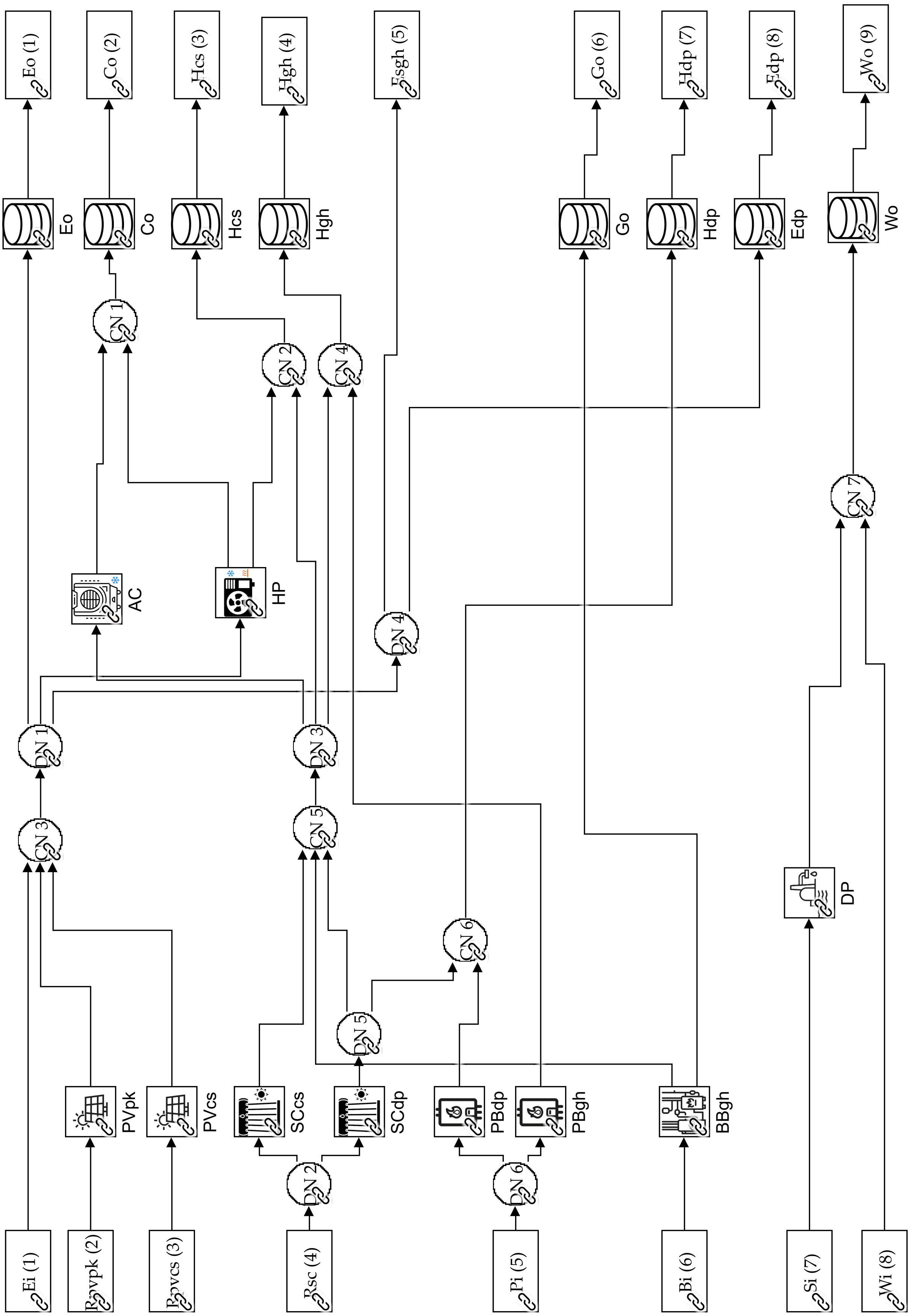

Figure 7.4. Case study of the EH defined through ODEHubs's blocks in Simulink®

Note that, in Figure 7.3, the missing arrows at the desalination plant (electricity and heat) and CO_2 storage input ports indicate that no conversion exists for these flows: they just represent the dependence of loads O_5, O_7 and O_8 on those devices, as their related binary variables also corroborate. Analogously, in Figure 7.4, the block corresponding to these devices are bypassed and the arrows are directly connected to their respective *Output* block. Therefore, in this case, ODEHubs defines the output activation matrix $\boldsymbol{\delta_O}$ as the nine-dimension identity matrix whose elements (5,5), (7,7), and (8,8) have been replaced by $\delta_{ch,6}$, $\delta_{D,12}$, and $\delta_{D,12}$.

The size of matrices $\boldsymbol{C}$, $\boldsymbol{C_i}$, $\boldsymbol{C_{di}}$ and $\boldsymbol{C_{do}}$ makes their mathematical representation difficult; hence they are defined in Tables 7.3–7.6, which contain their non-zero elements and their respective indexes. Readers are also referred to the Appendix for the full representation of these matrices. In addition, Table 7.7 shows—without mathematical notation, since its content does not refer to variables—the possible paths represented by vector $\boldsymbol{P}$. This is carried out automatically by ODEHubs, regardless of users' intervention, but it is included here for clarification.

Table 7.3. Matrix $\boldsymbol{C}$ of 9 × 30 elements

Row	Col.	Value	Row	Col.	Value	Row	Col.	Value	Row	Col.	Value
1	1	1	1	6	$\eta_{D,1}$	1	11	$\eta_{D,2}$	2	2	$\eta_{D,10}$
2	7	$\eta_{D,1}\eta_{D,10}$	2	12	$\eta_{D,2}\eta_{D,1}$	2	16	$\eta_{D,3}\eta_{D,9}$	2	19	$\eta_{D,4}\eta_{D,9}$
2	25	$\eta_{D,7}\eta_{D,9}$	3	3	$\eta_{D,11}$	3	8	$\eta_{D,1}\eta_{D,11}$	3	13	$\eta_{D,1}\eta_{D,11}$
3	17	$\eta_{D,3}$	3	20	$\eta_{D,4}$	3	26	$\eta_{D,7}$	4	18	$\eta_{D,3}$
4	21	$\eta_{D,4}$	4	24	$\eta_{D,6}$	4	27	$\eta_{D,7}$	5	5	1
5	10	$\eta_{D,1}$	5	15	$\eta_{D,2}$	6	28	$\eta_{D,8}$	7	22	$\eta_{D,4}$
7	23	$\eta_{D,5}$	8	4	1	8	9	$\eta_{D,1}$	8	14	$\eta_{D,2}$
9	29	$\eta_{D,12}$	9	30	1						

Table 7.4. Matrix $\boldsymbol{C_i}$ of 8 × 30 elements

Row	Col.	Value	Row	Col.	Value	Row	Col.	Value	Row	Col.	Value	Col.	Value	
1	1	1	1	2	1	1	3	1	1	4	1	1	5	1
2	6	1	2	7	1	2	8	1	2	9	1	2	10	1
3	11	1	3	12	1	3	13	1	3	14	1	3	15	1
4	16	1	4	17	1	4	18	1	4	19	1	4	20	1
4	21	1	4	22	1	5	23	1	5	24	1	6	25	1
6	26	1	6	27	1	7	29	1	8	30	1			

Table 7.5. Matrix $\boldsymbol{C_{di}}$ of 12 × 30 elements

Row	Col.	Value	Row	Col.	Value	Row	Col.	Value	Row	Col.	Value	Col.	Value	
1	6	1	1	7	1	1	8	1	1	9	1	1	10	1
2	11	1	2	12	1	2	13	1	2	14	1	2	15	1
3	16	1	3	17	1	3	18	1	4	19	1	4	20	1
4	21	1	4	22	1	5	23	1	6	24	1	7	25	1
7	26	1	7	27	1	8	28	1	9	16	$\eta_{D,3}$	9	19	$\eta_{D,4}$
9	25	$\eta_{D,7}$	10	2	1	10	7	$\eta_{D,1}$	10	12	$\eta_{D,2}$	11	3	1
11	8	$\eta_{D,1}$	11	13	$\eta_{D,2}$	12	29	1						

Table 7.6. Matrix $\boldsymbol{C_{do}}$ of 12×30 elements

Row	Col.	Value	Row	Col.	Value	Row	Col.	Value	Row	Col.	Value
1	6	$\eta_{D,1}$	1	7	$\eta_{D,1}$	1	8	$\eta_{D,1}$	1	9	$\eta_{D,1}$
1	10	$\eta_{D,1}$	2	11	$\eta_{D,2}$	2	12	$\eta_{D,2}$	2	13	$\eta_{D,2}$
2	14	$\eta_{D,2}$	2	15	$\eta_{D,2}$	3	16	$\eta_{D,3}$	3	17	$\eta_{D,3}$
3	18	$\eta_{D,3}$	4	19	$\eta_{D,4}$	4	20	$\eta_{D,4}$	4	21	$\eta_{D,4}$
4	22	$\eta_{D,4}$	5	23	$\eta_{D,5}$	6	24	$\eta_{D,6}$	7	25	$\eta_{D,7}$
7	26	$\eta_{D,7}$	7	27	$\eta_{D,7}$	8	28	$\eta_{D,8}$	9	16	$\eta_{D,3}\eta_{D,9}$
9	19	$\eta_{D,4}\eta_{D,9}$	9	25	$\eta_{D,7}\eta_{D,9}$	10	2	$\eta_{D,10}$	10	7	$\eta_{D,1}\eta_{D,10}$
10	12	$\eta_{D,2}\eta_{D,10}$	11	3	$\eta_{D,11}$	11	8	$\eta_{D,1}\eta_{D,11}$	11	13	$\eta_{D,2}\eta_{D,11}$
12	29	$\eta_{D,12}$									

Table 7.7. Path vector's elements for each path in the real plant

P_p	Path*	P_p	Path*	P_p	Path*
P_1	I1 → O1	P_2	I1 → D10 → O2	P_3	I1 → D11 → O3
P_4	I1 → O8	P_5	I1 → O5	P_6	I2 → D1 → O1
P_7	I2 → D1 → D10 → O2	P_8	I2 → D1 → D11 → O3	P_9	I2 → D1→ O8
P_{10}	I2 → D1→ O5	P_{11}	I3 → D2 → O1	P_{12}	I3 → D2 → D10 → O2
P_{13}	I3 → D2 → D11 → O3	P_{14}	I3 → D2 → O8	P_{15}	I3 → D2→ O5
P_{16}	I4 → D3 → D9 → O2	P_{17}	I4 → D3 → O3	P_{18}	I4 → D3 → O4
P_{19}	I4 → D4 → D9→ O2	P_{20}	I4 → D4 → O3	P_{21}	I4 → D4 → O4
P_{22}	I4 → D4 → O7	P_{23}	I5 → D5 → O7	P_{24}	I5 → D6 → O4
P_{25}	I6 → D7 → D9 → O2	P_{26}	I6 → D7 → O3	P_{27}	I6 → D7 → O4
P_{28}	I6 → D8 → O6	P_{29}	I7 → D12 → O9	P_{30}	I8 → O9

*I: input, O: output, D: device.

Finally, Equations (4.14)–(4.16) must be rearranged by ODEHubs to set suitable constraints for the EH presented in Figure 7.3: owing to the dependence of the electricity and water supply networks, Equations (7.1) and (7.2) are required,

$$\delta_{I,1}(k) + \delta_{M,1}(k) \leq 1, \tag{7.1}$$

$$\delta_{I,8}(k) + \delta_{M,9}(k) \leq 1, \tag{7.2}$$

where $\delta_{I,1}$ is the binary variable that allows the purchase of electricity from the grid, $\delta_{M,1}$ is the binary variable that allows the injection of electricity to the grid, $\delta_{I,8}$ is the binary variable that allows the purchase of water from the public network, and $\delta_{M,9}$ is the binary variable that allows the sale of water through the public network; the reversible heat pump is split into two virtual devices which cannot operate at the same time, as stated by Equation (7.3),

$$\delta_{D,10}(k) + \delta_{D,11}(k) \leq 1, \tag{7.3}$$

where $\delta_{D,10}$ is the binary variable that allows the use of the heat pump in heating mode, and $\delta_{D,11}$ is the binary variable that allows the use of the heat pump in cooling mode; and, since the biomass boiler produces both thermal energy and CO_2, consider Equation (7.4),

$$P_{25} + P_{26} + P_{27} = P_{28}, \tag{7.4}$$

where the left term of the equation represents the biomass flow for heat production whereas the right one represents the biomass flow for CO_2 production.

7.3.2 Operation Limits and Conversion Factors

Except for the solar systems, the upper and lower limits of the conversion devices, summarised in Table 7.8, correspond to static models based on their datasheet [57] and a previous study for the desalination plant [239]. Note that, Table 7.8 only contains values for $\mathbf{D_i}$ because the constraints are referred to devices' inputs, and the lower and upper limit of $\mathbf{D_o}$ are set to zero and infinity, respectively (i.e. $\mathbf{D_o}$ is unconstrained). For storage systems, either hypothetical values are assumed, or values obtained from experimentation are included [222], whereas lower and upper limit inputs are again set to zero and infinity, respectively. The market sales vector limits are not tabulated since they are zero for all their elements apart from M_1, M_6, and M_9. These, together with the input vector elements, have their lower limit set to zero whereas their upper limits are set to infinity, although the flows are indirectly limited by the production capacity of the conversion devices.

Table 7.8. Limits for converters, storage capacity, charge, and discharge flows

Variable	Min	Max	Variable	Min	Max
$D_{i,5}$	0 kg/h	20 kg/h	S_1	0 kWh	11 kWh
$D_{i,6}$	0 kg/h	6.8 kg/h	S_2	0 kWh	29 kWh
$D_{i,7}$	15 kg/h	40 kg/h	S_3	0 kWh	174.2 kWh
$D_{i,8}$	15 kg/h	40 kg/h	S_4	0 kWh	116.1 kWh
$D_{i,9}$	0 kW	100 kW	S_5	0 kWh	0 kWh
$D_{i,10}$	0 kW	26.5 kW	S_6	0 kg	25.2 kg
$D_{i,11}$	0 kW	26.5 kW	S_7	0 kWh	335.4 kWh
$D_{i,12}$	7.5 m^3/h	8.5 m^3/h	S_8	0 kWh	20 kWh
-	-	-	S_9	0 m^3	6 m^3
$Q_{ch,1}$	0 kW	3 kW	$Q_{dis,1}$	0 kW	3 kW
$Q_{ch,2}$	0 kW	20.9 kW	$Q_{dis,2}$	0 kW	20.9 kW
$Q_{ch,3}$	0 kW	125.4 kW	$Q_{dis,3}$	0 kW	125.4 kW
$Q_{ch,4}$	0 kW	104.5 kW	$Q_{dis,4}$	0 kW	104.5 kW
$Q_{ch,5}$	0 kW	0 kW	$Q_{dis,5}$	0 kW	0 kW
$Q_{ch,6}$	0 kg/h	51 kg/h	$Q_{dis,6}$	0 kg/h	51 kg/h
$Q_{ch,7}$	0 kW	250.8 kW	$Q_{dis,7}$	0 kW	250.8 kW
$Q_{ch,8}$	0 kW	3 kW	$Q_{dis,8}$	0 kW	3 kW
$Q_{ch,9}$	0 m^3/h	3 m^3/h	$Q_{dis,9}$	0 m^3/h	3 m^3/h

In contrast, devices 1 and 2 limits are set using real weather conditions and the models described in Chapter 5. The result of Equation 5.2 becomes both the upper and lower limits because it is assumed that there is no control system to adjust the irradiance received (only the electricity produced can be controlled through their maximum power point trackers, which are not connected to the data recording system). In the case of the PV parking area, these values are scaled to a tenth of its capacity to make the analysed situations more realistic: the Spanish self-consumption regulations (RD 900/2015) limited the power of PV facilities so this arrangement adapts the values of the energy produced to those typically demanded by the EH considered. Upper limits are calculated in a similar way, using the clear-sky model and the data from former studies, for both solar collector systems (the one in CIESOL [227] and the other in the desalination plant [228]) and, since their control system can regulate the inlet water flow, the lower limits are set to zero. As to conversion, degradation, charge, and discharge coefficient values, static models are used for most devices [57], as shown in Table 7.9.

Table 7.9. Conversion, degradation, charge, and discharge coefficients

Coeff.	Value	Coeff.	Value	Coeff.	Value	Coeff.	Value
$\eta_{D,5}$	11.54	$\eta_{s,1}$	0.02	$\eta_{ch,1}$	0.7	$\eta_{dis,1}$	0.8
$\eta_{D,6}$	11.54	$\eta_{s,2}$	0.06	$\eta_{ch,2}$	0.9	$\eta_{dis,2}$	0.9
$\eta_{D,7}$	4.25	$\eta_{s,3}$	0.06	$\eta_{ch,3}$	0.9	$\eta_{dis,3}$	0.9
$\eta_{D,8}$	1.76	$\eta_{s,4}$	0.06	$\eta_{ch,4}$	0.9	$\eta_{dis,4}$	0.9
$\eta_{D,9}$	0.7	$\eta_{s,5}$	0.02	$\eta_{ch,5}$	0.7	$\eta_{dis,5}$	0.8
$\eta_{D,10}$	2.9	$\eta_{s,6}$	0	$\eta_{ch,6}$	1	$\eta_{dis,6}$	1
$\eta_{D,11}$	3.1	$\eta_{s,7}$	0.06	$\eta_{ch,7}$	0.9	$\eta_{dis,7}$	0.9
$\eta_{D,12}$	0.32	$\eta_{s,8}$	0.02	$\eta_{ch,8}$	0.7	$\eta_{dis,8}$	0.8
-	-	$\eta_{s,9}$	0	$\eta_{ch,9}$	1	$\eta_{dis,9}$	1

Combustion system coefficients are determined according to the lower heating value (LHV) of each fuel and assuming a 90% global efficiency for thermal energy, a 98% combustion efficiency and a 45% carbon content in the biomass [57]. Both the reversible heat pump and the absorption chiller coefficients are obtained from their datasheets whereas the desalination plant conversion is obtained from [239]. For storage systems, either hypothetical values are assumed, or values obtained from experimentation are included [222].

7.3.3 Resource Prices

Firstly, the vectors $\boldsymbol{c}(k)$ and $\boldsymbol{s}(k)$ are defined through Equations (7.5) and (7.6) to express the price of the resource flows represented by $\boldsymbol{I}(k)$ and $\boldsymbol{M}(k)$, where zeros refer to cost-free resources.

$$\boldsymbol{c}(k) = \begin{bmatrix} c_1 & c_2 & c_3 & 0 & c_5 & c_6 & 0 & c_8 \end{bmatrix} \tag{7.5}$$

$$\boldsymbol{s}(k) = \begin{bmatrix} s_1 & 0 & 0 & 0 & 0 & 0 & 0 & 0 & s_9 \end{bmatrix} \tag{7.6}$$

Electricity cost $c_1 = 1.21 p_E$ is calculated according to the local supply company tariff with super off-peak time discrimination [240], for low-voltage contracted power over 15 kW, with winter and summer corresponding to daylight saving time periods. A 21 % value-added tax (VAT) is applied to prices (p_E) presented in Table 7.10.

Table 7.10. Local supply company tariff prices (p_E). Source: [240]

Period	Price	Winter (UTC+1)	Summer (UTC+2)
P1	0.168899 €/kWh	18-22 h	11-15 h
P2	0.093162 €/kWh	8-18 h / 22-24 h	8-11 h / 15-24 h
P3	0.073738 €/kWh	0-8 h	0-8 h

Photovoltaic energy costs $c_2 = \eta_{D,1} p_{PV}$ and $c_3 = \eta_{D,2} p_{PV}$ are obtained from variable charges over the 3.0A access fee [241] shown in Table 7.11. Since these prices (p_{PV}) refer to self-consumed energy, two adjustments are performed: prices in Table 7.11 are multiplied by $\eta_{D,1}$ and $\eta_{D,2}$ to get, respectively, c_2 and c_3 in terms of radiant power, and prices are aggregated to s_1 in order to take into account the portion of non-self-consumed energy (bear in mind the case for self-consumption type 2).

Table 7.11. Variable charges with the 3.0A access fee (p_{PV}). Source: [241]

Period	Price	Winter (UTC+1)	Summer (UTC+2)
P1	0.019894 €/kWh	18-22 h	11-15 h
P2	0.013147 €/kWh	8-18 h / 22-24 h	8-11 h / 15-24 h
P3	0.008459 €/kWh	0-8 h	0-8 h

With regard to the remaining $\boldsymbol{c}(k)$ elements, constant values are assumed based on local retailer prices: the propane cost c_5 is fixed at 1.4 €/kg plus 21 % VAT [242], the biomass cost c_6 is fixed at 0.255 €/kg (VAT included) [243] and the water cost c_8 is fixed at 0.497 €/m^3 plus 10 % VAT [244].

Regarding sales, electricity prices (7.7) from daily and intraday markets (p_{ES}), expressed in €/MWh, are considered together with the generation fee (0.5 €/MWh), the 7 % IVPEE and the non-self-consumed energy in order to calculate s_1 (7.7). Water (s_9) is considered to be sold at 90 % of the purchase price; in other words, 0.447 €/m^3. Note that the s_6 price is zero because M_6 expresses the amount of CO_2 released from storage.

$$s_1 = (0.93 p_{ES} - 0.5)/1000 + p_{PV} \tag{7.7}$$

7.4 Simulation Scenarios

7.4.1 Management Strategy

Assuming that the output vector, the weather conditions and the resource prices are known, or at least estimated with a high degree of confidence, for a period of H samples, different criteria (economic, environmental, etc.) can be considered to determine the operation schedule (i.e. the values for input, charge, discharge vectors and the binary variables, which are decision variables) minimising an objective function. In this case, the management strategy aimed at achieving the lowest operation cost is applied by solving the optimisation problem stated in Equation (4.25).

In real applications, the decision variables determined this way can constitute set-points for lower-level control loops, which adjust the operation for each device. Because of uncertainties in energy prices and demand, the decision variables must be dynamically determined and so the optimisation problem is solved iteratively in order to update the set-point values. Similar to MPC algorithms, a receding but variable horizon strategy is employed: operation schedule is calculated by repeatedly solving the above-mentioned problem with different values of H, only taking into account the decision variable values of the first sample.

For simplicity's sake, only resource cost is considered (self-consumption fixed charges and maintenance costs are not taken into account), so $\boldsymbol{c}(k)$ and $\boldsymbol{s}(k)$ are row vectors containing the price of each input or sold resource in terms of energy, mass or volume. Equation (4.25) is adjusted in ODEHubs to take into account the fact that the sample time T is defined in minutes, and the optimisation problem is actually formulated as in Equation (7.8),

$$\begin{aligned} \min \quad & \sum_{k=0}^{H-1} (\boldsymbol{c}(k)\boldsymbol{I}(k) - \boldsymbol{s}(k)\boldsymbol{M}(k))\frac{T}{60} \\ \text{s.t.} \quad & \text{Equations (4.1)–(4.16).} \end{aligned} \tag{7.8}$$

Both the legal framework and the electricity market have been detailed in this section to justify resource pricing and formulate the problem formally. The district can be sorted out as self-consumption type 2, and therefore the surplus energy produced in the photovoltaic facilities can be sold through the public utility network. Thus, electricity pricing plays a fundamental role in the optimisation problem since it delimits the H value and determines the first element of the $\boldsymbol{s}(k)$ vector. Although prices are updated four times in the daily market, only the FVDS price published before 17:00 h (UTC+1/UTC+2) is available for download; therefore, this time will be employed to determine the length of the optimisation horizon (see Figure 7.5) together with the intraday session's FHS publication time (the output vector, the weather conditions and the remaining resource prices are assumed to be known for any given time period).

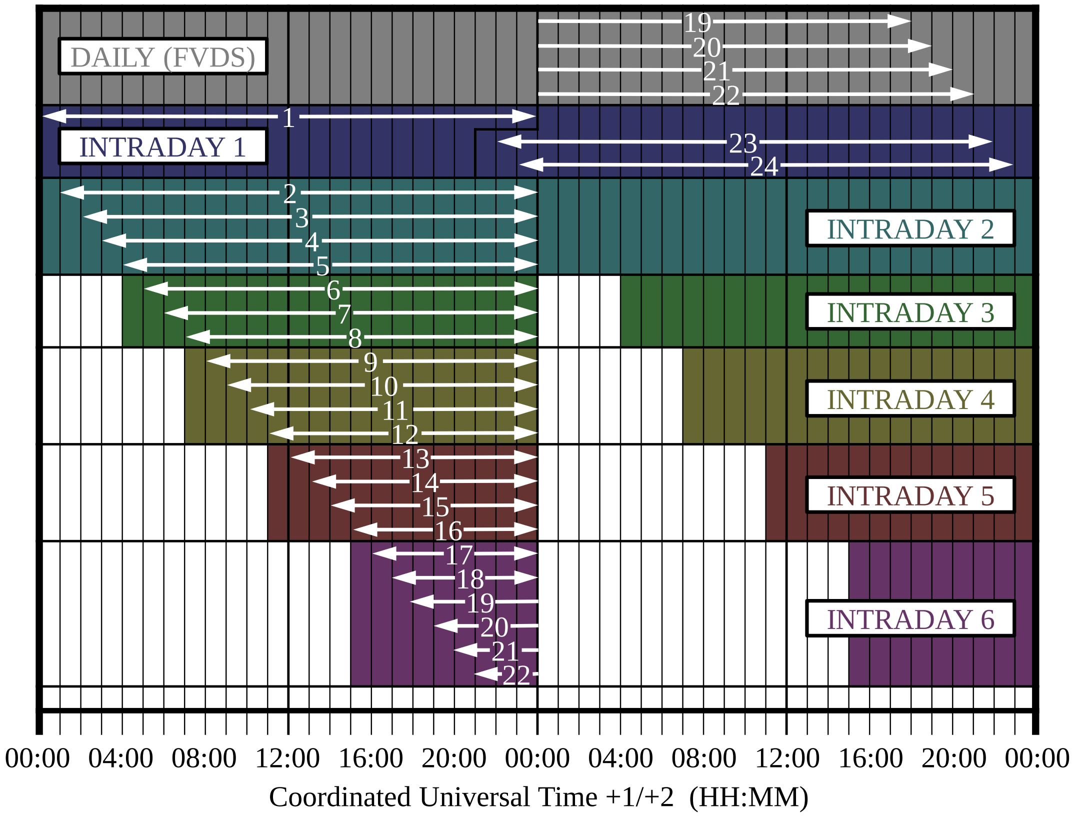

Figure 7.5. Optimisation horizons for each iteration performed to obtain the scheduling and to update the prices in each one (numbers between arrows delimit the intervals considered). In iterations 19 to 22, prices from both the daily market and the sixth session of the intraday are employed, so the arrows are divided to indicate the prices corresponding to each one. The time axis label refers to both summer (UTC+2) and winter periods (UTC+1).

- From 0 h to 18 h (UTC+1/UTC+2), the operation schedule is calculated by shortening H in order to make it equivalent to the difference between the current time and midnight, the period when the electricity price is known.
- From 18 h to 24 h (UTC+1/UTC+2), the electricity price is published for the whole of the following day, so H takes a value equivalent to 24 h (24 samples, given the sample time).

In both cases, the vector $\boldsymbol{s}(k)$ is updated according to the prices published by OMIE concerning daily and intraday markets, as detailed below, leaving an hour-long margin from the time when prices are published. The sample time can be fixed to sixty minutes, considering that electricity prices are published on this basis, and Figure 7.5 illustrate how the horizon's length is determined for the twenty-four iterations required to obtain the daily schedule.

7.4.2 Selected Experimental Data

With regard to weather conditions and demand profiles, two days are selected from the 2013–2017 period as an example of a summer (01/08/2014) and winter (31/01/2014) day. All the parameters characterising each kind of day (the output vector, the ambient temperature, the solar radiation and the electricity price) are depicted below in Figures 7.6–7.8. Since H can take a value equivalent to 24 h, the period of data corresponding to 02/08/2014 and 01/02/2014 are also included. All one-minute data were averaged over a sixty-minute period and the storage systems are supposed to be empty at the outset.

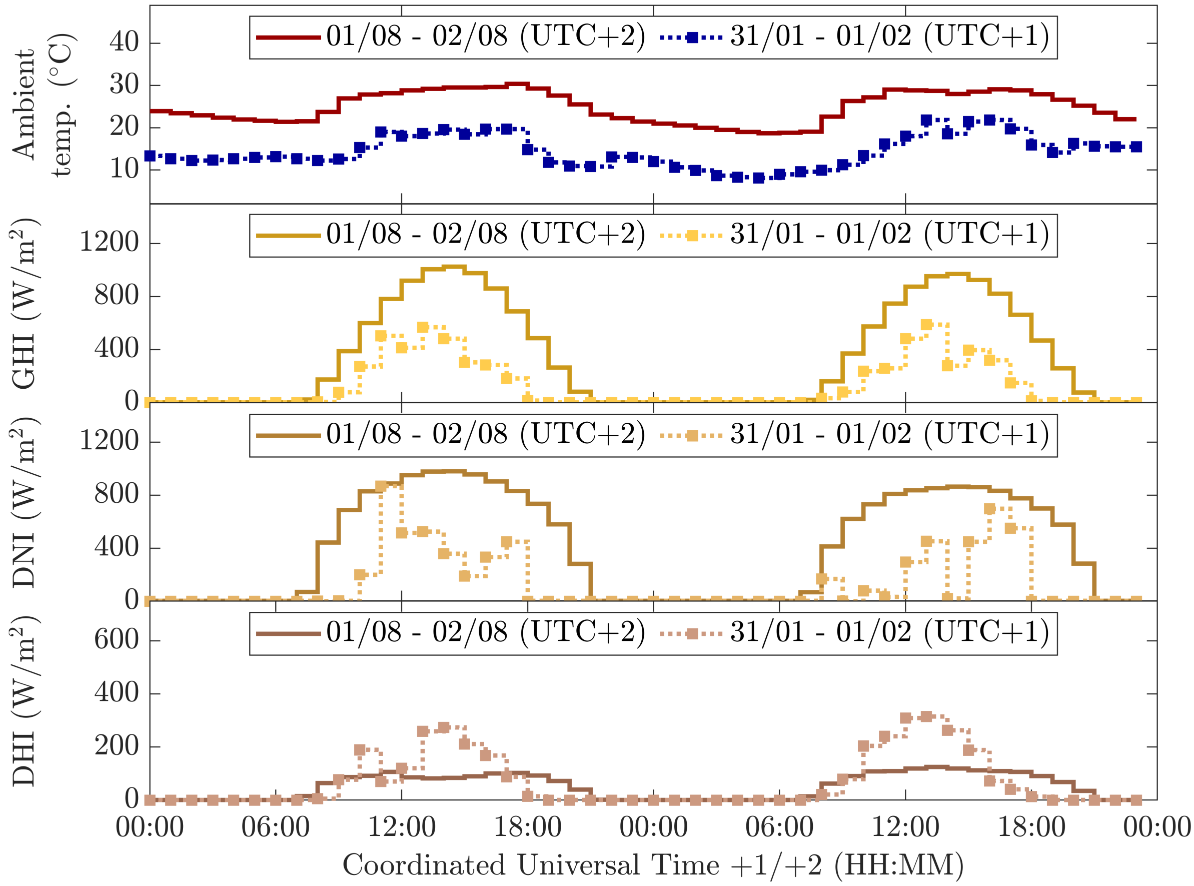

Figure 7.6. Weather conditions for the scenarios simulated. The summer period (01/08/2014-02/08/2014) corresponds to higher average levels of temperature and radiation versus the winter period (31/01/2014-01/02/2014). The time axis label refers to both summer (UTC+2) and winter periods (UTC+1), depending on the date.

Firstly, weather conditions directly affect the amount of energy produced in the solar systems: the available solar radiation is required to determine the lower and/or upper limit of certain devices and the ambient temperature is related to the performance of the same. In order to give an idea of the contrast between both days, Figure 7.6 illustrates the ambient temperature together with the global, direct beam, and diffuse radiation in each case. As can be observed, the summer period at the latitude considered is characterised by higher temperatures for both days, oscillating between 18.4 °C and 30.4 °C versus 8.1 °C and 21.8 °C in the winter period. Global horizontal irradiance (GHI), direct normal irradiance (DNI) in the first case also surpass those in the second whereas these data, together with the diffuse horizontal irradiance (DHI) profiles, reflect the presence of cloudiness on 31/01/2014 and 01/02/2014 (cloudiness increases the amount of DHI and diminishes the DNI).

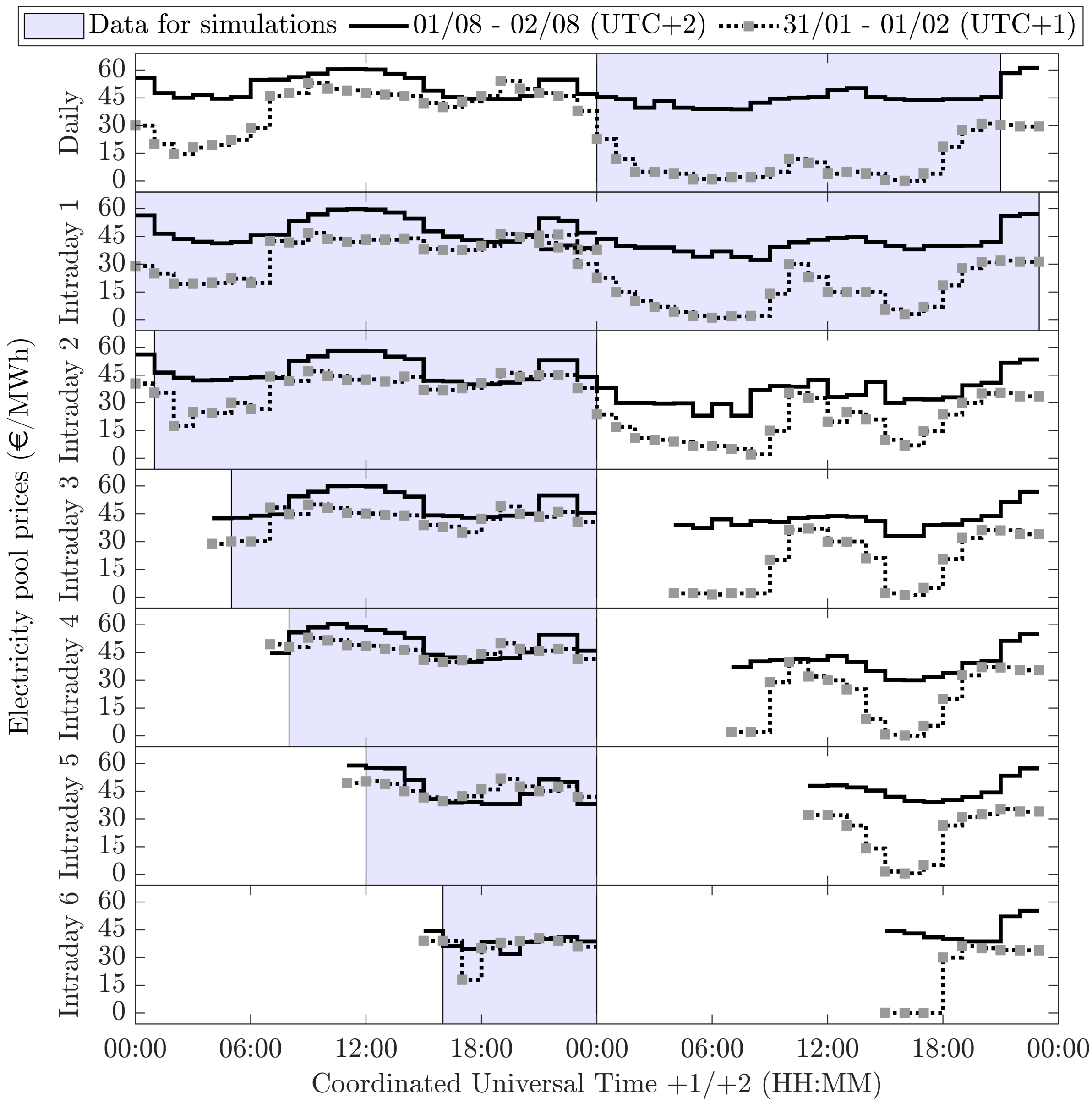

Figure 7.7. Electricity prices for the scenarios simulated. The shadowed areas indicate the data employed when the strategy proposed is applied (see Figure 7.5). In general, the energy is more expensive on the summer days (01/08/2014-02/08/2014) versus the winter days (31/01/2014-01/02/2014). The time axis label refers to both summer (UTC+2) and winter periods (UTC+1), depending on the date. Source: [229]

In addition, Figure 7.7 consists of the electricity prices from the daily (FVDS) and intraday markets, as published by OMIE for the periods considered. Because of the horizon of each session, the prices of Session 2 overlap between 21–24 h, whereas in Sessions 3–6, gaps appear in the hours prior to price publication. In accordance with the strategy proposed and the sample time of sixty minutes, the prices employed in each iteration are determined as shown in Figure 7.5; those employed for simulations have been shadowed in Figure 7.7.

Indirectly, the demand profiles are influenced by the weather conditions, so it is important to depict the output resources required for all the facilities, as presented in Figure 7.8, to understand the results. On the one hand, the electricity profiles are quite similar since, in both periods, a base power of around 65 kW is demanded. Thermal power demand is strongly related to the workday and the season of the year: in summer the workday is shorter and there is only cooling demand, which is concentrated during the morning (from 8 to 15 h on 01/08/2014), whereas in winter the workday usually last beyond 18 h and only heating is required. The 01/02/2014 date corresponds to a non-working day (Saturday) and therefore the heating profile is nil.

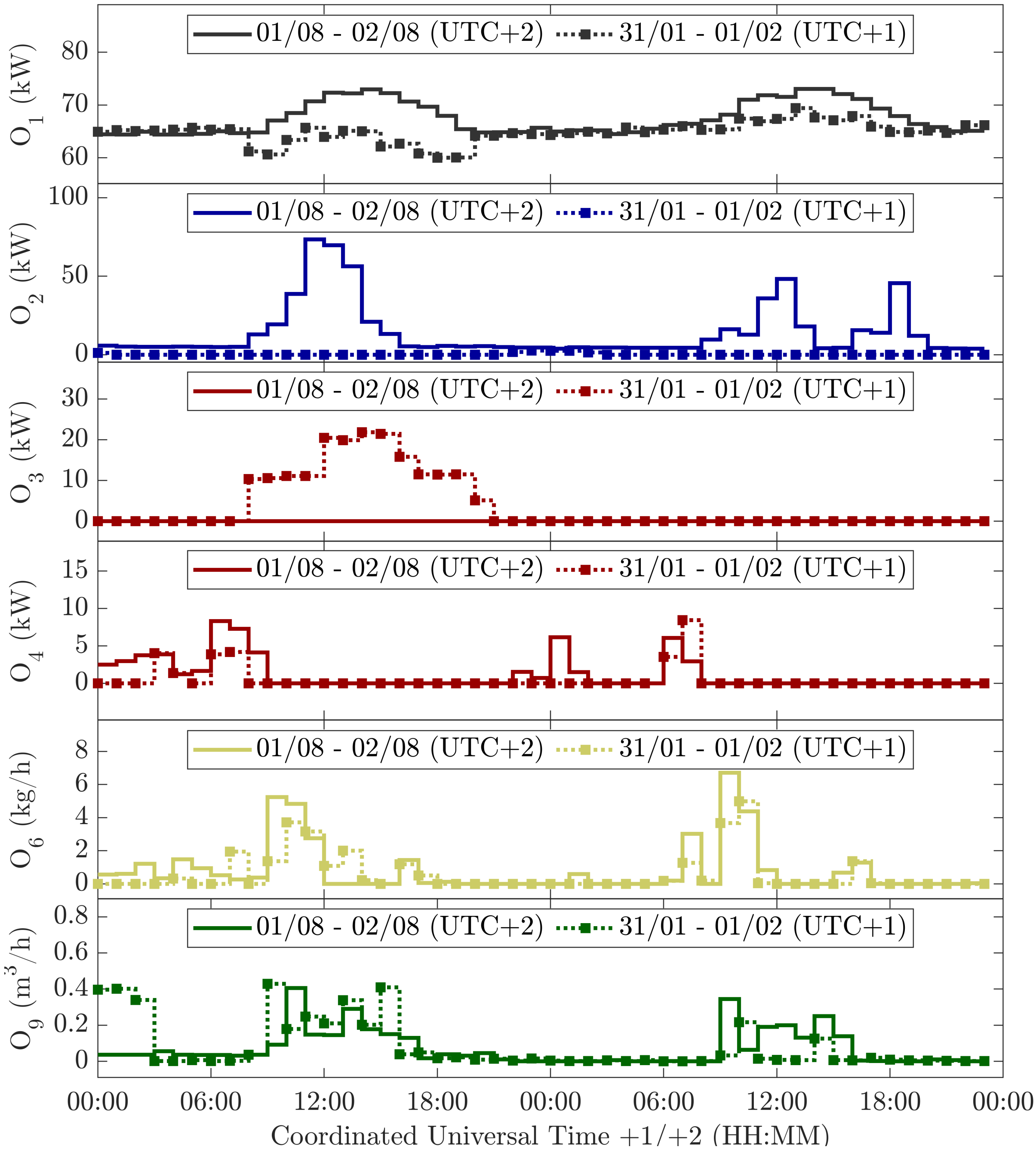

Figure 7.8. Demands for the scenarios simulated. From top to bottom: electricity or CIESOL and the greenhouse (O_1), thermal power (cooling) for CIESOL (O_2), thermal power (heating) for CIESOL (O_3), thermal power (heating) for the greenhouse (O_4), carbon dioxide for the greenhouse (O_6), and water for CIESOL and the greenhouse (O_9). The outputs attached to binary variables are not included since they are not known beforehand. The time axis label refers to both summer (UTC+2) and winter periods (UTC+1), depending on the date.

On the other hand, greenhouse's heating and CO_2 demands usually constitute opposite profiles since the former is needed at night, especially when the ambient temperature is lower (usually in winter) while the latter is related to photosynthetic activity, which only occurs in the presence of radiation (the availability of which is higher in summer) during the day. Figure 7.8 illustrates these facts since the thermal power demanded is higher on 31/01/2014 and on 01/02/2014; as does the CO_2 on 01/08/2014 and on 02/08/2014. With regard to water requirements, these increase during the workday, with peaks in periods of greenhouse irrigation, and with no significant differences between both simulated scenarios.

7.5 Resource Scheduling Results

The problem addressed is solved by running *intlinprog* MATLAB®'s solver [245] iteratively on an Intel® Core™ i7-6700K 4GHz CPU, taking less than two minutes for each scenario. Results for 01/08/2014 are shown in Figures 7.9, 7.11 and 7.13 and on 31/01/2014 in Figures 7.10, 7.12 and 7.14, employing colours according to each kind of resource as in Figure 7.3.

Each figure contains the hourly demand profiles (outputs), plotted with a thick line, and the market sales profile (M_o), stacked over the latter with a thin line; both are scaled to the left axis and expressed in terms of power or flow. The dashed line, scaled to the right axis, represent the evolution of the storage systems, corresponding to each output (S_o), in terms of energy, mass or volume. In each plot, the right axis upper limit corresponds to the storage maximum capacity (except for S_5). Coloured stacked bars (scaled to the left axis) indicate inputs for which demands are met (I_i); therefore, when they are over the demand and sales profiles, the storage systems are charged (so the dashed line has a positive slope) whereas they are discharged when under them. Because of the degradation assumed in certain stored resources (see Table 7.9), in some cases the storage profile has a negative slope, similar to a discharge, even when the demand and sales profiles are met (see for example S_1 in Figure 7.9 between 18 h and 24 h or S_2 in Figure 7.10 between 12 h and 22 h).

Figure 7.9 and Figure 7.10 combine the results obtained for the thermal power demanded by CIESOL and the electricity that it and the greenhouse need. Heating demand during the summer day is nil (O_3 in Figure 7.9) and this is almost the same with the cooling demand on the winter day (O_2 in Figure 7.10). The solar energy value is manifested in the remaining plots since the demand during the morning and the afternoon is covered by photovoltaic (see I_2 and I_3) or solar thermal power (I_4). This is because solar alternatives are cheaper than purchasing electricity (I_1), providing that sufficient radiation is available. A key difference between the summer and the winter day is that the electricity storage system (S_1) is not completely empty at day's end in summer. This is justified because the prices for the following day (see shadowed Daily Prices in Figure 7.7) make it profitable to store energy in the first case (01/08/2014) but not in the second (31/01/2014), when prices fall by around 30 €/MWh. The thermal storage system (S_2 and S_3) variations experience consistent behaviour: accumulating energy during the sun hours to utilise it during the evening and at night, instead of using electricity. The only exception to this is the biomass boiler (I_6) working during the night, at 0 h on 01/08/2014 and at 3 h on 31/01/2014, in order to take advantage of both the CO_2 and the heat demanded (see O_4 and O_6 in Figure 7.11 and Figure 7.12 at those times). With regard to electricity sales (M_1), these are clearly noticeable on 01/08/2014 during the afternoon and, to a lesser extent, on 31/01/2014 at 13 h.

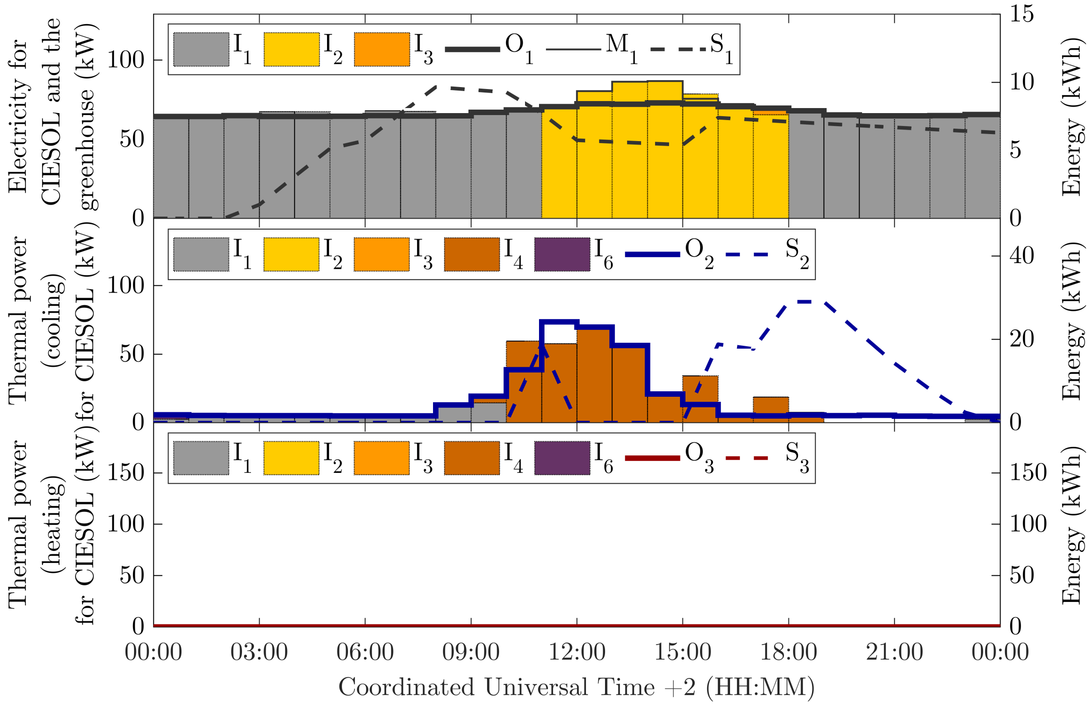

Figure 7.9. Simulation results on 01/08/2014 (first trio of variables). The figure contains the scheduling for each output (O_o) of the case study EH, sorted by number and including the evolution of each storage system (S_o), the inputs through which the demand is met (I_i), and the resources sold (M_o).

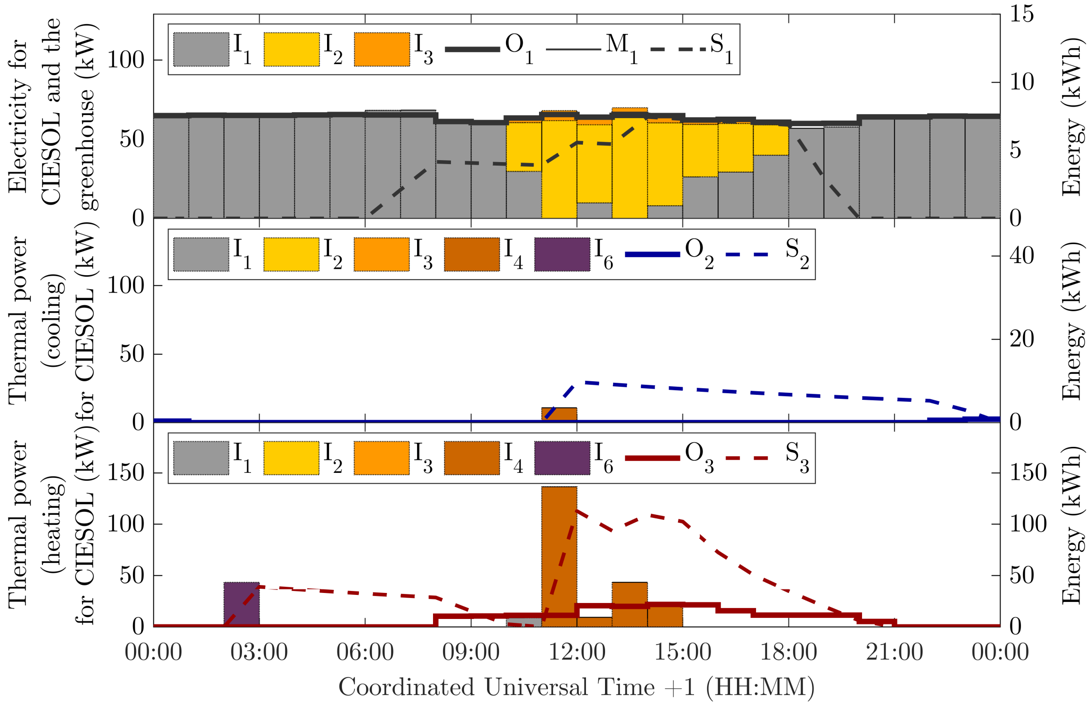

Figure 7.10. Simulation results on 31/01/2014 (first trio of variables). The figure contains the scheduling for each output (O_o) of the case study EH, sorted by number and including the evolution of each storage system (S_o), the inputs through which the demand is met (I_i), and the resources sold (M_o).

Figure 7.11 and Figure 7.12 contain the results related to the CO_2 and thermal power consumption of the greenhouse. Note that the coloured stacked bars corresponding to the inputs which meet the demands in each figure are presented at the same time (0 h on 01/08/2014 and 3 h on 31/01/2014). The explanations for the scheduling observed are as follows: the only source to produce carbon dioxide is the biomass boiler (I_6) but, on the one hand, its input mass flow is limited to a minimum of 15 kg/h (see Table 7.8) and, on the other, the cost of storing CO_2 increases with the number of times that the compressor activates (O_5). Therefore, as soon as the greenhouse requires this gas enrichment (O_6), the reasonable decision is to produce all the CO_2 required for the whole day in a single step so as to avoid wasting electricity with the compressor (O_5). Given that more CO_2 than required is produced because of the boiler's input lower limit, a portion is released (M_6) in both cases. Additionally, the thermal energy produced is stored (S_2, S_3, S_4) or employed to supply other demands (O_2, O_3, O_4), as shown in Figure 7.9 at the middle and bottom, and in Figure 7.11 at the top. Since the carbon dioxide is required (O_6) for the first time during the night in both cases, solar energy sources (I_2, I_3) cannot be employed to supply electricity to the compressor (O_5). The greenhouse thermal demand (O_4) is almost entirely covered with the heat produced by the boiler, except at 23 h on 01/08/2014 when the propane heater actuates as a support supply (I_5).

Figure 7.13 and Figure 7.14 include the scheduling for the water and the desalination plant demands. The main differences between both days is that powering the desalination plant (O_7, O_8) to produce water on 31/01/2014 was not worthwhile (Figure 7.14), even though this is not necessarily the general case in winter, since the energy from the sun (I_2, I_3, I_4) is not enough to cover the requirements of the whole EH (using propane and acquiring electricity increases the cost) and buying water instead (I_8) is more economical.

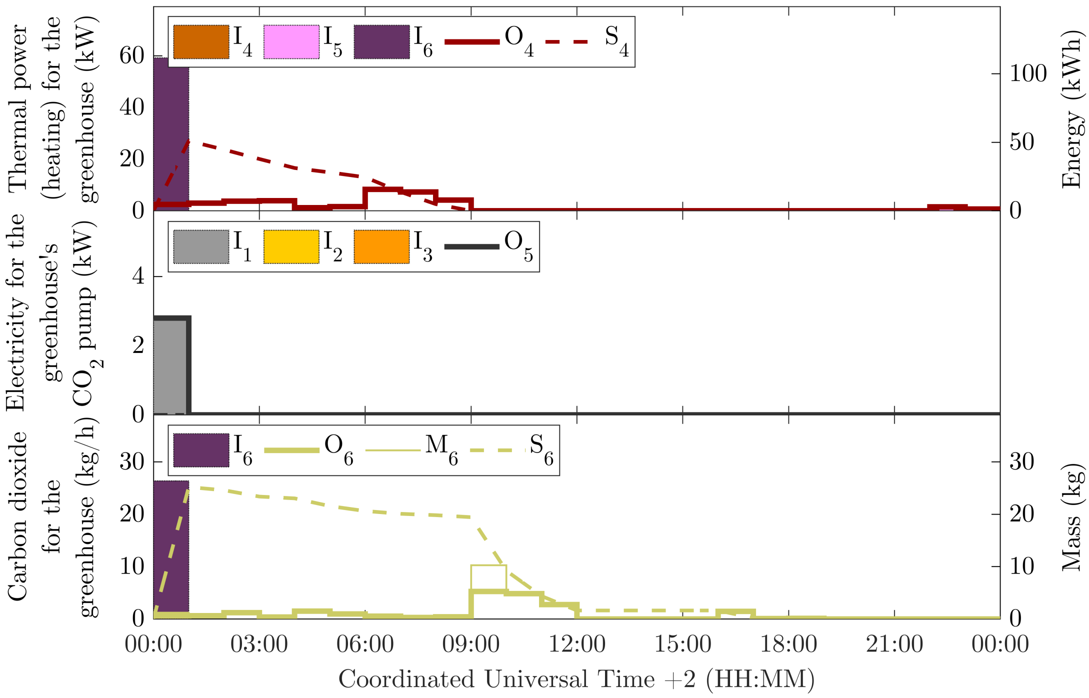

Figure 7.11. Simulation results on 01/08/2014 (second trio of variables). The figure contains the scheduling for each output (O_o) of the case study EH, sorted by number and including the evolution of each storage system (S_o), the inputs through which the demand is met (I_i), and the resources sold (M_o).

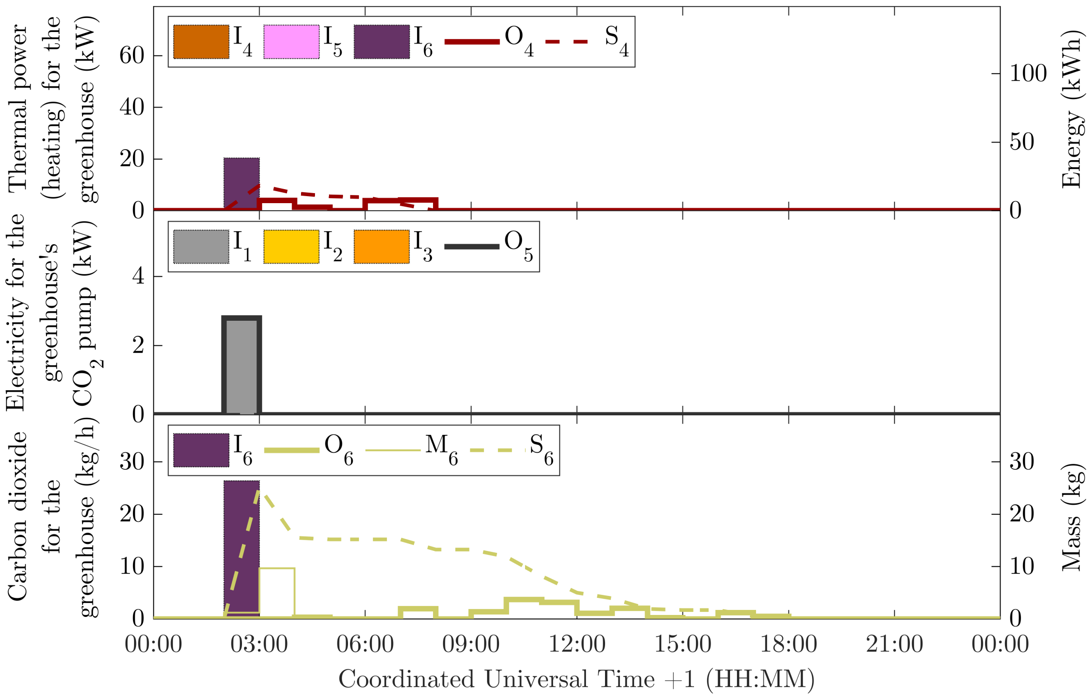

Figure 7.12. Simulation results on 31/01/2014 (second trio of variables). The figure contains the scheduling for each output (O_o) of the case study EH, sorted by number and including the evolution of each storage system (S_o), the inputs through which the demand is met (I_i), and the resources sold (M_o).

Figure 7.13 illustrates the opposite situation: the abundance of radiation allows seawater to be distilled at a lower cost. In this case, the amount of water produced (I_7) is more than needed (O_9) in order to sell the excess through the public network (M_9) or to store it (S_9) for the following day (when it would likewise be sold or consumed). The figure also shows how the desalination plant power demand (O_7, O_8) corresponds to the periods when water is produced (I_7). Although in this case the demands are met through the solar production facilities (I_2, I_3, I_4), the support of the power grid (I_1) and the propane boiler (I_5) could be necessary under certain circumstances to supply water profitably (for example complementing the photovoltaic and solar thermal production).

In addition, all these results are summarised in Table 7.12 in terms of demanded/supplied energy, mass or volume for vectors $\boldsymbol{I}$, $\boldsymbol{O}$ and $\boldsymbol{M}$ over the simulated days. Also, the total cost of importing (positive values) or selling resources (negative values) are included, according to vectors $\boldsymbol{c}$ and $\boldsymbol{s}$. Although demand differs between the summer and the winter day, especially that related to thermal power, in both cases the total operation cost is quite similar: less than a 3 € difference. Higher demands on 01/08/2014 were compensated for by electricity and water sales through the public utility networks. It is noticeable that the cost of self-consumed energy represents a 34.7%, in the summer day, and a 13.3%, in the winter day, of the total operation cost, which is however well worth it for the savings on the electricity imported from he grid. Since the case presented is based on the Royal Decree 900/2015, performing the same analysis considering the current situation (Royal Decree 244/2019) would give as a result lower operation costs, pointing up the benefits of RES.

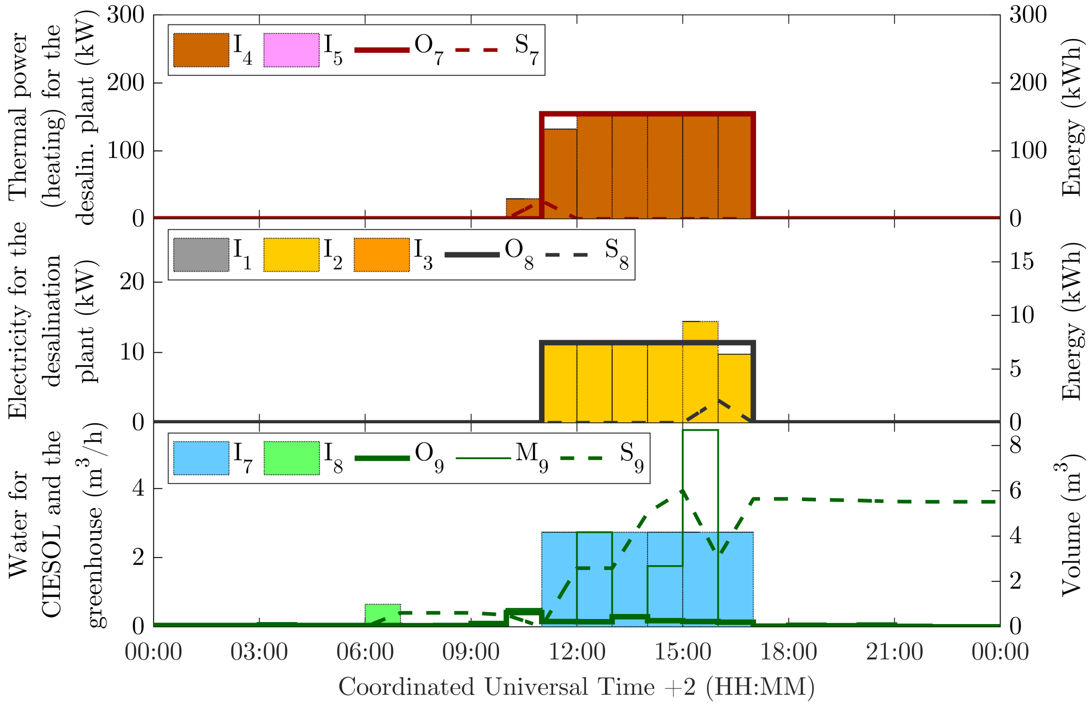

Figure 7.13. Simulation results on 01/08/2014 (third trio of variables). The figure contains the scheduling for each output (O_o) of the case study EH, sorted by number and including the evolution of each storage system (S_o), the inputs through which the demand is met (I_i), and the resources sold (M_o).

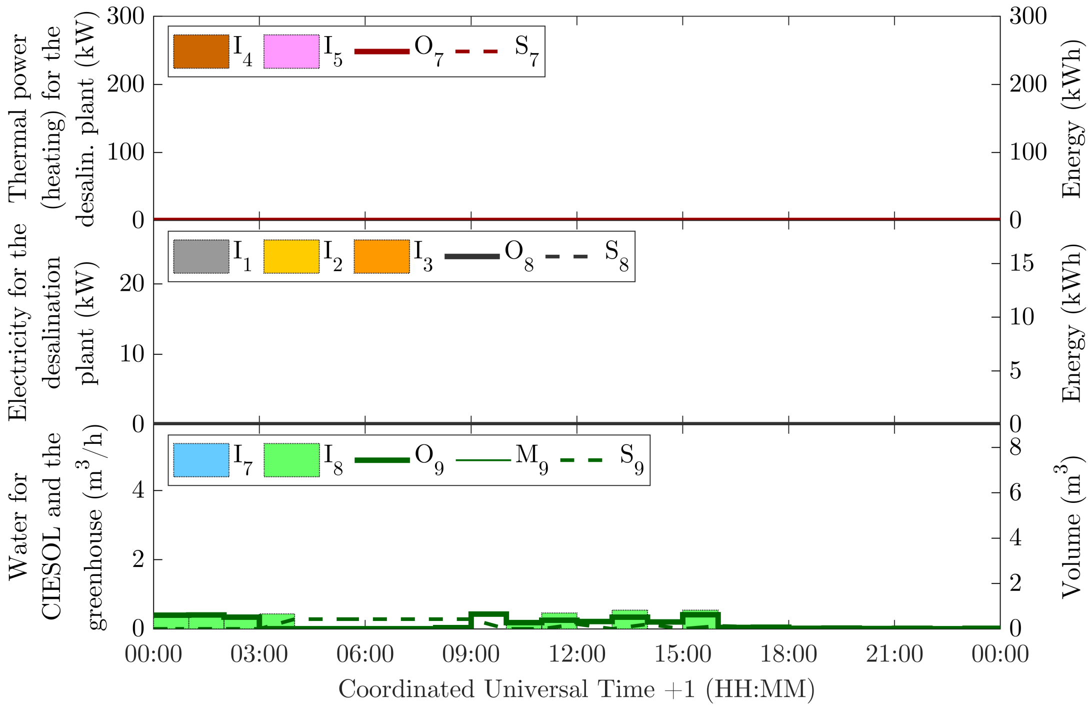

Figure 7.14. Simulation results on 31/01/2014 (third trio of variables). The figure contains the scheduling for each output (O_o) of the case study EH, sorted by number and including the evolution of each storage system (S_o), the inputs through which the demand is met (I_i), and the resources sold (M_o).

Table 7.12. Input, output, and market total demand/supply and costs

	Summer day		Winter day	
Variable	**Accumulated**	**Cost**	**Accumulated**	**Cost**
I_1	1150.28 kWh	116.81 €	1171.32 kWh	141.82 €
I_2	5102.92 kWh	60.73 €	2615.97 kWh	22.89 €
I_3	39.91 kWh	0.20 €	262.63 kWh	2.18 €
I_4	3189.96 kWh	0 €	606.42 kWh	0 €
I_5	0.19 kg	0.33 €	0 kg	0 €
I_6	15 kg	3.83 €	15 kg	3.83 €
I_7	51 m^3	0 €	0 m^3	0 €
I_8	0.97 m^3	0.53 €	3.42 m^3	1.87 €
O_1	1611.58 kWh	-	1530.25 kWh	-
O_2	386.96 kWh	-	5.37 kWh	-
O_3	0 kWh	-	182.24 kWh	-
O_4	37.93 kWh	-	13.48 kWh	-
O_5	2.8 kWh	-	2.8 kWh	-
O_6	20.74 kg	-	15.52 kg	-
O_7	927.00 kWh	-	0 kWh	-
O_8	68.4 kWh	-	0 kWh	-
O_9	2.02 m^3	-	3.37 m^3	-
M_1	41.32 kWh	-2.80 €	1.81 kWh	-0.11 €
M_6	5.65 kg	0 €	10.88 kg	0 €
M_9	9.82 m^3	-4.39 €	0 m^3	0 €
Total	-	175.23 €	-	172.48 €

7.6 Contributions and Related Publications

This chapter supports the same two core contributions as Chapter 4 as introduced in Section 1.4, and the two ones related to the practical knowledge of this thesis that have not been treated in the previous chapters (testing the validity of the proposed modelling framework and data processing). The results obtained in the selected scenarios demonstrate a logical operation schedule, validating the proposed approach, and they were published in the Applied Energy journal [41]. In addition, the legal reforms introduced in 2018, motivated a comparison study of the same plant against the previous situation [51], although the former framework has been considered in this chapter because it provides a more enriching demonstration on how fixing the cost of the acquired resources. Finally, the use of ODEHubs introduced in [44] has been elucidated in Section 7.3 with respect to the original analysis carried out for Applied Energy [41].

8. Contributions, Conclusion and Future Work

Chapter Summary

In this final chapter, the main ideas derived from the previous chapters serve to conclude this thesis. Section 8.1 reiterates the importance and originality of the contributions already presented in Chapter 1, Section 8.2 discusses some of the topics covered within the thesis, analysing their drawbacks and benefits, and Section 8.3 presents possible future lines of research to give continuity to the work developed.

8.1 Contributions Summary

As stated in Section 1.4, to which readers are referred for a full view of the contributions of this thesis with regard to the research objectives, they are recapped below in descending order of relevance and including the publications that support them.

- Formulation of a widely applicable generic modelling framework for representing multifarious EHs or MESs. [41, 43, 44]
- A software library called ODEHubs, based on the proposed framework, devised to ease the implementation of control or dispatch problems, and freely available on Github (https://github.com/ual-arm/odehubs). [44, 47, 53]
- Formalisation of the optimisation problem required to apply MPC-based or scheduling strategies for energy/resource management in EHs or MESs. [41, 43]
- Testing the proposed approach's validity on several case studies, although for the sake of conciseness, in this document only the most complex, but illustrative, modelling example has been presented in Chapter 7. [41, 43, 44, 46, 48, 49, 51, 53]
- Validation of a model for photovoltaic production based on the solar irradiance on sloped surfaces and the equivalent circuit for photovoltaic cells. [50]
- Combination, cleansing, and synchronisation of the databases of the facilities in order to identify consumption profiles for simulation purposes. [41]
- Preliminary arrangements in the software and the formulation to include chance constraints according to the presence of uncertainty in solar radiation forecasts. [44]

8.2 Conclusion

Taking into consideration Sections 2.1–2.3, which gave rise to the article submitted to IEEE Access [45], the most relevant ideas that can be extracted from that review, aimed at offering a global and straightforward view of the state-of-the-art to readers, are discussed in the following lines. As new design, scheduling, control and modelling techniques in production systems continue to be developed, it becomes palpable that without a comprehensive view on the terms and issues involved, resembling to the offered in this thesis, the identification of research opportunities can be really challenging. From a critical point of view, readers should regard the classification proposed in Chapter 2 as a non-exhaustive paradigm: classifying is intrinsically arguable since the level of detail might be at a certain point subjective. To the best of the author's capabilities, each publication has been scrutinised for identifying the required features in Tables 2.1–2.5, but some of them might not be accurate as the information available in the articles was unclear or insufficient.

In addition, some publications not covered by that review might consider different contexts, use other programming tools than the ones presented, and employ specific techniques that would fit better within a broader categorisation. As an ongoing topic, future research will introduce sooner or later new terms, methodologies and advances in software that could outdate the analysis performed. Currently, most works are focused on purely energetic issues with economic incentives, aimed at reaching clean, efficient, and sustainable production and transportation services for which RES need to be incorporated. Their contributions are however of interest when it comes to the management of heterogeneous resources (which can be both material and energetic), since similar methodologies are applicable, for example, in drinking water or CO_2 utility networks. On the integration of these, there are not many publications, and therefore it is an interesting topic for researchers, which might constitute the future evolution of the term MES to multi-resource system (MRS).

Another important fact that can be deducted from the review is that the denominations MG, VPP, EH, and MES, even though they may suggest being related with certain methodologies, they have more in common than not. Concretely, EHs have been sometimes associated with input–output models [16], but there are also examples of more complex models [73]. Thus, they can be indistinctly used for the vast majority of problems reviewed and actually some papers include more than one of these terms simultaneously [73]. In the same way, although in the field of MGs there are examples of experimental plants where real tests are carried out, many studies employ simulated systems. This is due to practical reasons, as most research is performed in academia and larger systems may belong to different agents or owners, which often makes experimenting unfeasible or too much expensive, particularly for testing designs on real environments (it would require developing prototypes). Something similar occurs with the consideration of uncertainty in models, which adds complexity to the problem and either can be ignored in not critical applications, or the tools to treat it are not sufficiently developed. To solve this issue MPC is presented sometimes as a deterministic approach (as discussed at the end of Section 1.1) that allows dealing with uncertainty. In summary, for practical use, the proposed classification is consistent enough and useful to detect some scientific gaps that could be tackled in future lines of research, which could complement the performed review by expanding it (regarding optimisation techniques and multi-criteria analyses) and make contributions in the field of production systems by pushing real test forward in other systems than MGs.

On the other hand, a holistic proposal for resource management such as the one presented in Chapter 4 can be a suitable instrument for resource scheduling problems. The results obtained in Chapter 7 are coherent with respect to the intuitively expected behaviour of the controller regarding the economic objective, and they prove that the approach adopted is appropriate even when the scheduling depends on mutually exclusive decisions (for example, resolving when a device must actuate or not) and bespeak the validity of the new elements introduced in the EH framework: the consideration of devices consuming a resource which is not related to the quantity of output produced, by attaching binary decision variables to certain energy hub outputs; the "path vector" which has been defined to take into account the flows of resources within the system instead of employing a variable for each branch between the components; and the introduction of the market sales vector to express the amount of output resources sold from the energy hub, including constraints for those resources which are exported and imported through the same medium.

The modelling approach proposed in Chapter 4 also helps one to augment the accuracy of the process represented without increasing computational complexity; this is achieved by defining the path vector rather than including a decision variable for each branch [21] between devices or between them and the input or output nodes. The computation times required for solving the scheduling problem of Chapter 7 allow one to increase the model complexity yet still make it applicable in real-time management. The choice of the receding horizon length, for instance, is one of the main computation time determinants and increasing it could improve the results obtained. However, this would require the development of electricity price estimators in addition to demand models, as suggested in the following section. There is still a tradeoff between an accurate representation of some nonlinear processes and the actual formulation as a MILP problem, which ensures the convergence to a global optimum whilst keeping the computational burden low. The current solution, however, allows the introduction of variable conversion coefficients (see Section 4.4), but the constraints could be adapted to consider nonlinear efficiencies due to partial loading [20].

Although in this thesis only a concrete case has been analysed [41], ODEHubs eases and expedites the simulation of not only different scenarios but also different EHs with arbitrary complexity, simply by defining their structures (inputs, outputs, devices and paths) in a straightforward way, as illustrated in Chapters 6 and 7. Thus, the tool will be useful in studying resource management strategies with different sets of real data and, because of its conception as a flexible tool, even in industrial, commercial, or home environments, as demonstrated in other articles derived from this thesis [44, 46–48]. In practice, it could be employed to asses multiple "what-if" scenarios (remember for instance the comparison study about the change in the self-consumption law [51]), including, for instance, the integration of the EH into the electricity market as a system agent (not just a self-consumer), as exemplified by Bordons et al. for MGs [192], although the presented approach is still valuable for a large number of "prosumers" who might benefit from the current self-consumption law. Another interesting analysis is the design of facilities, that is, determining which set of components/technologies better satisfy the needs of a plant, a problem which has been tackled in the literature by integrating the conversion and storage model into a bi-level approach where a genetic algorithm generates possible configurations of the EH [67]. For all the above reasons, it is hoped that the work developed in this thesis will be of interest to the wider scientific community and accessible to any user willing to exploit the capabilities of a free tool like ODEHubs.

8.3 Future Work

In terms of future work, the main perspectives include, but are not limited to, the issues discussed in this section. Firstly, the development of resource prediction models is one struggling task that was not achieved as expected and hindered, at a certain point, the formulation of the problem with chance constraints during the stay in Brazil.

Apart from refining the PV production model presented in Chapter 5, especially for the parking, more in-depth studies would help to improve the accuracy of some parameters (conversion factors and production limits) that have been assumed constant from the manufacturers' datasheet or to develop the above-mentioned models for their periodical estimation over time. This is germane to the prediction of demand profiles and resource prices, a prerequisite for implementing management strategies in real systems: even though using the certainty equivalent MPC approach with historical data is suitable for benchmarking—or demonstration purposes, as in this thesis—more pragmatic control systems will rely on these forecasts.

The model presented in Chapter 5 assumes that GHI, DHI, DNI and ambient temperature are known; it was feed with historical data in the simulations included in Chapter 7, but prediction data from the Spanish National Weather Agency (AEMET) [246], with whom the ARMs research group had an agreement to update weather forecast including those variables four times a day, or from any other sources, could be used instead. AEMET is a trustworthy authority that could provide data for future tests on the actual PV fields, which will require one to analyse their uncertainty by comparing the forecast corresponding to the period of March–December 2019 against the measurements of CIESOL's weather station. There is also another issue related to the prices published by OMIE: on the one hand, the deviations with respect to the FHS of each session alter the final price of the electricity and that is itself a matter to be considered into sensibility and uncertainty analyses; on the other, the development of models that allows ODEHubs to consider fixed a horizon (instead of shortening it as explained in Subsection 7.4.1) and their correlation with OMIE's prices is also a matter of interest for future research.

In line with the other objective (O_5), an opportunity presents itself to arrange the consequent probabilistic formulation of the problem after characterising the uncertainty in some of the variables (especially the demanded resources). The partial advances in chance-constrained optimisation during the stay in Brazil have opened the pathway to the inclusion of that technique in ODEHubs, which currently only implements the certainty equivalent MPC. This would allow giving a step forward in developing real applications for non-deterministic scenarios, where the predictions are not ideally exact and there is a mismatch between the energy demanded and produced; the yet useful approach presented in Chapter 4 would be employed for benchmarking. As introduced in Chapter 6, ODEHubs is already on its way to include in future releases a function to simulate the response of the EHs (*EH_system.m*), which will introduce variations in model's parameters with respect to controller's (*MPC_predictions.m*).

Other future implementations might incorporate the interconnection of EHs, the bases of which have been presented in Section 4.3 [43] and also already tackled in the literature [247], so agents with opposing interests can be considered in the dispatch problem. Once again, in terms of coding, it would require some modifications in ODEHubs and, regarding modelling, the mathematical representation of the transportation networks for each energy carrier or resource. On the other hand, there is another couple of pending issues that merit attention in relation with the equipment of which an EH is composed: one consists in their ageing due to usage, which can be taken into account in the cost function similarly as Bordons et al. did in the case of MGs [192]; the other involve devices operating at partial load, which might be represented in the current approach either by introducing virtual devices representing their performance at different operating points, or by turning the binary variables associated with them into integer variables. In both cases of the latter issue it will be necessary a suitable (and different) selection of their upper and lower limits and the binary (or integer) variables associated with them. Consequently, performing a comparison of those two with the stepwise approximation proposed by Evins et al. [20], in terms of size of the problem and computational burden, might prove to be an interesting analysis.

Finally, considering more technical aspects of ODEHubs, future upgrades consist of the addition of capabilities to incorporate elements from Simscape Simulink®'s library, which includes components to model different energy networks, such as power grids [248]; or the migration of the package to other languages, such as Python or Modelica®. Python programs are executed from a command line, similarly to MATLAB® scripts from the command prompt, and there are already some tools built in that language [97], and Modelica® is an object-oriented modelling language that has already been used to implement models of some of the components of the CHROMAE project [249].

In conclusion, future work should focus on adding capabilities to the proposed modelling framework in order to represent certain processes more accurately, developing precise models for conversion/storage devices and transportation networks, characterising uncertainty and formulating probabilistic control schemes accordingly, and implementing these features in ODEHubs, either in its current form or considering other programming paradigms and its integration within the so-called cyber-physical systems.

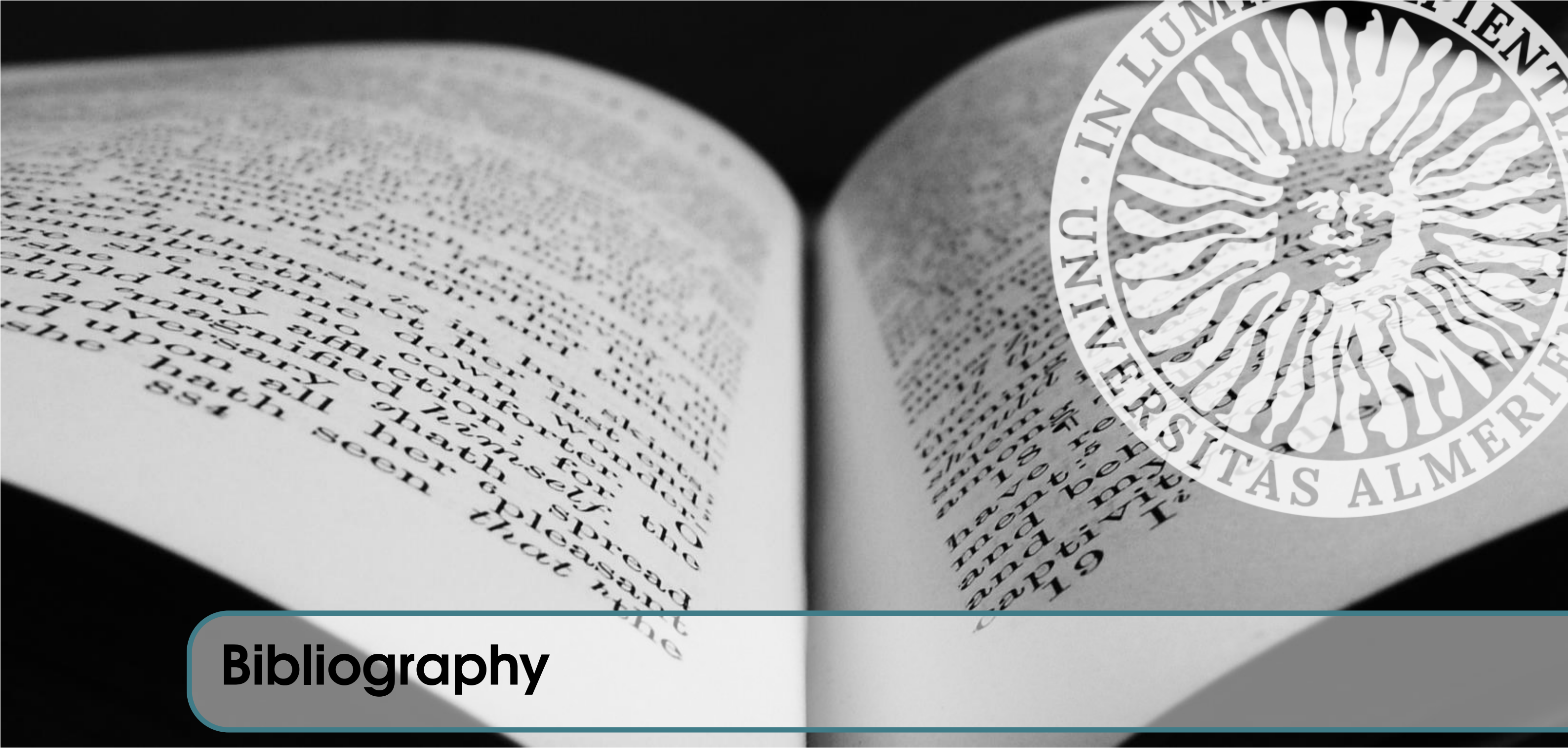

Bibliography

[1] M. Schlesinger, H. Kheshgi, J. Smith, F. de la Chesnaye, J. Reilly, T. Wilson, and C. Kolstad, Eds., *Human-Induced Climate Change: An Interdisciplinary Assessment*. Cambridge, United Kingdom: Cambridge University Press, 2007.

[2] Core Writing Team, R. K. Pachauri, and L. A. Meyer, Eds., "Climate Change 2014: Synthesis Report. Contribution of Working Groups I, II and III to the Fifth Assessment Report of the Intergovernmental Panel on Climate Change," Intergovernmental Panel on Climate Change, Geneva, Switzerland, Technical Report, 2014.

[3] M. Schlechtriem. (2020) Mapped: Impact of Climate Change on European Countries. Accessed: 01-Aug-2020. [Online]. Available: https://www.greenmatch.co.uk/.

[4] European Commission website. (2020) 2020 Climate and Energy Package. Accessed: 01-Aug-2020. [Online]. Available: https://ec.europa.eu/clima/policies/strategies/2020_en#tab-0-0.

[5] European Commission website. (2020) 2030 Climate and Energy Framework. Accessed: 01-Aug-2020. [Online]. Available: https://ec.europa.eu/clima/policies/strategies/2030_en.

[6] Looney, Bernard, "BP Statistical Review of World Energy (69th edition)," BP plc, London, United Kingdom, Technical Report, 2020.

[7] European Commission website. (2020) A European Green Deal. Accessed: 01-Aug-2020. [Online]. Available: https://ec.europa.eu/info/strategy/priorities-2019-2024/european-green-deal_en.

[8] BloombergNEF, Eaton, and Statkraft, "Sector coupling in europe: Powering decarbonization," Bloomberg New Energy Finance, London, United Kingdom and Berlin, Germany, Technical Report, 2020.

[9] H. Lund, A. N. Andersen, P. A. Østergaard, B. V. Mathiesen, and D. Connolly, "From electricity smart grids to smart energy systems—a market operation based approach and understanding," *Energy*, vol. 42, no. 1, pp. 96–102, 2012.

[10] C. D. Korkas, S. Baldi, I. Michailidis, and E. B. Kosmatopoulos, "Occupancy-based demand response and thermal comfort optimisation in microgrids with renewable energy sources and energy storage," *Applied Energy*, vol. 163, pp. 93–104, 2016.

[11] G. Chicco and P. Mancarella, "Distributed multi-generation: A comprehensive view," *Renewable and Sustainable Energy Reviews*, vol. 13, no. 3, pp. 535–551, 2009.

[12] K. Ghedamsi and D. Aouzellag, "Improvement of the performances for wind energy conversions systems," *International Journal of Electrical Power and Energy Systems*, vol. 32, no. 9, pp. 936–945, 2010.

[13] A. Ehsan and Q. Yang, "Optimal integration and planning of renewable distributed generation in the power distribution networks: A review of analytical techniques," *Applied Energy*, vol. 210, pp. 44–59, 2018.

[14] M. Guerrieri, M. L. Gennusa, G. Peri, G. Rizzo, and G. Scaccianoce, "University campuses as small-scale models of cities: Quantitative assessment of a low carbon transition path," *Renewable and Sustainable Energy Reviews*, vol. 113, p. 109263, 2019.

[15] S. Bolwig, G. Bazbauers, A. Klitkou, P. D. Lund, A. Blumberga, A. Gravelsins, and D. Blumberga, "Review of modelling energy transitions pathways with application to energy system flexibility," *Renewable and Sustainable Energy Reviews*, vol. 101, pp. 440–452, 2019.

[16] P. Mancarella, "MES (multi-energy systems): An overview of concepts and evaluation models," *Energy*, vol. 65, pp. 1–17, 2014.

[17] M. Geidl, G. Koeppel, P. Favre-Perrod, B. Klöckl, G. Andersson, and K. Fröhlich, "Energy hubs for the future," *IEEE Power and Energy Magazine*, vol. 5, no. 1, pp. 24–30, 2006.

[18] M. Geidl and G. Andersson, "Optimal power flow of multiple energy carriers," *IEEE Transactions on Power Systems*, vol. 22, no. 1, pp. 145–155, 2007.

[19] A. Parisio, C. Del Vecchio, and A. Vaccaro, "A robust optimisation approach to energy hub management," *International Journal of Electrical Power & Energy Systems*, vol. 42, no. 1, pp. 98–104, 2012.

[20] R. Evins, K. Orehounig, V. Dorer, and J. Carmeliet, "New formulations of the 'energy hub' model to address operational constraints," *Energy*, vol. 73, pp. 387–398, 2014.

[21] Y. Wang, J. Cheng, N. Zhang, and C. Kang, "Automatic and linearised modelling of energy hub and its flexibility analysis," *Applied Energy*, vol. 211, pp. 705–714, 2018.

[22] D. Setlhaolo, S. Sichilalu, and J. Zhang, "Residential load management in an energy hub with heat pump water heater," *Applied Energy*, vol. 208, pp. 551–560, 2017.

[23] C. Hernández-Hernández, F. Rodríguez, J. C. Moreno, P. R. da Costa Mendes, J. E. Normey-Rico, and J. L. Guzmán, "The comparison study of short-term prediction methods to enhance the model predictive controller applied to microgrid energy management," *Energies*, vol. 10, no. 7, p. 884, 2017.

[24] P. R. C. Mendes, L. V. Isorna, C. Bordons, and J. E. Normey-Rico, "Energy management of an experimental microgrid coupled to a V2G system," *Journal of Power Sources*, vol. 327, pp. 702–713, 2016.

[25] S. D. Beigvand, H. Abdi, and M. La Scala, "A general model for energy hub economic dispatch," *Applied Energy*, vol. 190, pp. 1090–1111, 2017.

[26] P. Gabrielli, M. Gazzani, E. Martelli, and M. Mazzotti, "Optimal design of multi-energy systems with seasonal storage," *Applied Energy*, vol. 219, pp. 408–424, 2018.

[27] M. Mohammadi, Y. Noorollahi, B. Mohammadi-Ivatloo, and H. Yousefi, "Energy hub: From a model to a concept—A review," *Renewable and Sustainable Energy Reviews*, vol. 80, pp. 1512–1527, 2017.

[28] C. Klessmann, A. Held, M. Rathmann, and M. Ragwitz, "Status and perspectives of renewable energy policy and deployment in the European Union—What is needed to reach the 2020 targets?" *Energy Policy*, vol. 39, no. 12, pp. 7637–7657, 2011.

[29] J. Vasconcelos, "Survey of regulatory and technological developments concerning smart metering in the European Union electricity market," *EUI RSCAS PP, 2008/01, Florence School of Regulation, Energy*, 2008.

[30] H. Farhangi, "The path of the smart grid," *IEEE Power and Energy Magazine*, vol. 8, no. 1, pp. 18–28, 2010.

[31] C. E. García, D. M. Prett, and M. Morari, "Model predictive control: Theory and practice-A survey," *Automatica*, vol. 25, no. 3, pp. 335–348, 1989.

[32] S. Long, "Generalised modelling framework for multi-energy systems with model predictive control applications," Ph.D. dissertation, University of Manchester, 2019.

[33] E. F. Camacho and C. Bordons, *Model Predictive Control*, ser. Advanced Textbooks in Control and Signal Processing. London, United Kingdom: Springer-Verlag London, 2004.

[34] D. J. am Ende and M. T. am Ende, *Chemical Engineering in the Pharmaceutical Industry: Drug Product Design, Development, and Modelling*. John Wiley & Sons, 2019.

[35] E. Aydın, Y. Arkun, and G. Is, "Economic model predictive control (EMPC) of an industrial diesel hydroprocessing plant," *IFAC-PapersOnLine*, vol. 49, no. 7, pp. 568–573, 2016.

[36] T. Tran, K. Ling, and J. M. Maciejowski, "Economic model predictive control—a review," in *Proceedings of the International Symposium on Automation and Robotics in Construction*, vol. 31. IAARC Publications, 2014, p. 1.

[37] J. Skaf and S. P. Boyd, "Design of affine controllers via convex optimization," *IEEE Transactions on Automatic Control*, vol. 55, no. 11, pp. 2476–2487, 2010.

[38] S. Long, O. Marjanovic, and A. Parisio, "Generalised control-oriented modelling framework for multi-energy systems," *Applied Energy*, vol. 235, pp. 320–331, 2019.

[39] M. Nassourou, J. Blesa, and V. Puig, “Optimal energy dispatch in a smart micro-grid system using economic model predictive control,” *Proceedings of the Institution of Mechanical Engineers, Part I: Journal of Systems and Control Engineering*, vol. 234, no. 1, pp. 96–106, 2020.

[40] Automatic Control, Robotics and Mechatronics Research Group (ARM-TEP197). ENERPRO project. Accessed: 01-Aug-2020. [Online]. Available: http://www2.ual.es/enerpro/.

[41] J. Ramos-Teodoro, F. Rodríguez, M. Berenguel, and J. L. Torres, “Heterogeneous resource management in energy hubs with self-consumption: Contributions and application example,” *Applied Energy*, vol. 229, pp. 537–550, 2018.

[42] Automatic Control, Robotics and Mechatronics Research Group (ARM-TEP197). (2017) CHROMAE Project (DPI2017-85007-R). Accessed: 01-Aug-2020. [Online]. Available: http://www2.ual.es/chromae/.

[43] J. Ramos-Teodoro, F. Rodríguez, M. Castilla, and M. Berenguel, “Modelling production, consumption and storage of heterogeneous resources of an agro-industrial district with renewable energies,” in *Proceedings of the X Iberian Congress on Agro-Engineering*, Huesca, Spain, 2019, pp. 190–198, (in Spanish).

[44] J. Ramos-Teodoro, A. Giménez-Miralles, F. Rodríguez, and M. Berenguel, “A flexible interactive tool for modelling and optimal dispatch of resources in agri-energy hubs,” *Sustainability*, vol. 11, no. 21, p. 8820, 2020.

[45] J. Ramos-Teodoro, F. Rodríguez, and M. Berenguel, “Cutting-edge approaches in control, management and design of distributed production systems: Microgrids, virtual power plants, energy hubs, and multi-energy systems,” *IEEE Access*, (submitted to journal and under review).

[46] J. Ramos-Teodoro, F. Rodríguez, and M. Berenguel, “Modelling based on the energy hub paradigm of a greenhouse agricultural exploitation with support of renewable energies,” in *Proceedings of the I Iberian Symposium on Horticultural Engineering*, Lugo, Spain, 2018, (in Spanish).

[47] A. Giménez-Miralles, J. Ramos-Teodoro, F. Rodríguez, and M. Berenguel, “Case study of the ODEHubs tool for energetic and material resources management of a Mediterranean traditional greenhouse,” in *Proceedings of the II Iberian Symposium on Horticultural Engineering*, Ponte de Lima, Portugal, 2020, (in Spanish).

[48] J. Ramos-Teodoro, M. Castilla, J. D. Álvarez, F. Rodríguez, and M. Berenguel, “Economic dispatch of a bioclimatic office building considering thermal energy, electricity and water demands,” in *Proceedings of the 18th International Conference on Renewable Energies and Power Quality*, Granada, Spain, 2020.

[49] J. Ramos-Teodoro, J. D. Álvarez, F. Rodríguez, and M. Berenguel, “Economic management of energy hubs with heterogeneous resources through MINLP,” in *Proceedings of the IV CEA Symposium on Modelling, Simulation and Optimisation*, Valladolid, Spain, 2018, (in Spanish).

[50] J. Ramos-Teodoro, F. Rodríguez, and M. Berenguel, “Photovoltaic facilities modelling for an energy hub management with heterogeneous resources,” in *Proceedings of the XVI CEA Symposium on Control Engineering*, Almeria, Spain, 2018, pp. 23–30, (in Spanish).

[51] J. Ramos-Teodoro, F. Rodríguez, and M. Berenguel, "Comparative study of energy management in a agro-industrial plant with self-consumption," in *Proceedings of the I Congress for Young Researchers on Agri-Food Science*, Almeria, Spain, 2018, (in Spanish).

[52] F. Rodríguez, J. Ramos-Teodoro, M. Berenguel, and P. Lorenzo, "Economic management of the carbon enrichment in a tomato greenhouse with different sources of CO_2," in *Proceedings of the "Adding Value to CO_2" Congress (3rd edition)*, Madrid, Spain, 2019, (in Spanish).

[53] J. Ramos-Teodoro, A. Giménez-Miralles, F. Rodríguez, and M. Berenguel, "Simulation of scenarios of economic dispatch in multi-energy systems," in *Proceedings of the XVIII CEA Symposium on Control Engineering*, Murcia, Spain, 2020, (in Spanish).

[54] J. Ramos-Teodoro, "Energy management strategies in production environments with support of solar energy," in *Proceedings of the I Annual Meeting of the PhD Programme in Informatics of the University of Almeria*, Almeria, Spain, 2018, (in Spanish).

[55] J. Ramos-Teodoro, "Heterogeneous resource management in energy hubs with self-consumption," in *Proceedings of the II Annual Meeting of the PhD Programme in Informatics of the University of Almeria*, Almeria, Spain, 2019, (in Spanish).

[56] J. Ramos-Teodoro, "Contributions to control and management of distributed production systems: State-of-the-art and development of a library for simulations," in *Proceedings of the III Annual Meeting of the PhD Programme in Informatics of the University of Almeria*, Almeria, Spain, 2020, (in Spanish).

[57] J. Ramos-Teodoro, "Energy management of a heterogeneous production system under the energy hub paradigm," Master's thesis, Department of Systems Engineering and Automation, University Carlos III of Madrid, Madrid, Spain, 2017, (in Spanish).

[58] A. Giménez-Miralles, "Design of a graphic interface for modelling and analysing energy hubs," Bachelor's thesis, University of Almeria, 2019, (in Spanish).

[59] L. A. Marchi, "Modelling of an agri-food district under the cyber-physical systems paradigm," Bachelor's thesis, University of Almeria, 2019.

[60] M. Castilla, F. Rodríguez, J. D. Álvarez, J. G. Donaire, and J. Ramos-Teodoro, "Design of a prototype based on the hardware-in-the-loop paradigm for practical classes of automation in engineering degrees," in *2019 Teaching Innovation Meeting*, Almeria, Spain, 2019, (in Spanish).

[61] M. Castilla, F. Rodríguez, J. D. Álvarez, J. G. Donaire, and J. Ramos-Teodoro, "A hardware-in-the-loop prototype to design benchmarks for automation and control education," in *Proceedings of the 21st IFAC World Congress*, Berlin, Germany, 2020.

[62] M. P. Groover, *Automation, Production Systems, and Computer-Integrated Manufacturing*, 4th ed. Pearson, 2015.

[63] S. Howell, Y. Rezgui, J.-L. Hippolyte, B. Jayan, and H. Li, "Towards the next generation of smart grids: Semantic and holonic multi-agent management of distributed energy resources," *Renewable and Sustainable Energy Reviews*, vol. 77, pp. 193–214, 2017.

[64] J. F. Burnham, "Scopus database: A review," *Biomedical digital libraries*, vol. 3, no. 1, p. 1, 2006.

[65] H. Sadeghi, M. Rashidinejad, M. Moeini-Aghtaie, and A. Abdollahi, "The energy hub: An extensive survey on the state-of-the-art," *Applied Thermal Engineering*, vol. 161, 2019.

[66] A. S. Dagoumas and N. E. Koltsaklis, "Review of models for integrating renewable energy in the generation expansion planning," *Applied Energy*, vol. 242, pp. 1573–1587, 2019.

[67] R. Evins, "Multi-level optimisation of building design, energy system sizing and operation," *Energy*, vol. 90, pp. 1775–1789, 2015.

[68] T. Rodríguez-Blanco, D. Sarabia, and C. De Prada, "Real-time optimisation using the modifier adaptation methodology," *Revista Iberoamericana de Automática e Informática Industrial*, vol. 15, no. 2, pp. 133–144, 2018, (in Spanish).

[69] M. Kalliski, J. L. Pitarch, C. Jasch, and C. De Prada, "Support to decision-making in a network of industrial evaporators," *Revista Iberoamericana de Automática e Informática Industrial*, vol. 16, no. 1, pp. 26–35, 2018, (in Spanish).

[70] J. D. Vergara-Dietrich, M. Menezes Morato, P. R. da Costa Mendes, A. A. Cani, J. E. Normey-Rico, and C. Bordons, "Advanced chance-constrained predictive control for the efficient energy management of renewable power systems," *Journal of Process Control*, vol. 74, pp. 120–132, 2019.

[71] E. Fabrizio, V. Branciforti, A. Costantino, M. Filippi, S. Barbero, G. Tecco, P. Mollo, and A. Molino, "Monitoring and managing of a micro-smart grid for renewable sources exploitation in an agro-industrial site," *Sustainable Cities and Society*, vol. 28, pp. 88–100, 2017.

[72] K. Orehounig, R. Evins, and V. Dorer, "Integration of decentralised energy systems in neighbourhoods using the energy hub approach," *Applied Energy*, vol. 154, pp. 277–289, 2015.

[73] M. C. Bozchalui, C. A. Cañizares, and K. Bhattacharya, "Optimal energy management of greenhouses in smart grids," *IEEE Transactions on Smart Grid*, vol. 6, no. 2, pp. 827–835, 2015.

[74] M. Mohammadi, R. Ghasempour, F. R. Astaraei, E. Ahmadi, A. Aligholian, and A. Toopshekan, "Optimal planning of renewable energy resource for a residential house considering economic and reliability criteria," *International Journal of Electrical Power & Energy Systems*, vol. 96, pp. 261–273, 2018.

[75] J. Czyzyk, M. P. Mesnier, and J. J. Moré, "The NEOS server," *IEEE Journal on Computational Science and Engineering*, vol. 5, no. 3, pp. 68–75, 1998.

[76] E. D. Dolan, "The NEOS server 4.0 administrative guide," Mathematics and Computer Science Division, Argonne National Laboratory, Technical Memorandum ANL/MCS-TM-250, 2001.

[77] W. Gropp and J. J. Moré, "Optimisation environments and the NEOS server," in *Approximation Theory and Optimisation*, M. D. Buhman and A. Iserles, Eds. Cambridge University Press, 1997, pp. 167–182.

[78] M. Mohammadi, Y. Noorollahi, B. Mohammadi-ivatloo, H. Yousefi, and S. Jalilinasrabady, "Optimal scheduling of energy hubs in the presence of uncertainty—A review," *Journal of Energy Management and Technology*, vol. 1, no. 1, pp. 1–17, 2017.

[79] J. Ombach, "A short introduction to stochastic optimisation," *Schedae Informaticae*, vol. 23, pp. 9–20, 2014.

[80] A. G. Zamani, A. Zakariazadeh, and S. Jadid, "Day-ahead resource scheduling of a renewable energy based virtual power plant," *Applied Energy*, vol. 169, pp. 324–340, 2016.

[81] L. J. Hong and G. Liu, "Monte Carlo estimation of value-at-risk, conditional value-at-risk and their sensitivities," in *2011 Winter Simulation Conference (WSC)*. IEEE, 2011, pp. 95–107.

[82] International Business Machines Corporation (IBM). (2019) IBM ILOG CPLEX Optimisation Studio. Accessed: 01-Aug-2020. [Online]. Available: https://www.ibm.com/es-es/products/ilog-cplex-optimization-studio. Armonk, New York, United States.

[83] J. Bisschop and A. Meeraus, "On the development of a general algebraic modelling system in a strategic planning environment," in *Applications*, ser. Mathematical Programming Studies. Springer Berlin Heidelberg, 1982, vol. 20, pp. 1–29.

[84] R. Fourer, D. M. Gay, and B. Kernighan, "AMPL: A mathematical programming language," in *Algorithms and Model Formulations in Mathematical Programming*, S. W. Wallace, Ed. Berlin & Heidelberg, Germany: Springer-Verlag, 1989, pp. 150–151.

[85] The MathWorks, Inc. (2020) {MATLAB R2020a}. Accessed: 01-Aug-2020. [Online]. Available: http://es.mathworks.com/products/\glsxtrshort{MATLAB}/. Natick, Massachusetts, United States.

[86] Gurobi Optimisation, LLC. (2019) Gurobi optimiser reference manual. Accessed: 01-Aug-2020. [Online]. Available: http://www.gurobi.com.

[87] N. Sahinidis. (2019) BARON v. 2019.7.13: Global optimisation of mixed-integer nonlinear programs, *User's Manual*. Accessed: 01-Aug-2020. [Online]. Available: http://www.minlp.com/downloads/docs/baron%20manual.pdf.

[88] J. Löfberg, "YALMIP: A toolbox for modelling and optimisation in MATLAB," in *2004 IEEE International Conference on Robotics and Automation*, 2004, pp. 284–289.

[89] K. Holmström, A. O. Göran, and M. M. Edvall. (2010) User's Guide for TOMLAB 7. Accessed: 01-Aug-2020. [Online]. Available: https://tomopt.com/docs/TOMLAB.pdf.

[90] C. Marnay, G. Venkataramanan, M. Stadler, A. Siddiqui, R. Firestone, and B. Chandran, "Optimal technology selection and operation of commercial-building microgrids," *IEEE Transactions on Power Systems*, vol. 23, no. 3, pp. 975–982, 2008.

[91] B. H. Bakken, H. I. Skjelbred, and O. Wolfgang, "eTransport: Investment planning in energy supply systems with multiple energy carriers," *Energy*, vol. 32, no. 9, pp. 1676–1689, 2007.

[92] T. Givler and P. Lilienthal, "Using HOMER software, NREL's micropower optimisation model, to explore the role of gen-sets in small solar power systems—Case study: Sri Lanka," National Renewable Energy Laboratory, Golden, Colorado, United States, Technical Report, 2005.

[93] D. B. Crawley, C. O. Pedersen, L. K. Lawrie, and F. C. Winkelmann, "EnergyPlus: Energy simulation program," *ASHRAE Journal*, vol. 42, pp. 49–56, 2000.

[94] F. Bünning, R. Sangi, and D. Müller, "A Modelica library for the agent-based control of building energy systems," *Applied Energy*, vol. 193, pp. 52–59, 2017.

[95] J. Allegrini, K. Orehounig, G. Mavromatidis, F. Ruesch, V. Dorer, and R. Evins, "A review of modelling approaches and tools for the simulation of district-scale energy systems," *Renewable and Sustainable Energy Reviews*, vol. 52, pp. 1391–1404, 2015.

[96] I. van Beuzekom, M. Gibescu, and J. Slootweg, "A review of multi-energy system planning and optimisation tools for sustainable urban development," in *2015 IEEE Eindhoven PowerTech*. Eindhoven, The Netherlands: IEEE, 2015, pp. 1–7.

[97] M. Groissböck, "Are open source energy system optimisation tools mature enough for serious use?" *Renewable and Sustainable Energy Reviews*, vol. 102, pp. 234–248, 2019.

[98] H.-K. Ringkjøb, P. M. Haugan, and I. M. Solbrekke, "A review of modelling tools for energy and electricity systems with large shares of variable renewables," *Renewable and Sustainable Energy Reviews*, vol. 96, pp. 440–459, 218.

[99] J. Bisschop, *AIMMS—Optimisation Modelling*. Haarlem, The Netherlands: Paragon Decision Technology B.V, 2006.

[100] R Core Team—R Foundation for Statistical Computing. (2013) R: A language and environment for statistical computing. Accessed: 01-Aug-2020. [Online]. Available: http://www.r-project.org/. Vienna, Austria.

[101] G. Van Rossum and F. L. Drake Jr, *Python Reference Manual*. Centrum voor Wiskunde en Informatica Amsterdam, 1995.

[102] L. A. Bollinger and V. Dorer, "The Ehub modelling tool: A flexible software package for district energy system optimisation," *Energy Procedia*, vol. 122, pp. 541–546, 2017.

[103] G. Darivianakis, A. Georghiou, R. S. Smith, and J. Lygeros. (2015) EHCM toolbox. Accessed: 01-Aug-2020. [Online]. Available: https://people.ee.ethz.ch/{~{}}building/ehcmToolbox/EHCM{_}Documentation.pdf.

[104] R. D. Zimmerman and C. E. Murillo-Sánchez. (2019) MATPOWER optimal scheduling tool (MOST) User's Manual, Version 1.0.2. Accessed: 01-Aug-2020. [Online]. Available: https://github.com/MATPOWER/most/blob/master/docs/MOST-manual.pdf.

[105] M. R. Kühne, "Drivers of energy storage demand in the German power system: An analysis of the influence of methodology and parameters on modelling results ," Ph.D. dissertation, Technical University of Munich, 2016.

[106] K. den Bergh, K. Bruninx, E. Delarue, and W. D'haeseleer, "LUSYM: A unit commitment model formulated as a mixed-integer linear program," *KU Leuven Energy Institute, TME Branch (Energy and Environment)*, vol. 7, 2014.

[107] C. Brancucci Martinez-Anido, "Electricity without borders—The need for cross-border transmission investment in Europe ," Ph.D. dissertation, Delft University of Technology, 2013.

[108] N. Hatziargyriou, H. Asano, R. Iravani, and C. Marnay, "Microgrids," *IEEE Power and Energy Magazine*, vol. 5, no. 4, pp. 78–94, 2007.

[109] M. Braun and P. Strauss, "A review on aggregation approaches of controllable distributed energy units in electrical power systems," *International Journal of Distributed Energy Resources*, vol. 4, no. 4, pp. 297–319, 2008.

[110] W. Gu, Z. Wu, R. Bo, W. Liu, G. Zhou, W. Chen, and Z. Wu, "Modelling, planning and optimal energy management of combined cooling, heating and power microgrid: A review," *International Journal of Electrical Power & Energy Systems*, vol. 54, pp. 26–37, 2014.

[111] A. Mohammed, S. S. Refaat, S. Bayhan, and H. Abu-Rub, "AC microgrid control and management strategies: Evaluation and review," *IEEE Power Electronics Magazine*, vol. 6, no. 2, pp. 18–31, 2019.

[112] M. F. Zia, M. Benbouzid, E. Elbouchikhi, S. Muyeen, K. Techato, and J. M. Guerrero, "Microgrid transactive energy: Review, architectures, distributed ledger technologies, and market analysis," *IEEE Access*, vol. 8, pp. 19 410–19 432, 2020.

[113] S. Ghaem Sigarchian, M. S. Orosz, H. F. Hemond, and A. Malmquist, "Optimum design of a hybrid PV-CSP-LPG microgrid with particle swarm optimisation technique," *Applied Thermal Engineering*, vol. 109, pp. 1031–1036, 2016.

[114] G. Kyriakarakos, A. Dounis, S. Rozakis, K. Arvanitis, and G. Papadakis, "Polygeneration microgrids: A viable solution in remote areas for supplying power, potable water and hydrogen as transportation fuel," *Applied Energy*, vol. 88, no. 12, 2011.

[115] P. Velarde, L. Valverde, J. M. Maestre, C. Ocampo-Martinez, and C. Bordons, "On the comparison of stochastic model predictive control strategies applied to a hydrogen-based microgrid," *Journal of Power Sources*, vol. 343, pp. 161–173, 2017.

[116] C. Bordons, F. Garcia-Torres, and M. Á. Ridao, "Model predictive control of interconnected microgrids and electric vehicles," *Revista Iberoamericana de Automática e Informática Industrial*, vol. 17, no. 3, pp. 239–253, 2020, (in Spanish).

[117] Y. Zhang, T. Zhang, R. Wang, Y. Liu, B. Guo, S. Barberis, M. Rivarolo, A. Traverso, and A. F. Massardo, "Optimal operation of a smart residential microgrid based on model predictive control by considering uncertainties and storage impacts," *Solar Energy*, vol. 122, pp. 1052–1065, 2015.

[118] C. Phurailatpam, B. S. Rajpurohit, and L. Wang, "Planning and optimisation of autonomous DC microgrids for rural and urban applications in India," *Renewable and Sustainable Energy Reviews*, vol. 82, pp. 194–204, 2018.

[119] P. Firouzmakan, R.-A. Hooshmand, M. Bornapour, and A. Khodabakhshian, "A comprehensive stochastic energy management system of micro-CHP units, renewable energy sources and storage systems in microgrids considering demand response programs," *Renewable and Sustainable Energy Reviews*, vol. 108, pp. 355–368, 2019.

[120] H. Ali, A. Hussain, V. Bui, and H. Kim, “Consensus algorithm-based distributed operation of microgrids during grid-connected and islanded modes,” *IEEE Access*, vol. 8, pp. 78 151–78 165, 2020.

[121] M. Mehdi, C. Kim, and M. Saad, “Robust centralised control for DC islanded microgrid considering communication network delay,” *IEEE Access*, vol. 8, pp. 77 765–77 778, 2020.

[122] F. Garcia-Torres, D. G. Vilaplana, C. Bordons, P. Roncero-Sanchez, and M. A. Ridao, “Optimal management of microgrids with external agents including battery/fuel cell electric vehicles,” *IEEE Transactions on Smart Grid*, vol. 10, no. 4, pp. 4299–4308, 2019.

[123] J. L. Torres-Moreno, A. Giménez-Fernández, M. Pérez-García, and F. Rodríguez, “Energy management strategy for micro-grids with PV-battery systems and electric vehicles,” *Energies*, vol. 11, no. 3, p. 522, 2018.

[124] X. Gong, F. Dong, M. A. Mohamed, O. M. Abdalla, and Z. M. Ali, “A secured energy management architecture for smart hybrid microgrids considering proton-exchange-membrane-fuel cell and electric vehicles,” *IEEE Access*, vol. 8, pp. 47 807–47 823, 2020.

[125] M. S. Orosz and A. V. Mueller, “Dynamic simulation of performance and cost of hybrid PV-CSP-LPG generator micro grids with applications to remote communities in developing countries,” in *ASME 2015 9th International Conference on Energy Sustainability*, 2015.

[126] D. Pudjianto, C. Ramsay, and G. Strbac, “Virtual power plant and system integration of distributed energy resources,” *IET Renewable Power Generation*, vol. 1, no. 1, pp. 10–16, 2007.

[127] G. Zhang, C. Jiang, and X. Wang, “Comprehensive review on structure and operation of virtual power plant in electrical system,” *IET Generation, Transmission & Distribution*, vol. 13, no. 2, pp. 145–156, 2019.

[128] S. Yu, F. Fang, Y. Liu, and J. Liu, “Uncertainties of virtual power plant: Problems and countermeasures,” *Applied Energy*, vol. 239, pp. 454–470, 2019.

[129] Z. Liang, Q. Alsafasfeh, T. Jin, H. Pourbabak, and W. Su, “Risk-constrained optimal energy management for virtual power plants considering correlated demand response,” *IEEE Transactions on Smart Grid*, vol. 10, no. 2, pp. 1577–1587, 2019.

[130] L. Ju, R. Zhao, Q. Q. Tan, Y. Lu, Q. Q. Tan, and W. Wang, “A multi-objective robust scheduling model and solution algorithm for a novel virtual power plant connected with power-to-gas and gas storage tank considering uncertainty and demand response,” *Applied Energy*, vol. 250, pp. 1336–1355, 2019.

[131] F. J. Heredia, M. D. Cuadrado, and C. Corchero, “On optimal participation in the electricity markets of wind power plants with battery energy storage systems,” *Computers & Operations Research*, vol. 96, pp. 316–329, 2018.

[132] D. Wozabal and G. Rameseder, “Optimal bidding of a virtual power plant on the Spanish day-ahead and intraday market for electricity,” *European Journal of Operational Research*, vol. 280, no. 2, pp. 639–655, 2020.

[133] H. Pandžić, I. Kuzle, and T. Capuder, "Virtual power plant mid-term dispatch optimisation," *Applied Energy*, vol. 101, pp. 134–141, 2013.

[134] O. Sadeghian, A. M. Shotorbani, and B. Mohammadi-Ivatloo, "Generation maintenance scheduling in virtual power plants," *IET Generation, Transmission & Distribution*, vol. 13, no. 12, pp. 2584–2596, 2019.

[135] M. Pasetti, S. Rinaldi, and D. Manerba, "A virtual power plant architecture for the demand-side management of smart prosumers," *Applied Sciences*, vol. 8, no. 3, p. 432, 2018.

[136] A. Baringo, L. Baringo, and J. M. Arroyo, "Day-ahead self-scheduling of a virtual power plant in energy and reserve electricity markets under uncertainty," *IEEE Transactions on Power Systems*, vol. 34, no. 3, pp. 1881–1894, 2019.

[137] C. Wei, J. Xu, S. Liao, Y. Sun, Y. Jiang, D. Ke, Z. Zhang, and J. Wang, "A bi-level scheduling model for virtual power plants with aggregated thermostatically controlled loads and renewable energy," *Applied Energy*, vol. 224, pp. 659–670, 2018.

[138] X. Kong, J. Xiao, C. Wang, K. Cui, Q. Jin, and D. Kong, "Bi-level multi-time scale scheduling method based on bidding for multi-operator virtual power plant," *Applied Energy*, vol. 249, pp. 178–189, 2019.

[139] D. Koraki and K. Strunz, "Wind and solar power integration in electricity markets and distribution networks through service-centric virtual power plants," *IEEE Transactions on Power Systems*, vol. 33, no. 1, pp. 473–485, 2018.

[140] E. Dall'Anese, S. S. Guggilam, A. Simonetto, Y. C. Chen, and S. V. Dhople, "Optimal regulation of virtual power plants," *IEEE Transactions on Power Systems*, vol. 33, no. 2, pp. 1868–1881, 2018.

[141] P. Li, Y. Liu, H. Xin, and X. Jiang, "A robust distributed economic dispatch strategy of virtual power plant under cyber-attacks," *IEEE Transactions on Industrial Informatics*, vol. 14, no. 10, pp. 4343–4352, 2018.

[142] A. Alahyari, M. Ehsan, and M. Mousavizadeh, "A hybrid storage-wind virtual power plant (VPP) participation in the electricity markets: A self-scheduling optimisation considering price, renewable generation, and electric vehicles uncertainties," *Journal of Energy Storage*, vol. 25, p. 100812, 2019.

[143] A. Maroufmashat, S. T. Taqvi, A. Miragha, M. Fowler, and A. Elkamel, "Modelling and optimisation of energy hubs: A comprehensive review," *Inventions*, vol. 4, no. 3, p. 50, 2019.

[144] F. Brahman, M. Honarmand, and S. Jadid, "Optimal electrical and thermal energy management of a residential energy hub, integrating demand response and energy storage system," *Energy and Buildings*, vol. 90, pp. 65–75, 2015.

[145] Y. Wang, N. Zhang, Z. Zhuo, C. Kang, and D. Kirschen, "Mixed-integer linear programming-based optimal configuration planning for energy hub: Starting from scratch," *Applied Energy*, vol. 210, pp. 1141–1150, 2018.

[146] W. Zhong, C. Yang, K. Xie, S. Xie, and Y. Zhang, “Admm-based distributed auction mechanism for energy hub scheduling in smart buildings,” *IEEE Access*, vol. 6, pp. 45 635–45 645, 2018.

[147] M. F. Tahir, C. Haoyong, K. Mehmood, N. Ali, and J. A. Bhutto, “Integrated energy system modelling of China for 2020 by incorporating demand response, heat pump and thermal storage,” *IEEE Access*, vol. 7, pp. 40 095–40 108, 2019.

[148] A. Mirzapour-Kamanaj, M. Majidi, K. Zare, and R. Kazemzadeh, “Optimal strategic coordination of distribution networks and interconnected energy hubs: A linear multi-follower bi-level optimisation model,” *International Journal of Electrical Power & Energy Systems*, vol. 119, p. 105925, 2020.

[149] M. Alipour, K. Zare, and M. Abapour, “MINLP probabilistic scheduling model for demand response programs integrated energy hubs,” *IEEE Transactions on Industrial Informatics*, vol. 14, no. 1, pp. 79–88, 2018.

[150] M. Menezes Morato, P. R. da Costa Mendes, J. E. Normey-Rico, and C. Bordons, “Optimal operation of hybrid power systems including renewable sources in the sugar cane industry,” *IET Renewable Power Generation*, vol. 11, no. 8, pp. 1237–1245, 2017.

[151] M. Batić, N. Tomašević, G. Beccuti, T. Demiray, and S. Vraneš, “Combined energy hub optimisation and demand side management for buildings,” *Energy and Buildings*, vol. 127, pp. 229–241, 2016.

[152] L. Kriechbaum, G. Scheiber, and T. Kienberger, “Grid-based multi-energy systems-modelling, assessment, open source modelling frameworks and challenges,” *Energy, Sustainability and Society*, vol. 8, no. 35, pp. 1–19, 2018.

[153] E. Guelpa, A. Bischi, V. Verda, M. Chertkov, and H. Lund, “Towards future infrastructures for sustainable multi-energy systems: A review,” *Energy*, vol. 184, pp. 2–21, 2019.

[154] X. Liu and P. Mancarella, “Modelling, assessment and Sankey diagrams of integrated electricity-heat-gas networks in multi-vector district energy systems,” *Applied Energy*, vol. 167, 2016.

[155] M. Minutillo, A. Perna, and A. Sorce, “Combined hydrogen, heat and electricity generation via biogas reforming: Energy and economic assessments,” *International Journal of Hydrogen Energy*, vol. 44, no. 43, pp. 23 880–23 898, 2019.

[156] S. Clegg and P. Mancarella, “Integrated electricity-heat-gas modelling and assessment, with applications to the Great Britain system. Part II: Transmission network analysis and low carbon technology and resilience case studies,” *Energy*, vol. 184, pp. 191–203, 2019.

[157] S. Clegg and P. Mancarella, “Integrated electricity-heat-gas modelling and assessment, with applications to the Great Britain system. Part I: High-resolution spatial and temporal heat demand modelling,” *Energy*, vol. 184, pp. 180–190, 2019.

[158] E. Fabrizio, V. Corrado, and M. Filippi, “A model to design and optimise multi-energy systems in buildings at the design concept stage,” *Renewable Energy*, vol. 35, no. 3, pp. 644–655, 2010.

[159] W. Huang, N. Zhang, J. Yang, Y. Wang, and C. Kang, "Optimal configuration planning of multi-energy systems considering distributed renewable energy," *IEEE Transactions on Smart Grid*, vol. 10, no. 2, pp. 1452–1464, 2019.

[160] J. Wang, Z. Hu, and S. Xie, "Expansion planning model of multi-energy system with the integration of active distribution network," *Applied Energy*, vol. 253, p. 113517, 2019.

[161] H. Fan, Q. Yuan, S. Xia, J. Lu, and Z. Li, "Optimally coordinated expansion planning of coupled electricity, heat and natural gas infrastructure for multi-energy system," *IEEE Access*, vol. 8, pp. 91 139–91 149, 2020.

[162] E. A. Martinez Cesena and P. Mancarella, "Energy systems integration in smart districts: Robust optimisation of multi-energy flows in integrated electricity, heat and gas networks," *IEEE Transactions on Smart Grid*, vol. 10, no. 1, pp. 1122–1131, 2019.

[163] N. Good and P. Mancarella, "Flexibility in multi-energy communities with electrical and thermal storage: A stochastic, robust approach for multi-service demand response," *IEEE Transactions on Smart Grid*, vol. 10, no. 1, pp. 503–513, 2017.

[164] S. Lu, W. Gu, J. Zhou, X. Zhang, and C. Wu, "Coordinated dispatch of multi-energy system with district heating network: Modelling and solution strategy," *Energy*, vol. 152, pp. 358–370, 2018.

[165] J. Liu, A. Wang, C. Song, R. Tao, and X. Wang, "Cooperative operation for integrated multi-energy system considering transmission losses," *IEEE Access*, vol. 8, pp. 96 934–96 945, 2020.

[166] C. Liu, D. Wang, and Y. Yin, "Two-stage optimal economic scheduling for commercial building multi-energy system through internet of things," *IEEE Access*, vol. 7, pp. 174 562–174 572, 2019.

[167] B. Chen, J. Wang, and M. Shahidehpour, "Cyber-physical perspective on smart grid design and operation," *IET Cyber-Physical Systems: Theory & Applications*, vol. 3, no. 3, pp. 129–141, 2018.

[168] L. Zeng, Y. Sun, X. Zhou, B. Li, and B. Qi, "Demand dispatch in cyber-physical load aggregation system with multilevel incentives," *Journal of Modern Power Systems and Clean Energy*, vol. 6, no. 5, pp. 968–978, 2018.

[169] W. Pei, X. Ma, W. Deng, X. Chen, H. Sun, and D. Li, "Industrial multi-energy and production management scheme in cyber-physical environments: A case study in a battery manufacturing plant," *IET Cyber-Physical Systems: Theory & Applications*, vol. 4, no. 1, pp. 13–21, 2019.

[170] Z. Yuan, S. Wogrin, and M. R. Hesamzadeh, "Towards the Power Synergy Hub (PSHub): Coordinating the energy dispatch of super grid by modified Benders decomposition," *Applied Energy*, vol. 205, pp. 1419–1434, 2017.

[171] Y. Jiang, J. Xu, Y. Sun, C. Wei, J. Wang, D. Ke, X. Li, J. Yang, X. Peng, and B. Tang, "Day-ahead stochastic economic dispatch of wind integrated power system considering demand response of residential hybrid energy system," *Applied Energy*, vol. 190, pp. 1126–1137, 2017.

[172] Y. Fang, S. Zhao, N. Wang, Z. Li, and J. Liu, "Power system stochastic optimal dispatch considering thermal and electrical coordination," *International Journal of Electrical Power & Energy Systems*, vol. 110, pp. 772–780, 2019.

[173] S. Wenzel, R. Paulen, G. Stojanovski, S. Krämer, B. Beisheim, and S. Engell, "Optimal resource allocation in industrial complexes by distributed optimisation and dynamic pricing," *Automatisierungstechnik*, vol. 64, no. 6, pp. 428–442, 2016.

[174] Y. Fu, Z. Lu, W. Hu, S. Wu, Y. Wang, L. Dong, and J. Zhang, "Research on joint optimal dispatching method for hybrid power system considering system security," *Applied Energy*, vol. 238, pp. 147–163, 2019.

[175] J. D. Gil, J. D. Álvarez, L. Roca, J. A. Sánchez-Molina, M. Berenguel, and F. Rodriguez, "Optimal thermal energy management of a distributed energy system comprising a solar membrane distillation plant and a greenhouse," *Energy Conversion and Management*, vol. 198, p. 111791, 2019.

[176] M. Geidl, "Integrated modelling and optimisation of multi-carrier energy systems," Ph.D. dissertation, ETH Zurich, 2007.

[177] Energy Science Center. ESC website. Accessed: 01-Aug-2020. [Online]. Available: https://esc.ethz.ch/research/research-projects.html.

[178] Empa. Urban Energy Systems Laboratory website. Accessed: 01-Aug-2020. [Online]. Available: https://www.empa.ch/web/s313.

[179] G. Mavromatidis, K. Orehounig, and J. Carmeliet, "A review of uncertainty characterisation approaches for the optimal design of distributed energy systems," *Renewable and Sustainable Energy Reviews*, vol. 88, pp. 258–277, 2018.

[180] Swiss Competence Centre for Energy Research. Future Energy Efficient Buildings & Districts website. Accessed: 01-Aug-2020. [Online]. Available: https://www.sccer-feebd.ch/.

[181] Institute for Data Science & Artificial Intelligence. (2020) Electrical Energy and Power Systems website. Accessed: 01-Aug-2020. [Online]. Available: http://www.datascience.manchester.ac.uk/research/application-areas/physical-sciences/electrical-engineering/electrical-energy-and-power-systems/.

[182] P. Mancarella, G. Andersson, J. Pecas-Lopes, and K. Bell, "Modelling of integrated multi-energy systems: Drivers, requirements, and opportunities," in *2016 Power Systems Computation Conference (PSCC)*. IEEE, 2016, pp. 1–22.

[183] S. Long, A. Parisio, and O. Marjanovic, "A conversion model for nodes in multi-energy systems," in *2017 IEEE Manchester PowerTech*. IEEE, 2017, pp. 1–6.

[184] Community Research and Development Information Service. (2017) District information modelling and management for energy reduction. Accessed: 01-Aug-2020. [Online]. Available: https://cordis.europa.eu/project/id/609084/es.

[185] Community Research and Development Information Service. (2020) CORDIS website. Accessed: 01-Aug-2020. [Online]. Available: https://cordis.europa.eu/es.

[186] Joint Research Centre. (2020) Smart Grid projects map. Accessed: 01-Aug-2020. [Online]. Available: https://ses.jrc.ec.europa.eu/project-maps.

[187] EnergyVille. (2020) SmarThor: Research platform for multi-energy systems and markets. Accessed: 01-Aug-2020. [Online]. Available: https://www.energyville.be/en/research/smarthor-research-platform-multi-energy-systems-and-markets.

[188] Community Research and Development Information Service. (2017) Dynamic management of physically coupled systems of systems. Accessed: 01-Aug-2020. [Online]. Available: https://cordis.europa.eu/project/id/611281.

[189] Community Research and Development Information Service. (2020) Improved energy and resource efficiency by better coordination of production in the process industries. Accessed: 01-Aug-2020. [Online]. Available: https://cordis.europa.eu/project/id/723575/es.

[190] Community Research and Development Information Service. (2020) Synergistic approach of multi-energy models for an European optimal energy system management tool. Accessed: 01-Aug-2020. [Online]. Available: https://cordis.europa.eu/project/id/773897.

[191] Community Research and Development Information Service. (2020) Integrated planning of multi-energy systems. Accessed: 01-Aug-2020. [Online]. Available: https://cordis.europa.eu/project/id/863922/es.

[192] C. Bordons, F. García-Torres, and L. Valverde, "Optimal energy management for renewable energy microgrids," *Revista Iberoamericana de Automática e Informática Industrial*, vol. 12, no. 2, pp. 117–132, 2015, (in Spanish).

[193] A. del Real, A. Arce, and C. Bordons, "Optimisation strategy for element sizing in hybrid power systems," *Journal of Power Sources*, vol. 193, no. 1, 2009.

[194] C. Bordons, F. Garcia-Torres, and M. A. Ridao, *Model Predictive Control of Microgrids*. Springer, 2020.

[195] A. J. del Real Torres, "An integrated framework for distributed model predictive control of large scale networks. Applications to power networks," Ph.D. dissertation, University of Seville, 2011.

[196] F. K. Pour, V. Puig, and G. Cembrano, "Economic reliability-aware MPC-LPV for operational management of flow-based water networks including chance-constraints programming," *Processes*, vol. 8, no. 1, p. 60, 2020.

[197] Y. Wang, V. Puig, and G. Cembrano, "Non-linear economic model predictive control of water distribution networks," *Journal of Process Control*, vol. 56, pp. 23–34, 2017.

[198] M. Arriaga, C. A. Canizares, and M. Kazerani, "Long-term renewable energy planning model for remote communities," *IEEE Transactions on Sustainable Energy*, vol. 7, no. 1, pp. 221–231, 2016.

[199] P. Czop, G. Kost, D. Sławik, and G. Wszołek, "Formulation and identification of first-principle data-driven models," *Journal of Achievements in Materials and Manufacturing Engineering*, vol. 44, no. 2, pp. 179–186, 2011.

[200] J. D. Gil, "Hierarchical control and optimisation strategies applied to solar membrane distillation facilities," Ph.D. dissertation, University of Almeria, 2020.

[201] J. A. Duffie and W. A. Beckman, *Solar Engineering of Thermal Processes*. Hoboken, New Jersey, United States: John Wiley & Sons, Inc., 2013.

[202] A. Luque and S. Hegedus, *Handbook of Photovoltaic Science and Engineering*, A. Luque and S. Hegedus, Eds. Chichester, United Kingdom: John Wiley & Sons, Ltd, 2010.

[203] W. de Soto, S. A. Klein, and W. A. Beckman, "Improvement and validation of a model for photovoltaic array performance," *Solar Energy*, vol. 80, no. 1, pp. 78–88, 2006.

[204] L. Martín, L. F. Zarzalejo, J. Polo, A. Navarro, R. Marchante, and M. Cony, "Prediction of global solar irradiance based on time series analysis: Application to solar thermal power plants energy production planning," *Solar Energy*, vol. 84, no. 10, pp. 1772–1781, 2010.

[205] F. O. Hocaoğlu, Ö. N. Gerek, and M. Kurban, "Hourly solar radiation forecasting using optimal coefficient 2-D linear filters and feed-forward neural networks," *Solar Energy*, vol. 82, no. 8, pp. 714–726, 2008.

[206] W. Ji and K. C. Chee, "Prediction of hourly solar radiation using a novel hybrid model of ARMA and TDNN," *Solar Energy*, vol. 85, no. 5, pp. 808–817, 2011.

[207] C. Voyant, M. Muselli, C. Paoli, and M.-L. Nivet, "Numerical weather prediction (NWP) and hybrid ARMA/ANN model to predict global radiation," *Energy*, vol. 39, no. 1, pp. 341–355, 2012.

[208] R. Perez, S. Kivalov, J. Schlemmer, K. Hemker, D. Renné, and T. E. Hoff, "Validation of short and medium term operational solar radiation forecasts in the US," *Solar Energy*, vol. 84, no. 12, pp. 2161–2172, 2010.

[209] H.-x. Zhao and F. Magoulès, "A review on the prediction of building energy consumption," *Renewable and Sustainable Energy Reviews*, vol. 16, no. 6, pp. 3586–3592, 2012.

[210] L. A. House-Peters and H. Chang, "Urban water demand modelling: Review of concepts, methods, and organising principles," *Water Resources Research*, vol. 47, no. 5, p. W05401, 2011.

[211] M. Herrera, L. Torgo, J. Izquierdo, and R. Pérez-García, "Predictive models for forecasting hourly urban water demand," *Journal of Hydrology*, vol. 387, no. 1-2, pp. 141–150, 2010.

[212] F. Rodríguez, M. Berenguel, J. L. Guzmán, and A. Ramírez-Arias, *Modelling and Control of Greenhouse Crop Growth*, ser. Advances in Industrial Control. London, United Kingdom: Springer International Publishing, 2014.

[213] CIESOL. Solar Energy Research Center web site. Accessed: 01-Aug-2020. [Online]. Available: http://www.ciesol.es/index.php?Idioma=EN&Opcion=6&Pagina=80.

[214] M. Castilla, J. D. Álvarez, F. Rodríguez, and M. Berenguel, *Comfort Control in Buildings*, ser. Advances in Industrial Control. London, United Kingdom: Springer-Verlag London, 2014.

[215] Solar Platform of Almeria. PSA website. Accessed: 01-Aug-2020. [Online]. Available: http://www.psa.es/en/index.php.

[216] P. Palenzuela, D. Alarcón, G. Zaragoza, J. Blanco, and M. Ibarra, "Parametric equations for the variables of a steady-state model of a multi-effect desalination plant," *Desalination and Water Treatment*, vol. 51, no. 4-6, pp. 1229–1241, 2013.

[217] D. C. Alarcón Padilla, J. Blanco Gálvez, L. García Rodríguez, W. Gernjak, and S. Malato Rodríguez, "First experimental results of a new hybrid solar/gas multi-effect distillation system: The AQUASOL project," *Desalination*, vol. 220, no. 1-3, pp. 619–625, 2008.

[218] J. D. Gil, L. Roca, A. Ruiz-Aguirre, G. Zaragoza, and M. Berenguel, "Optimal operation of a solar membrane distillation pilot plant via nonlinear model predictive control," *Computers & Chemical Engineering*, vol. 109, pp. 151–165, 2018.

[219] A. I. Sánchez-Pelegrina, F. Rodríguez, I. Oller, M. Berenguel, and S. Malato, "Modelling and control of a pilot nanofiltration plant applied to the reuse of wastewater in agriculture," in *Proceedings of the XXXIX Annual Meeting of Automatics*, Badajoz, Spain, 2018, (in Spanish).

[220] C. Foundation, "Cajamar Experimental Station," https://www.fundacioncajamar.es/es/comun/estacion-experimental-palmerillas/, accessed on 01/09/2020, 2020.

[221] J. A. Sánchez-Molina, F. Rodríguez, J. L. Guzmán, and M. R. Arahal, "Virtual sensors for designing irrigation controllers in greenhouses," *Sensors*, vol. 12, no. 11, pp. 15 244–15 266, 2012.

[222] J. A. Sánchez-Molina, J. V. Reinoso, F. G. Acién, F. Rodríguez, and J. C. López, "Development of a biomass-based system for nocturnal temperature and diurnal CO_2 concentration control in greenhouses," *Biomass and Bioenergy*, vol. 67, pp. 60–71, 2014.

[223] F. J. Mañas-Álvarez, J. L. Blanco-Claraco, J. L. Torres-Moreno, and A. G. Giménez-Fernández, "Modelling and multi-variable control of the urban electric vehicle UAL-eCARM," *Revista Iberoamericana de Automática e Informática Industrial*, vol. 17, no. 2, pp. 144–155, 2020, (in Spanish).

[224] Klein, S. A. et al., "TRNSYS 18: A Transient System Simulation Program," Solar Energy Laboratory, University of Wisconsin, Madison, United States, Technical Report, 2017.

[225] W. Zhou, H. Yang, and Z. Fang, "A novel model for photovoltaic array performance prediction," *Applied Energy*, vol. 84, no. 12, pp. 1187–1198, 2007.

[226] T. Ma, H. Yang, and L. Lu, "Solar photovoltaic system modeling and performance prediction," *Renewable and Sustainable Energy Reviews*, vol. 36, pp. 304–315, 2014.

[227] M. Pasamontes, J. D. Álvarez, J. L. Guzmán, and M. Berenguel, "Hybrid modelling of a solar cooling system," *IFAC Proceedings Volumes (IFAC-PapersOnline)*, vol. 3, no. 1, pp. 26–31, 2009.

[228] L. Roca, M. Berenguel, L. Yebra, and D. C. Alarcón-Padilla, "Solar field control for desalination plants," *Solar Energy*, vol. 82, no. 9, pp. 772–786, 2008.

[229] OMI-Polo Español (OMIE). Files Access. Accessed: 01-Aug-2020. [Online]. Available: https://www.omie.es/es/file-access-list.

[230] Spanish Ministry of Industry, Energy and Tourism. Royal Decree 900/2015, of 9 October, regulating the administrative, technical and economic conditions on modalities of electricity supply and generation with self-consumption. BOE no. 243, of 10/10/2015 (In Spanish). Accessed: 01-Aug-2020. [Online]. Available: https://www.boe.es/buscar/doc.php?id=BOE-A-2015-10927.

[231] Head of State. Royal Decree-Law 15/2018, of 6 October, on urgent measures for the energy transition and the protection of consumers. BOE no. 242, of 06/10/2018 (In Spanish). Accessed: 01-Aug-2020. [Online]. Available: https://www.boe.es/buscar/doc.php?id=BOE-A-2018-13593.

[232] Spanish Ministry for Ecological Transition. Royal Decree 244/2019, of 6 April, regulating the administrative, technical and economic conditions of the self-consumption of electric energy. BOE no. 83, of 06/04/2019 (In Spanish). Accessed: 01-Aug-2020. [Online]. Available: https://www.boe.es/diario_boe/txt.php?id=BOE-A-2019-5089.

[233] Spanish Ministry of Industry, Tourism and Commerce. Royal Decree 1544/2011, of 31 October, establishing the transport and distribution network access fees to be paid by electricity producers. BOE no. 276, of 16/11/2011 (In Spanish). Accessed: 01-Aug-2020. [Online]. Available: https://www.boe.es/buscar/doc.php?id=BOE-A-2011-17891.

[234] Head of State. Law 15/2012, of 27 December, on tax measures for energy sustainability. BOE no. 312, of 28/12/2012 (In Spanish). Accessed: 01-Aug-2020. [Online]. Available: https://www.boe.es/buscar/doc.php?id=BOE-A-2012-15649.

[235] OMI-Polo Español (OMIE). OMIE web site. Accessed: 01-Aug-2020. [Online]. Available: http://www.omie.es/en/inicio.

[236] Red Eléctrica de España (REE). REE web site. Accessed: 01-Aug-2020. [Online]. Available: http://www.ree.es/en.

[237] EPEX SPOT, Nord Pool, OMIE, OPCOM, GME, OTE, TGE (PCR PXs). Euphemia public description. PCR market coupling algorithm. Accessed: 01-Aug-2020. [Online]. Available: https://www.nordpoolspot.com/globalassets/download-center/pcr/euphemia-public-documentation.pdf.

[238] Spanish Ministry of Energy, Tourism and Digital Agenda. Resolution, of 9 May 2018, of the Secretary of State for Energy, approving the operation rules for the daily and intraday electricity markets of electric energy production. BOE no. 115, of 11/05/2018 (In Spanish). Accessed: 01-Aug-2020. [Online]. Available: https://www.boe.es/buscar/act.php?id=BOE-A-2018-6295.

[239] J. A. Carballo, J. Bonilla, L. Roca, A. de la Calle, P. Palenzuela, and M. Berenguel, "Optimal operating conditions analysis of a multi-effect distillation plant," *Desalination and Water Treatment*, vol. 69, pp. 229–235, 2017.

[240] Endesa. Latest Electricity and Gas Rates. Accessed: 01-Aug-2020. [Online]. Available: https://www.endesaclientes.com/articles/latest-gas-light-regulated-rates.html.

[241] Spanish Ministry of Energy, Tourism and Digital Agenda. Error Correction of the Order ETU/1282/2017, of 22 December, establishing electricity access fees for 2018. BOE no. 315, of 28/12/2017 (In Spanish). Accessed: 01-Aug-2020. [Online]. Available: https://www.boe.es/boe/dias/2017/12/28/pdfs/BOE-A-2017-15608.pdf.

[242] Spanish Biomass Association (AVEBIOM). Biomass Prices Index. Accessed: 01-Aug-2020. [Online]. Available: http://www.avebiom.org/es/ind-precios-biomasa.

[243] Profielectra S.L. Propane price. Accessed: 01-Aug-2020. [Online]. Available: https://propanogas.com/faq/precio-propano.

[244] FCC AQUALIA. Water Tariffs. Accessed: 01-Aug-2020. [Online]. Available: http://www.aqualia.com/es/web/aqualia-almeria/atencion-al-cliente/tarifas-de-agua.

[245] The MathWorks Inc. Documentation: intlinprog. Accessed: 01-Aug-2020. [Online]. Available: https://es.mathworks.com/help/optim/ug/intlinprog.html.

[246] Spanish State Meteorological Agency (AEMET). (2020) AEMET website. Accessed: 01-Aug-2020. [Online]. Available: http://www.aemet.es/es/portada.

[247] G. T. Ayele, P. Haurant, B. Laumert, and B. Lacarrière, "An extended energy hub approach for load flow analysis of highly coupled district energy networks: Illustration with electricity and heating," *Applied Energy*, vol. 212, pp. 850–867, 2018.

[248] O. D. Montoya, W. Gil-González, S. Avila-Becerril, A. Garces, and G. Espinosa-Pérez, "Distributed energy resources integration in AC grids: a family of passivity-based controllers," *Revista Iberoamericana de Automática e Informática Industrial*, vol. 16, no. 2, pp. 212–221, 2019, (in Spanish).

[249] F. J. Gómez, L. J. Yebra, A. Giménez, and J. L. Torres-Moreno, "Modelling of batteries for application in light electric urban vehicles," *Revista Iberoamericana de Automática e Informática Industrial*, vol. 16, no. 4, pp. 459–466, 2019, (in Spanish).

Appendix

Full Representation of the Sparse Matrices in Chapter 7

$$
\boldsymbol{C_i} = \begin{bmatrix}
1&1&1&1&1&0&0&0&0&0&0&0&0&0&0&0&0&0&0&0&0&0&0&0&0&0&0&0&0&0\\
0&0&0&0&0&1&1&1&1&1&0&0&0&0&0&0&0&0&0&0&0&0&0&0&0&0&0&0&0&0\\
0&0&0&0&0&0&0&0&0&0&1&1&1&1&1&0&0&0&0&0&0&0&0&0&0&0&0&0&0&0\\
0&0&0&0&0&0&0&0&0&0&0&0&0&0&0&1&1&1&1&1&1&1&0&0&0&0&0&0&0&0\\
0&0&0&0&0&0&0&0&0&0&0&0&0&0&0&0&0&0&0&0&0&0&1&1&0&0&0&0&0&0\\
0&0&0&0&0&0&0&0&0&0&0&0&0&0&0&0&0&0&0&0&0&0&0&0&1&1&1&0&0&0\\
0&0&0&0&0&0&0&0&0&0&0&0&0&0&0&0&0&0&0&0&0&0&0&0&0&0&0&0&1&0\\
0&0&0&0&0&0&0&0&0&0&0&0&0&0&0&0&0&0&0&0&0&0&0&0&0&0&0&0&0&1
\end{bmatrix}
$$

$$
\boldsymbol{C_{di}} = \begin{bmatrix}
0&0&0&0&0&1&1&1&1&1&0&0&0&0&0&0&0&0&0&0&0&0&0&0&0&0&0&0&0&0\\
0&0&0&0&0&0&0&0&0&0&1&1&1&1&1&0&0&0&0&0&0&0&0&0&0&0&0&0&0&0\\
0&0&0&0&0&0&0&0&0&0&0&0&0&0&0&1&1&1&0&0&0&0&0&0&0&0&0&0&0&0\\
0&0&0&0&0&0&0&0&0&0&0&0&0&0&0&0&0&0&1&1&1&1&0&0&0&0&0&0&0&0\\
0&0&0&0&0&0&0&0&0&0&0&0&0&0&0&0&0&0&0&0&0&0&1&0&0&0&0&0&0&0\\
0&0&0&0&0&0&0&0&0&0&0&0&0&0&0&0&0&0&0&0&0&0&0&1&0&0&0&0&0&0\\
0&0&0&0&0&0&0&0&0&0&0&0&0&0&0&0&0&0&0&0&0&0&0&0&1&1&1&0&0&0\\
0&0&0&0&0&0&0&0&0&0&0&0&0&0&0&0&0&0&0&0&0&0&0&0&0&0&0&1&0&0\\
0&0&0&0&0&0&0&0&0&0&0&0&0&0&0&\eta_{D,3}&0&0&\eta_{D,4}&0&0&0&0&0&\eta_{D,7}&0&0&0&0&0\\
0&1&0&0&0&0&\eta_{D,1}&0&0&0&0&\eta_{D,2}&0&0&0&0&0&0&0&0&0&0&0&0&0&0&0&0&0&0\\
0&0&1&0&0&0&0&\eta_{D,1}&0&0&0&0&\eta_{D,2}&0&0&0&0&0&0&0&0&0&0&0&0&0&0&0&0&0\\
0&0&0&0&0&0&0&0&0&0&0&0&0&0&0&0&0&0&0&0&0&0&0&0&0&0&0&0&1&0
\end{bmatrix}
$$

$$
\boldsymbol{C} = \begin{bmatrix}
1 & 0 & 0 & 0 & 0 & \eta_{D,1} & 0 & 0 & 0 & 0 & \eta_{D,2} & 0 & 0 & 0 & 0 & 0 & 0 & 0 & 0 & 0 & 0 & 0 & 0 & 0 & 0 & 0 & 0 & 0 & 0 & 0 \\
0 & \eta_{D,10} & 0 & 0 & 0 & 0 & \eta_{D,1}\eta_{D,10} & 0 & 0 & 0 & 0 & \eta_{D,2}\eta_{D,1} & 0 & 0 & 0 & \eta_{D,3}\eta_{D,9} & 0 & 0 & \eta_{D,4}\eta_{D,9} & 0 & 0 & 0 & 0 & 0 & \eta_{D,7}\eta_{D,9} & 0 & 0 & 0 & 0 & 0 \\
0 & 0 & \eta_{D,11} & 0 & 0 & 0 & 0 & \eta_{D,1}\eta_{D,11} & 0 & 0 & 0 & 0 & \eta_{D,1}\eta_{D,11} & 0 & 0 & 0 & \eta_{D,3} & 0 & 0 & \eta_{D,4} & 0 & 0 & 0 & 0 & 0 & \eta_{D,7} & 0 & 0 & 0 & 0 \\
0 & 0 & 0 & 0 & 0 & 0 & 0 & 0 & 0 & 0 & 0 & 0 & 0 & 0 & 0 & 0 & 0 & \eta_{D,3} & 0 & 0 & \eta_{D,4} & 0 & 0 & \eta_{D,6} & 0 & 0 & \eta_{D,7} & 0 & 0 & 0 \\
0 & 0 & 0 & 0 & 1 & 0 & 0 & 0 & 0 & \eta_{D,1} & 0 & 0 & 0 & 0 & \eta_{D,2} & 0 & 0 & 0 & 0 & 0 & 0 & 0 & 0 & 0 & 0 & 0 & 0 & 0 & 0 & 0 \\
0 & 0 & 0 & 0 & 0 & 0 & 0 & 0 & 0 & 0 & 0 & 0 & 0 & 0 & 0 & 0 & 0 & 0 & 0 & 0 & 0 & 0 & 0 & 0 & 0 & 0 & 0 & \eta_{D,8} & 0 & 0 \\
0 & 0 & 0 & 0 & 0 & 0 & 0 & 0 & 0 & 0 & 0 & 0 & 0 & 0 & 0 & 0 & 0 & 0 & 0 & 0 & 0 & \eta_{D,4} & \eta_{D,5} & 0 & 0 & 0 & 0 & 0 & 0 & 0 \\
0 & 0 & 0 & 1 & 0 & 0 & 0 & 0 & \eta_{D,1} & 0 & 0 & 0 & 0 & \eta_{D,2} & 0 & 0 & 0 & 0 & 0 & 0 & 0 & 0 & 0 & 0 & 0 & 0 & 0 & 0 & 0 & 0 \\
0 & 0 & 0 & 0 & 0 & 0 & 0 & 0 & 0 & 0 & 0 & 0 & 0 & 0 & 0 & 0 & 0 & 0 & 0 & 0 & 0 & 0 & 0 & 0 & 0 & 0 & 0 & 0 & \eta_{D,12} & 1
\end{bmatrix}
$$

$$
\boldsymbol{C_{do}} = \begin{bmatrix}
0 & 0 & 0 & 0 & 0 & \eta_{D,1} & \eta_{D,1} & \eta_{D,1} & \eta_{D,1} & \eta_{D,1} & 0 & 0 & 0 & 0 & 0 & 0 & 0 & 0 & 0 & 0 & 0 & 0 & 0 & 0 & 0 & 0 & 0 & 0 & 0 & 0 \\
0 & 0 & 0 & 0 & 0 & 0 & 0 & 0 & 0 & 0 & \eta_{D,2} & \eta_{D,2} & \eta_{D,2} & \eta_{D,2} & \eta_{D,2} & 0 & 0 & 0 & 0 & 0 & 0 & 0 & 0 & 0 & 0 & 0 & 0 & 0 & 0 & 0 \\
0 & 0 & 0 & 0 & 0 & 0 & 0 & 0 & 0 & 0 & 0 & 0 & 0 & 0 & 0 & \eta_{D,3} & \eta_{D,3} & \eta_{D,3} & 0 & 0 & 0 & 0 & 0 & 0 & 0 & 0 & 0 & 0 & 0 & 0 \\
0 & 0 & 0 & 0 & 0 & 0 & 0 & 0 & 0 & 0 & 0 & 0 & 0 & 0 & 0 & 0 & 0 & 0 & \eta_{D,4} & \eta_{D,4} & \eta_{D,4} & \eta_{D,4} & 0 & 0 & 0 & 0 & 0 & 0 & 0 & 0 \\
0 & 0 & 0 & 0 & 0 & 0 & 0 & 0 & 0 & 0 & 0 & 0 & 0 & 0 & 0 & 0 & 0 & 0 & 0 & 0 & 0 & 0 & \eta_{D,5} & 0 & 0 & 0 & 0 & 0 & 0 & 0 \\
0 & 0 & 0 & 0 & 0 & 0 & 0 & 0 & 0 & 0 & 0 & 0 & 0 & 0 & 0 & 0 & 0 & 0 & 0 & 0 & 0 & 0 & 0 & \eta_{D,6} & 0 & 0 & 0 & 0 & 0 & 0 \\
0 & 0 & 0 & 0 & 0 & 0 & 0 & 0 & 0 & 0 & 0 & 0 & 0 & 0 & 0 & 0 & 0 & 0 & 0 & 0 & 0 & 0 & 0 & 0 & \eta_{D,7} & \eta_{D,7} & \eta_{D,7} & 0 & 0 & 0 \\
0 & 0 & 0 & 0 & 0 & 0 & 0 & 0 & 0 & 0 & 0 & 0 & 0 & 0 & 0 & 0 & 0 & 0 & 0 & 0 & 0 & 0 & 0 & 0 & 0 & 0 & 0 & \eta_{D,8} & 0 & 0 \\
0 & 0 & 0 & 0 & 0 & 0 & 0 & 0 & 0 & 0 & 0 & 0 & 0 & 0 & 0 & \eta_{D,3}\eta_{D,9} & 0 & 0 & \eta_{D,4}\eta_{D,9} & 0 & 0 & 0 & 0 & 0 & \eta_{D,7}\eta_{D,9} & 0 & 0 & 0 & 0 & 0 \\
0 & \eta_{D,10} & 0 & 0 & 0 & 0 & \eta_{D,1}\eta_{D,10} & 0 & 0 & 0 & 0 & \eta_{D,2}\eta_{D,10} & 0 & 0 & 0 & 0 & 0 & 0 & 0 & 0 & 0 & 0 & 0 & 0 & 0 & 0 & 0 & 0 & 0 & 0 \\
0 & 0 & \eta_{D,11} & 0 & 0 & 0 & 0 & \eta_{D,1}\eta_{D,11} & 0 & 0 & 0 & 0 & \eta_{D,2}\eta_{D,11} & 0 & 0 & 0 & 0 & 0 & 0 & 0 & 0 & 0 & 0 & 0 & 0 & 0 & 0 & 0 & 0 & 0 \\
0 & 0 & 0 & 0 & 0 & 0 & 0 & 0 & 0 & 0 & 0 & 0 & 0 & 0 & 0 & 0 & 0 & 0 & 0 & 0 & 0 & 0 & 0 & 0 & 0 & 0 & 0 & 0 & \eta_{D,12} & 0
\end{bmatrix}
$$

These are my principles.
If you don't like them
I've got others.

Groucho Marx

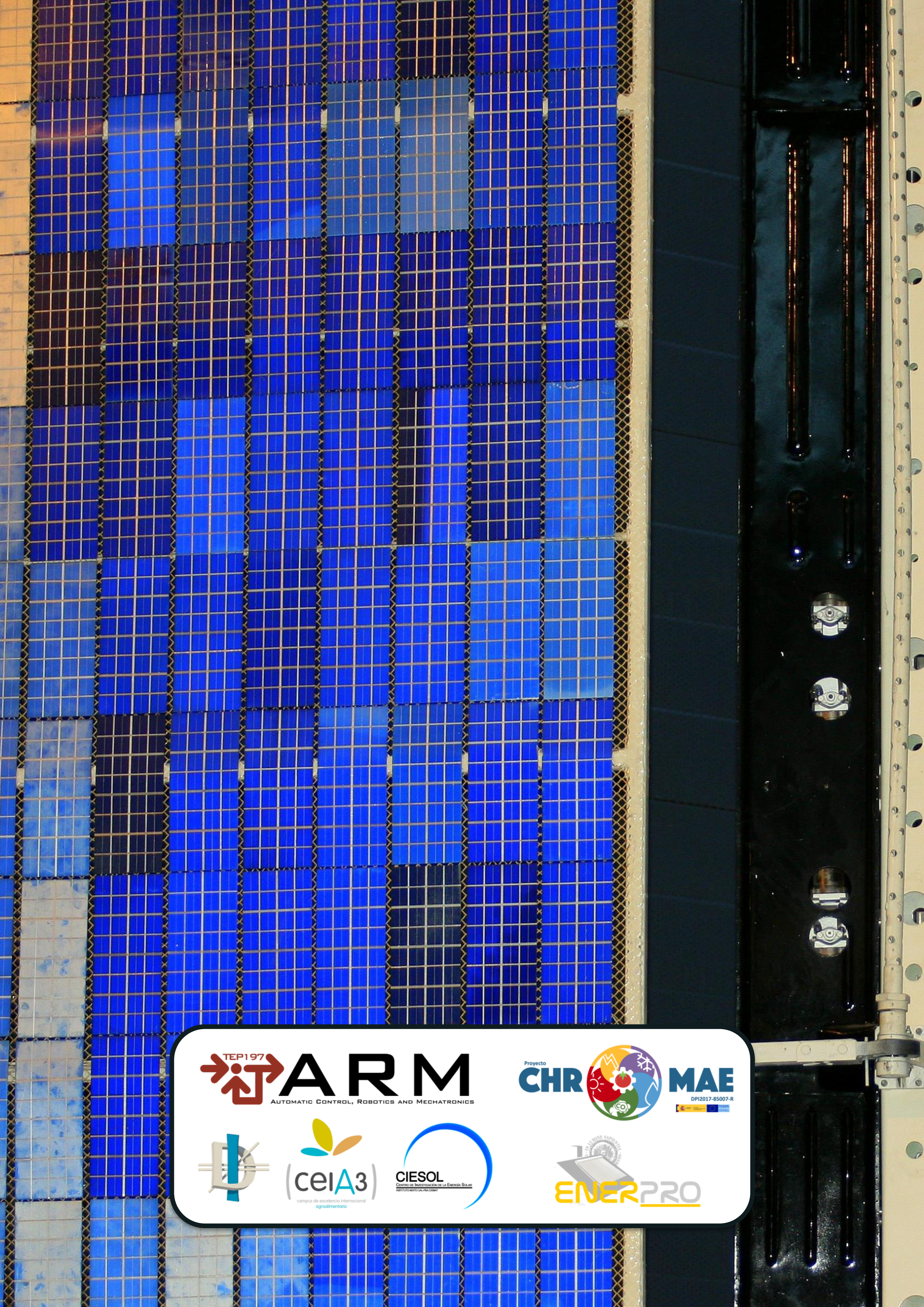

TEP197
ARM
Automatic Control, Robotics and Mechatronics
Proyecto
CHROMAE
DPI2017-85007-R
ceiA3
campus de excelencia internacional agroalimentario
CIESOL
Centro de Investigación de la Energía Solar
ENERPRO